ANALYSIS OF THE MOVEMENT OF WATER FROM RECHARGE CHANNELS AND PITS

RESEARCH PROJECT No. 71/30

Burdekin Artificial Recharge Study

ANALYSIS OF THE MOVEMENT OF WATER FROM RECHARGE CHANNELS AND PITS
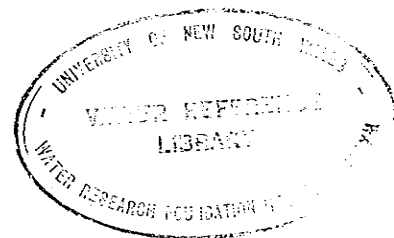
by
S.N. Webb
and
K.K. Watson   *Keith Watson*
School of Civil Engineering
University of New South Wales

TABLE OF CONTENTS

ACKNOWLEDGEMENTS

Membership of the project reference panel was as follows:

Dr. N.O. Jones (Chairman)   - Canberra College of Advanced Education.

Mr. W.M. Day   - Irrigation and Water Supply Commission, Queensland.

Mr. R.G. Shepherd   - Department of Mines, South Australia.

Prof. K.K. Watson   - University of New South Wales

Prof. K.P. Stark   - James Cook University, Queensland.

Prof. C. Burdon-Jones   - James Cook University, Queensland.

Mr. G.B. Stirk   - CSIRO Division of Soils, St. Lucia, Queensland.

Dr. P.L. Airey   - A.A.E.C. Research Establishment, New South Wales.

Mr. S.E. James   - Irrigation and Water Supply Commission, Queensland.

Dr. J. Gordon-Smith, Department of Environment, Housing and Community Development, Canberra and later Mr. K. Johnson, Department of National Resources, Canberra, acted as secretary to the reference panel.

NOTE ON APPENDICES

In Part A of this study reference is made to three appendices relating to computer program listings and in Part B reference is made to one such appendix. These appendices, which appeared in the original report, have not been included in this reproduction because of space considerations.

B	=	constant in acceleration term,
C	=	specific water capacity ($d\theta/dh$),
D	=	constant in finite difference equations,
d	=	depth of ponding (cm),
E	=	constant in finite difference equations,
F	=	constant in finite difference equations,
G	=	constant in finite difference equations,
H	=	constant in finite difference equations,
H	=	translation of origin (cm),
h	=	pressure head (cm of water),
i	=	iteration number,
K	=	hydraulic conductivity (cm min^{-1}),
K_o	=	saturated hydraulic conductivity (cm min^{-1}),
K_{bo}	=	saturated hydraulic conductivity at some index point $\bar{x}_o$, $\bar{y}_o$, $\bar{z}_o$ (cm min^{-1}),
K_x, K_y, K_z	=	hydraulic conductivities in x, y and z directions (cm min^{-1}),
K_s	=	sum of K values at surrounding node points (cm min^{-1}),
$\bar{K}$	=	dimensionless relative hydraulic conductivity,
L	=	length scaling factor (profile depth normally) (cm),
M	=	hydraulic conductivity coupling ratio,
m	=	index in x direction,
N	=	number of equations in one dimensional grid,
n	=	index in z direction,
p	=	time index,
P	=	constant in finite difference equations,
Q	=	constant in finite difference equations,
R	=	constant in finite difference equations,
R'	=	flux - positive upward (cm min^{-1}),
r	=	iteration counter,
S	=	constant in finite difference equations,
T	=	constant in finite difference equations,
t	=	time (min),
Δt	=	time step (min),
v_x, v_y, v_z	=	macroscopic flow velocities in x, y and z directions (cm min^{-1}),

$\bar{v}$ = macroscopic velocity vector (cm min^{-1}),

w = over-relaxation or under-relaxation factor,

x = cartesian space co-ordinate,

y = cartesian space co-ordinate,

z = cartesian space co-ordinate (positive upward),

z = positive head relative to some datum (cm),

$\bar{x},\bar{y},\bar{z}$ = dimensionless space co-ordinates,

$\bar{x}_0,\bar{y}_0,\bar{z}_0$ = dimensionless space co-ordinates at an index point,

$\Delta x, \Delta y, \Delta z$ = increments in co-ordinate directions (cm),

α, β = constants in top flux boundary condition,

θ = water content (cm^3 cm^{-3}),

ϕ = hydraulic head (cm of water),

$\bar{\phi}$ = dimensionless hydraulic head,

ω = acceleration term in finite difference equations,

μ = angle of inclination of plane (radians),

ρ = density of water (gm cm^{-3}).

PART A

NUMERICAL STUDIES

1. INTRODUCTION

1.1 GENERAL

The onshore portion of the Burdekin Delta in Northern Queensland covers an area of 500 km^2 and is intensively cultivated for agricultural purposes, the predominant crop being sugar cane. Sugar cane requires regular and substantial quantities of irrigation water for efficient year-round crop management; to meet this irrigation need it has been necessary to extract much of the water from groundwater storage. Annual extraction of groundwater is now well in excess of 300 x 10^6 m^3. Natural recharge, which is supplied partly by seasonal precipitation and partly by bed and bank leakage from the Burdekin River, has been estimated to have a mean annual volume of 210 x 10^6 m^3. The continual extraction of this water, particularly when paralleled by a succession of low rainfall years has resulted in periods when there have been depressed water table levels in the deltaic sediments with the consequent danger of sea water intrusion. To alleviate this situation a comprehensive programme of works on the north and south sides of the Burdekin River has resulted in the construction of a regional groundwater recharge system in which water is pumped from the river during times of flow into natural and artificial recharge channels and pits thus inducing seepage into the underlying sediments. Pumpage for artificial recharge is now approaching 100 x 10^6 m^3 per year. Details of the regional recharge scheme have been presented by O'Shea (1967).

Several problems have arisen in implementing the artificial recharge programme. These include siltation of the artificial recharge channels and pits with a consequent reduction in intake rates. Clogging of the bottom and sides of the recharge pits by algal material has also resulted in a reduction in potential intake rates. In order to study these and related problems of artificial recharge management, the Australian Water Resources Council financed in 1971 a group of four research projects. These projects are:

(1) 71/28 Numerical modelling of an aquifer system with intermittent recharge. The objective of this study was to provide a means of predicting future aquifer response and improve management practice. Volker and Stark (1973) have discussed the modelling approach used in this work.

(2) 71/29 The effects of siltation on recharge rates.
Regional studies, along the main recharge channels were
carried out to determine the longitudinal variation of
seepage rates due to differences in silt deposition.
Several seepage meters were tested in the process of
this investigation with varying degrees of success.
This project also provided a data collection service
for projects 71/28, 71/30 and 71/39 as well as assisting
the Australian Atomic Energy Commission.

(3) 71/30 Analysis of the movement of water from recharge
channels and pits. Early in this project it was found
that the local seepage flow from channels was very small
compared to the flow from the equivalent length of
artificial recharge pit. As a consequence of this both
the numerical and field studies were concentrated on
understanding the flow regime beneath artificial recharge
pits. Preliminary results on this study were reported in
Watson and Webb (1974).

(4) 71/39 Biological aspects of the aquifer recharge in the
Burdekin Delta. The objective of this project was to
evaluate the biological factors involved in the recharge
environment and their effect on recharge retardation.

In addition to these funded projects the Australian Atomic
Energy Commission has been studying the tritium dating of the ground-
waters in the stratified aquifers of the delta to provide data on the
age of the groundwater currently being extracted and the age pattern of
the water in the different aquifer systems. The work has been discussed
by Airey et al. (1974). The A.A.E.C. has also participated in seepage
meter studies in conjunction with project 71/29. Carbon-14 age determin-
ations have been carried out on bore water samples and the A.A.E.C. has
made studies of the penetration of labelled clay minerals into the sand
below an artificial recharge pit. Valuable assistance has also been
provided to several of the projects by the Division of Soils, CSIRO.

This report presents the results of A.W.R.C. project 71/30. The
primary objectives of this study were:-

(a) To investigate the nature of the process of the movement of water from recharge channels and pits to an aquifer and to develop a numerical model of this process;

(b) to examine and calculate design criteria relevant to the future development of the recharge scheme using the results of the work in (a);

(c) to investigate the problem of clogging at the recharge channel soil interface by means of soil tension measurements near the soil surface.

This investigation was concentrated on the behaviour of artificial recharge pits, in particular Shands No. 2 Pit and Iyah Creek No. 1 Pit. These two pits were investigated in preference to examining the seepage flow from natural channels, because almost complete flexibility in management is possible in artificial pits, whereas only limited management decisions can be implemented for natural channels. The intake rate per unit intake area is also several orders greater for artificial pits resulting in significant flow profile development under the pits.

The authorities conducting the recharge operations are particularly interested in optimising the recharge-drying cycle of the pits to give the most efficient operation. A rational basis for such decisions can only be made following detailed experimental and numerical studies of the movement of water from the pits to the water table and the manner in which the movement is controlled by surface sealing.

This report is presented in two Parts. Part A discusses the numerical part of the investigation, and Part B presents the field experimental results derived using tensiometers and neutron moisture meter equipment. A summary of Part A is given below.

1.2 SUMMARY OF PART A

The numerical analyses and results are presented in four chapters. The first of these (Chapter 2) details the theoretical bases of the computer programs used to derive the results in the succeeding three chapters. It is logical to present the theory in one chapter as the basic flow equations controlling one and two dimensional flow, and both steady and unsteady flow, are closely related. Chapter 3 discusses flow profile development under unsteady surface clogging conditions for

a homogeneous soil profile such as under Shands No. 2 Pit. A one dimensional unsteady state computer program is used. It should be noted that both the one and two dimensional unsteady state programs only simulate homogeneous profiles. Hence the introduction of beach sand in Shands No. 2 Pit part way through the project, creating in fact a non-homogeneous profile, made the simulation of the response of this pit more difficult. Fortunately this problem was overcome by using a steady state program capable of solving flow problems in non-homogeneous profiles. It was possible to use a one dimensional program to study surface clogging, as the flow from a recharge pit to a water table is predominantly vertical (see Chapter 5) and a one dimensional program provides a satisfactory approximation to the true flow regime.

Chapter 4 describes a study of Shands No. 2 Pit carried out using a two dimensional unsteady state model. Although such a model gives an accurate representation of the flow regime under this pit before the beach sand was introduced, the technique requires a large amount of computer time to derive representative results. To overcome this problem, and to expand the work to include non-homogeneous profiles, an investigation was carried out using a steady state computer program which could be used to model flow in one, two, or three dimensions. Chapter 5 discusses the results produced using this program. A wide variety of heterogeneous soil profiles are discussed including several representations of both Shands No. 2 Pit and Iyah Creek No. 1 Pit. Steady state surface clogging examples are also described for both pits. The computer programs used in the study are described in detail in the chapter in which they are used. Conclusions are presented at the end of each chapter.

2. NUMERICAL PROCEDURES

2.1 UNSTEADY STATE SOLUTIONS

Unsteady state solutions were obtained for both one dimensional and two dimensional flow configurations. In both cases it was assumed that the profile was rigid and homogeneous and that isothermal conditions existed. The flow equations were developed in a manner which permitted a unified analysis of water movement in the saturated and unsaturated zones.

A finite difference solution process was used for both the one dimensional and two dimensional cases. The form of the finite difference equations is similar for the two cases; the main difference is the addition of an acceleration parameter in the two dimensional analysis.

The general partial differential equation for flow in unsaturated porous media can be derived by combining Darcy's law with the equation of continuity. Darcy's law can be expressed as

$$\bar{v} = -K\nabla\phi \tag{2.1}$$

where

$\bar{v}$ = macroscopic velocity vector ($cm\ min^{-1}$),

K = hydraulic conductivity ($cm\ min^{-1}$),

ϕ = hydraulic head (cm of water).

The equation of continuity for a rigid soil-water system is

$$\partial\theta/\partial t = -\nabla.\bar{v}$$

This can be expressed as

$$\partial\theta/\partial t = -(\partial v_z/\partial z + \partial v_x/\partial x + \partial v_y/\partial y) \tag{2.2}$$

where

θ = volumetric water content ($cm^3 cm^{-3}$),

t = time (min),

x,y,z = cartesian space co-ordinates. In this study the vertical ordinate z is taken positive upwards,

v_x, v_y, v_z = macroscopic flow velocities in x, y, z directions respectively.

Combining (2.1) and (2.2) gives

$$\partial\theta/\partial t = \partial[K_z(\partial\phi/\partial z)]/\partial z + \partial[K_x(\partial\phi/\partial x)]/\partial x + \partial[K_y(\partial\phi/\partial y)]/\partial y \tag{2.3}$$

where

K_x, K_y, K_z = hydraulic conductivities in x, y and z directions respectively.

$$\text{Now} \quad \phi = h + z$$

$$\text{where} \quad h = \text{pressure head (cm of water)},$$

$$z = \text{position head relative to some datum (cm)}.$$

$$\therefore \quad \partial\phi/\partial z = \partial h/\partial z + 1,$$

$$\partial\phi/\partial x = \partial h/\partial x, \text{ and } \partial\phi/\partial y = \partial h/\partial y.$$

It should be noted that for flow in unsaturated materials θ and K are dependent on the pressure head h. In addition $\theta(h)$ exhibits strong hysteresis depending on the history of wetting and draining of the profile. The hysteresis of $\theta(h)$ is reflected in $K(h)$ but little, if any, hysteresis is apparent in $K(\theta)$.

On substituting for ϕ, K, and θ, Equation (2.3) becomes

$$\partial\theta(h)/\partial t = \partial[K_z(h) \, \partial h/\partial z]/\partial z + \partial[K_z(h)]/\partial z + \partial[K_x(h) \, \partial h/\partial x]/\partial x$$

$$+ \partial[K_y(h) \, \partial h/\partial y]/\partial y \tag{2.4}$$

If the specific water capacity C(h) is defined as

$$C(h) = d\theta/dh$$

then Equation (2.4) may be written entirely in terms of h.

$$C(h) \, \partial h/\partial t = \partial[K_z(h) \, \partial h/\partial z]/\partial z + \partial[K_z(h)]/\partial z$$

$$+ \partial[K_x(h) \, \partial h/\partial x]/\partial x + \partial[K_y(h) \, \partial h/\partial y]/\partial y \tag{2.5}$$

In an isotropic medium $K_x = K_y = K_z$

For the case of one dimensional vertical flow, Equation (2.5) becomes

$$C(h) \, \partial h/\partial t = \partial[K(h) \, \partial h/\partial z]/\partial z + \partial[K(h)]/\partial z \tag{2.6}$$

The appropriate form of Equation (2.5) for two dimensional unsaturated flow in an isotropic medium is

$$C(h) \, \partial h/\partial t = \partial[K(h) \, \partial h/\partial z]/\partial z + \partial[K(h)]/\partial z + \partial[K(h) \, \partial h/\partial x]/\partial x \tag{2.7}$$

2.1.1 One Dimensional System

The numerical approach summarized here is that developed in the School of Civil Engineering in recent years and detailed by Perrens (personal communication). It is similar to that used by Richtmeyer and Morton (1967), Whisler and Klute (1967), and Whisler and Watson (1969). One departure in the approach is the numbering of the node points downwards from the top boundary, with z still being positive in the upward direction. A consequence of this approach is that the sign of the incremental distance in vertical direction (Δz) is negative. The principal advantage of numbering the nodes from the

surface downwards is the ease with which moving lower boundary problems can be analysed. Considerable savings in computer time are also achieved since finite difference equations need only be applied over that section of the profile where changes are occurring.

The one dimensional partial differential equation for unsteady flow in a rigid, isotropic porous medium was defined in Section 2.1 as

$$C(h) \ \partial h/\partial t = \partial[K(h) \ \partial h/\partial z]/\partial z + \partial[K(h)]/\partial z \tag{2.6}$$

To solve this equation numerically a grid of points is imposed on the region $t \geq 0$, $-L \leq z \leq 0$ where L is the profile depth. The z axis is divided into $N + 1$ intervals, the nodes being numbered from 0 at the top to $N + 1$ at the base. The spatial node points are defined by

$$z_n = -n\Delta z \qquad n = 0,1,2 \ldots N + 1$$

$$\Delta z = L/(N+1)$$

$$t_o = 0$$

and $\qquad t_p = t_{p-1} + \Delta t \qquad p = 1,2,3 \ldots$

where $\qquad$ t is time and p is the index of time.

It should be noted that t_p is not a simple multiple of Δt because the size of Δt is different for each time step. When rapid changes are occurring it will tend to be small, and as the profile approaches a steady state condition, Δt will tend to be larger.

a) Development of Finite Difference Equations

The partial derivatives in Eq. (2.6) are approximated by the finite difference equations given below. To find the finite difference expression at node n, the pressure heads and soil characteristics at the node above n (node n-1) and the node below n (node n+1) are required

$$h_{n+1}^{p+\frac{1}{2}} \simeq (h_{n+1}^{p} + h_{n+1}^{p+1})/2$$

$$h_{n}^{p+\frac{1}{2}} \simeq (h_{n}^{p} + h_{n}^{p+1})/2$$

$\therefore$ at $n + \frac{1}{2}$, $p + \frac{1}{2}$

$$\partial h/\partial z \simeq (h_{n+1}^{p} + h_{n+1}^{p+1} - h_{n}^{p} - h_{n}^{p+1})/(2\Delta z)$$

Let $\qquad K_{n+\frac{1}{2}}^{p+\frac{1}{2}} = (K_{n}^{p} + K_{n}^{p+1} + K_{n+1}^{p} + K_{n+1}^{p+1})/4$

then at $n+\frac{1}{2}$, $p+\frac{1}{2}$

$$K(\partial h/\partial z) \simeq K_{n+\frac{1}{2}}^{p+\frac{1}{2}} (h_{n+1}^{p} + h_{n+1}^{p+1} - h_{n}^{p} - h_{n}^{p+1})/(2\Delta z)$$

Similarly at $n-\frac{1}{2}$, $p+\frac{1}{2}$

$$K(\partial h/\partial z) \simeq K_{n-\frac{1}{2}}^{p+\frac{1}{2}} (h_{n}^{p} + h_{n}^{p+1} - h_{n-1}^{p} - h_{n-1}^{p+1})/(2\Delta z)$$

$\therefore$ $\partial[K(\partial h/\partial z)]/\partial z$ at $n, p+\frac{1}{2}$

$$\simeq [K_{n+\frac{1}{2}}^{p+\frac{1}{2}} (h_{n+1}^{p} + h_{n+1}^{p+1} - h_{n}^{p} - h_{n}^{p+1})$$

$$- K_{n-\frac{1}{2}}^{p+\frac{1}{2}} (h_{n}^{p} + h_{n}^{p+1} - h_{n-1}^{p} - h_{n-1}^{p+1})]/(2\Delta z^2) \tag{2.8}$$

The remaining two partial derivatives in Eq. (2.6) are evaluated from the following expressions.

At $n, p+\frac{1}{2}$ $\partial K/\partial z \simeq (K_{n+\frac{1}{2}}^{p+\frac{1}{2}} - K_{n-\frac{1}{2}}^{p+\frac{1}{2}})/\Delta z$ $\tag{2.9}$

Let $C_{n}^{p+\frac{1}{2}} = (C_{n}^{p+1} + C_{n}^{p})/2$

then at $n, p+\frac{1}{2}$

$$C(\partial h/\partial t) \simeq C_{n}^{p+\frac{1}{2}} (h_{n}^{p+1} - h_{n}^{p})/\Delta t \tag{2.10}$$

The finite difference approximations given in Equations (2.8), (2.9) and (2.10) are substituted in Eq. (2.6) to obtain a set of N equations of the form

$$E h_{n-1}^{p+1} + F h_{n}^{p+1} + G_{n+1}^{p+1} = H \tag{2.11}$$

where $E = -K_{n-\frac{1}{2}}^{p+\frac{1}{2}}/(2\Delta z^2)$

$$G = -K_{n+\frac{1}{2}}^{p+\frac{1}{2}}/(2\Delta z^2)$$

$$F = C_{n}^{p+\frac{1}{2}}/\Delta t + K_{n+\frac{1}{2}}^{p+\frac{1}{2}}/(2\Delta z^2) + K_{n-\frac{1}{2}}^{p+\frac{1}{2}}/(2\Delta z^2)$$

$$= C_{n}^{p+\frac{1}{2}}/\Delta t - E - G$$

$$H = -E h_{n-1}^{p} - h_{n}^{p} (-C_{n}^{p+\frac{1}{2}}/\Delta t - E - G)$$

$$-G h_{n+1}^{p} + 2\Delta z (-G + E)$$

It should be noted that E, F, G and H can be evaluated in Eq.(2.11), so the only unknowns are the N+2 values of h at time (p+1) on the left hand side of the expression. There are therefore N equations in N+2 unknowns. Two more equations are necessary to make a solution possible and these are derived by applying the appropriate boundary conditions at the top and base of the soil profile.

b)   Boundary Conditions

Two broad categories of boundary conditions may be defined.

1.   Specified pressure head at a boundary.
   (i)   imposed hydrostatic pressure (e.g. ponded surface condition).
   (ii)   water table condition. This is a special case of (i). The pressure head is zero.
   (iii)   constant pressure ($\partial h/\partial t = 0$) at the base of a semi-infinite profile (this infers zero flux across the boundary).
   (iv)   impervious boundary. This is treated similarly to (iii).

2.   Imposed flux at a boundary.
   (i)   surface rainfall.
   (ii)   controlled flux into a profile.
   (iii)   zero flux condition.

The flux boundary conditions are treated in a similar manner by using the expression

$$\partial\theta/\partial t \simeq [-R' - K(\partial h/\partial z + 1)]/(\Delta z/2) \qquad (2.12)$$

where $R' = $ flux   (positive upward in cm min^{-1}; precipitation would therefore be $-R'$).

To illustrate the pressure head boundary condition we will consider cases 1(i) and 1(ii). Firstly case 1(i), which is ponding at the surface of the profile.

The form of Eq.(2.11) for the node below the surface is

$$E_1 h_0^{p+1} + F_1 h_1^{p+1} + G_1 h_2^{p+1} = H_1 \qquad (2.13)$$

But $h_0^{p+1} = d$ (i.e. pressure head at the surface is equal to ponding depth).

Then Eq. (2.13) becomes

$$F_1 \, h_1^{p+1} + G_1 \, h_2^{p+1} = H_1 - E_1 d$$

The inclusion of this boundary condition therefore eliminates one unknown, h_o^{p+1}.

The second example of a pressure head boundary is case 1(ii) which is the water table boundary condition. The form of Eq.(2.11) for the node one above the water table is

$$E_N \, h_{N-1}^{p+1} + F_N \, h_N^{p+1} + G_N \, h_{N+1}^{p+1} = H_N$$

But at a water table the pressure head is zero, hence

$$h_{N+1}^{p+1} = 0$$

$$\therefore \quad E_N \, h_{N-1}^{p+1} + F_N \, h_N^{p+1} = H_N$$

The inclusion of this boundary condition therefore eliminates the unknown, h_{N+1}^{p+1}.

The general case of flux at a boundary can now be considered. Each flux case (evaporation, zero flux, precipitation) can be simulated by substituting the appropriate value of R' in the general equation.

By substituting the appropriate finite difference expressions in Eq.(2.12), and applying the equation across the top half node of the profile, the form of Eq. (2.11) for the node below the top boundary becomes

$$(F_1 + E_1 \alpha) \, h_1^{p+1} + G_1 \, h_2^{p+1} = H_1 - E_1 \beta$$

where $\quad \alpha = (E_1 \Delta z)/[E_1 \Delta z - C_o^{p+\frac{1}{2}} (\Delta z/2)]$

and $\quad \beta = [E_1 \Delta z (h_1^p - h_o^p + 2\Delta z) - R'$

$$-(C_o^{p+\frac{1}{2}} \, h_o^p \, \Delta z)/(2\Delta t)]/[E_1 \Delta z - C_o^{p+\frac{1}{2}} (\Delta z/2)]$$

The unknown h_o^{p+1} is thus eliminated by the inclusion of this boundary condition.

c)   The Solution Process

To solve for a particular soil profile, N equations of the form of Eq.(2.11) are set up and appropriate boundary conditions are imposed at the top and bottom of the profile. The combination of N equations similar to Eq.(2.11) with an equation for both the top and bottom boundaries leads to

a set of N+2 equations in N+2 unknowns. This system of equations is thus capable of solution by numerical means. Because the equations are nonlinear, an iterative process has to be used to obtain a solution.

The solution proceeds from an initial assumed head distribution h_n^p to a new solution h_n^{p+1} where the time at (p+1) = time at (p) plus Δt. The value of Δt is optimised within the solution process to minimise the computer time requirements without decreasing the accuracy of the solution.

After a value of Δt is calculated for the next time step, the coefficients E, F, G, and H are evaluated using the current pressure head distribution h_n^p and the corresponding $K_n^{p+\frac{1}{2}}$ and $C_n^{p+\frac{1}{2}}$ values. The resulting set of linear algebraic equations are solved using an algorithm formulation for the tri-diagonal matrix to obtain an estimate of the pressure distribution h_n^{p+1}. These values are then used in turn to derive improved values of E, F, G, and H, and the process repeated until the new estimate of h_n^{p+1} differs by a specified small amount from the previous estimate. This final head distribution is then accepted as the solution at time (p+1). A new value of Δt is evaluated and the solution process repeated until the time reaches a pre-determined value, where the solution process is terminated.

2.1.2 Two Dimensional System

The numerical approach used to solve a two dimensional flow problem is similar to that used for the one dimensional case described in Section 2.1.1. However, the solution is necessarily more complex because of the need to distribute head changes in two dimensions, and because the soil characteristics and pressure heads at the four nodes surrounding a point have to be considered in calculating the coefficients and determining a solution.

The first investigator to present a two dimensional numerical model of unsteady state flow applicable to the saturated-unsaturated soil-water regime was Rubin (1968). His work was based on a finite difference scheme utilising the alternating direction implicit (ADI) method developed mainly by Peaceman and Rachford (1955) and Douglas et al (1959). Other studies in this area have been presented by Amerman (1969), Verma and Brutsaert (1970), Brutsaert (1971), Freeze (1971), and Nwa et al (1971).

The numerical approach detailed below is basically that used by Perrens (personal communication). The general equation for two dimensional unsaturated flow in a porous medium was derived in Section 2.1 as

$$C(h)\ \partial h/\partial t = \partial[K(h)\ \partial h/\partial z]/\partial z + \partial[K(h)]/\partial z$$
$$+ \partial[K(h)\ \partial h/\partial x]/\partial x \tag{2.7}$$

If the same process were used to solve this equation as in the one dimensional case, considerable difficulties would be encountered. The number of simultaneous equations requiring solution would be the product of the number of rows and number of columns in the two dimensional grid. Sinc the amount of computer time required to solve such a system of equations is approximately proportional to the square of the number of nodes, the comput time required to obtain a solution for even a moderate-sized grid could be prohibitive. Another problem which would increase the computer time requir ments would be the lack of a convenient tri-diagonal form as used in the one dimensional system.

To facilitate the solution of two dimensional problems Peaceman and Rachford (1955) proposed the ADI technique in which the equations are reduced to a convenient tri-diagonal form. The technique solves Eq.(2.7) by introducing an intermediate non-usable time step which allows the soluti(to proceed column by column and then row by row. Initially the values of h in the x direction (horizontal) are expressed explicitly in terms of known values and the values of h in the z direction are determined implicitly giving

$$C(h) \ \partial h/\partial t_{(i)} = \partial[K(h) \ \partial h/\partial x]/\partial x_{(i)} + \partial[K(h)]/\partial z_{(i+\frac{1}{2})}$$

$$+ \ \partial[K(h) \ \partial h/\partial z]/\partial z_{(i+\frac{1}{2})} \qquad (2.14)$$

where i is the iteration number.

The values of h in the z direction determined from Eq.(2.14) are then used explicitly and the values of h in the x direction are determined by implicit means giving

$$C(h) \ \partial h/\partial t_{(i+\frac{1}{2})} = \partial[K(h) \ \partial h/\partial x]/\partial x_{(i+1)} + \partial[K(h)]/\partial z_{(i+\frac{1}{2})}$$

$$+ \ \partial[K(h) \ \partial h/\partial z]/\partial z_{(i+\frac{1}{2})} \qquad (2.15)$$

Effectively therefore by using head values at the ith iteration it is possible to obtain a solution at an 'imaginary' time step at $(i+\frac{1}{2})$. This solution is then used to obtain a new set of pressure heads for the (i+1)th iteration. As is the case with the one dimensional flow system, several iterations are required to obtain a solution at the next time step. The iteration process is continued until the maximum pressure head difference between two successive iterations is less than a small pre-determined value.

In order to speed convergence of the solution, Douglas et al (1959) included an acceleration parameter in the equations. Eqs. (2.14) and (2.15) then become

$$C(h) \; \partial h/\partial t_{(i)} - \omega_{(i)} \; (h_{(i+\frac{1}{2})} - h_{(i)}) = \partial[K(h) \; \partial h/\partial x]/\partial x_{(i)}$$

$$+ \; \partial[K(h)]/\partial z_{(i+\frac{1}{2})} + \partial[K(h) \; \partial h/\partial z]/\partial z_{(i+\frac{1}{2})} \qquad (2.16)$$

$$C(h) \; \partial h/\partial t_{(i+\frac{1}{2})} - \omega_{(i)} \; (h_{(i+1)} - h_{(i+\frac{1}{2})}) = \partial[K(h) \; \partial h/\partial x]/\partial x_{(i+1)}$$

$$+ \; \partial[K(h)]/\partial z_{(i+\frac{1}{2})} + \partial[K(h) \; \partial h/\partial z]/\partial z_{(i+\frac{1}{2})} \qquad (2.17)$$

Douglas et al (1959) suggest that the form of the acceleration parameter should be

$$\omega_{(i)} = K_s B^i$$

where K_s = sum of surrounding K values,

B = 0.22,

i = iteration number; varies cyclically 0,1,2,...6.

There are several difficulties involved in the choice of a suitable acceleration parameter. The form suggested above is suitable for some flow conditions but is completely unusable with others. Problems encountered in using the acceleration parameter are discussed in more detail in Chapter 4.

The partial differentials in Eqs. (2.16) and (2.17) can be approximated in a similar way to the one dimensional case discussed in the preceding section. Eq. (2.16) can be expressed in the following form (note that the values are at iteration i unless otherwise noted). The node index in the x direction is m, and in the z direction is n.

$$C_{m,n}^{p+\frac{1}{2}} \; (h_{m,n}^{p+1,i+\frac{1}{2}} - h_{m,n}^{p})/\Delta t - \omega_{(i)} \; (h_{m,n}^{p+1,i+\frac{1}{2}} - h_{m,n}^{p+1})$$

$$= [K_{m+\frac{1}{2},n}^{p+\frac{1}{2}} \; (h_{m+1,n}^{p+1} - h_{m,n}^{p+1}) - K_{m-\frac{1}{2},n}^{p+\frac{1}{2}} \; (h_{m,n}^{p+1} - h_{m-1,n}^{p+1})]/(2\Delta x^2)$$

$$+ [K_{m,n+\frac{1}{2}}^{p+\frac{1}{2}} \; (h_{m,n+1}^{p+1,i+\frac{1}{2}} - h_{m,n}^{p+1,i+\frac{1}{2}}) - K_{m,n-\frac{1}{2}}^{p+\frac{1}{2}} \; (h_{m,n}^{p+1,i+\frac{1}{2}} - h_{m,n-1}^{p+1,i+\frac{1}{2}})]/(2\Delta z^2)$$

$$+ [K_{m+\frac{1}{2},n}^{p+\frac{1}{2}} \; (h_{m+1,n}^{p} - h_{m,n}^{p}) - K_{m-\frac{1}{2},n}^{p+\frac{1}{2}} \; (h_{m,n}^{p} - h_{m-1,n}^{p})]/(2\Delta x^2)$$

$$+ [K_{m,n+\frac{1}{2}}^{p+\frac{1}{2}} \; (h_{m,n+1}^{p} - h_{m,n}^{p}) - K_{m,n-\frac{1}{2}}^{p+\frac{1}{2}} \; (h_{m,n}^{p} - h_{m,n-1}^{p})]/(2\Delta z^2)$$

$$+ (K_{m,n+\frac{1}{2}}^{p+\frac{1}{2}} - K_{m,n-\frac{1}{2}}^{p+\frac{1}{2}})/\Delta z \qquad (2.18)$$

Eq.(2.17) can be expressed in the following form

$$C_{m,n}^{p+\frac{1}{2}} (h_{m,n}^{p+1,i+1} - h_{m,n}^{p})/\Delta t - \omega_{(i)} (h_{m,n}^{p+1,i+1} - h_{m,n}^{p+1,i+\frac{1}{2}})$$

$$= [K_{m+\frac{1}{2},n}^{p+\frac{1}{2}}(h_{m+1,n}^{p+1,i+1} - h_{m,n}^{p+1,i+1}) - K_{m-\frac{1}{2},n}^{p+\frac{1}{2}} (h_{m,n}^{p+1,i+1} - h_{m-1,n}^{p+1,i+1})]/(2\Delta x^2)$$

$$+ [K_{m,n+\frac{1}{2}}^{p+\frac{1}{2}} (h_{m,n+1}^{p+1,i+\frac{1}{2}} - h_{m,n}^{p+1,i+\frac{1}{2}}) - K_{m,n-\frac{1}{2}}^{p+\frac{1}{2}} (h_{m,n}^{p+1,i+\frac{1}{2}} - h_{m,n-1}^{p+1,i+\frac{1}{2}})]/(2\Delta z^2)$$

$$+ [K_{m+\frac{1}{2},n}^{p+\frac{1}{2}} (h_{m+1,n}^{p} - h_{m,n}^{p}) - K_{m-\frac{1}{2},n}^{p+\frac{1}{2}} (h_{m,n}^{p} - h_{m-1,n}^{p})]/(2\Delta x^2)$$

$$+ [K_{m,n+\frac{1}{2}}^{p+\frac{1}{2}} (h_{m,n+1}^{p} - h_{m,n}^{p}) - K_{m,n-\frac{1}{2}}^{p+\frac{1}{2}} (h_{m,n}^{p} - h_{m,n-1}^{p})]/(2\Delta z^2)$$

$$+ (K_{m,n+\frac{1}{2}}^{p+\frac{1}{2}} - K_{m,n-\frac{1}{2}}^{p+\frac{1}{2}})/\Delta z \tag{2.19}$$

where Δt is the time step,

        i is the iteration number,

        K and C are respectively the conductivity and capacity terms.

They are evaluated in a similar manner to that used in the one dimensional case (see Section 2.1.1).

The acceleration term in the above two equations is evaluated from the following expression

$$\omega_{(i)} = B^i (K_{m-\frac{1}{2},n}^{p+\frac{1}{2}} + K_{m+\frac{1}{2},n}^{p+\frac{1}{2}} + K_{m,n-\frac{1}{2}}^{p+\frac{1}{2}} + K_{m,n+\frac{1}{2}}^{p+\frac{1}{2}})$$

where B = 0.22 if the acceleration parameter suggested by Douglas et al (1959) is used.

Eqs. (2.18) and (2.19) can be expressed in a form suitable for tri-diagonal solution. Firstly, Eq. (2.18) can be expressed as

$$P\, h_{m,n-1}^{p+1,i+\frac{1}{2}} + Q\, h_{m,n}^{p+1,i+\frac{1}{2}} + R\, h_{m,n+1}^{p+1,i+\frac{1}{2}} = S + T \tag{2.20}$$

and secondly Eq. (2.19) takes the form

$$D\, h_{m-1,n}^{p+1,i+1} + E\, h_{m,n}^{p+1,i+1} + F\, h_{m+1,n}^{p+1,i+1} = H + T \tag{2.21}$$

where coefficients P,Q,R,S and T in Eq. (2.20) are derived by grouping the appropriate terms in Eq. (2.18). They consist of known values at the ith iteration.

Coefficients D,E,F and H in Eq. (2.21) are similarly found by grouping the appropriate terms in Eq. (2.19). These consist of values known at the $(i+\frac{1}{2})$th iteration. It should be noted that T consists of terms common to both equations. Eqs. (2.20) and (2.21) are similar in form to Eq. (2.11)

used in the one dimensional case. In fact the same solution algorithm can be used to solve both the one dimensional and two dimensional cases. Eq. (2.20) is first solved for all columns in the grid using the appropriate boundary conditions at the top and bottom of the grid. The $h^{i+\frac{1}{2}}$ terms derived in this first pass are used to derive the coefficients for the second pass, which solves for all rows in the grid using Eq. (2.21) and the appropriate boundary conditions at each end. Pressure head values derived in the second pass give the new estimates of the pressure head at time (p+1). This pressure head grid is compared with the heads at the ith iteration, and if the maximum head difference is less than a small pre-determined value, the latest head estimate is accepted as the new solution. Another cycle of iterations is then initiated to determine the pressure distribution at the next time step.

The boundary condition equations used are of the same form as those used in the one dimensional case. In addition a special type of boundary condition, representing a no flow boundary or mirror boundary, will be discussed here since it occurs frequently in two dimensional flow systems. For example, if the left hand boundary of a profile is a no flow boundary, the row equation for the second pass in the solution process will relate to the node next to the boundary. Hence

$$D \, h_{0,n}^{p+1,i+1} + E \, h_{1,n}^{p+1,i+1} + F \, h_{2,n}^{p+1,i+1} = H + T$$

By positioning the boundary half way between the first two nodes, then

$$h_{0,n}^{p+1,i+1} = h_{1,n}^{p+1,i+1}$$

and the general equation for the node next to the boundary becomes

$$(D + E) \, h_{1,n}^{p+1,i+1} + F \, h_{2,n}^{p+1,i+1} = H + T$$

which eliminates the unknown

$$h_{0,n}^{p+1,i+1}$$

from the solution process. This boundary condition, together with others discussed in Section 2.1.1b), can be used to eliminate the unknowns in each row and each column of the grid. The resulting N + 2 equations involve N + 2 unknowns and a numerical solution is then possible.

A large part of the computer program consists of routines to determine the best value of Δt for the succeeding time step as in the one dimensional case. Further details on the derivation of the optimum Δt value, and other techniques used to improve the solution process, are discussed in Chapter 4.

2.2 TWO DIMENSIONAL STEADY STATE SOLUTIONS

The previous sections in this chapter have considered the numerical procedures to be adopted under exacting unsteady state conditions. However, the hydraulic behaviour of a recharge pit may often approximate a steady state flow condition, the numerical analysis to be used for such a case is detailed in this section. The numerical results are given in Chapter 5.

The computer program used to derive the results presented in Chapter 5 has been adapted from details presented in two publications. The first publication, Nelson (1962), describes the mathematical and numerical formulation of the steady state flow equations. A second report, Reisenauer et al (1963), describes the computer program, provides examples of typical results, and gives a copy of the program listing. The equations derived in the first report relating to two dimensional unsaturated flow problems will be discussed in this section. Details of the computer program will be presented in Chapter 5.

The two basic equations used to derive the unsteady state equations in Section 2.1 are again used to define flow in a steady state system. Accordingly

$$\bar{v} = -K\nabla\phi \qquad (2.1)$$

where

$\bar{v}$ = macroscopic velocity vector (cm min^{-1}),

K = hydraulic conductivity (cm min^{-1}),

ϕ = potential, or hydraulic head (this is expressed in a dimensionless form for the steady state case).

The form of the equation of continuity for the steady state case is different from that used in the unsteady state solutions since there is no change of storage (i.e. water content) with time. The equation of continuity for steady state flow can be expressed in the following form

$$\text{div } \rho \, \bar{v} = 0 \qquad (2.22)$$

where ρ is the density of water (gm cm^{-3}).

Combining Eqs. (2.1) and (2.22) leads to the following general equation of steady flow in heterogeneous saturated soils

$$\bar{K}(\partial^2\bar{\phi}/\partial\bar{x}^2 + \partial^2\bar{\phi}/\partial y^2 + \partial^2\bar{\phi}/\partial z^2) + (\partial\bar{K}/\partial x)(\partial\bar{\phi}/\partial\bar{x})$$
$$+ (\partial\bar{K}/\partial\bar{y})(\partial\bar{\phi}/\partial\bar{y}) + (\partial\bar{K}/\partial\bar{z})(\partial\bar{\phi}/\partial\bar{z}) = 0 \qquad (2.23)$$

where $\bar{x}$, $\bar{y}$, $\bar{z}$ are the dimensionless space co-ordinates ($\bar{z}$ is in the vertical

direction, $\bar{x}$ is in the horizontal, and $\bar{y}$ is in a direction perpendicular to the z - x plane). The x, y, z co-ordinates are reduced to dimensionless form by dividing by the vertical length dimension (i.e. the depth of the profile). ϕ is similarly expressed in dimensionless form $(\bar{\phi})$ by dividing by the profile depth. In all the cases considered in this report, the value of $\bar{\phi}$ will be set to zero at the water table. $\bar{K}$ is also in dimensionless form in Eq. (2.23). It is expressed in dimensionless form by applying the following expression

$$\bar{K} = (K/K_o) (K_o/K_{bo}) = (K/K_o)M$$

where

$\bar{K}$ = the relative hydraulic conductivity in dimensionless form,

K = hydraulic conductivity at the pressure existing at any point, $\bar{x}$, $\bar{y}$, $\bar{z}$ (cm min^{-1}),

K_o = saturated hydraulic conductivity at any location $\bar{x}$, $\bar{y}$, $\bar{z}$ (cm min^{-1}),

K_{bo} = saturated hydraulic conductivity at some index point $\bar{x}_o$, $\bar{y}_o$, $\bar{z}_o$ in the flow system (cm min^{-1}),

M = hydraulic conductivity coupling ratio. This ratio allows several soils, each expressed in terms of its own relative hydraulic conductivity but having different saturated hydraulic conductivities, to be interrelated.

To evaluate the relative hydraulic conductivity at any point in the grid, the pressure head at that point requires calculation, and this is used in a table look-up procedure to determine K. It should be noted that boundary rewet data were used in this analysis, hence K could be related directly to a pressure head value. The expression used to evaluate K from the potential at a point is reasonably complicated and will be discussed more fully in Chapter 5.

Eq. (2.23) was expressed in a finite difference form suitable for solution by the modified Gauss-Seidel iterative method. Central differences were used to evaluate the first derivatives while the second derivatives were approximated by combined forward and backward differences. In deriving the finite difference equations the node spacing was assumed to be uniform in all directions. Since only the two dimensional case is considered in this report, the finite difference expressions for the three dimensional case will not be given. The finite difference form of Eq. (2.23) applicable to

steady state flow in two dimensions is

$$\overline{\phi}_{m,n} = (\overline{\phi}_{m,n+1} + \overline{\phi}_{m,n-1} + \overline{\phi}_{m+1,n} + \overline{\phi}_{m-1,n})/4$$

$$+ (\overline{K}_{m,n+1} - \overline{K}_{m,n-1}) (\overline{\phi}_{m,n+1} - \overline{\phi}_{m,n-1})/[8(\overline{K}_{m,n+1} + \overline{K}_{m,n-1})]$$

$$+ (\overline{K}_{m+1,n} - \overline{K}_{m-1,n}) (\overline{\phi}_{m+1,n} - \overline{\phi}_{m-1,n})/[8(\overline{K}_{m+1,n} + \overline{K}_{m-1,n})] \qquad (2.$$

where   m = node index used in the x direction (horizontal),
         n = node index used in the z direction (vertical).

This equation is also referred to as an improvement formula, as the potential $\overline{\phi}_{m,n}$ is 'improved' by using the surrounding values of $\overline{\phi}$ and $\overline{K}$ to determine a better estimate of $\overline{\phi}_{m,n}$.

The solution proceeds from an initial assumed value of $\overline{\phi}$ over all the grid points to a final value by successively sweeping through the grid using the latest values of $\overline{\phi}$ and $\overline{K}$ to find better estimates. This process is continued until the maximum improvement in $\overline{\phi}$ for a complete sweep is less than some specified small value. Boundary conditions are applied along each side of the grid. They are applied in a similar way to the boundary condition for the unsteady state solutions but are considerably simpler. There are basically two types of boundary condition possible. These are the fixed potential boundary

$$\overline{\phi} = \text{constant},$$

and the no-flow or zero flux boundary

$$\partial\overline{\phi}/\partial\overline{x} \text{ or } \partial\overline{\phi}/\partial\overline{z} = 0$$

The fixed potential boundary can be used to simulate a water table (usually $\overline{\phi} = 0$), or ponding at the surface of the profile (usually $\overline{\phi} = 1$). At a fixed head boundary no calculation is carried out on the boundary nodes and the potential head remains at the initial assumed value. However the value of $\overline{\phi}$ at the boundary is used to calculate an improved value for $\overline{\phi}$ at the nodes adjacent to the boundary.

The no-flow boundary is simulated by setting up an imaginary node outside the real boundary node, and setting the potential value at that point at the same value as the node adjacent to the boundary. This simulates no flow across the boundary, but the potential at the boundary can vary.

Other boundary conditions such as a constant flux (e.g. evaporation), are simulated by choosing an appropriate fixed potential boundary which results in the desired flux.

Another important feature of the process used to derive the steady state solutions is the use of an optimum over-relaxation factor. The solution process described above is normally stable for saturated flow, although some instabilities can occur in heterogeneous profiles. In unsaturated soil profiles the use of an over-relaxation factor, and sometimes an under-relaxation factor, is essential for obtaining a stable solution. The factor is derived from an expression involving the sum of the corrections applied to all nodes in the grid on the previous sweep. When a new value of $\bar{\phi}^{\,i}_{m,n}$ is calculated (i is the iteration number) a corrected value is computed from the following expression

$$\bar{\phi}^{\,I}_{m,n} = \bar{\phi}^{\,i-1}_{m,n} + w(\bar{\phi}^{\,i}_{m,n} - \bar{\phi}^{\,i-1}_{m,n})$$

where
$$\bar{\phi}^{\,I}_{m,n} = \text{'corrected' value of } \bar{\phi}_{m,n} \text{ at ith iteration,}$$

$$\bar{\phi}^{\,i-1}_{m,n} = \bar{\phi}_{m,n} \text{ at the preceding iteration,}$$

$$\bar{\phi}^{\,i}_{m,n} = \text{newly calculated value of } \bar{\phi}_{m,n} \text{ from Eq. (2.24),}$$

$$w = \text{over-relaxation or under-relaxation factor (over-relaxation if > 1).}$$

For further details on the derivation of w the reader is referred to Reisenauer et al (1963).

The solution process used in the steady state program is inefficient as judged by current numerical techniques and, as a consequence, requires quite large amounts of computer time. Over 1000 iterations are sometimes needed to obtain a solution. However, the computer time requirements are still small compared with the requirements of unsteady state solutions. Further details of the mechanisms of the program are discussed in Chapter 5.

3. ONE DIMENSIONAL SIMULATION
OF SURFACE CLOGGING

3.1 INTRODUCTION

The operation of artificial recharge pits in the Burdekin Delta area is characterised by decreasing intake rates with time. There are several factors which contribute towards this phenomenon. Undoubtedly the major factors involved are the growth of different types of algae in the pits and the clogging of the bottom and sides of the pits due to the build-up of a layer of sediment deposited from the recharge water. Another factor which may contribute to the reduction in flux in particular circumstances is the formation of an excessively high water table mound underneath the pit. The relative importance of these factors depends on environmental conditions involving water temperature, amount of sunlight, and sediment load in the recharge water.

Part B of the report on this research project studies from an experimental viewpoint the complex interactions existing between the mechanisms involved in the clogging process. The physical and biological complexities are such that it is not possible at this time to insert into a numerical model of the flow process a detailed simulation of the dynamic surface clogging phenomenon. However, it is desirable that the physical conditions existing in the soil profile during a reduction in surface flux due to clogging be studied. To this end a one dimensional simulation of surface clogging has been completed using a computer program written by S.J. Perrens. The program computes for the one dimensional unsteady flow system described in Section 2.1.1 the time-dependent water content and pressure head distributions. Three different top boundary conditions involving a time-dependent surface flux were used in the program. They were

(a) an exponential reduction in flux with time
(b) a linear reduction in flux over a medium time interval (1 day)
(c) a linear reduction in flux over a short time interval (1 hour)

The surface of the profile was assumed to be at the base of the recharge pit, and the bottom of the profile at the water table. The results are discussed in Section 3.3.

Ideally the one dimensional unsteady state studies discussed in this chapter should be extended to a two dimensional unsteady flow system. This has not proved possible in this investigation because of certain problems encountered in the two dimensional unsteady state solution. These problems are discussed in Chapter 4. However surface clogging studies have been carried out using a two dimensional steady state program. The results of these studies are presented in Section 5.3.3.

3.2 THE COMPUTER PROGRAM

The computer program used in the one dimensional simulation of surface clogging was written by S.J. Perrens in Programming Language One (PL/1) for use on the IBM 360/50 computer. The program is capable of solving flow regimes in homogeneous saturated and unsaturated profiles using a uniform grid spacing. More recent versions of this program have been developed by other research workers in the School of Civil Engineering and these versions can be used to solve non-homogeneous systems. Grid-refining can now be included in the programs if there is an area in the profile, such as the interface between two soils, where pressures and moisture contents vary over short distances.

The PL/1 program used to carry out the investigations described in this chapter is reproduced in Appendix A. The program consists of a MAIN program together with 8 subroutines. The functions carried out by each part of the program are described below.

MAIN Program

As its name implies, the MAIN program forms the core of the one dimensional program. It includes most of the input statements, generates the starting information, calls the subroutines to perform their respective functions, and generally controls the iteration and time-stepping sequences. The coefficients E, F, G and H (see Section 2.1.1) are calculated in the MAIN program, but the solution is computed in subroutine SOLVE. The MAIN program is written so that it can be used for many different types of flow configurations without requiring amendment. This is accomplished by putting those parts of the program which require frequent change into a series of subroutines. By using this device it is possible to reduce the amount of compilation time when setting up a new profile, since only those subroutines which require changes are compiled.

Subroutine STIMER

This subroutine is part of the library in the IBM 360/50 operating system. The subroutine is called early in the MAIN program and a value

called INTERVAL is passed to it. This value is the time that the program
is allowed to run before STIMER sets a variable in the MAIN program,
called INDICATOR, to 1. At the end of each time step the value of INDICATO)
is tested. If it remains at its initial value of 0 then the program con-
tinues; however if it has a value of 1, the program switches to a terminatii
routine which punches out the current head profile and the values of the
control variables. This enables the program to be started again from this
point if the job had not progressed to a satisfactory solution in the
allotted time.

Subroutine SOLVE

This subroutine carries out the solution of the tri-diagonal system of
equations described in Section 2.1.1. It has been written in optimum form
to ensure the minimum amount of computer time usage. The subroutine is
accessed several thousand times in a normal computer run and for this reason
it is essential that it be in optimum form. It has been written in Assemble
language for the IBM 360/50. The Assembler version is not reproduced in
this report since it is unlikely that it would be compatible with the
Assembler language available at other computer installations.

Subroutine LIMIT

This subroutine is used to find the maximum difference between any pair
of values contained in two arrays. It is used for two purposes within the
MAIN program. In the first case it is accessed after each iteration to find
the maximum change in head between the current iteration and the preceding
one. If this value is less than a pre-set variable then the solution process
is assumed to have converged. The subroutine is used a second time, after
a solution has been obtained, to find the change in head between the precedir
time step and the current solution. If the maximum head change is greater
than a pre-set value, then the time step interval is decreased, and the
calculations repeated. The purpose of doing this is to minimise the errors
involved in allowing large head changes within a time step in the nonlinear
system. LIMIT is accessed many times within the one computer run; accordingl
it has also been written in Assembler language for the IBM 360/50.

Subroutine SETSOIL, with entry points, LCURVE and LOKSOIL

The main entry to this subroutine (SETSOIL) sets up the arrays contain-
ing pressure head, moisture content, conductivity and capacity, and then
returns control to the MAIN program. The entry LCURVE acts as a dummy when
the soil characteristics are defined by either the main redrain data or main
rewet data. However, when hysteresis data is being used in the solution

process, LCURVE is used to find which curve each node in the profile is following. This information is then used in LOKSOIL to look up the appropriate conductivity, capacity, and moisture content values for a given head. Each of the hydrologic parameters of the soil is defined by a table of values for different pressure heads. Linear interpolation is used to find the conductivity, capacity, and moisture content for a calculated value of head. The SETSOIL listing in Appendix A refers to #17 sand. If it is desired to use a different soil, only the data within the main entry to SETSOIL requires changing (i.e. LCURVE and LOKSOIL remain the same). When hysteresis data is needed by the program, different versions of SETSOIL, LCURVE and LOKSOIL are used. The form of the hysteresis subroutine is given in the listing of the two dimensional unsteady state flow program in Appendix B (subroutine SETSOIL is identical for the one dimensional and two dimensional programs).

Subroutine TOP

Subroutine TOP is made up of a main entry TOP, and two entry points TOPA and TOPB. The main entry prints out a heading showing what type of top boundary condition exists and sets a variable to -1 or +1 depending on whether the top boundary is a flux condition or ponding condition respectively. Control is then returned to MAIN. Within each iteration loop the entry TOPA is called before the tri-diagonal solution is calculated, and the entry TOPB is called after a solution is obtained. The entry TOPA sets the coefficients at the node one down from the top boundary to new values depending on the type of top boundary condition imposed. Since the flux at the surface was varied according to a pre-determined equation, a new value of surface flux had to be calculated each time TOPA was entered to find the flux applying at that time. After the solution is obtained the head at the surface node is calculated in TOPB. The equation used to derive this value depends on the type of boundary condition imposed at the surface of the profile.

Subroutine BASE

This subroutine is very similar in form to subroutine TOP. It consists of a main entry BASE, and two entry points BASEA and BASEB. Several types of base boundary condition are possible and these are described in Section 2.1.1. The example given in the listing in Appendix A refers to a water table base being the one used in the one dimensional study of surface clogging. As can be seen in the listing, the main entry to BASE prints out a heading and returns control to the MAIN program. The entry BASEA, called before entering the tri-diagonal solution algorithm, is in fact a dummy

entry when the subroutine is used to simulate a water table base. For other base boundary conditions the entry adjusts the coefficients at the node above the base. After the solution is obtained BASEB is called and this sets the pressure head at the base node to zero.

Subroutine ITOUT

This subroutine is used to print out array values after each iteration. It is only accessed if an index value is set to a value greater than 1. In normal operation of the program, this subroutine is not used as it generates a large amount of output. However, it is useful when there are stability problems in the solution process and the numerical information being generated requires detailed analysis.

Subroutine OUTPUT

As its name implies this subroutine is used as the main output facility of the program. It is used to print the pressure head and moisture content profiles when a solution has been obtained. By selecting various options in the MAIN program it is possible to access OUTPUT after every time step or after a pre-set number of time steps have been completed.

3.3 RESULTS

As discussed in the Introduction to this chapter, three different flux equations were used to simulate the reduction in flux at the top node of the soil profile. This study was completed when data on the actual degree of flux reduction was very limited and, accordingly, although the reduction patterns are realistic they do not specifically refer to the Burdekin sites. The main value of this analysis lies in its description of physical conditions* in the profile during surface flux reduction.

3.3.1 Exponential Reduction in Flux

The assumed form of the flux equation for the results presented in this sub-section was

$$FLUX = -[0.594/EXP(0.001569 \times t) + 0.066] \qquad (3.1)$$

where   EXP indicates exponentiation,

t = time from the start of the flux
reduction process in minutes.

It should be noted that a negative flux indicates infiltration into the profile. This follows from the assumption in Section 2.1, that the z direction (vertical) is positive upwards. A positive flux would indicate evaporation from the surface. A consequence of this convention is that a reduction in flux into the profile corresponds to an increase in the numerical value of the flux as the flux assumes less negative values. Therefore in this chapter a reference to a 'reduction in flux' should be taken to mean that the absolute value of the flux into the profile is reduced.

Botany sand data were used to simulate the soil profile below the artificial recharge pits. The main redrain $\theta(h)$ curve for this sand is given in Figure 3.1 and the $K(\theta)$ data are presented in Figure 3.2. The profile used in the study was 100 cm in depth with a node spacing of 1 cm. Initially saturated conditions were assumed with the absolute value of the flux being the same as the saturated conductivity of the sand, namely 0.66 cm min^{-1}. As a consequence of this initial flux condition the initial pressure head was zero throughout the profile, and unit hydraulic gradient conditions existed.

The time-dependent surface flux was determined by using Eq. (3.1) starting at time t = 0. Substituting t = 0 into this equation gives a flux of -0.66 cm min^{-1} initially, reducing to -0.128 cm min^{-1} at 1440 minutes (one day), and tending towards a flux of -0.066 at t = ∞.

Pressure head and water content profiles at various times from the commencement of the simulation are given in Figures 3.3 and 3.4. It can be seen from these figures that the profile remains saturated until the pressure at the surface reaches the air entry value for Botany sand (-38 cm). This pressure occurs 350 minutes from the start of the test. As can be seen from Figure 3.4, there has been a small amount of drainage at 390 minutes when the flux is -0.388 cm min^{-1}. After this time the pressure head distribution at a particular instant can be defined by two straight lines joined by a short curvilinear section where the water content changes rapidly with depth. In the upper part of the profile flow occurs under sensibly unit hydraulic gradient conditions (uniform pressure head) with a corresponding uniform water content. Within the saturated region in the lower part of the profile, the pressure head can again be described by a straight line with a slope such that the flux through this region is slightly greater than the flux through the surface of the profile.

It should be noted that since drainage is occurring, the flux out of the profile must be greater than the flux into the profile. However, for this flux reduction example, there is only a small difference between the flux in
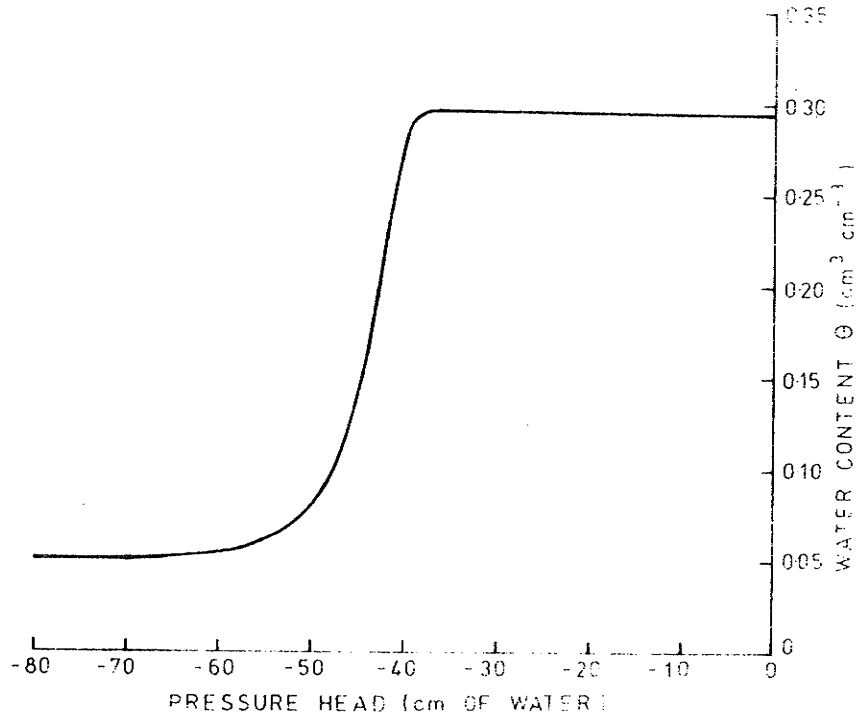
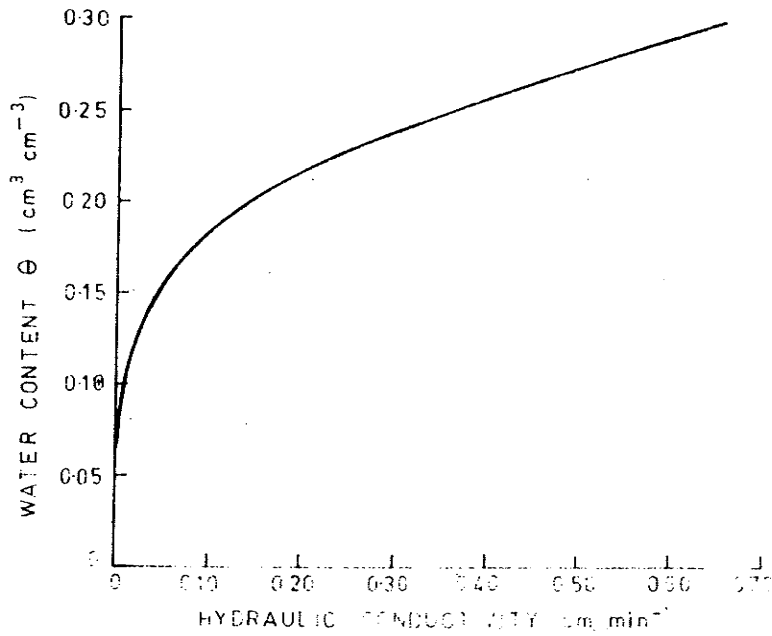Fig.3.1: Pressure head-water content relationship
for Botany sand.

Fig.3.2: Hydraulic conductivity-water content
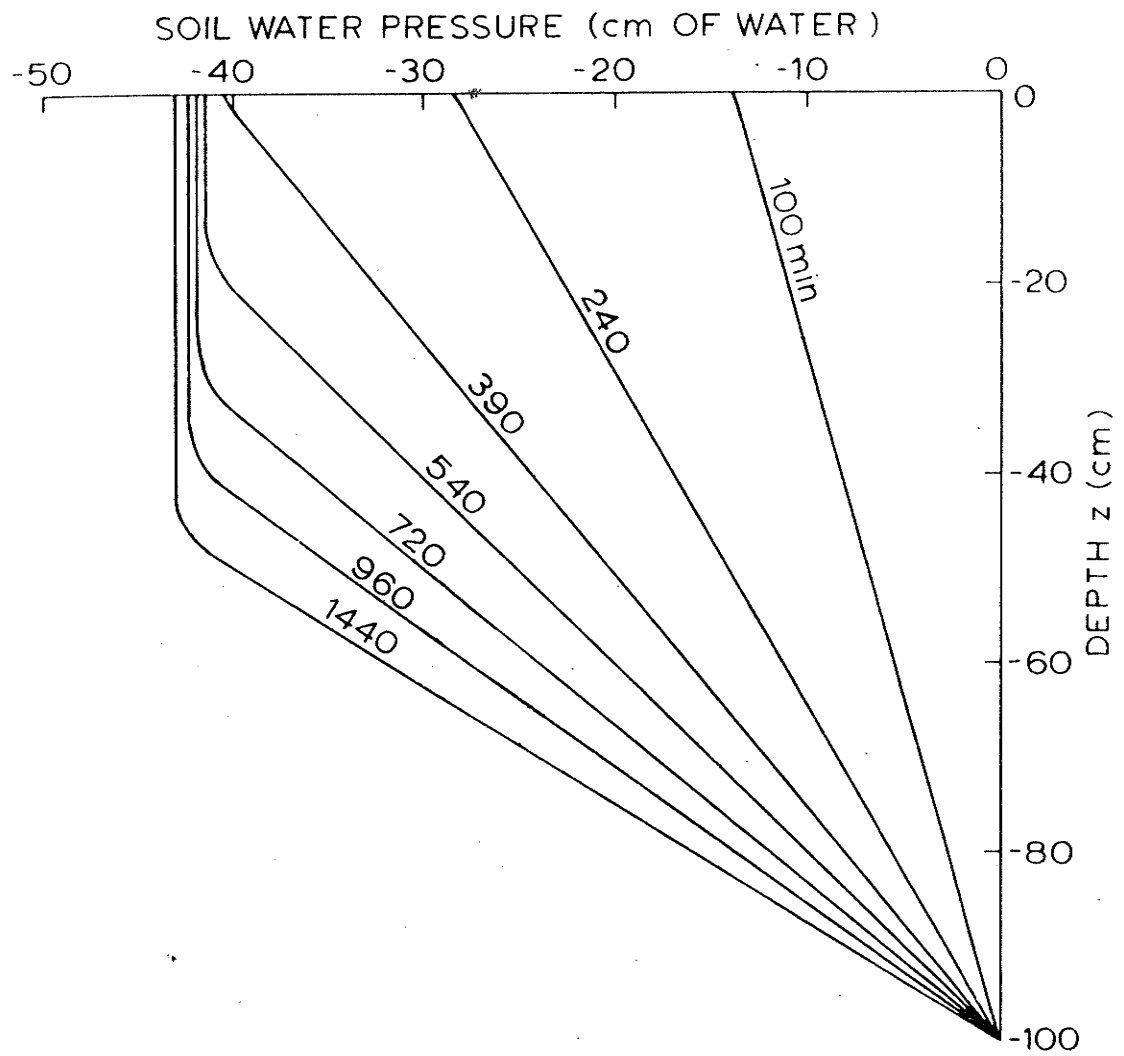relationship for Botany sand.

Figure 3.3: h(z) profiles during drainage of Botany sand under an exponential reduction in flux.
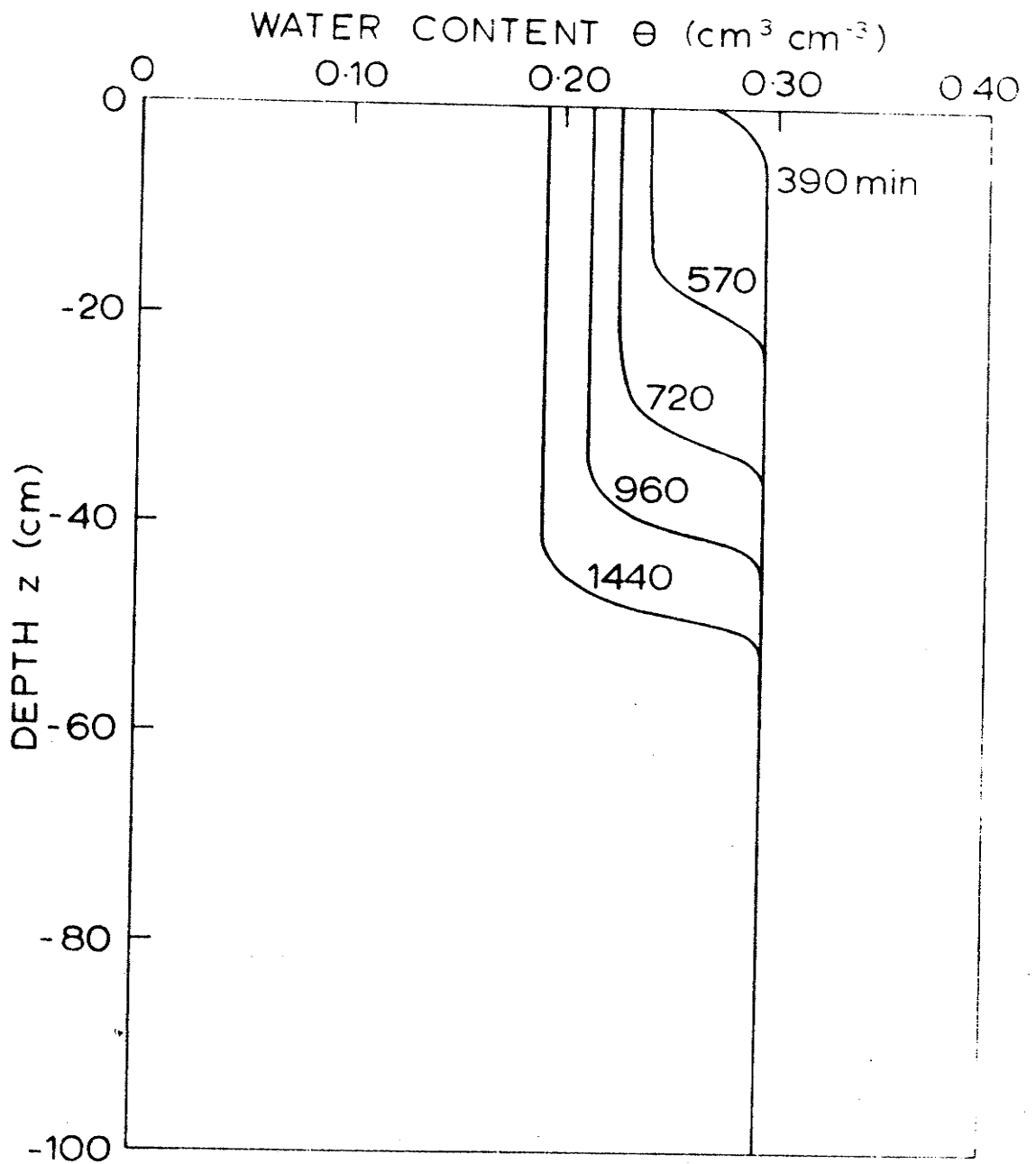
Figure 3.4: $\theta(z)$ profiles corresponding to $h(z)$ profiles given in Figure 3.3.

and the flux out. This occurs because the flux is being reduced at a relatively slow rate at the surface enabling the profile to attain a series of almost steady state configurations. For example at 1440 minutes the flux through the surface from Eq. (3.1) is -0.128 cm min^{-1}. The flux out of the base at that time can be calculated from the slope of the hydraulic head distribution near the base and the saturated hydraulic conductivity of the sand; this calculation gives a flux of -0.132 cm min^{-1}. The small difference between the fluxes into and out of the profile represents the 'instantaneous' drainage component.

A study of Figures 3.3 and 3.4 also indicates that in general terms the hydraulic conductivity at the surface should be numerically equivalent to the instantaneous flux there. In order to check this the pressure head at 1440 minutes in the upper part of the profile (-43.04 cm) was used to derive the hydraulic conductivity in this zone. From the Botany sand data the conductivity corresponding to this pressure head is 0.127 cm min^{-1} giving a satisfactory comparison with the flux of -0.128 cm min^{-1}.

It should be noted in this analysis of exponential flux reduction that the reduction in the flux to -0.128 cm min^{-1} only decreases the water content in the surface zone from 0.295 cm^3 cm^{-3} to 0.193 cm^3 cm^{-3}. As discussed above, at this θ value the decrease of the hydraulic conductivity to 0.127 cm min^{-1} represents only a moderate reduction. It is this moderate reduction in hydraulic conductivity as well as the rate at which the flux decreases which produces the quasi steady state condition. When the flux is reduced to a much smaller value (say -0.01 cm min^{-1} as in the following examples) the consequent small hydraulic conductivity at the surface results in a departure from a profile of the steady state type.

3.3.2 Linear Reduction in Flux (24 hr period)

The surface flux condition used for the analysis presented in this sub-section can be described by the following equations:

$$\text{FLUX} = -[0.66 - (0.0004515 \times t)] \text{ cm min}^{-1} \tag{3.2}$$

for the period $0 < t \le 1440$ minutes and

$$\text{FLUX} = -0.01 \text{ cm min}^{-1} \tag{3.3}$$

for times greater than 1440 minutes. t is the time from the start of the flux reduction process in minutes.

The Botany sand data used in Section 3.3.1 was again utilised for this analysis. The profile was 100 cm deep with the nodes defined at 1 cm intervals. Initially the profile was assumed to be saturated with a steady

flux (-0.66 cm min^{-1}) equal to the saturated conductivity. Eqs.(3.2) and (3.3) describe an initial flux of -0.66 cm min^{-1} reducing linearly to a flux of -0.01 cm min^{-1} at 1440 minutes. For t > 1440 minutes the flux is maintained at -0.01 cm min^{-1}.

Pressure head and water content profiles at several times are given in Figures 3.5 and 3.6. No drainage occurs until the time from the commencement of the test exceeds 555 minutes. At this time the pressure head at the surface becomes more negative than the air entry value for Botany sand (-38.0 cm) and drainage commences.

In Figure 3.3 as previously discussed, the pressure profiles can be divided into two straight line components joined by a short curvilinear section. For the current analysis the same pattern is apparent up to t = 1200 minutes (see Figure 3.5). However for t > 1200 min the h(z) profile departs in shape from the characteristic steady state form as drainage becomes dominant. This is apparent by studying the difference between the flux into the top of the profile and the flux out of the base. At 1620 minutes, after the flux has been constant at -0.01 cm min^{-1} for 180 minutes, a sensibly constant profile of the expected steady state configuration is obtained.

The fluxes into and out of the profile have been calculated at several times and these are shown in Table 3.1.

Table 3.1: Flux Values during Linear Flux Reduction (24 hr period)

Time (t) from start of Flux Change (min) (1)	Flux through the Surface at time t (cm min^{-1}) (2)	Flux out of the Base at time t (cm min^{-1}) (3)	Flux Difference Col.(3)-Col.(2) (cm min^{-1}) (4)
630	-0.376	-0.378	-0.002
720	-0.335	-0.341	-0.006
900	-0.254	-0.261	-0.007
1200	-0.118	-0.127	-0.009
1380	-0.037	-0.054	-0.017
1440	-0.010	-0.035	-0.025
1620	-0.010	-0.012	-0.002

and (3.3)

x of

ntained

ven in

encement

he

d

be

ar

profile

e

n the

20

inutes,

n is

everal

d)

| fference
-Col.(2)
in⁻¹)
4) |
| --- |
| 02 |
| 06 |
| 07 |
| 09 |
| 17 |
| 25 |
| 02 |
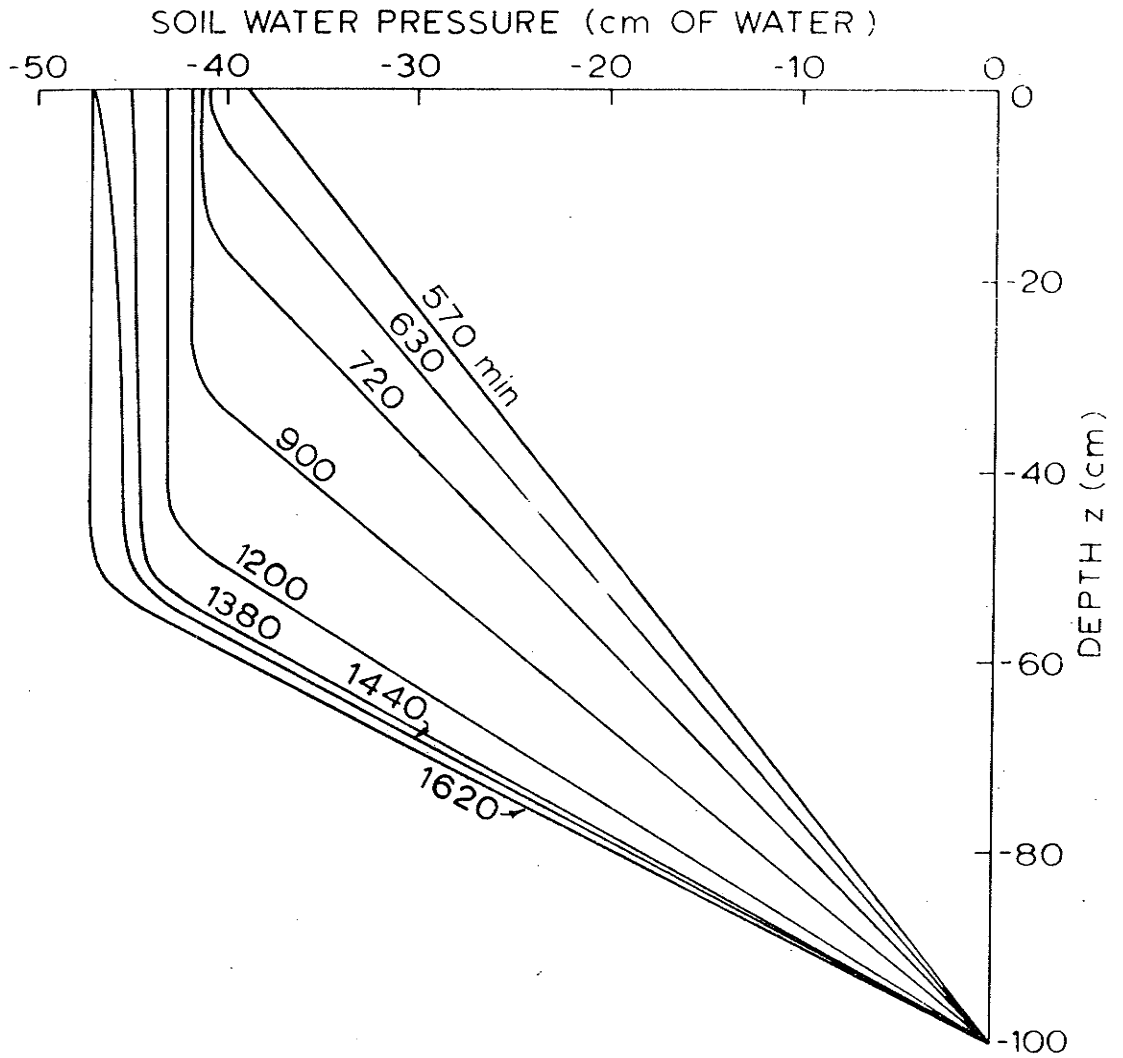
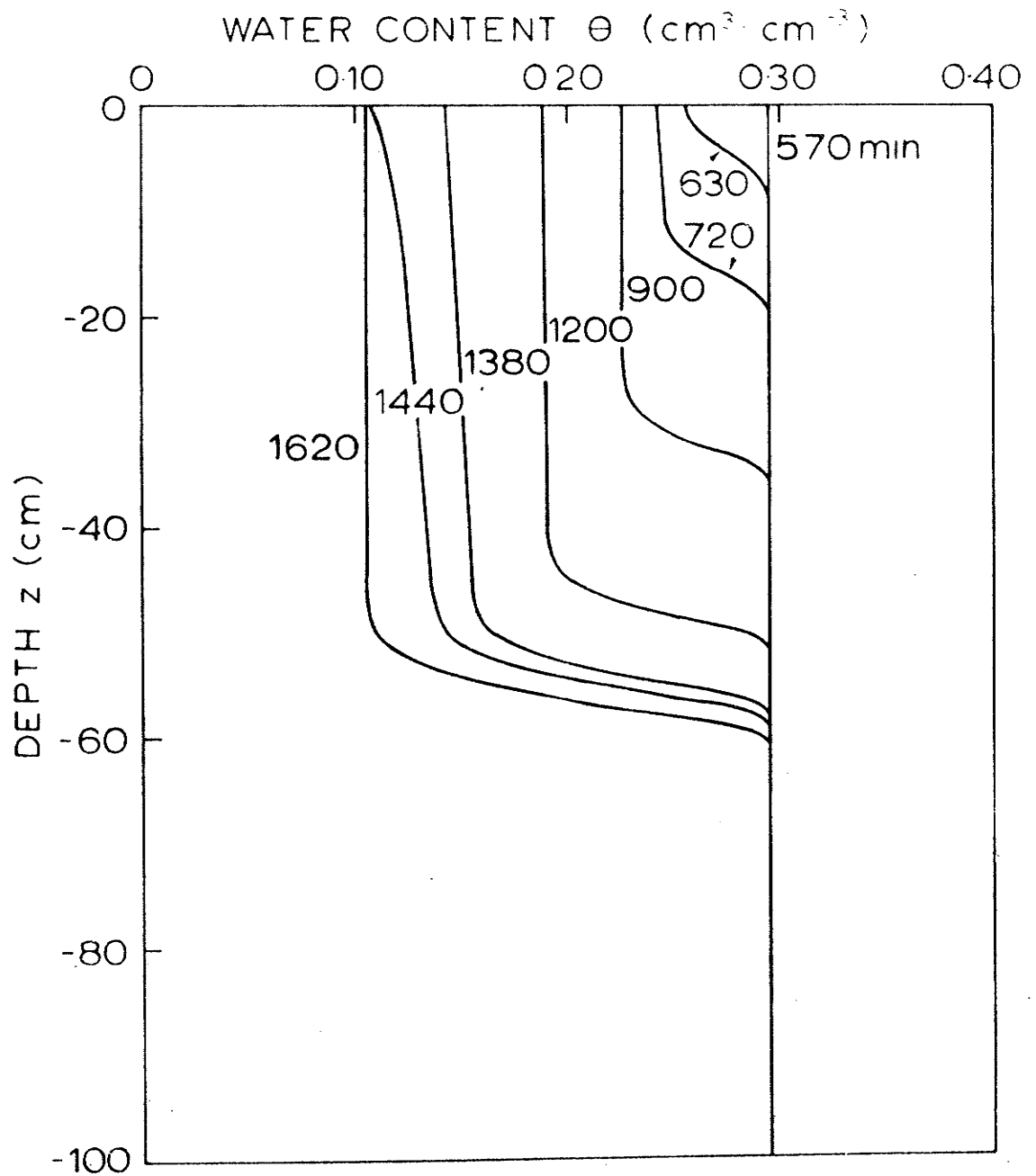Figure 3.5: h(z) profiles during drainage of Botany sand under a linear reduction in flux (24 hour period).

Figure 3.6: θ(z) profiles corresponding to h(z) profiles given in Figure 3.5.

A comparison of columns (2) and (3) in Table 3.1 indicates the manner in which the flux from the base of the profile gradually becomes larger than the input flux. This is dominantly so for times greater than 1200 minutes. A qualitative explanation of the development of this more definite unsteady state condition is given below.

It has been noted previously that at early times as the flux slowly decreases the hydraulic changes in the profile occur at a slow enough rate to allow unit gradient conditions to exist in the top section of the profile with the hydraulic conductivity in the region effectively equalling the flux appropriate to that time. Since the flux-time relationship is linear a casual consideration of the problem might tend to suggest that the steady state type configuration could exist through the entire flux range. However, this does not occur. The shape of the $K(\theta)$ curve is such that a small decrement in K (which would correspond to a similar decrement in flux under unit gradient conditions) at the higher water content end of the relationship results in a smaller θ change than would occur from a similar change in K at the drier end of the $K(\theta)$ curve. Therefore if unit gradient conditions were to exist through the entire range of flux change more water would have to drain from the surface in a given time at later times compared with early times. When the decrease of flux occurs too rapidly for the greater amount of water to drain effectively, the higher water content ('higher' in terms of the water content at which K equals the flux) results in a K value greater than the flux at that time. Flow continuity at the surface requires therefore that $d\phi/dz$ decrease there; this results in a curved $h(z)$ profile in the surface region of the shape shown in Figure 3.5 at 1440 min. In the upper region of the profile above the drainage front zone $d\phi/dz$ increases with depth and K also increases with depth (since θ increases with depth) resulting in an increase of flux with depth confirming the trend given in Table 3.1. At a given instant of time the flux in the lower saturated zone is uniform and therefore equal to the flux from the base of the profile.

In the following sub-section the above behaviour is illustrated more significantly by utilizing a faster reduction in flux.

3.3.3 Linear Reduction in Flux (1 hr period)

The surface flux condition used to derive the results presented in this sub-section can again be described by two equations:

$$\text{FLUX} = -[0.402 - (0.00653 \times t)] \text{ cm min}^{-1} \tag{3.4}$$

for the period $0 < t \leq 60$ minutes, and

$$\text{FLUX} = -0.01 \text{ cm min}^{-1} \qquad\qquad (3.5)$$

for times greater than 60 minutes.

The profile again consisted of 100 cm of Botany sand with the nodes spaced at 1 cm. A water table was used as the base boundary condition. In the previous analyses unit gradient saturated conditions were assumed at the start of the test with a consequent initial flux of -0.66 cm min^{-1}. However, as would be expected, it was seen in these analyses that a straight line pressure profile was maintained until desaturation started at the surface. Therefore, to save computer time, zero time for this analysis was taken to be that time when drainage was incipient at the surface. The assumed initial pressure head distribution was linear with pressure head values of -39.1 cm at the surface and zero at the water table. For these conditions the potential gradient was 0.609. The initial uniform flux can then be calculated, its value being -0.402 cm min^{-1}. This value is consistent with Eq. (3.4) for t=0. The value of h at the surface at t = 0 has been made marginally greater than the air entry value but this has a negligible effect on the results.

The computer analysis was carried out using Eqs. (3.4) and (3.5) to describe the time-dependent top boundary condition. The h(z) and θ(z) profiles at several times are presented in Figures 3.7 and 3.8. These figures show that under this rapid flux reduction a steady state type configuration was not formed. Included in Figure 3.7 is the h(z) profile that is established when the steady state condition is finally reached under the constant flux of -0.01 cm min^{-1}.

The fluxes into and out of the profile have been calculated at the same times as the plots given in Figures 3.7 and 3.8. These are presented in Table 3.2. It can be seen from the table that the flux difference reaches a maximum at 60 minutes after the start of drainage, which is the time a constant flux of -0.01 cm min^{-1} is established at the surface. Comparing Tables 3.1 and 3.2 the expected result is apparent, namely that the flux difference is much greater for the latter case.

(3.5)

les

. In

at the

:raight

s was

·ad

ese

can

0 has

to

figures

ation

tablished

flux

ʒ

ıted

reaches

a

ing

ıx

SOIL WATER PRESSURE (cm OF WATER)

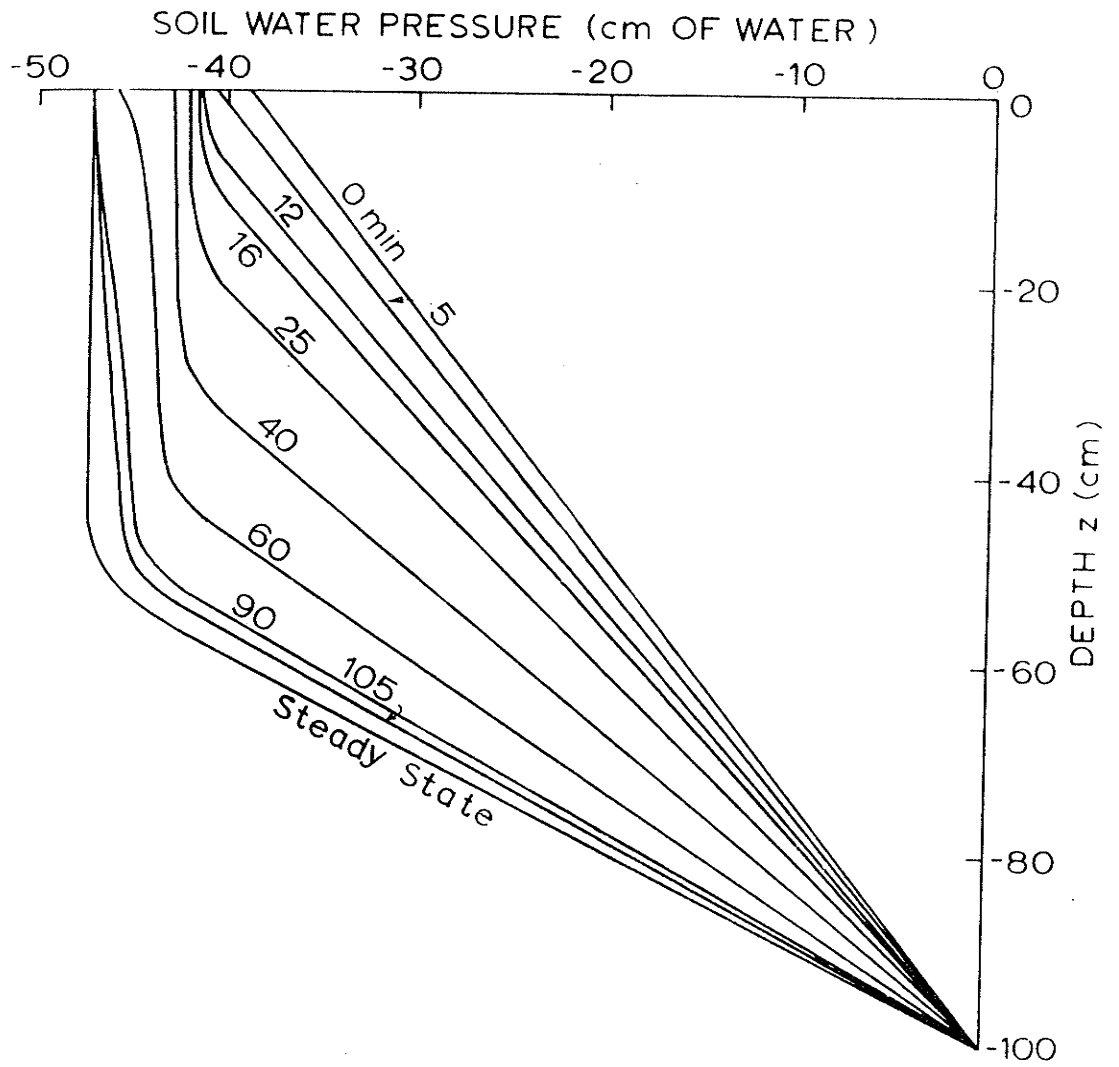Figure 3.7: h(z) profiles during drainage of Botany sand
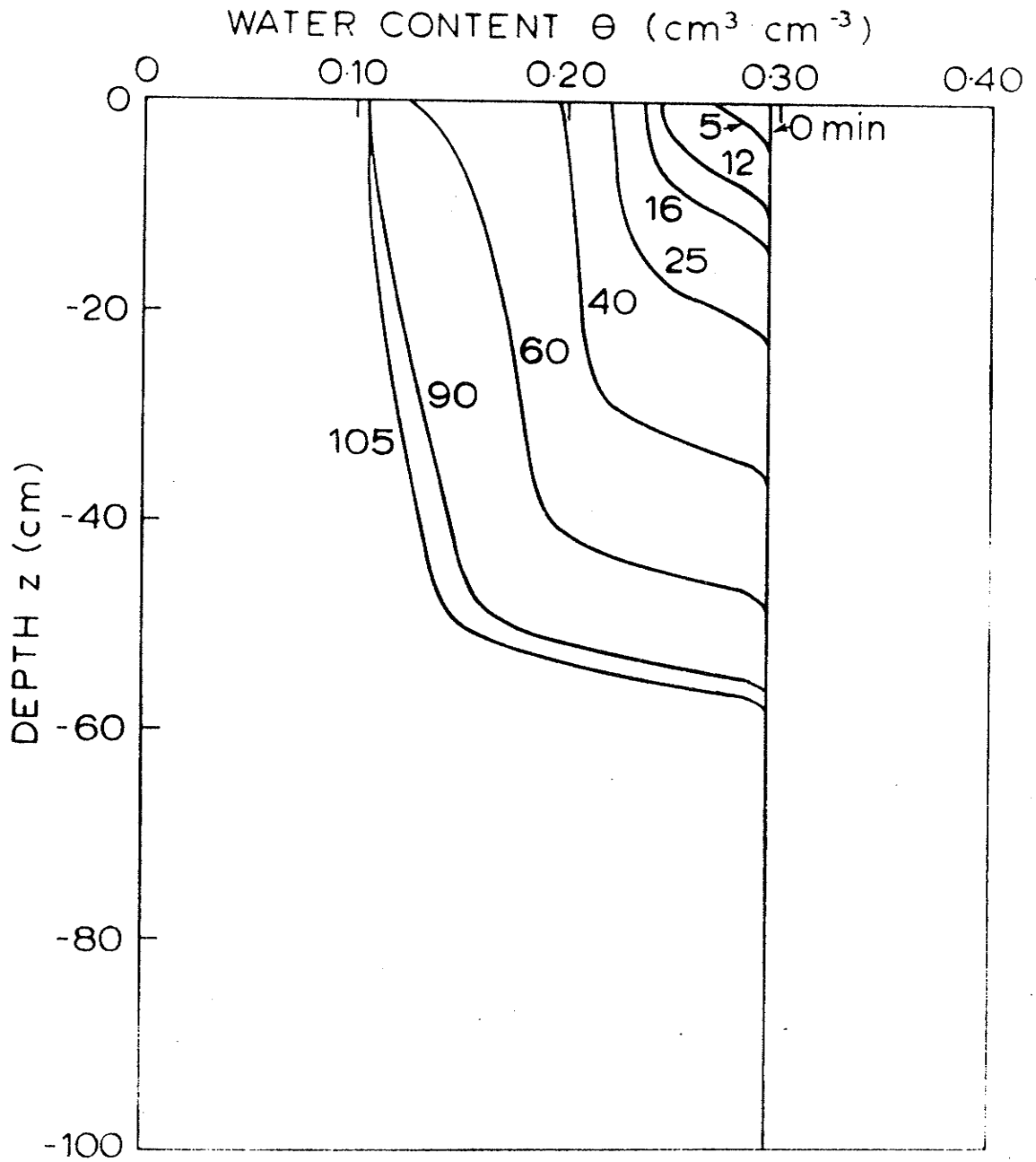under a linear reduction in flux (1 hour period).

Figure 3.8: θ(z) profiles corresponding to h(z) profiles
given in Figure 3.7.

Table 3.2:   Flux Values During Linear Flux Reduction (1 hr period)

Time (t) from start of Flux Change (min) (1)	Flux through the Surface at time t (cm min^{-1}) (2)	Flux out of the Base at time t (cm min^{-1}) (3)	Flux Difference Col.(3)-Col.(2) (cm min^{-1}) (4)
0	-0.402	-0.402	0
5	-0.369	-0.391	-0.022
12	-0.324	-0.372	-0.048
16	-0.298	-0.360	-0.062
25	-0.239	-0.327	-0.088
40	-0.141	-0.259	-0.118
60	-0.010	-0.166	-0.156
90	-0.010	-0.073	-0.063
105	-0.010	-0.050	-0.040
∞	-0.010	-0.010	0

3.4   SUMMARY

1.   The objective of the study presented in this chapter has been to determine the pressure head and water content profiles which may exist between the base of a recharge pit and the underlying water table during conditions of changing surface flux. A computer program for one dimensional flow in unsaturated porous materials has been extended to simulate the hydraulic conditions existing beneath the recharge pit. The decreasing surface fluxes were simulated by a time-dependent flux boundary condition at the upper boundary. The hydrologic characteristics used as data in the computer model were those of a medium sand known as Botany sand. The hydraulic properties were similar to those of the natural sand in the profile at Shands No. 2 Pit. Accordingly, it would be expected that the results are reasonably representative of the conditions at Shands No. 2 Pit under similar flux changes.

2.   The time-dependent flux boundary conditions were described by equations representing

(i)   an exponential reduction in flux with time;

(ii)   a linear reduction in flux over one day;

(iii) a linear reduction in flux over one hour.

The above reduction patterns were not based on any measurements taken on site but were chosen to develop a physical understanding of the system. However, if measurements of a changing flux with time were available from field measurements they could be readily used as boundary data in the computer program to simulate the behaviour of the recharge pit. The form of the flux reduction relationship in the field would probably be very complicated with changes in the flux being caused by several factors. Principal amongst these would be changes in the algae activity level, variations in the turbidity of the recharge water and hence non-uniform build up with time of the sediment layer on the base of the pit. Variations in the height of the water table mound, and fluctuations in the pit water level due to changes in flow rate in the supply channel, would also affect the intake rate. A periodic change in the flux-time relationship is caused by the diurnal variation in the level of algae activity. This work is detailed in Part B of this report. It is clear therefore that although the surface flux reduces with time, the relationship defining this reduction is complex, and can depend on several factors. However it can be concluded from the results in this chapter, that for reasonably slow flux changes such as those which occur in the field, steady state pressure head profiles derived using the current surface flux, will approximate satisfactorily the pressure head profiles determined from unsteady state analysis.

3.   The one dimensional analysis is theoretically only applicable to conditions on the centreline of the trench. However, the studies given in Chapter 5 for steady state flow indicate a predominantly vertical flow pattern to the water table. Under these circumstances the one dimensional analysis forms a reasonable approximation to the field regime.

4. ANALYSIS OF TWO DIMENSIONAL UNSTEADY FLOW

4.1 INTRODUCTION

The relatively long length of Shands No. 2 Pit compared with its width allows two dimensional flow equations to be used to simulate the flow of recharge water from the pit to the water table. The flow would not be two dimensional near the ends of the pit but these areas are of relatively minor importance in the overall transmission of water from the pit to the water table. The pit was considered to be symmetrical about its centreline for measurement and simulation purposes. This resulted in only one side of the pit being instrumented; in addition, the two dimensional computer models used in this chapter and Chapter 5 were also only used to model flow from the centre of the pit outwards in one direction.

Considerable difficulties were encountered in the numerical analysis of the two dimensional unsteady flow cases examined in this investigation. This occurred because the analysis of interacting saturated - unsaturated flow regimes as one system is still in its formative stages. Although the numerical techniques available provided good solutions under some flow conditions, the results under others were unstable. These problems are discussed in detail in the following sections.

As a consequence of the problems encountered in the numerical analysis of the two dimensional unsteady recharge flow, only two cases are reported in this study. These relate to flow from a recharge pit to a gravel substratum under initial conditions of uniform water content and flow from a pit through a profile with an impermeable base for similar initial conditions. The development of a water table mound was simulated in the latter case.

It was originally intended to simulate surface clogging using the two dimensional unsteady state model but this proved to be impracticable because of stability problems with the numerical solution. However, successful two dimensional studies of this problem were carried out using a steady state model. Another limitation of the two dimensional model was the difficulty of analysing heterogeneous profiles. The program could be extended to include such profiles but this would further complicate the solution process and could introduce additional stability problems at the soil interfaces.

The solutions presented in this chapter provide detailed information on the development of a water table mound under a recharge pit. The steady state solutions in the following chapter give a more complete picture of the fully-developed flow nets under a recharge pit for various combinations of profile patterns.

4.2   THE COMPUTER PROGRAM

The listing of the computer program used in this investigation is reproduced in Appendix B.   It is similar in structure to the one dimensional program discussed in the preceding chapter; it might be noted that the subroutines have the same names and perform similar functions.   The program was originally written by S.J. Perrens in Programming Language One (PL/1) for the IBM 360/50 computer.   It was later translated into FORTRAN IV and the listing reproduced in the Appendix is the most up-to-date version in this language.   In the following sub-sections the program is described in detail.

4.2.1   Program Structure

The two dimensional unsteady state program consists of a MAIN program with 12 sub-programs, several of these having multiple entry points.   In Appendix B the listings for all these routines are reproduced together with modified versions of some of the subroutines which are used to simulate different profiles.   The function carried out by each of these routines is described in turn.

MAIN Program

The MAIN program is the nucleus of the two dimensional unsteady state program.   It is similar in form to the MAIN used in the one dimensional program but is more complex.   The MAIN program is denoted by TWDIM on the right hand side of the listing.   The major functions performed by MAIN are -

- initialisation of variables,
- reading of initial and control variables
     from card input,
- control of time step interval,
- calculation of coefficients for solution of
     Equations (2.20) and (2.21) in Chapter 2,
- testing of head differences at each iteration
     and each time step,
- calling of sub-programs,
- output of initial variables and output of
     terminating information.

One of the most complex parts of the program is involved in deriving the time interval for the next time step.   This aspect of the program is particularly important because the efficiency and accuracy of the program is intimately connected with the size of the time step.   Theoretically the ADI

solution technique is stable for any time interval, but in practice the nonlinearities in the derivation of the coefficients make the solution highly unstable if too large a time step is taken when pressures at any point in the profile are changing rapidly. However, if the time step is too small, computer time is wasted, and several computer runs may be required to obtain a solution whereas one run may have been sufficient with an efficient time-stepping mechanism.

The segment of the program in which the coefficients are calculated has been written so that the maximum computational efficiency is obtained. It might also be noted that after the first two iterations, the soil characteristics (K and C) are not recalculated at each iteration. From experience it has been found that after the first two iterations the head values do not change significantly. There is therefore little point in re-calculating the soil characteristics for succeeding iterations.

Subroutine INCTYM

This subroutine has been written to perform a similar function to STIMER which is the built-in function available in PL/1. The FORTRAN version of the two dimensional unsteady state program is in a form compatible with the CYBER 72-26 computer, and the INCTYM routine is based on the library function SECOND available in the KRONOS operating system library. This function returns a value which is the elapsed central processor time in seconds since the job commenced. This value is tested against a constant read in the MAIN program, and if it is greater, an integer is reset from 0 to 1. Later in the program the value of 1 is detected and the program automatically terminates after outputting on cards the current head distribution and the values of all the control variables. The main contribution of this subroutine to the two dimensional program is that it enables a long computation to be split into several smaller units, each unit producing terminating output which can be used to start the next unit. This is particularly necessary when an infiltration sequence is being simulated. INCTYM is one of a set of 'commonly-used subroutines' denoted by COMSUB on the right hand side of the listing in Appendix B.

Subroutine SOLVE

This subroutine carries out the tri-diagonal solution of the N+2 equations for each column and for each row in the grid. It performs the same function as SOLVE for the one dimensional case, but is complicated by the fact that the same routine is used for both the horizontal and vertical passes. This

necessitates using indices to define the start and end point nodes so that the correct coefficient values can be looked up in the storage arrays. A version of the subroutine was produced in Assembler for the IBM 360/50 but it was only marginally faster than the FORTRAN version. No attempt has therefore been made to write an Assembler-type program for the CYBER 72-26. This subroutine is also denoted by COMSUB on the right hand side of the listing in Appendix B.

Function FLIMIT

This function is used in a similar way to LIMIT for the one dimensional program. The only essential difference is that it searches over a two dimensional grid to find the maximum difference between any two arrays, instead of just searching along a vector. FLIMIT is denoted by AFLIM on the right hand side of the listing given in Appendix B.

Subroutine STSOIL, with entry points LCURVE and LKSOIL

This subroutine is very similar in form to SETSOIL used in the one dimensional case. In fact the FORTRAN versions of both the one dimensional and two dimensional soil characteristic look-up subroutines are exactly the same. It should be noted that two versions of this subroutine are reproduced in Appendix B. The first, denoted by ASSHY17 on the right hand side of the listing, contains hysteresis information on #17 sand. Seven primary draining and seven primary wetting curves are tabulated for both moisture content and capacity. A separate subroutine CONDCT is called to calculate the conductivity values from the moisture contents. The subroutine ASSHY17 is quite complex since it has the capacity to interpolate between the primary curves and determine higher order scanning curves as cycles of wetting and draining are carried out using the program. The subroutine was written by S.J. Perrens in PL/1 and has since been translated into FORTRAN IV. It might be noted that it is almost as long as the MAIN program. The second version of the STSOIL subroutine denoted by ASTS17 in Appendix B, provides main rewet soil data when all the profile can be considered to be wetting up from an initially drained equilibrium state. The subroutine is identical to the one reproduced in Appendix A (one dimensional program) except that it is written in FORTRAN instead of PL/1.

Subroutine ZOT, with entry point ZOTA

The subroutine sets the number of iterations to be carried out before the time step is reduced and a repeat cycle initiated. If satisfactory convergence is achieved within the pre-determined number of iterations a

repeat cycle is not carried out. The subroutine also calculates the iteration-dependent part of the acceleration term. This is the B^i term in the expression for $\omega_{(i)}$ given in Section 2.1.2. Many different versions of this subroutine were used in the course of this investigation. They are discussed in Section 4.2.3. Subroutine ZOT is denoted by AZOT on the right hand side of the listing given in Appendix B.

BLOCK DATA Sub-Program

This sub-program is used to initialise several character arrays and set the maximum array dimension used in the two dimensional program. It is one of the subroutines denoted by COMSUB on the right hand side of the listing.

Subroutine TOP, with entry points TOPA and TOPB

This subroutine is accessed before and after a column of the two dimensional grid is solved. It is of the same form as the TOP subroutine used for the one dimensional case. It can be used to apply a top flux condition (either rainfall or evaporation) or a ponding condition at the surface of the profile. Two versions of the subroutine are reproduced in Appendix B. TOP10CM is used when the node spacing is 10 cm and TOP5CM is used when it is 5 cm. It might be noted in TOP10CM that the nodes numbered from 2 to 13 can be set to either ponding or flux conditions and the nodes from 14 to the right hand limit of the profile are set to a flux boundary condition. The reasons for this will become clear in later sections where the simulated profile is discussed. In subroutine TOP5CM the respective zones are from 2 to 25 and from 26 to the right hand boundary.

Subroutine BASE, with entry points BASEA and BASEB

Three versions of this subroutine are given in the listing in Appendix B. The structure of the subroutine is similar to that of the subroutine of the same name used in the one dimensional study. It is called before and after the columns are solved in the two dimensional grid. On the first call BASEA sets up corrections for the coefficients at the base-1 node depending on what the base boundary condition is at that point. After SOLVE has been accessed for each column in the grid BASEB is called to calculate the head at the base node depending on the new head derived at the base-1 node.

The version of BASE which is used to simulate an impermeable base (such as basement rock) is denoted by BASIM on the right hand side of the listing. BASWTIM is a more complicated version of BASE which was used to simulate a gravel substratum base across part of the profile, and an impermeable base across

the rest. This device was necessary to overcome instability problems which developed when the wetting front moving down from the pit reached the zone near the top of the capillary fringe. By using BASWTIM it was possible to set up an impermeable base initially and then change this to an h = 0 condition when the wetting front arrived at the boundary. This is an approximation to an h = 0 base boundary condition which includes a fully developed capillary fringe but the errors introduced by the approximation have been gauged to be minimal.

Another version of BASE - BASS - is also given in the listing in Appendix B. This version is used to simulate a shifting base boundary condition in which the base boundary is lowered by two nodes whenever the wetting zone reaches the current base limit. The advantage of this version is that only the top part of the profile needs to be simulated in the early stages of infiltration, and this saves a considerable amount of computer time compared with simulating the whole profile.

Subroutine LEFT, with entry points LEFTA and LEFTB

Subroutine LEFT (designated by LEFTM on the right hand side of the listing in Appendix B) sets up a mirror or no-flow boundary on the left hand side of the profile. This type of boundary condition was discussed in Section 2.1.2 and is used when a half profile is being simulated. Normally for convenience the right hand side of the total profile is simulated and this makes the left hand boundary the line of symmetry of the recharge pit. No flow can occur across such a boundary. LEFTA adjusts the coefficients at the left + 1 node to allow for the fact that the head at the boundary must equal the head at the boundary + 1 node for no flow. In LEFTB the boundary node pressure heads are set equal to the newly-calculated heads at the left boundary node + 1.

Subroutine RIGHT with entry points RIGHTA and RIGHTB

The version of this subroutine listed in Appendix B is used to simulate shifting right boundary condition and is designated by RIGHTS on the right hand side of the listing. It functions in a similar way to BASS discussed above in that the boundary is shifted to the right whenever a change in pressure is detected approaching the boundary. In RIGHTA the coefficients for the nodes adjacent to the right boundary are adjusted before solving for all rows in the two dimensional grid. After a solution has been obtaine RIGHTB is accessed to set the head values at the boundary. A check is also performed at this entry to determine whether the wetting front has reached

the boundary. If it has, the boundary is shifted further to the right. This subroutine can only be used when one is simulating infiltration into a fully drained profile. For other initial conditions different versions of this subroutine would have to be used such as one that simulates a no-flow boundary.

Subroutine ITOUT

This subroutine is used to print out pressure profiles at each iteration. It carries out similar functions to the subroutine of the same name used in the one dimensional program. The subroutine is only used as a diagnostic tool where inconsistencies develop in the solution process. If the pressure head values were printed out at every iteration in normal circumstances a large volume of computer output would be generated. For this reason an integer read from a data card is used to indicate to the program whether iteration printouts are required or not. This subroutine is one of several denoted by COMSUB in the listing in Appendix B.

Subroutine OUTPUT

This subroutine is also similar to the subroutine of the same name used in the one dimensional program. Since it is necessary to output the head and moisture content profiles at various points in the MAIN program, it is more efficient to write one output routine and access it every time a printout is required, rather than have the same programming statements repeated several times. An integer read from a data card sets the elapsed number of time steps between printouts of the head and moisture content profiles. If these were printed at every time step an excessive amount of output would be generated. Printouts are also produced at preselected times from the beginning of the simulation process. These times are read in from data cards. Subroutine OUTPUT is one of the subroutines denoted by COMSUB on the right hand side of the listing in Appendix B.

4.2.2 Program Development

The original program for the simulation of two dimensional unsteady state problems was written by Mr. S.J. Perrens of the School of Civil Engineering. The partial differential equations were approximated using a similar technique to that used by Rubin (1968). Initially the program was written in Programming Language One (PL/1) for the IBM 360/50 computer. At a later stage Mr. D.G. Doran translated the program to FORTRAN so that it could be run on the CYBER 72-26 computer. During the course of the investigation reported in this chapter many modifications were made to the program to improve stability and

increase the speed of convergence.

Modifications were also made to the acceleration parameter subroutine ZOT in an attempt to reduce oscillations in the solution. This problem is discussed in further detail in Section 4.2.3. The program at its current stage of development is suitable for simulating infiltration and redistribution sequences into an infinite profile. However difficulties may be encountered in simulating a water table or impermeable base boundary condition. These cases can be simulated, but as is discussed in a later section, problems may be encountered as the profile approaches a steady state condition.

4.2.3 The Acceleration Parameter

Approximately twenty different versions of the acceleration parameter subroutine ZOT were tested in the course of this investigation. Initially the acceleration parameter suggested by Douglas et al (1959) was used (see Section 2.1.2) but it was found that the solution became unstable resulting in unsatisfactory pressure profile development. It appears that this acceleration parameter is not suitable for simulating wetting up from a ponded surface condition into an initially drained profile. Other computer simulations have been carried out using the two dimensional program with a flux condition at the top boundary and an initially drained profile. Under these conditions the acceleration parameter suggested by Douglas et al (1959) was found to be satisfactory.

Perrens and Watson (1976) used another version of the acceleration parameter which was a function of the square of the surrounding conductivity values and also a function of the capacity. They found this to be satisfactory under conditions of surface flux into an infinite profile, but it was found to be unsuitable for the cases reported in this chapter.

Since both the available acceleration parameters were found to be unsatisfactory under surface ponding conditions, an investigation was initiated to find a better technique. It was found that statistical texts gave optimum acceleration parameters for the solution of partial differential equations with constant coefficients, but not for the case where the coefficients are functions of the pressure head. It was therefore necessary to use trial and error techniques to arrive at a satisfactory form of the acceleration parameter Two factors had to be considered in choosing a suitable acceleration parameter. Firstly the solution should be stable (i.e. pressure heads should vary systematically from one time step to another and not oscillate erratically) and secondly the solution should converge in as few iterations as possible.

With these two objectives in mind a systematic series of tests was carried out to find an optimum acceleration parameter. It was found that the use of the capacity terms in the expression for the acceleration parameter could cause instability problems in the zone where the profile was wetting up from a drained state. An expression was eventually derived in which the acceleration parameter increases with the iteration number (note that in the approach of Douglas et al (1959) the acceleration parameter value decreases with increasing iteration number). The expression is

$$\omega_{(i)} = K_s \cdot 5^{(i-1)}$$

where
K_s = sum of surrounding K values,
i = iteration number; varies cyclically $0,1,2\ldots\ldots5$.

It was found that this expression produced generally stable solutions for the cases examined in this report, except at large times when the profile approached steady state conditions. However for surface flux conditions this expression is not suitable and the relations used by Douglas et al (1959), or Perrens and Watson (1976) should be used.

It was apparent that developmental work needs to be done to derive a suitable acceleration parameter that can be used with confidence over a range of different flow conditions. The present situation, of having to derive a new acceleration parameter for each profile type using trial and error procedures, is obviously unsatisfactory. However the derivation of a suitable acceleration parameter may not be simple because of the non-linearity of the flow equations.

4.3 FLOW FROM A RECHARGE PIT TO A GRAVEL SUBSTRATUM

The two dimensional unsteady state program was used to model the flow regime under Shands No. 2 Pit in the Burdekin Delta. Two cases were considered. Firstly, infiltration from a ponded surface into a uniformly drained profile with a gravel substratum (h=0) at 1.2 metres, and secondly similar top boundary and initial conditions but with an impermeable base at 1.2 metres from the surface. The first case will be considered here and the second in the next section.

Referring to Figure 4.1 it can be seen that the left hand boundary of the profile is a centreline. This is because the centre of the recharge pit was assumed to be a line of symmetry and only half the cross-section of
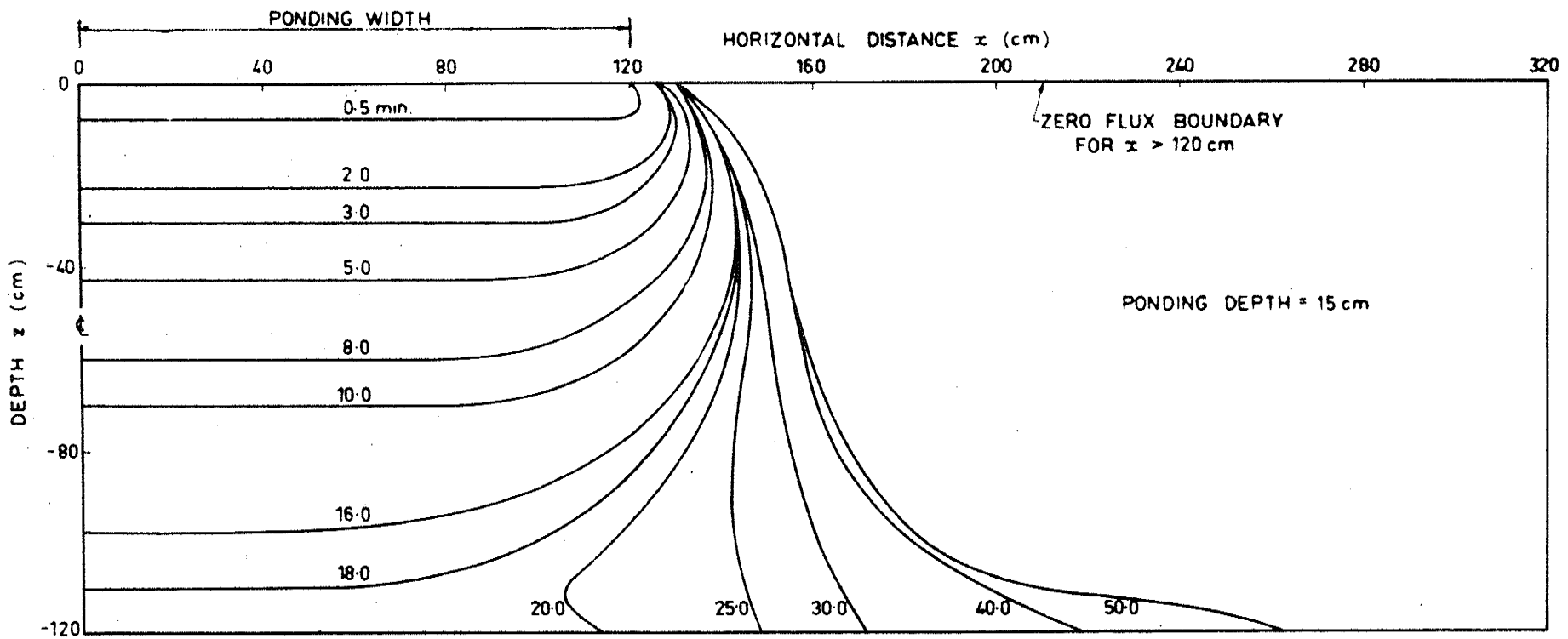
Figure 4.1: Position of saturated front with time during infiltration into #17 sand. Gravel substratum base.

the pit was simulated. The top of the profile was set at the same level as the bottom of the recharge pit. This meant that water in the pit constituted a ponding top boundary condition and the clay bank material was approximated by a zero flux top boundary on the right hand side of the profile. The width of ponding was set at 1.2 metres which is half of the total recharge pit width of 2.4 metres at the bottom of the pit. The assumed ponding depth was 15 cm which corresponds closely with the average depth of water in the pit in the initial stages of infiltration.

The porous material used in this analysis was a uniform silica sand, known as #17 sand. The hydrologic characteristics of this sand have been summarized by Watson and Curtis (1974). At time zero the profile was assumed to be at a uniformly drained pressure head of -120 cm. Since this is 'outside' the hysteresis loop of #17 sand, the wetting up process could be assumed to follow the main rewet curve except in the capillary fringe above the base boundary. Moving base boundary and right boundary subroutines were used so that the region of calculation was kept to a minimum. As the wetting front neared either of these boundaries, the boundary was moved a further two nodes ahead of the approaching front. When the wetting front neared the base the hysteresis STSOIL subroutine was used as the points wetting up near the water table could no longer be assumed to follow the main rewet curve.

Because of instability and convergence problems with the two dimensional unsteady state program it was not possible to simulate a gravel substratum base directly. It was found that if the base was set up in the normal way, with zero pressure head at the base node and a zone of saturation corresponding to the capillary fringe above it, then when the wetting front moving down from the surface intersected with this zone, the calculated pressure head distribution became unstable. This was probably due to the sharp gradients across the zone between the two saturated regions. If it had been possible to have grid refining (i.e. a closer spacing of node points) across this region, the program may have been able to produce a satisfactory result. Since grid refining is beyond the capacity of the present program another device was used to overcome the problem.

The bottom boundary of the profile was initially assumed to be an impermeable base with no zone of saturation above it. When the wetting front approached the base the pressure heads along the base increased from negative values initially, and when they reached zero the pressure head was fixed at

zero, effectively simulating a gravel substratum boundary condition. Since the wetting front reached the base near the left hand boundary first (this corresponds to the centreline of the pit) the base boundary is gradually transformed from an impermeable boundary to zero pressure head boundary. The subroutine used for this purpose is denoted by BASWTIM in the listing in Appendix B.

The use of this combined base boundary condition instead of a direct h = 0 condition would introduce minor errors in the simulation of the profile near the base, but the general development of the saturated zone shown in Figure 4.1 would not be significantly affected.

Figures 4.1 to 4.4 describe the development of the saturated region under a recharge pit during infiltration. Figure 4.1 shows the position of the wetting front at various times from the time the water first enters the pit. Figures 4.2 to 4.4 give the pressure head distributions at 5, 14.5, and 50 minutes from the start. The profile outside the -120 cm line remains virtually unchanged from the initial state except for a minor redistribution of water due to the vertical potential gradient (the pressure gradient in the vertical direction is zero but there is a gravity component which causes soil water to move downward).

It can be seen from Figures 4.2 and 4.3 that the wetting front has a very sharp gradient. As the profile approaches steady state in Figure 4.4, the steepness of the gradient becomes less severe. It is believed that one of the main causes of the stability problems encountered in the simulation of two dimensional unsteady state profiles is the coarseness of the grid spacing. Although the node spacing was initially 2.5 cm in the vertical and 5 cm in the horizontal direction, these had to be changed to 5 cm and 10 cm respectively as the wetting front moved downward and outward. This resulted in very few nodes being located across the steep wetting front and gave poor definition of the pressure gradients. Any increase in the number of node points used would have exceeded the computer storage capacity or reduced the computational speed to an unacceptable level.

Comparing the position of the wetting front in Figure 4.1 at 50 minutes with the pressure distribution at the same time shown in Figure 4.4, it can be seen that although the pressures have been affected by the infiltration process for some distance out from the edge of the ponding zone, the wetting front has stabilized at approximately 40 cm from this point. This indicates that the movement of the recharge water from the pit to the water table is predominantly vertical. In Chapter 5 steady state solutions

Since
(this
ally
ary.
sting
irect
a
zone
gion
tion
ions
ot
adient
a
has
gure 4.4,
at one
lation
grid
ical
n
rd.
g front
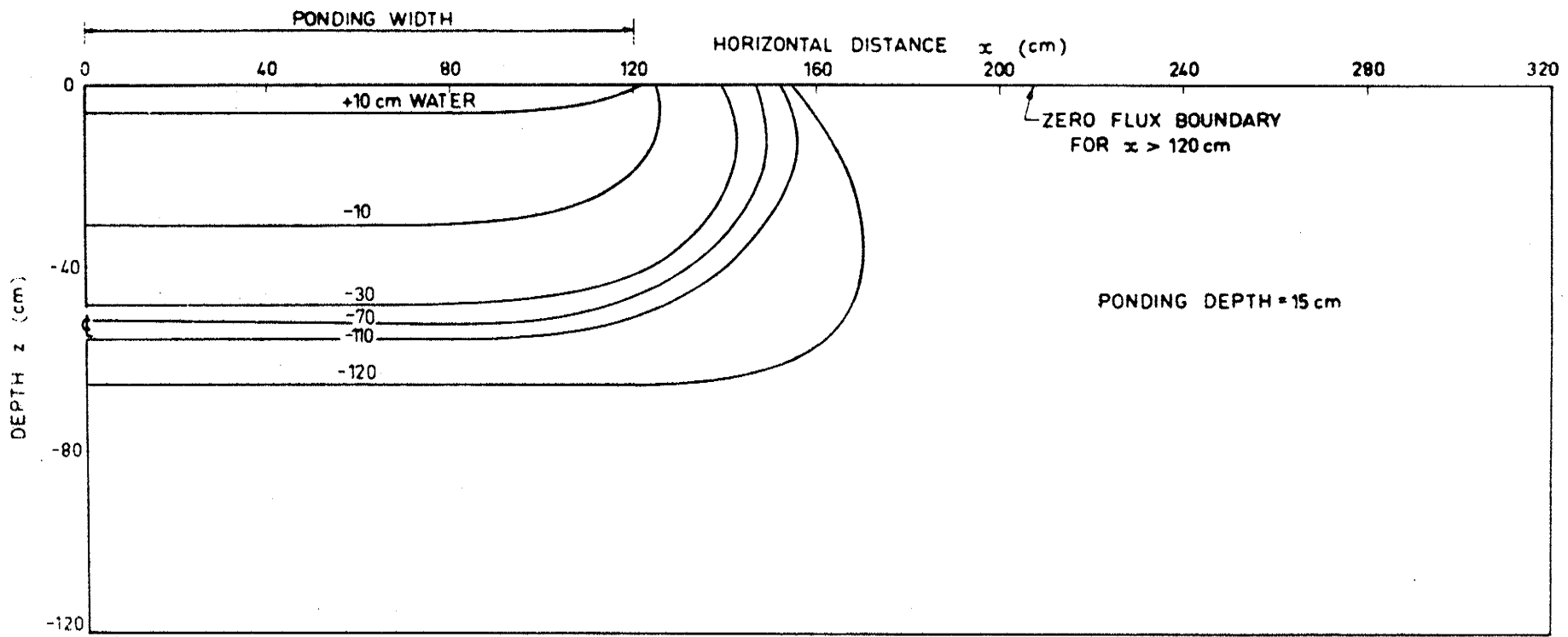the
capacity
minutes
it can
ration
This
water
s

Figure 4.2: Pressure head distribution after 5.0 minutes of infiltration into a uniformly drained profile of #17 sand.
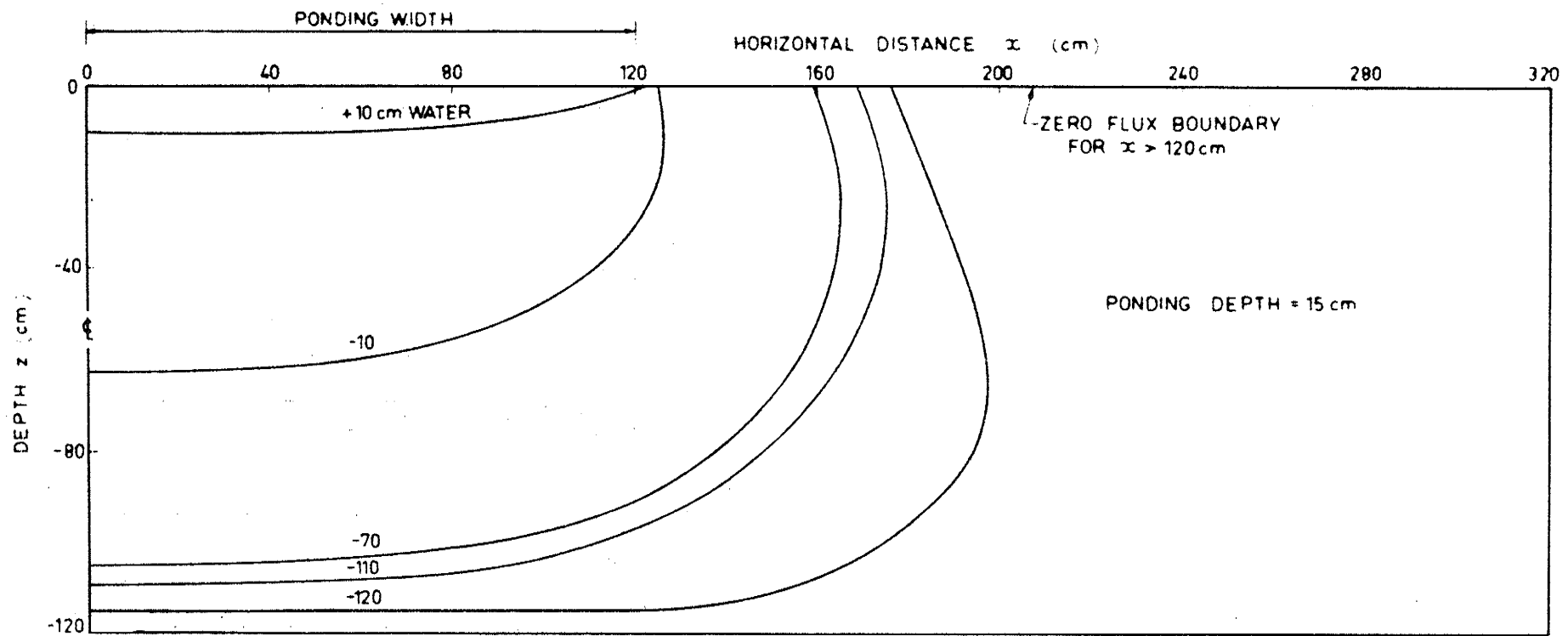
Figure 4.3: Pressure head distribution after 14.5 minutes of infiltration into a uniformly drained profile of #17 sand.
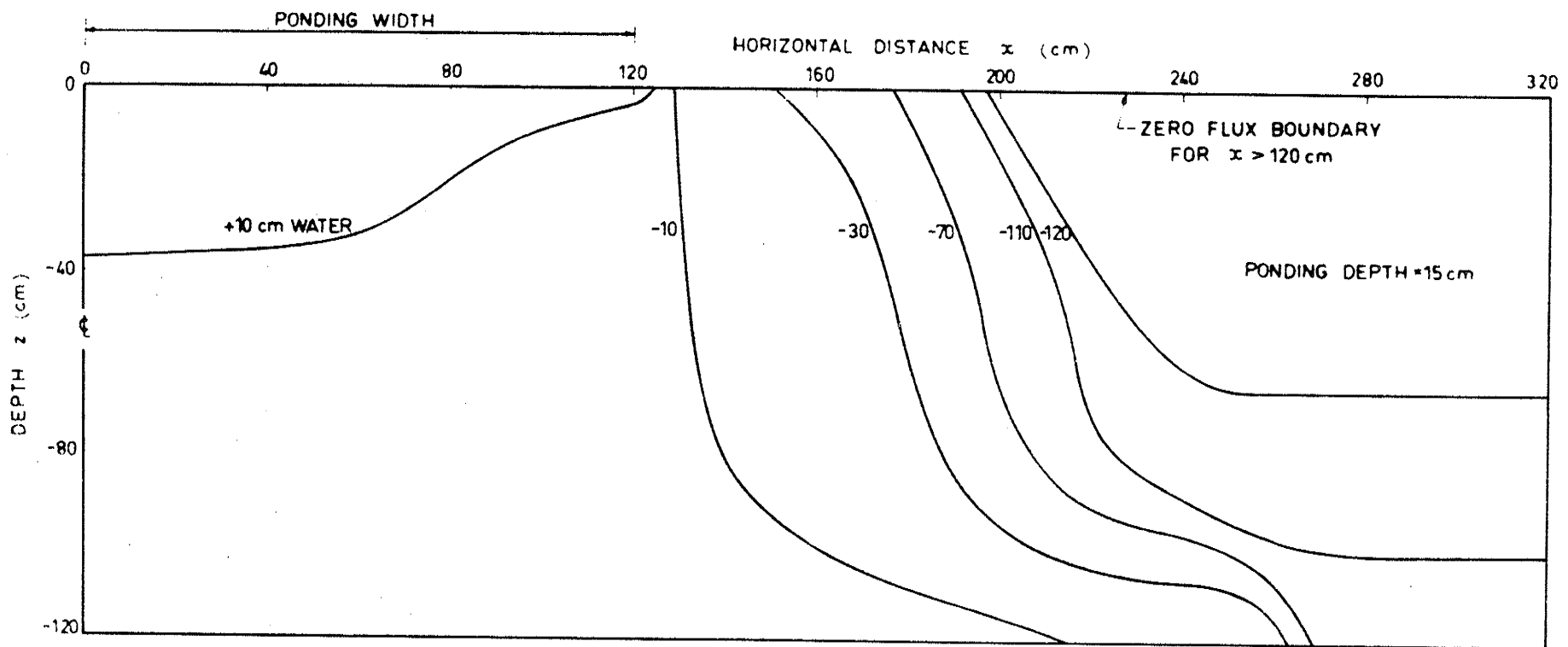
Figure 4.4: Pressure head distribution after 50.0 minutes of infiltration into a uniformly drained profile of #17 sand. Gravel substratum base.

confirm this observation. The development of the wetting front shown in Figure 4.1 is not given beyond 50 minutes because at this time the profile has virtually reached steady state conditions. It was also at 50 minutes that the unsteady state program started producing erratic results. A steady state solution for the same profile used to produce the results in Figures 4.1 to 4.4 is given in Chapter 5, and the saturation line almost coincides with the wetting front at 50 minutes.

4.4 FLOW FROM A RECHARGE PIT TO AN IMPERMEABLE BASE

In Section 4.3 above the development of pressure and moisture content profiles with time, for a two dimensional profile, was described. A gravel substratum base boundary condition was simulated although an impermeable base was used in the initial stages to overcome certain computational difficulties. In this section the same profile is examined with the same initial and boundary conditions, except that an impermeable base is used throughout the infiltration sequence.

Figure 4.5 shows the position of the saturated front with time from the commencement of infiltration. It should be noted that the pressure profile development for this case is identical to the one described in the preceding section for the first 18 minutes of infiltration. This is because the influence of the base boundary condition is insignificant until the wetting front approaches the base. The pressure profiles shown in Figures 4.2 and 4.3 for the former case are therefore identical to the pressure profiles for an impermeable base at 5.0 and 14.5 minutes respectively. Hence, for an impermeable base, the pressure profile development can be described by Figures 4.2 and 4.3, and Figure 4.6 gives the pressure profile at 60.0 minutes.

There are several differences between the profiles at corresponding times for the two different base boundary conditions. Comparing the wetting front development shown in Figures 4.1 and 4.5 it can be seen that with an impermeable base, the front progresses further in the horizontal direction for the same period of infiltration. The pressures along a large portion of the base are positive showing that a water table mound has developed. At times greater than 60 minutes the mound would move further to the right away from the pit. The steady state profile that would eventually develop if the boundary conditions did not change, would resemble a steady state case described in Chapter 5. In that example the right hand boundary positioned at some finite distance from the pit has a zone of saturation near the base through which flow occurs away from the pit.

in
ofile
utes

s

he base
itioned
e case
p if
ght away
ped. At
direction
rtion
ith
wetting
ding

be
profile
y.
re
igures
the
because
in the
re
from

sed
same

ble
gravel
ntent
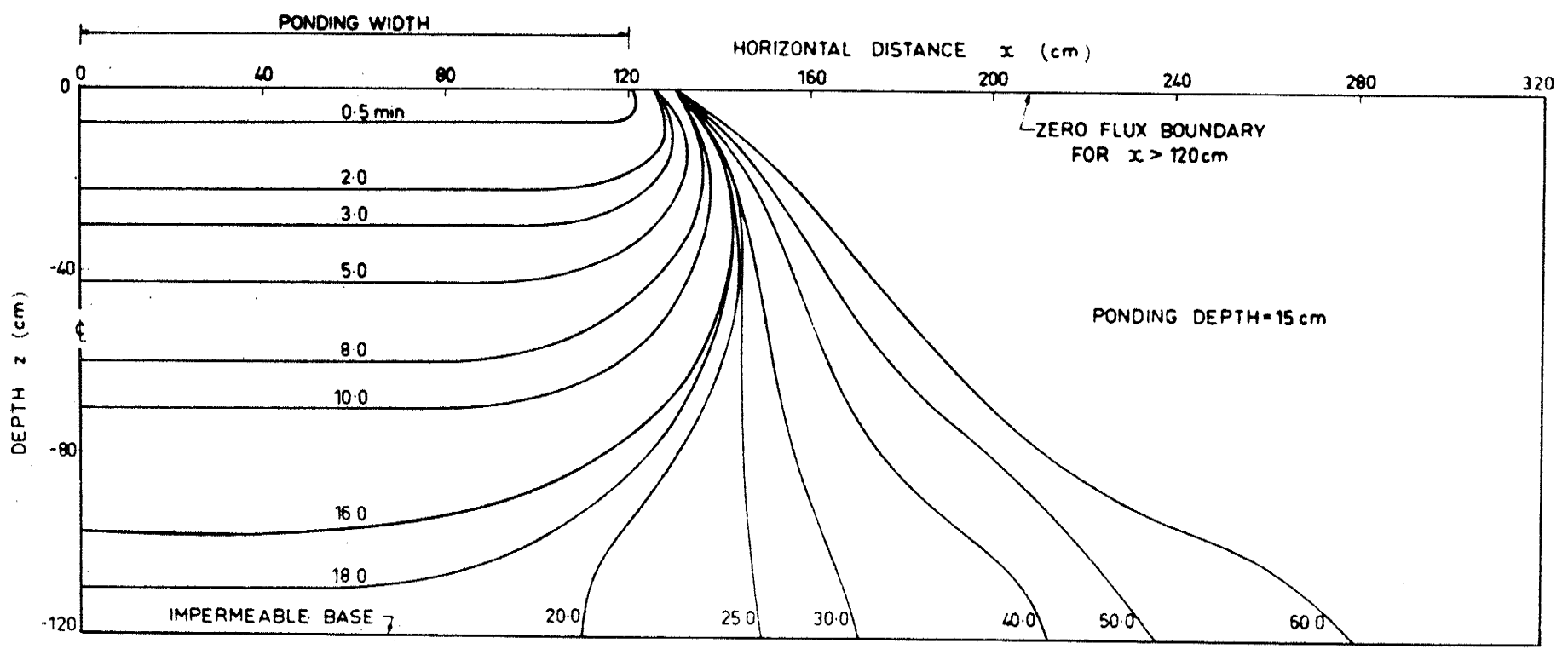
Figure 4.5: Position of saturated front with time during infiltration into #17 sand. Impermeable base.

PONDING WIDTH

HORIZONTAL DISTANCE x (cm)

ZERO FLUX BOUNDARY
FOR x > 120 cm

+10 cm WATER   -10   -30   -70   -110 -120   PONDING DEPTH = 15 cm

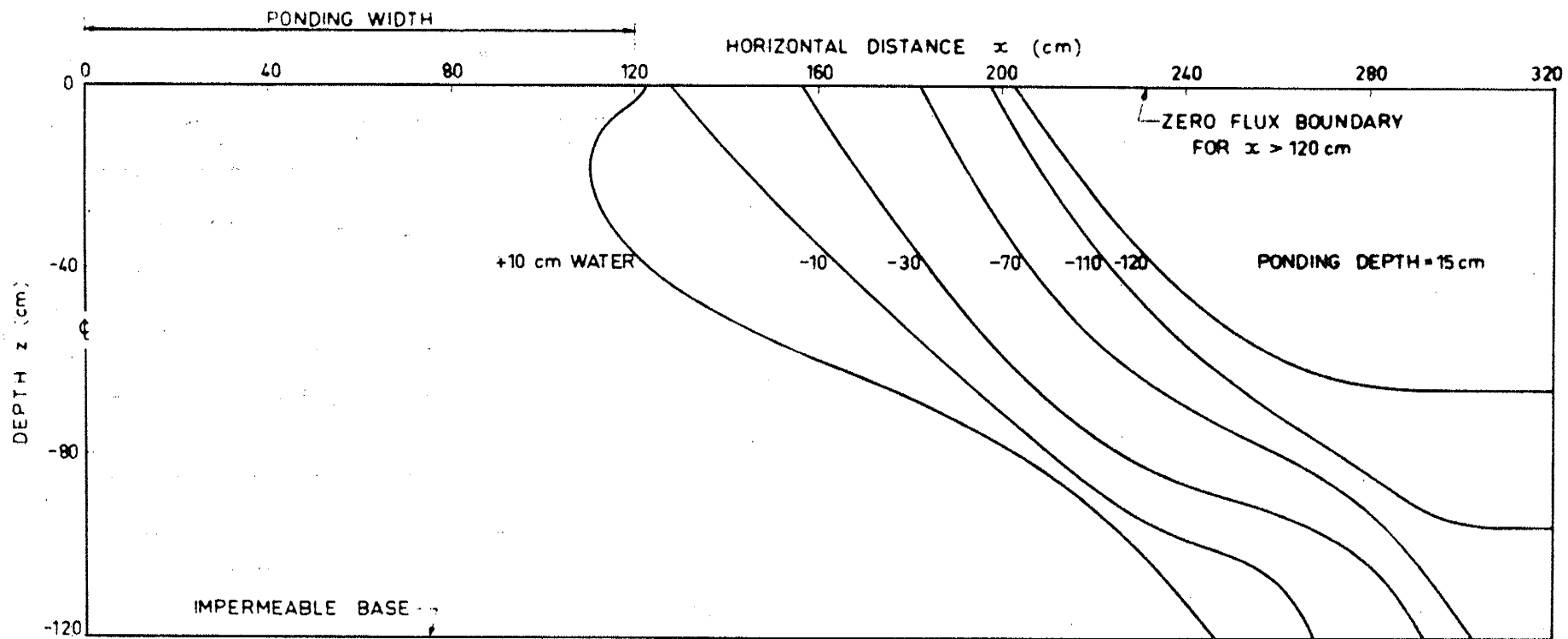DEPTH z (cm)

IMPERMEABLE BASE

56.

Figure 4.6:   Pressure head distribution after 60.0 minutes of infiltration into a uniformly drained profile
of #17 sand.   Impermeable base.

The pressure profiles at large times for the two base boundary types also differ in several aspects. Comparing Figures 4.4 and 4.6, which give the pressure profiles at 50 and 60 minutes respectively for the two cases, it can be seen that the pressures are generally higher for the impermeable base case, and the profile has developed further to the right away from the recharge pit. Although the pressure profile for the h = 0 base has almost reached steady state at 50 minutes, the profile for the impermeable base is still developing at 60 minutes. If the unsteady state program had been performing satisfactorily the profile could have been plotted for a longer period of infiltration.

The profile development under the pit where a 'true' water table exists is probably more similar to that experienced with an impermeable base than the h = 0 base. A water table mound develops under the pit and the horizontal potential gradient causes the recharge water to flow down-ward and outward from the pit, with the flow approaching horizontal at large distances from the pit. Also some flow would occur within the initial water table zone. Accordingly, the actual development of a water table mound beneath a recharge pit would not be as pronounced as that obtained with an impermeable base at the level corresponding to the initial water table.

4.5 CONCLUSIONS

A two dimensional unsteady state computer program was developed for simulating the movement of water in the saturated and unsaturated zones under a recharge pit. Satisfactory solutions were obtained for times up to approximately 50 minutes from the start of infiltration. For times greater than 50 minutes instabilities occurred but that was not a limitation in this investigation, as steady state solutions were available to provide the limiting solutions at very large times.

Two different base boundary conditions were simulated to provide solutions for two extreme cases. The actual water table base boundary under field conditions lies somewhere between the h = 0 base boundary and an impermeable boundary, and is more likely to resemble the latter for homogeneous profiles.

It was shown that in a uniform sand profile the flow of recharge water from the pit to the base of the profile was predominantly vertical except in the region near the base. The horizontal component of flow was more

significant for the case with an impermeable base boundary condition. The moisture characteristics of #17 sand, which was used in this simulation, are similar to that of the natural sand under Shands No. 2 Pit (see Chapter 5). It can therefore be expected that the pressure head profiles and saturation profiles simulated in this chapter closely resemble the actual behaviour of Shands No. 2 Pit.

The wetting front which proceeds downward and outward from a recharge pit during the initial stages of infiltration has a steep pressure gradient in the region near the front. This makes the simulation of the progress of the front difficult when a fixed node spacing is used in both directions. It seems likely that an improvement in accuracy and speed of solution could be achieved if a finer grid spacing could be used in the region near the wetting front.

5. STEADY STATE STUDIES OF FLOW FROM A RECHARGE PIT

5.1 INTRODUCTION

Steady state studies of the hydraulic behaviour of artificial recharge pits were carried out to complement the unsteady state studies discussed in Chapter 4, and to investigate a wider range of problems than could be examined using the current two dimensional unsteady state program. Because of the relatively high conductivity of the sands under the recharge pits investigated in this study, the flow pattern rapidly approaches equilibrium and can be readily approximated by a steady state solution. As discussed in Section 2.2, the computer program used in this study was adapted from a program published by Nelson (1962) and Reisenauer et al (1963). The prime advantages of using a steady state program such as this, instead of an unsteady state program, are that the solution is more easily obtained and less computer time is required; in addition, heterogeneous profiles can be easily accommodated.

A wide variety of cases was examined in this investigation. One model was set up to simulate Shands No. 2 Pit with both the original profile and after the beach sand was introduced. Several cases similar to Iyah Creek No. 1 Pit were examined to determine the effects of having different widths of beach sand in the excavated slot in the middle of the pit. The effects of surface clogging due to biological activity and sediment deposition were simulated also for both the Shands and Iyah Creek Pits. In addition, the development of a water table mound was simulated for Shands No. 2 Pit. The results for each of these cases are presented in the form of flow nets and corresponding water content profiles. From the flow nets it was possible to calculate flux rates for each configuration. Conclusions could then be drawn on the effects changes in the pit design would have on recharge rates.

In the following sections the computer program is described briefly and the results are presented for each case investigated.

5.2 THE COMPUTER PROGRAM

The computer program used in the steady state investigation of saturated and unsaturated flow was adapted from a program presented by Reisenauer et al (1963). Further background to the underlying assumptions made in writing the program were obtained from Nelson (1962). The program was not in a form suitable for the CYBER 72-26 computer used at the University of New South Wales and several changes had to be made. These are detailed in the following sections. A listing of the current program used to produce the
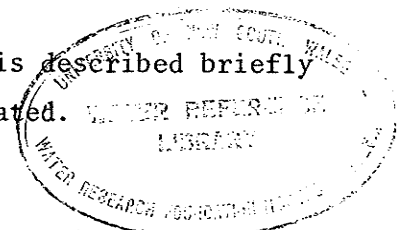
results in this chapter is presented in Appendix C. The basic theory of steady state flow in unsaturated soils was discussed in Section 2.2. Only the working details of the computer program will be presented here.

5.2.1 Program Structure

The program is made up of a MAIN program and 14 subroutines. It has the capacity to simulate one, two, or three dimensional steady state saturated or unsaturated flow systems. Flow systems containing both saturated and unsaturated regions can also be accommodated.

Two computer runs are needed to evaluate both the hydraulic head solution and the corresponding water content profile. In the first run the hydraulic head is calculated using the conductivity at each node, and the boundary conditions, to obtain a solution. Conductivity versus pressure head data are obtained from subroutine KAY. Once a solution has been obtained the hydraulic head solution matrix can be used in a second computer run to evaluate the water content profile, and for this run subroutine KAY contains data relating water content to pressure head. An integer (NDUM3) is set to zero for the first run and to any integer value for the second run. NDUM3 switches the program into the appropriate calculation loop for each case.

The program in its present form can accommodate up to 6000 nodes and occupies 120K words on the CYBER 72-26 computer. The functions carried out by each part of the program are discussed in turn below.

MAIN Program

This program reads in all the initial information and calculates the basic indices and parameters used in the calculation phase. It also carries out various tests to determine whether there are any contradictions in the input data which would prevent a solution being obtained. The complexity of the MAIN program is largely due to the generality of this computer program. If it was written to simulate just two dimensional unsaturated flow conditions for example, then only a fraction of the programming statements would be needed. The generality of the program also contributes to the slowness of the solution process, but with a moderate-sized grid, the solution is obtained in a relatively short time compared with an unsteady state solution. The input format for the initial data is very flexible and also quite complicated. A clear step by step description of this is given in Reisenauer et al (1963), and this must be followed closely to ensure a successful computer run. At the end of the MAIN program, subroutine CHAIN2 is called and from this point on control is not returned to MAIN until a solution is obtained.

This saves computer storage space but complicates the initialization of the data. Full details on how to set up these relations in a form suitable for the program are given in Reisenauer et al (1963). KAY is called from within the calculation loop in CHAIN2.

Subroutine FHI

This subroutine evaluates the terms in Eq. (2.24) in Section 2.2. It has several branches within it, the appropriate one being dependent on whether the problem is in one, two, or three dimensions. The subroutine is called within the calculation loop in CHAIN2.

Subroutine STEP

This subroutine controls the sequence of stepping from the origin of calculation through all the nodes in the grid. The origin can be set at any point in the grid, the optimum point being at the predominant boundary where large changes in hydraulic head are likely to occur. Subroutine STEP also carries out corrections to impose the appropriate boundary conditions at each node. If the calculation node is in the middle of the grid then no corrections are performed. However if the node lies on a boundary then appropriate corrections are applied. This subroutine is accessed at the beginning of the calculation loop in CHAIN2.

Subroutine OUT

Subroutine OUT contains most of the output statements for the program. The output format for the program is very flexible. One of its best features is that matrix output can be selected. In this format the hydraulic heads are plotted at even spacings in the horizontal and vertical directions corresponding to the two dimensional grid pattern. The water content profile can be outputted in a similar way. Using this format it is possible to cut the computer printout sheets and join them together to form a representation of the flow profile. Equipotentials and flowlines, or lines of equal water content, can then be drawn on the computer paper. For this investigation the plots on computer printout were reduced by photocopying, traced, and then photographically reduced to the size presented in this report. The use of the matrix output option probably halved the time required compared with plotting all the points by hand. Subroutine OUT is accessed from CHAIN2.

Subroutine INPUT

This subroutine is used to print all the initial information read in the MAIN program. It is accessed from subroutine OUT.

Subroutine CHAIN2

This subroutine controls the calculation phase of the program. The parts of the subroutine in which repetitive functions are carried out are contained in separate subroutines. Almost all the output is controlled by subroutine OUT. A large part of CHAIN2 involves IF statements which are used to define the specific case being investigated from the general cases the program is capable of solving. If a solution is not obtained within the predetermined number of iterations specified, subroutine SAVE is accessed and the current hydraulic head matrix is outputted onto cards so that it can be used as initial data for a continuation run. Subroutine CHAIN2 is called at the end of the MAIN program.

Subroutine TEST

This subroutine carries out tests on the choice of calculation type at each node point to see if it is compatible with the initial and boundary conditions. Such a subroutine is necessary because the generality of the program makes it easy to select wrong combinations of parameters for a particular flow case. Test is called from the MAIN program after the control variables have been read in.

Subroutine CUTTER

This subroutine was not used in this investigation but could be useful in more complicated flow configurations. It allows the number of node points to be reduced in the calculation region if the program is progressing too slowly towards a solution, or if there are more node points than are needed to define the problem. This subroutine is called from the MAIN program.

Subroutine RELAX

This subroutine calculates the over-relaxation (or under-relaxation) factor used in the solution algorithm. The function of this factor in the solution process is discussed in Section 2.2. The subroutine is called from within the iteration loop in subroutine CHAIN2.

Subroutine KAY

As discussed above, this subroutine determines the conductivity corresponding to the calculated pressure heads in unsaturated flow problems. For saturated flow the subroutine is not needed as conductivities at given points do not change with pressure head changes. This subroutine is also used to evaluate the water content from the pressure head at a point. The conductivity versus pressure head (or water content versus pressure head) data used in KAY are defined by a series of straight lines, tabulated points, and fitted curves.

Subroutines ADDRS, GMAN, GNO

Subroutines ADDRS, GMAN and GNO were written in an assembler language (FAP), which is not compatible with the CYBER 72-26 computer currently used at the University of New South Wales. As a consequence they had to be rewritten in FORTRAN IV to carry out the same objective, which was reduction in computer storage usage. Subroutine ADDRS is accessed at the beginning of CHAIN2 and merges the material and type of calculation integers at each node into one computer word. Subroutine GMAN (also accessed from CHAIN2) retrieves the material matrix from the merged matrix. Similarly GNO retrieves the calculation type matrix from the merged matrix. GNO is accessed from subroutine STEP.

Subroutine ZERO

This subroutine is used to initialize to zero the array which will contain the initial hydraulic head values. It is accessed early in the MAIN program.

Subroutine SAVE

Subroutine SAVE in the original program was also unusable at the computer installation available at the University of New South Wales. It was written in FAP and was used for outputting terminating information on magnetic tape if continuation runs were required. A simpler version of this subroutine was written in FORTRAN IV for this investigation. It outputs on cards the current hydraulic head profile, and this can be used to start a continuation run if this is necessary. SAVE is accessed from CHAIN2.

5.2.2 Modifications of the Original Program

Several changes had to be made to the original published program before it could be used in this investigation. As discussed in the preceding section, the parts of the program written in FAP had to be interpreted and rewritten in FORTRAN IV. It was not considered necessary to rewrite the subroutines in the local assembler language (COMPASS) as all the subroutines written in FAP are accessed relatively infrequently. The COMMON statements were rewritten in labelled blocks so that the appropriate variables could be made available in each subroutine. In the original form there was considerable danger of variables and arrays being overwritten.

Several errors in the matrix output option were detected and corrected. Subroutine ZERO had to be written to initialize an array to zero. In some computer installations storage space is automatically set to zero at the beginning of a job but this is not a feature of the CYBER 72-26 system.

The program in the form reproduced in the listing in Appendix C is believed to be generally free of errors. However there are so many different possible loops for a particular flow problem to follow, depending on the number of dimensions, whether it is a saturated or unsaturated flow problem, and several other factors, that it is impossible to assert that there are no other errors. The program has been thoroughly tested on both two dimensional and three dimensional unsaturated flow, and two dimensional saturated flow.

5.2.3 Limitations of the Program

According to the originators of the program, convergence and stability problems can arise in some unsaturated flow cases. In all the cases discussed in this chapter no problems were encountered in this regard. If problems do arise they can be overcome in several ways. The judicious selection of an initial hydraulic head distribution must make a solution faster and easier to obtain. The selection of the origin of solution can apparently have an important effect on the speed of solution. It is suggested by Reisenauer et al (1963) that this point be selected on a boundary on which large hydraulic head changes could occur during the solution process. There is no further information supplied on the choice of this point, so in an actual case in which convergence problems were encountered, it would be advisable to do several computer runs with different origins of calculation until a solution was obtained. Experience in the use of the program would undoubtedly help in choosing an optimum origin.

The solution technique used in the program (Gauss-Seidel with an under-relaxation or over-relaxation factor) could be considered to be inadequate by present day standards. Over 1000 iterations are sometimes needed to obtain a solution, and this involves quite a large amount of computer time (up to 25 minutes CPU time for a 28 x 100 two dimensional grid on the CYBER 72-26 computer). However with a smaller grid (say 20 x 20) the program rapidly converges to a solution.

The main limitation of the steady state program appears to be in the technique used to derive the under-relaxation or over-relaxation factor. If a more flexible technique was devised to derive this factor, a much faster rate of convergence could probably be obtained. There is very little information in either of the publications describing the program, detailing how the acceleration factors were derived. Trial and error techniques probably played a large part in their determination.

The preparation of input data for the program is quite complicated. This is largely due to the wide variety of options offered by the program. Very careful attention has to be paid to the description of the input data preparation given in Reisenauer et al (1963). The description is inadequate in some places particularly in the detailing of the setting up of the boundary conditions. The derivation of the pressure head at a point, from the hydraulic head and several other variables, is also poorly described (see Section 5.2.4).

In general however the program produces good results for a wide variety of steady state flow problems. It is slow because of the wide range of options and an outdated solution algorithm, but if computer time is freely available this is not a serious limitation. In comparison the solution of an equivalent unsteady state flow problem could take several orders of magnitude longer on the same computer.

5.2.4 Evaluation of the Conductivity from the Hydraulic Head

As mentioned above, the expression used to derive the pressure head from the hydraulic head at a point, is quite complicated. The various parameters in the expression are not clearly defined in the reports describing the program. It appears that several of the terms have been derived for special applications of the program, and in general they are not needed. The pressure head is derived in CHAIN2 and is then passed to subroutine KAY. The following expression is used to derive the pressure head

$$h = [\bar{\phi} - D\bar{z} \cos \mu + E\bar{x} \sin \mu - (F.H/L)] \cdot L \qquad (5.1)$$

where

h = pressure head (cm of water).

$\bar{\phi}$ = hydraulic head (dimensionless).

D,E,F = constants. Called control parameters in the original reports. Their functions are not clear but normally they have the value unity except when simulating large profiles.

H = parameter used for translating the origin (cm of water). Useful when a problem contains only unsaturated flow. Set to zero for this investigation.

μ = angle of inclination of the flow system in radians. Useful when simulating flow on a sloping plane. Had the value zero for all the cases examined in this report.

L = length scaling factor (cm). Usually convenient to have it equal to the distance between the lowest and highest $\bar{\phi}$ values in the vertical direction. For this investigation it was set to the total depth of the profile.

$\overline{x}, \overline{z}$ = dimensionless distances taken from the origin of co-ordinates at the bottom left hand corner of the two dimensional grid. $\overline{z}$ was taken in the vertical direction and $\overline{x}$ in the horizontal. The distances were made dimensionless by dividing by L.

For all the cases examined in this chapter Eq. (5.1) could be reduced to

$$h = (\overline{\phi} - \overline{z}) \cdot L \qquad (5.2)$$

which can be written as

$$\phi = h + z,$$

the familiar expression relating hydraulic head and pressure head.

The value of h calculated from Eq. (5.2) is used to evaluate the conductivity (water content in the second computer run) for that point, by accessing subroutine KAY.

5.3 RESULTS

Because of the large number of cases investigated in the steady state study, the results have been presented in several separate sections, each one of these describing a particular flow problem. The results are presented in Figures 5.1 to 5.36 in the form of flow nets and corresponding water content patterns. In the following sections the figures are discussed in detail but general comments applying to all the figures are given in this section.

The odd numbered figures give the flow nets for each case and the following even numbered figures give the corresponding water content profiles. All the figures are presented together so that comparisons can be made more easily. It should be noted that in each case the left hand boundary is situated at the centreline of the pit, and the boundary is considered to be a line of symmetry for simulation purposes. The properties of the six soils used in this investigation are listed in Table 5.1. They are indicated on the flow net figures by the codes SOIL 1, SOIL 2, etc.

The dimensionless hydraulic head $\overline{\phi}$ (shown as ϕ in the figures) was set to 1.0 in the ponding zone and 0.0 at the water table. The water table is defined by h = 0 in this chapter and consequently, for a fixed water table position, this infers that there is uninhibited vertical flow of water as with a gravel substratum. Both the ground surface and pit centreline were assumed to be no-flow boundaries. In all cases

except Figures 5.35 and 5.36 the right hand boundary was a no-flow boundary, but it was situated at a large distance from the pit so that it would have a negligible effect on the flow net pattern (note that the right hand border shown in these figures is not the location of the right hand boundary, this being much further to the right).

Table 5.1: Properties of Soils Used in the Steady State Study

Soil Code	Saturated K $(cm\ min^{-1})$	Saturated θ $(cm^3\ cm^{-3})$	Moisture Characteristic Curve	Remarks
SOIL 1	0.80	0.292	#17 Sand Main Rewet	For properties of this soil see Watson & Curtis (1974).
SOIL 2	0.03	0.380	Rubicon Sandy Loam Main Rewet	Properties of this soil given in Topp (1969).
SOIL 3	2.214	0.360	G1 Sand Main Drain	Properties given in Watson (1971).
SOIL 4	0.353	0.292	#17 Sand Main Rewet	Saturated K found from dry-packed field sample. Shape of h-K curve same as #17 sand.
SOIL 5	1.110	0.360	G1 Sand Main Drain	Saturated K found from wet-packed field sample. Shape of h-K curve same as G1 sand.
SOIL 6	1.468	0.360	G1 Sand Main Drain	Saturated K found from dry-packed field sample. Shape of h-K curve same as G1 sand.

The recharge rate (also called intake rate) for each case has been calculated based on the assumption that the recharge pit is 92 metres long. Intake rates are listed in Table 5.2.

In the following four sections results are presented for Shands No.2 Pit and Iyah Creek No. 1 Pit together with studies of surface clogging and a study of water table mounding.

Table 5.2: Intake Rates for each of the Steady State Flow Cases

Recharge Pit Simulated	Low Conductivity Layer Under Pit?	Figure Number	Intake Rate m^3 day^{-1}
Shands #2	No	5.1	4540
Shands #2	No	5.3	4260
Shands #2	No	5.5	6280
Shands #2	No	5.7	3690
Shands #2	No	5.9	7000
Shands #2	No	5.11	6950
Shands #2	No	5.13	13900
Iyah Creek #1	No	5.15	3070
Iyah Creek #1	No	5.17	4750
Iyah Creek #1	No	5.19	6220
Shands #2	Yes	5.21	3690
Shands #2	Yes	5.23	1040
Shands #2	Yes	5.25	6110
Shands #2	Yes	5.27	3120
Iyah Creek #1	Yes	5.29	2430
Iyah Creek #1	Yes	5.31	4120
Iyah Creek #1	Yes	5.33	5800
Shands #2	No	5.35	4470
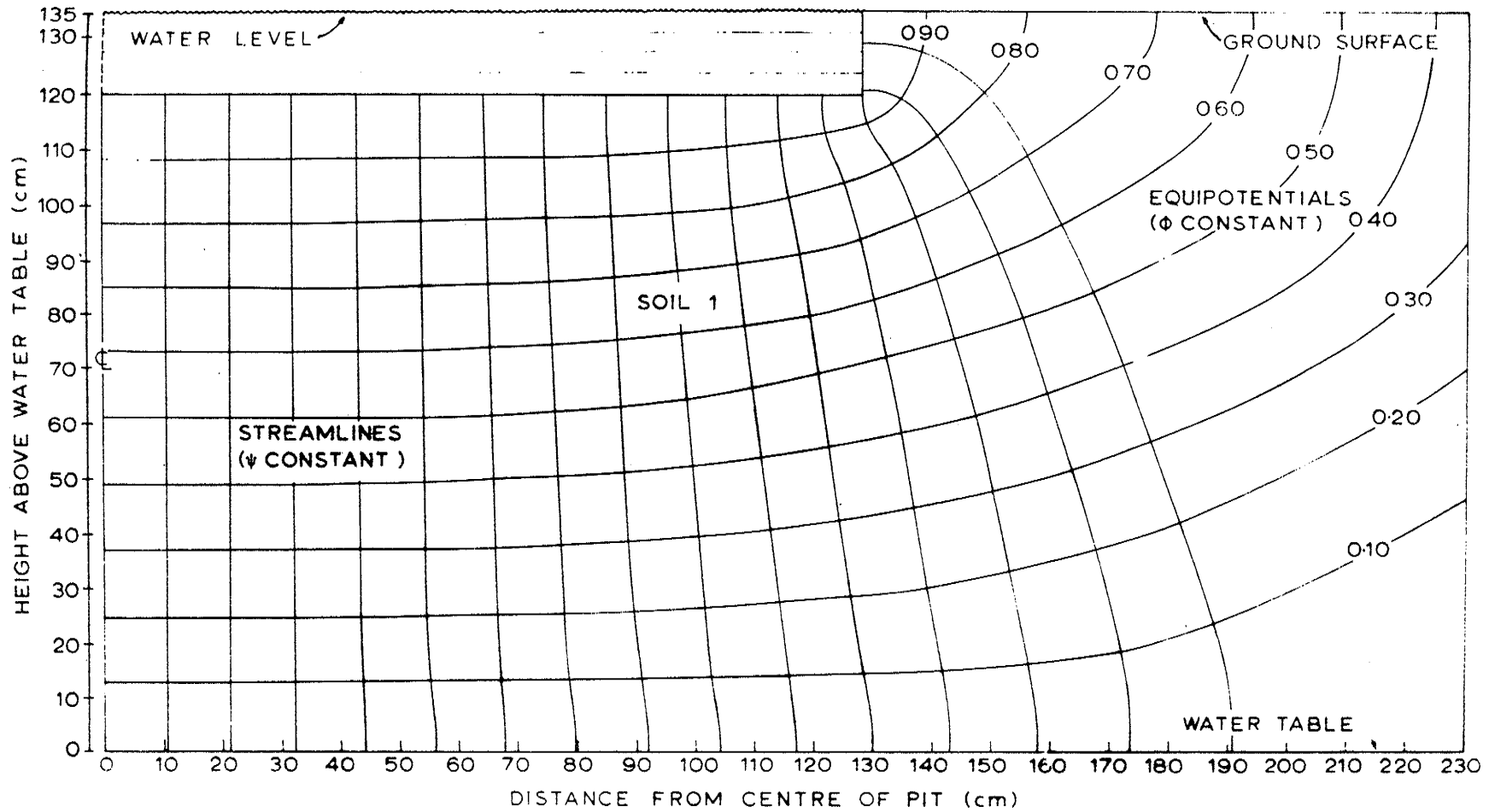
Figure 5.1: Shands No. 2 Pit. Flow net for 15 cm depth of ponding into a uniform profile.

69.
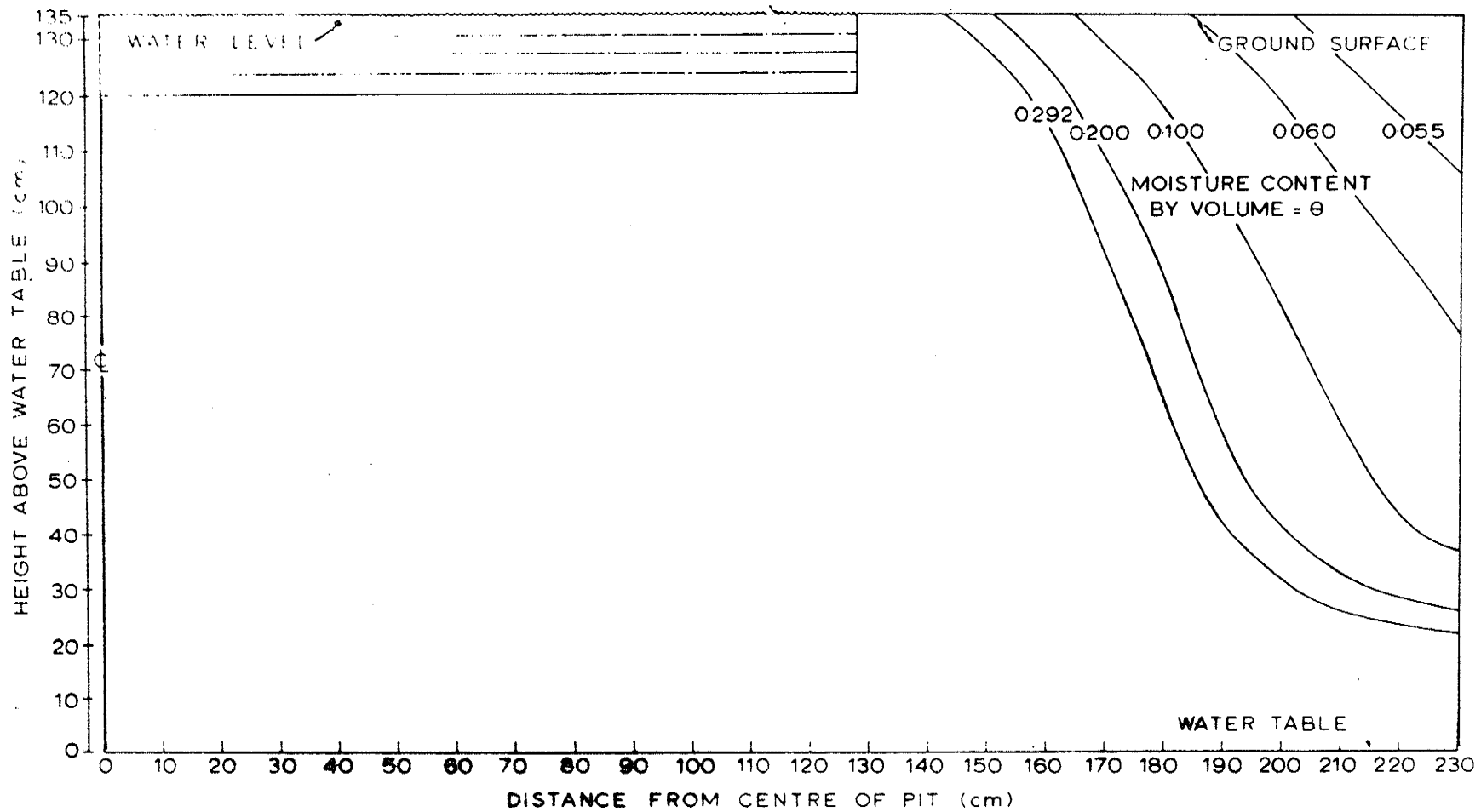
Figure 5.2:   Shands No. 2 Pit.   Water content profile corresponding to flow net given in Figure 5.1.
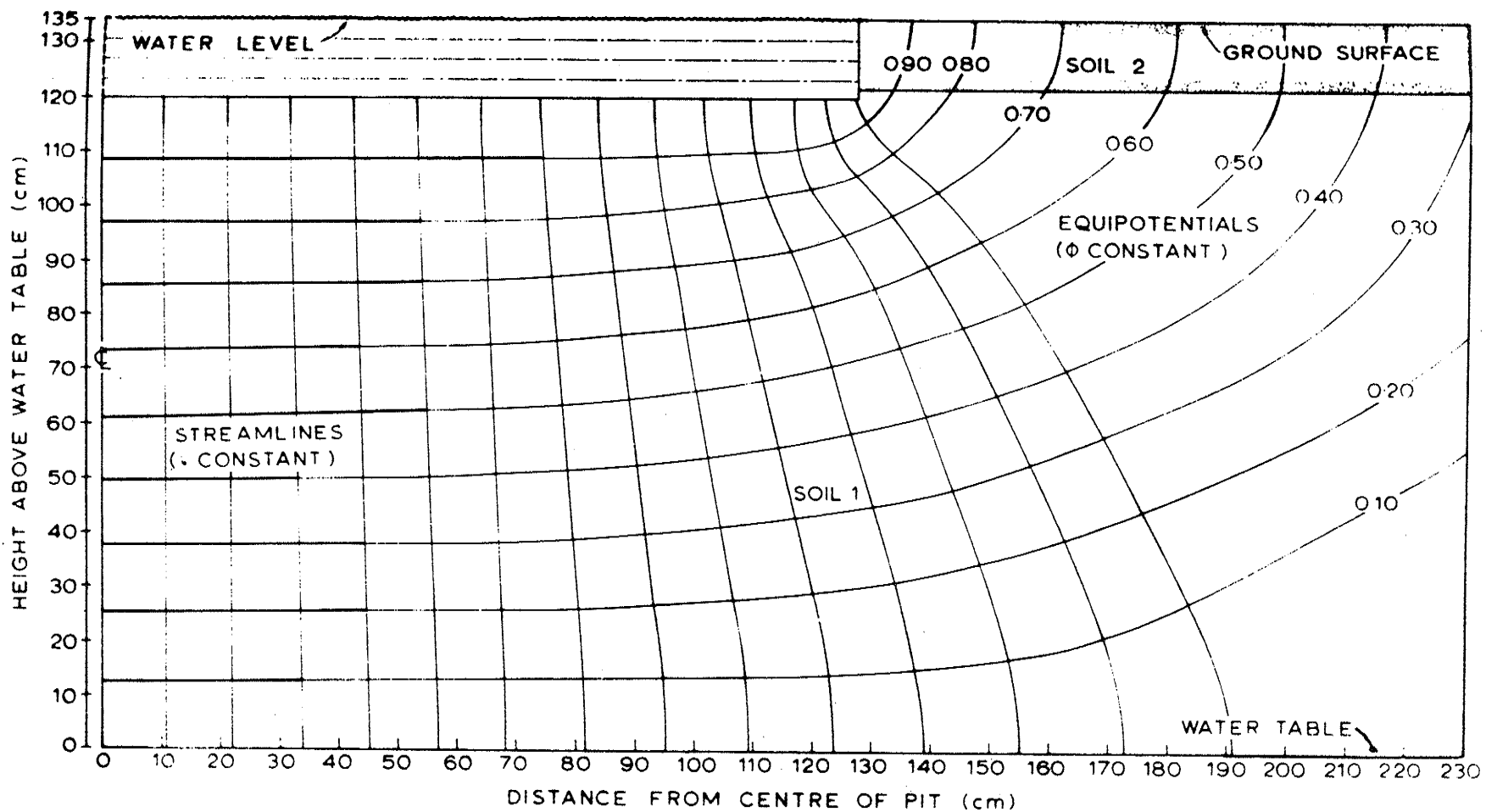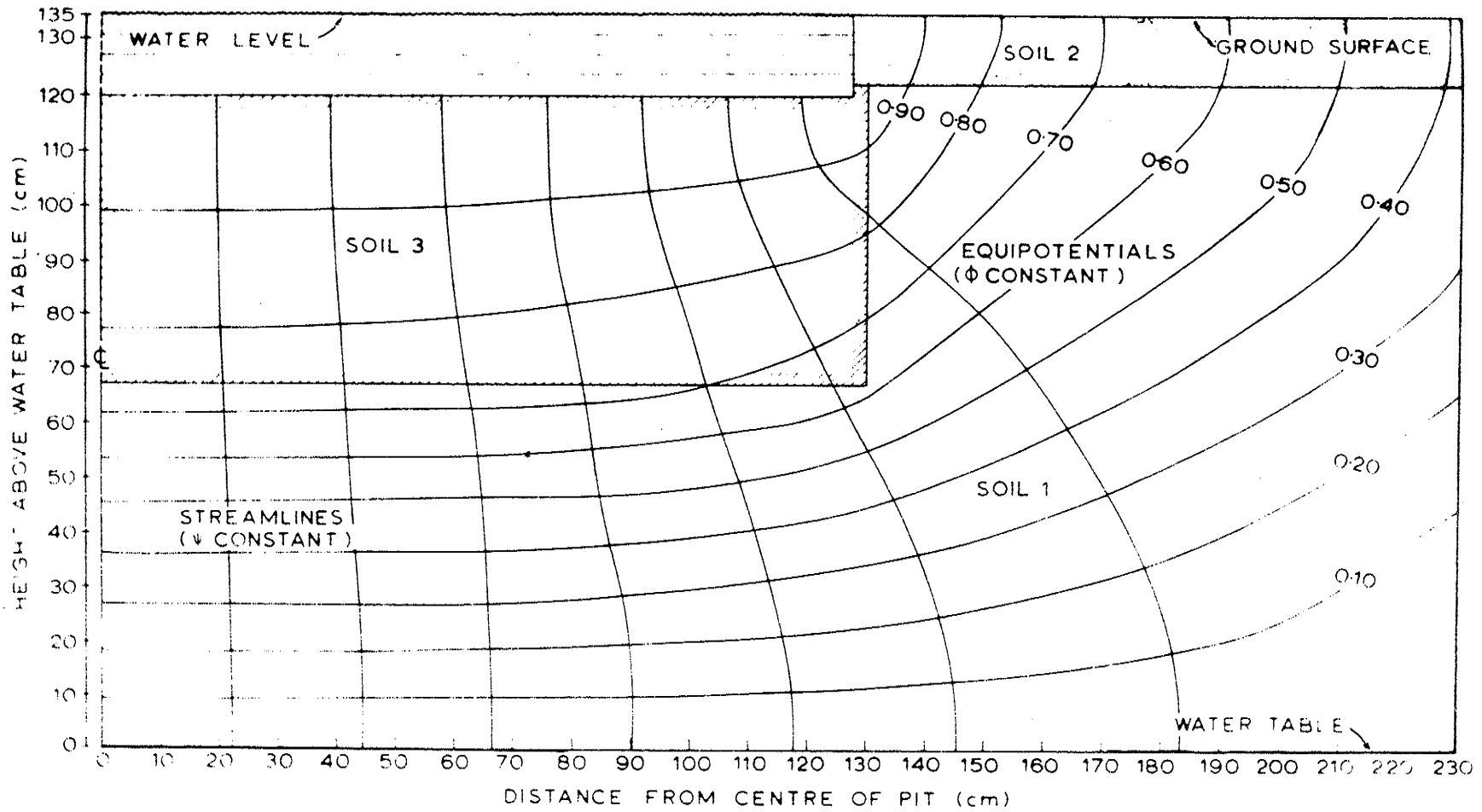
Figure 5.3: Shands No. 2 Pit. Flow net for 15 cm depth of ponding into a uniform profile with a low conductivity bank zone.
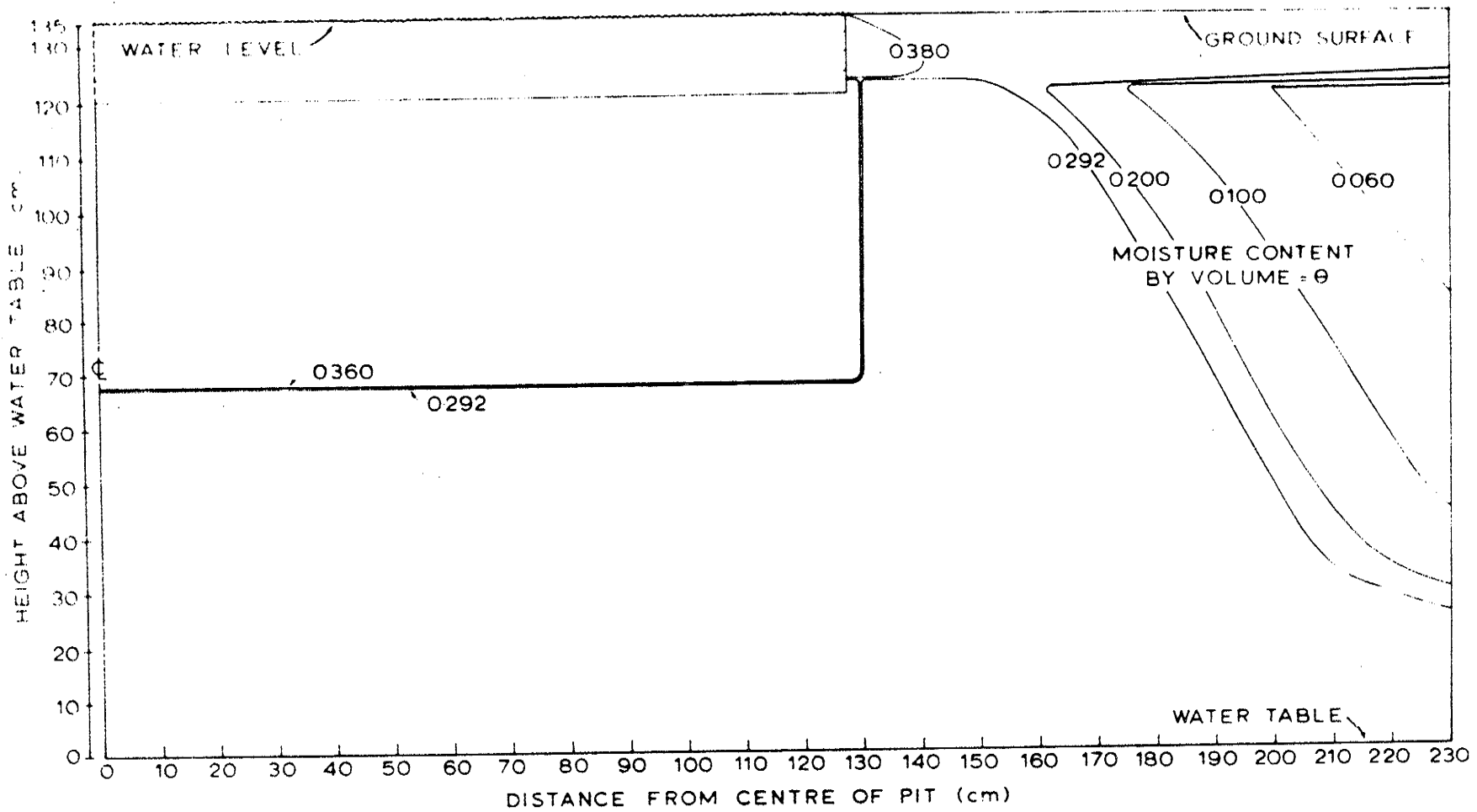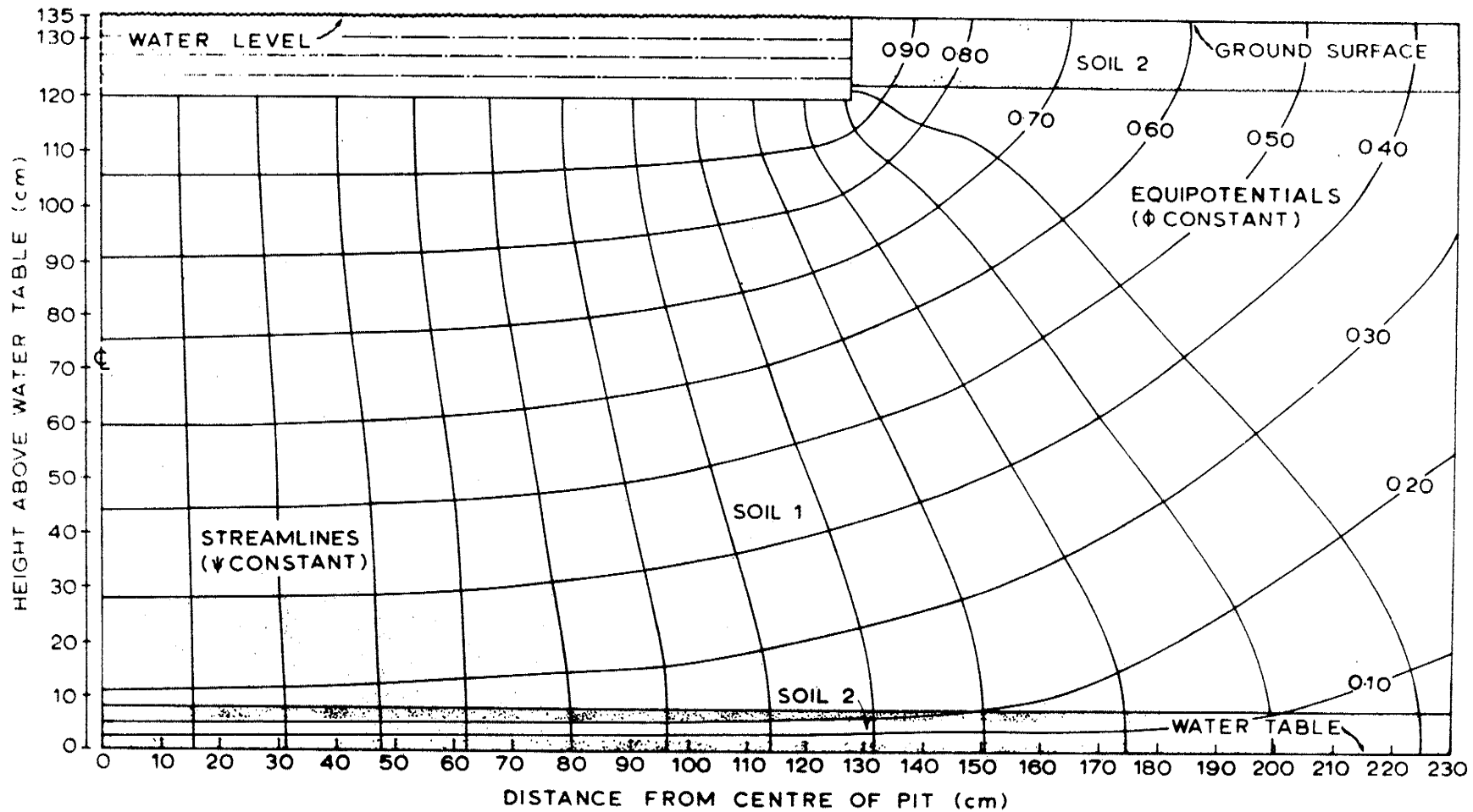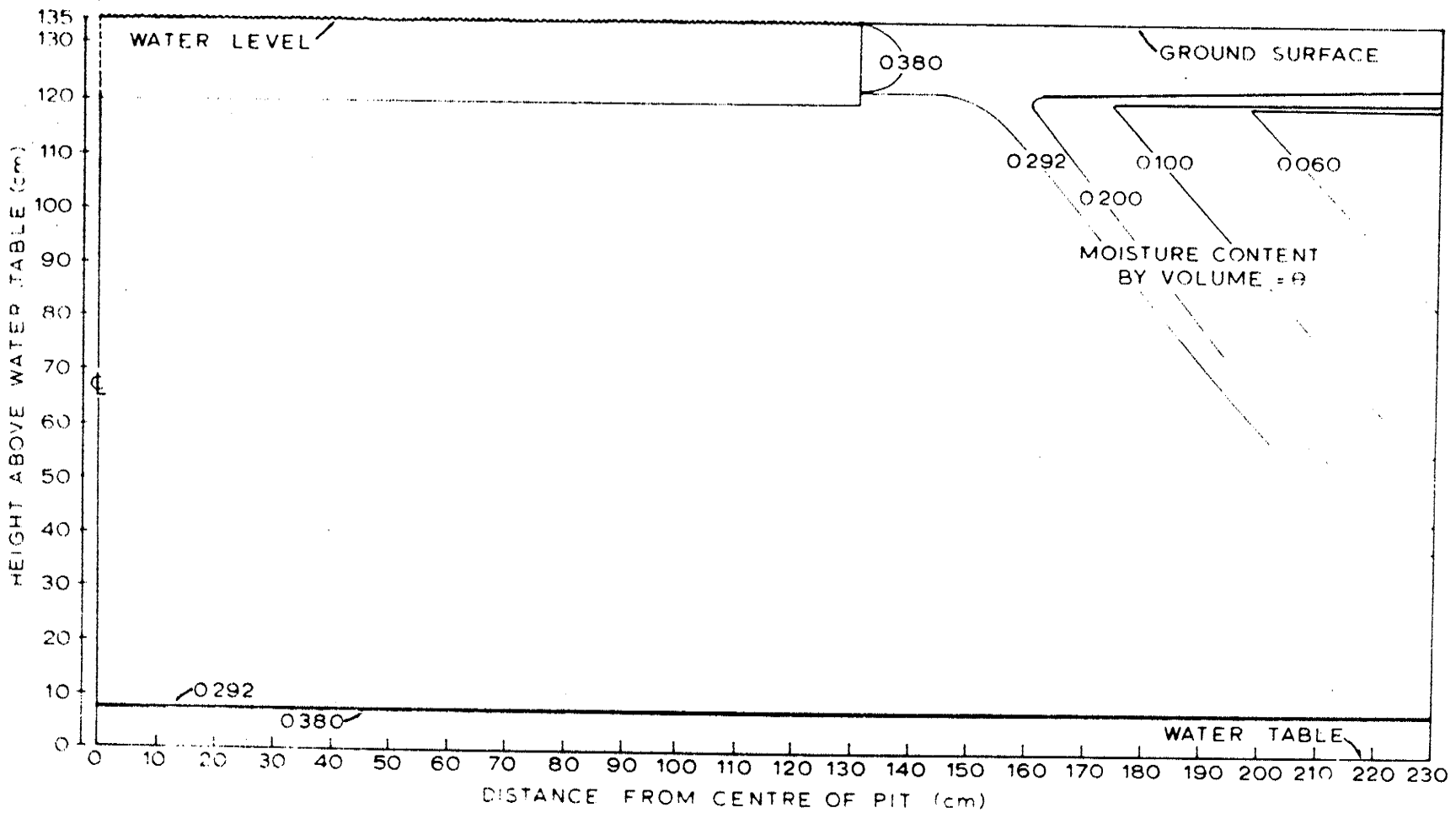
71.
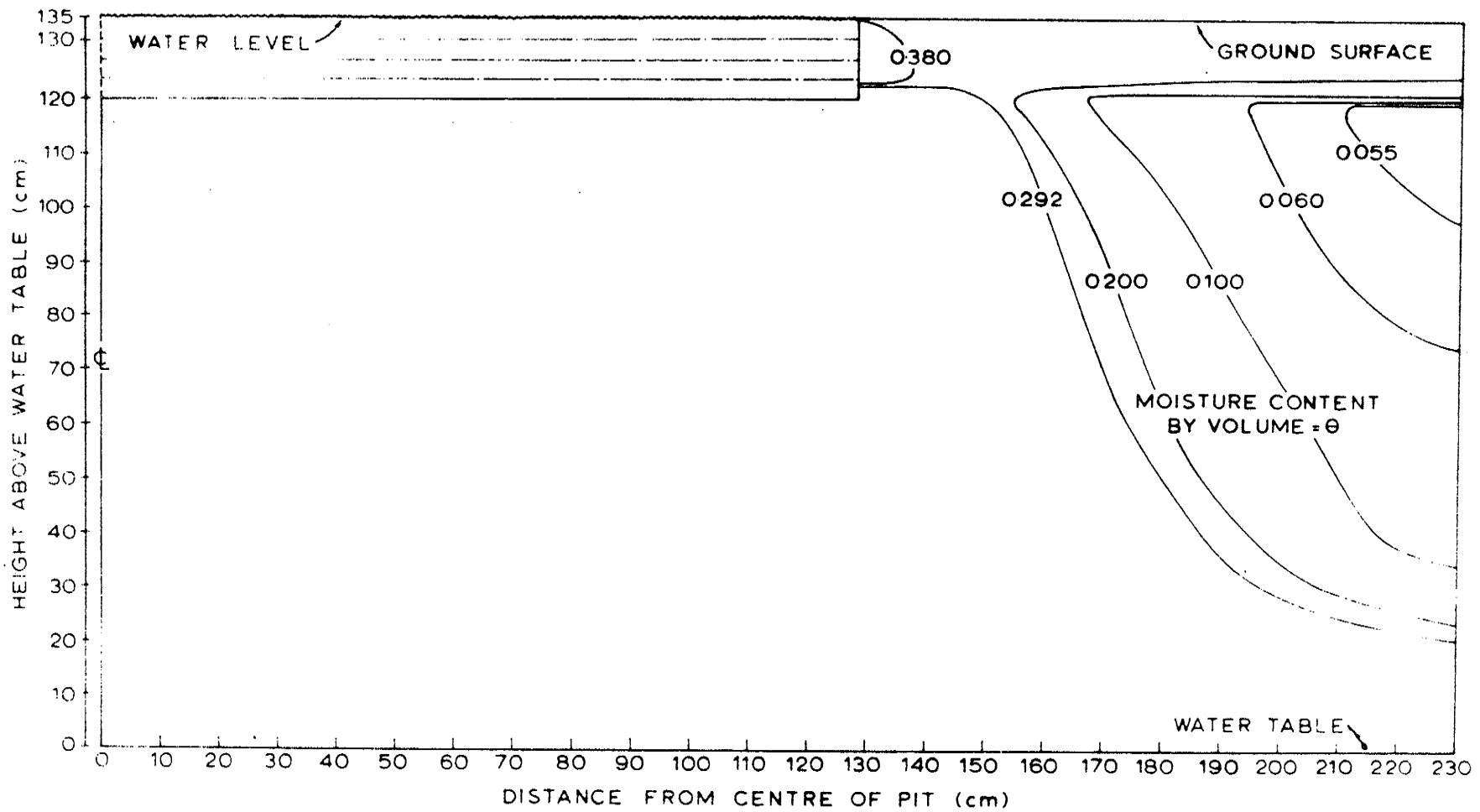
Figure 5.4: Shands No. 2 Pit. Water content profile corresponding to flow net given in Figure 5.3.

Figure 5.4: Shands No. 2 Pit. Water content profile corresponding to flow net given in Figure 5.3.

Figure 5.5: Shands No. 2 Pit. Flow net for 15 cm depth of ponding into a combined profile with a low conductivity bank zone.

Figure 5.6: Shands No. 2 Pit. Water content profile corresponding to flow net given in Figure 5.5.

Figure 5.7:   Shands No. 2 Pit.   Flow net for 15 cm depth of ponding into a uniform profile with a low conductivity layer across the base and a low conductivity bank zone.

Figure 5.8: Shands No. 2 Pit. Water content profile corresponding to flow net given in Figure 5.7.
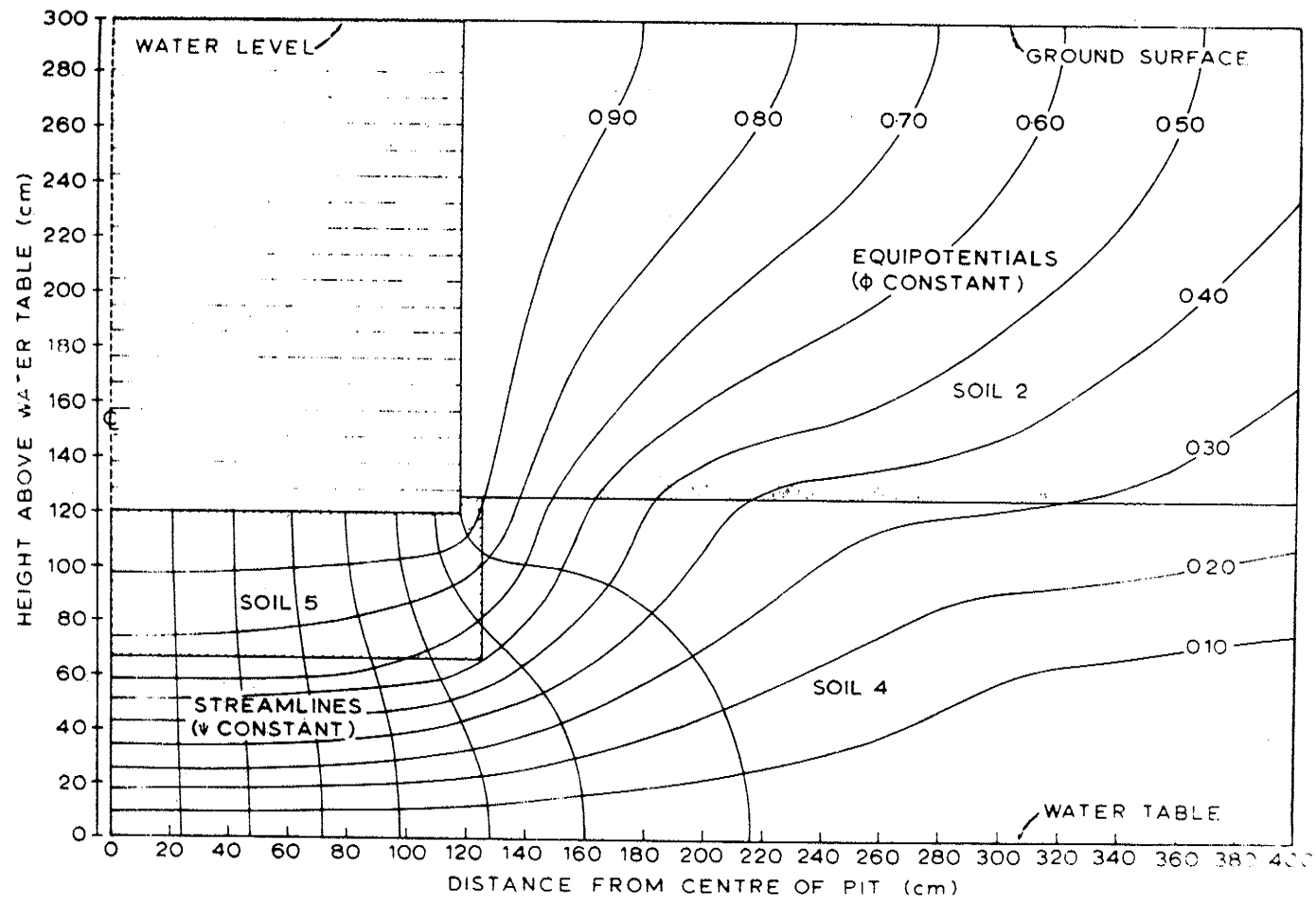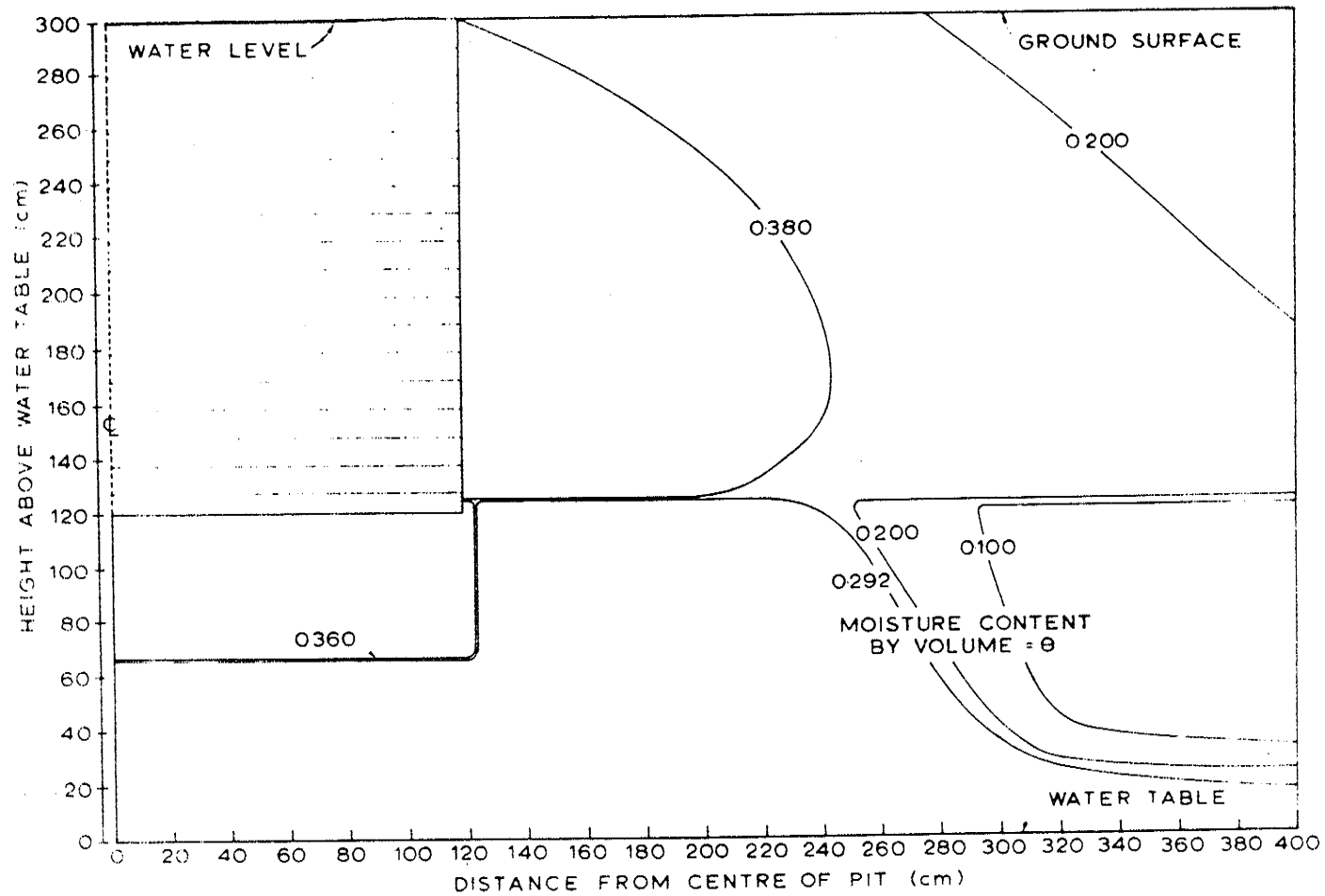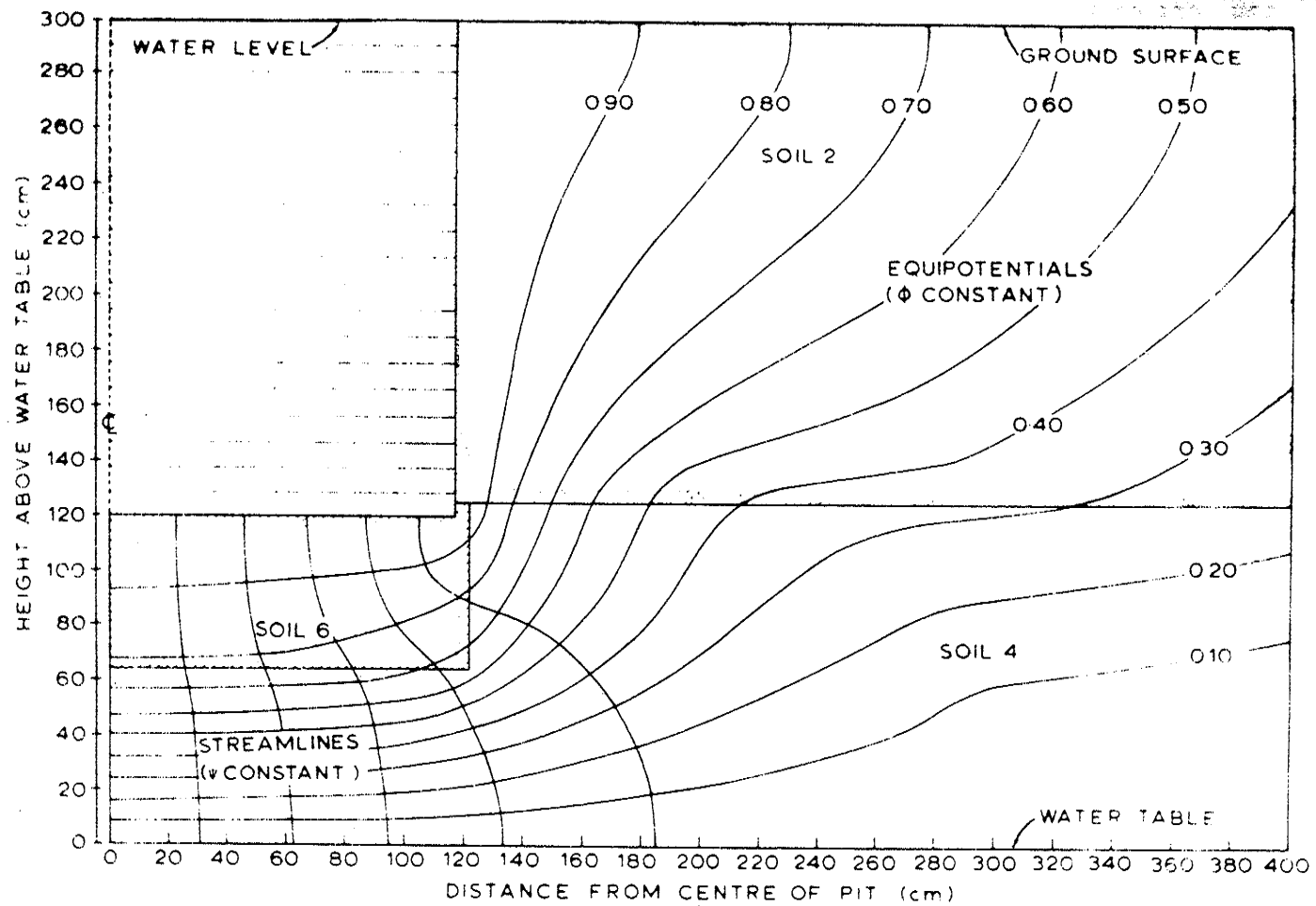
Figure 5.9:   Shands No. 2 Pit. Flow net for 180 cm depth of ponding into a combined profile with a low conductivity bank zone.

Figure 5.10: Shands No. 2 Pit. Water content profile corresponding to flow net given in Figure 5.9.

Figure 5.11: Shands No. 2 Pit. Flow net for 180 cm depth of ponding into a combined profile with a low conductivity bank zone.
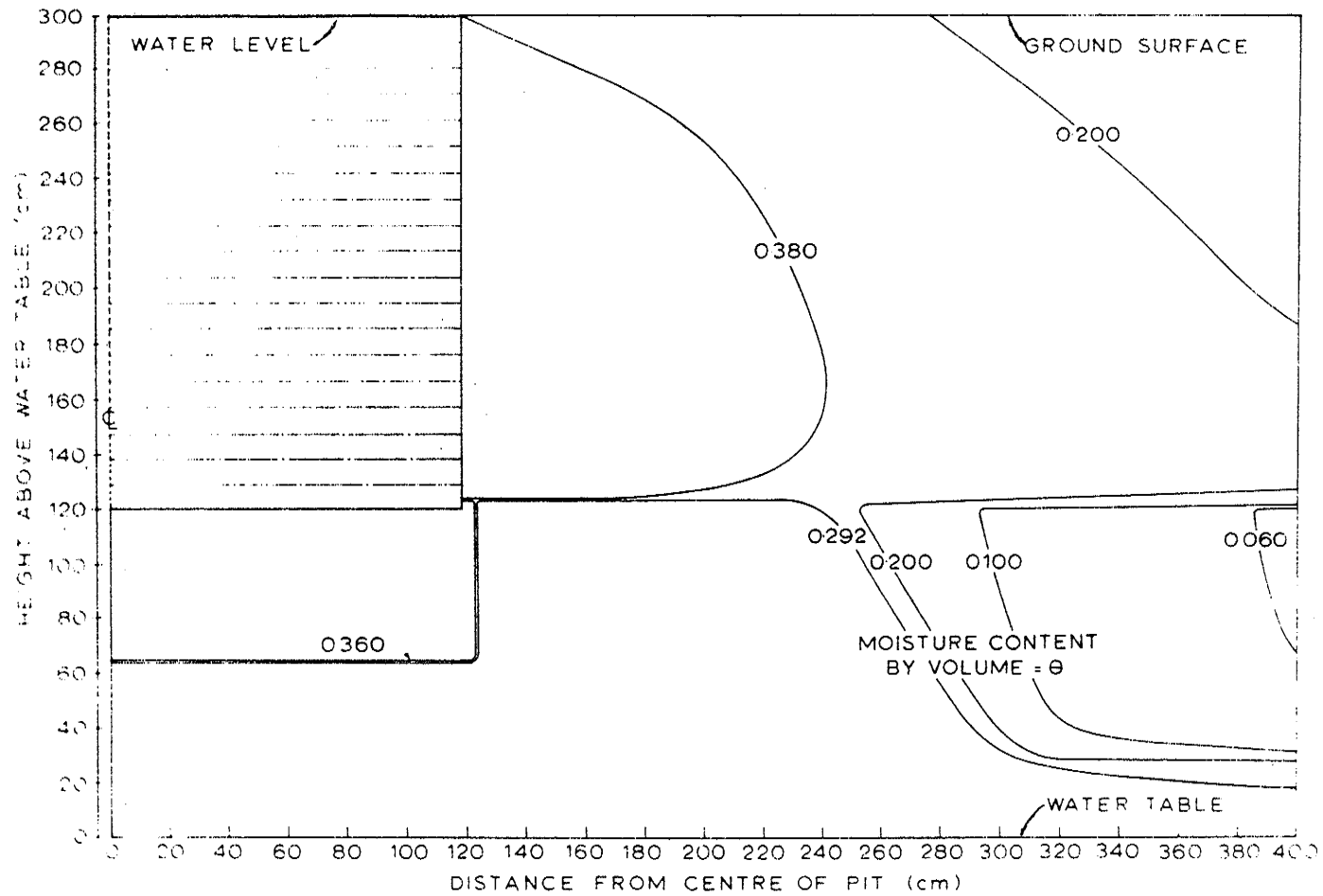
Figure 5.12: Shands No. 2 Pit. Water content profile corresponding to flow net given in Figure 5.11.
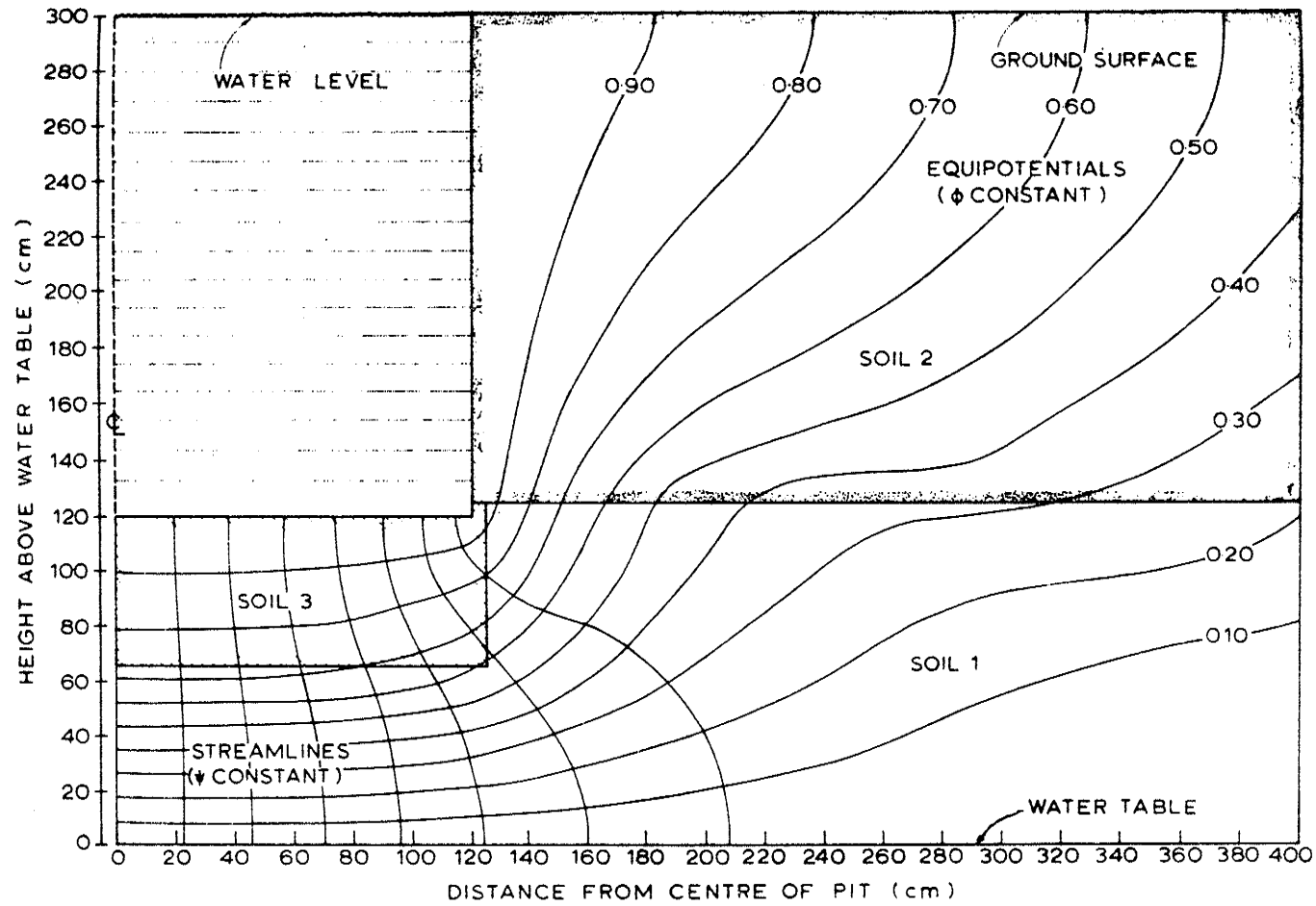
Figure 5.14: Shands No. 2 Pit. Flow net for 180 cm depth of ponding into a
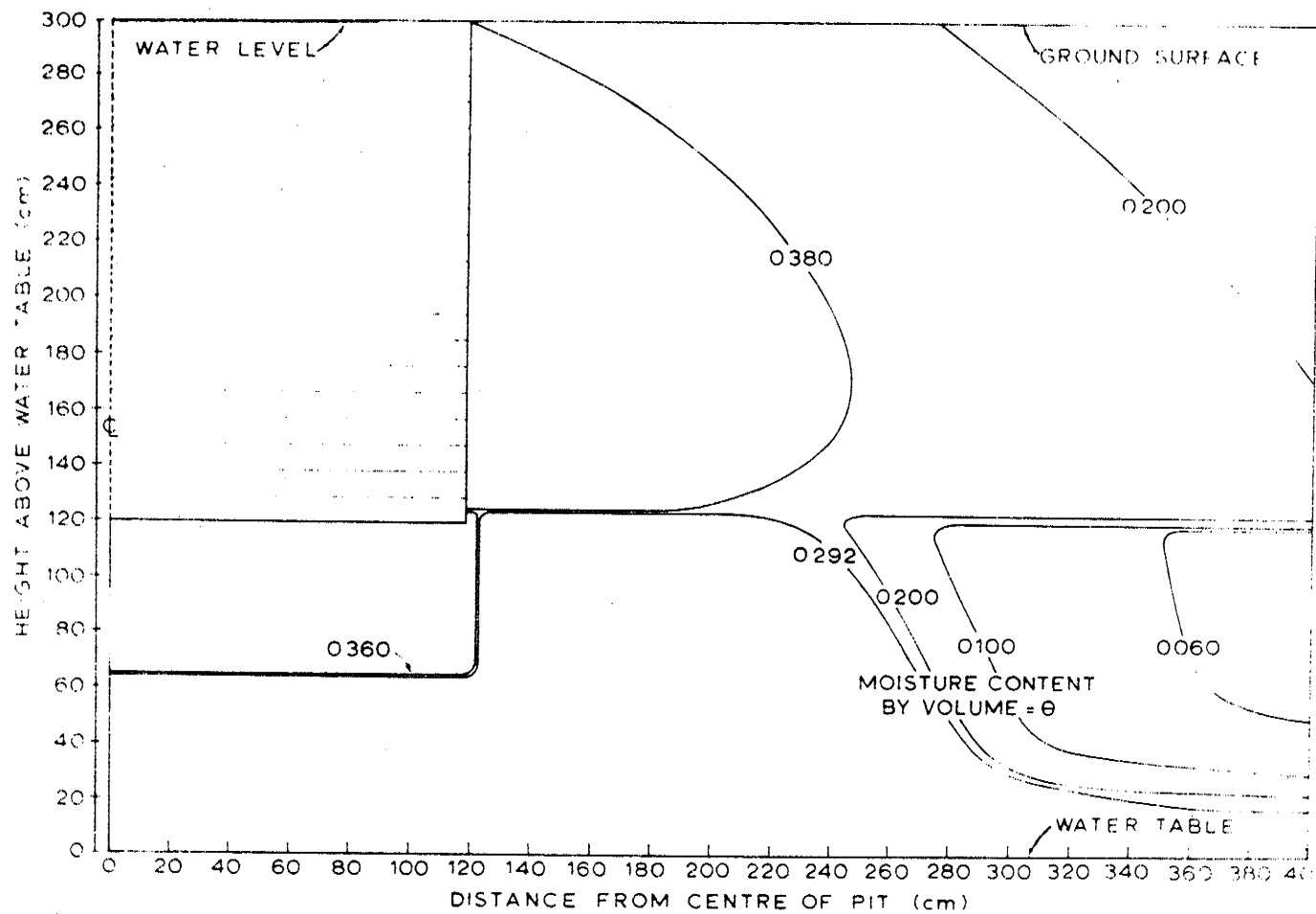combined profile with a low conductivity bank zone.

Figure 5.14:   Shands No. 2 Pit. Water content profile corresponding to flow net given in Figure 5.13.

Figure 5.15: Iyah Creek No. 1 Pit. Flow net for 60 cm depth of ponding into a 70 cm wide slot of high conductivity sand.

Figure 5.16: Iyah Creek No. 1 Pit. Water content profile corresponding to flow net given in Figure 5.15.

Figure 5.17: Iyah Creek No. 1 Pit. Flow net for 60 cm depth of ponding into a 130 cm wide slot of high conductivity sand.
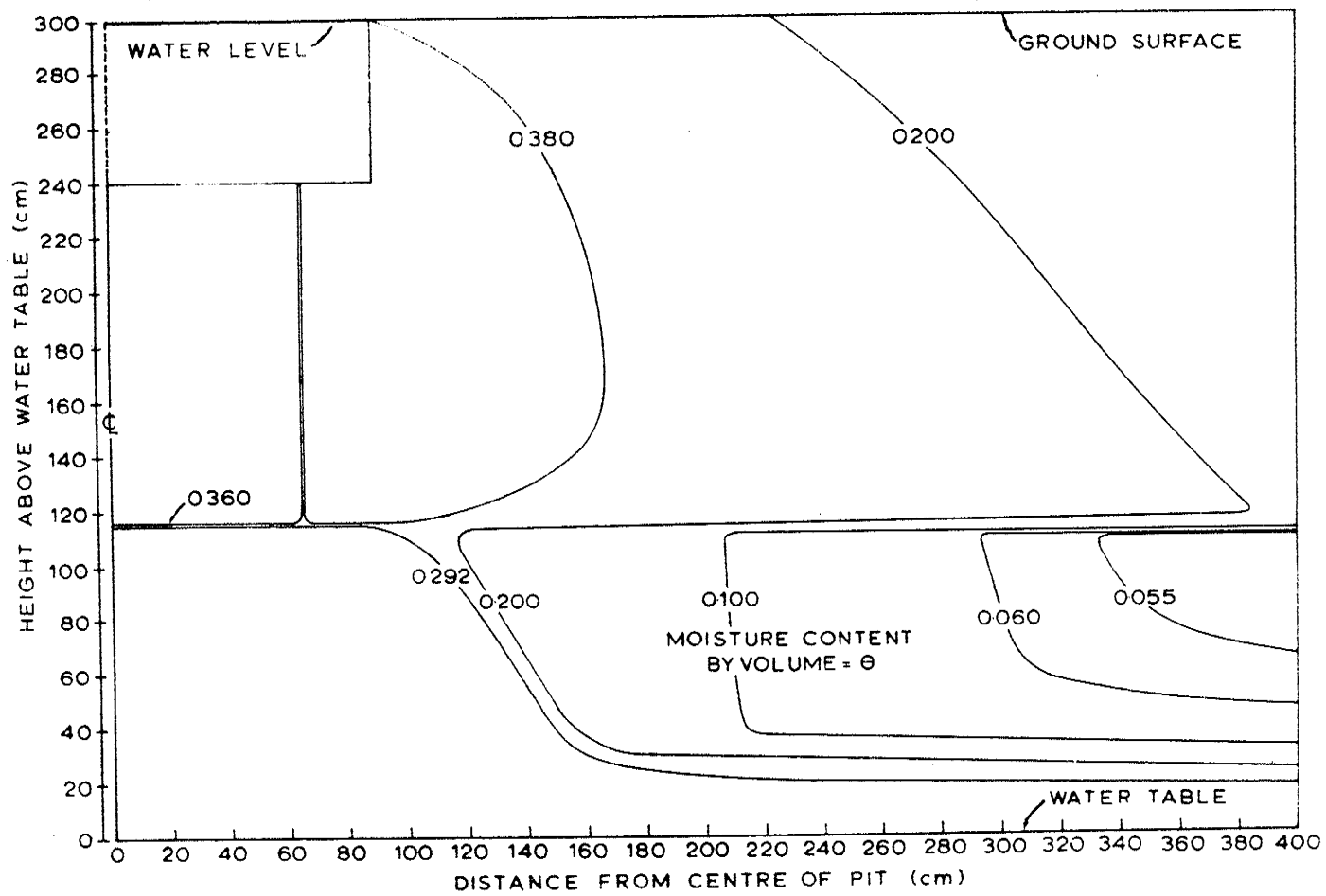
Figure 5.18: Iyah Creek No. 1 Pit. Water content profile corresponding to flow net given in Figure 5.17.
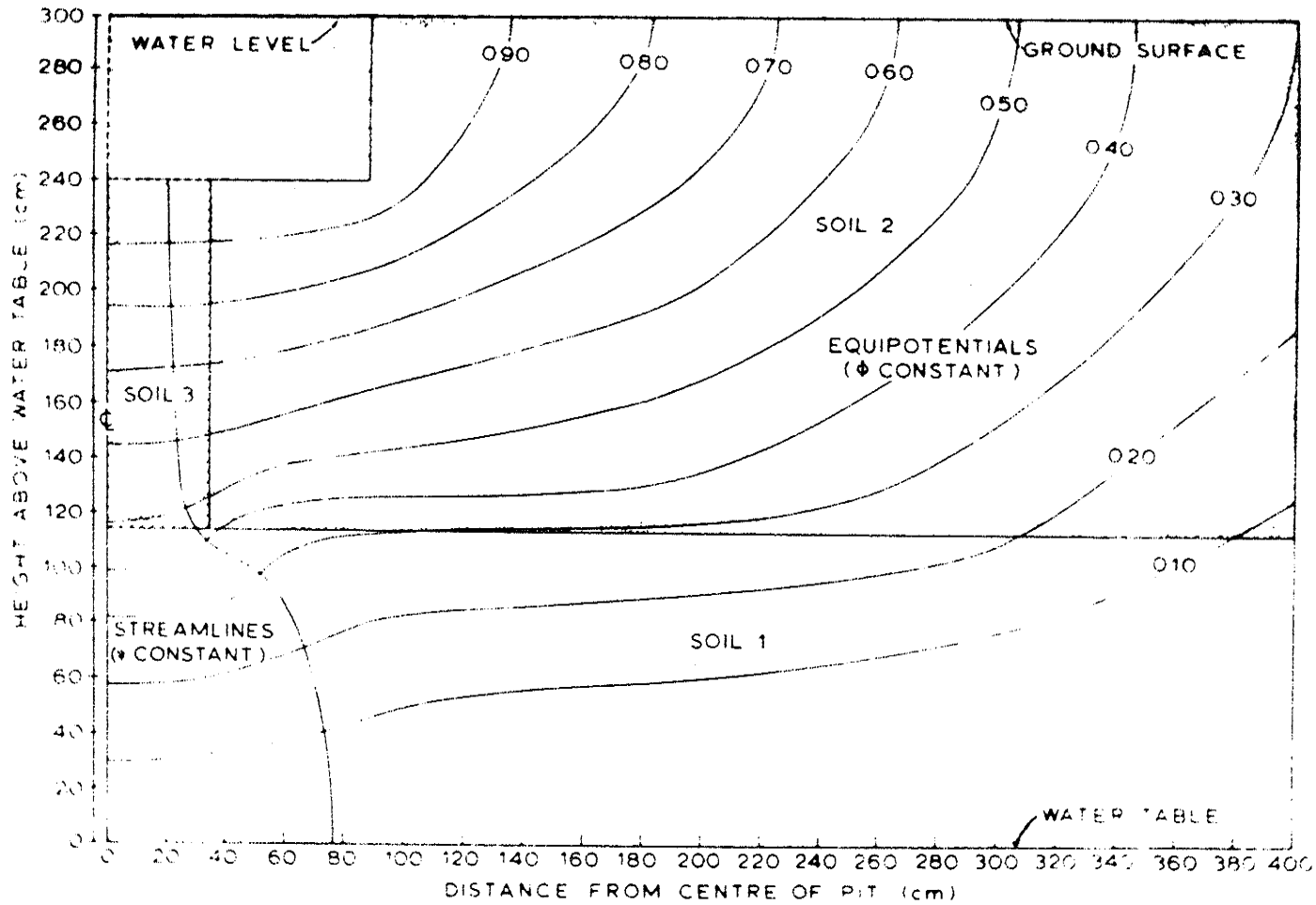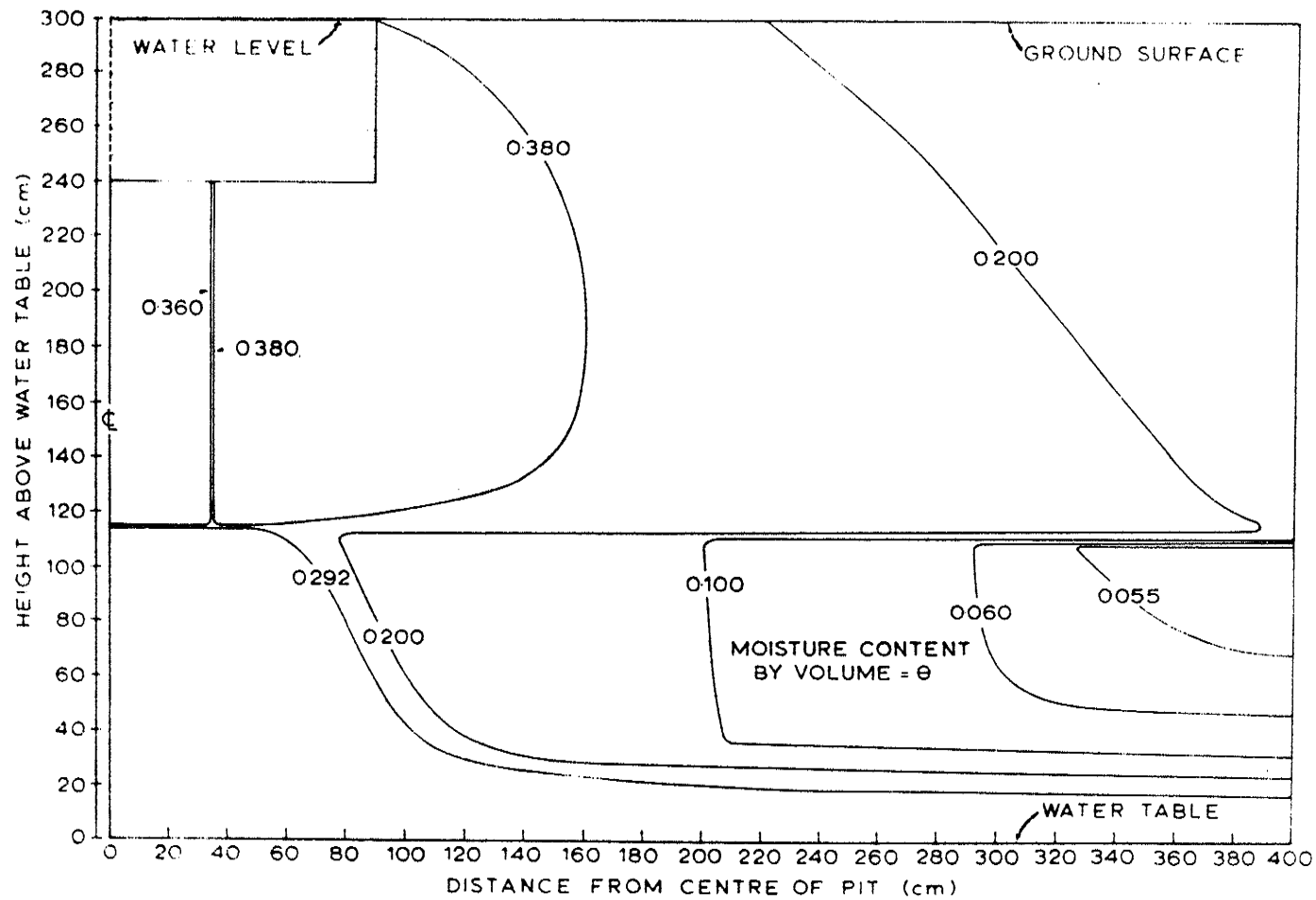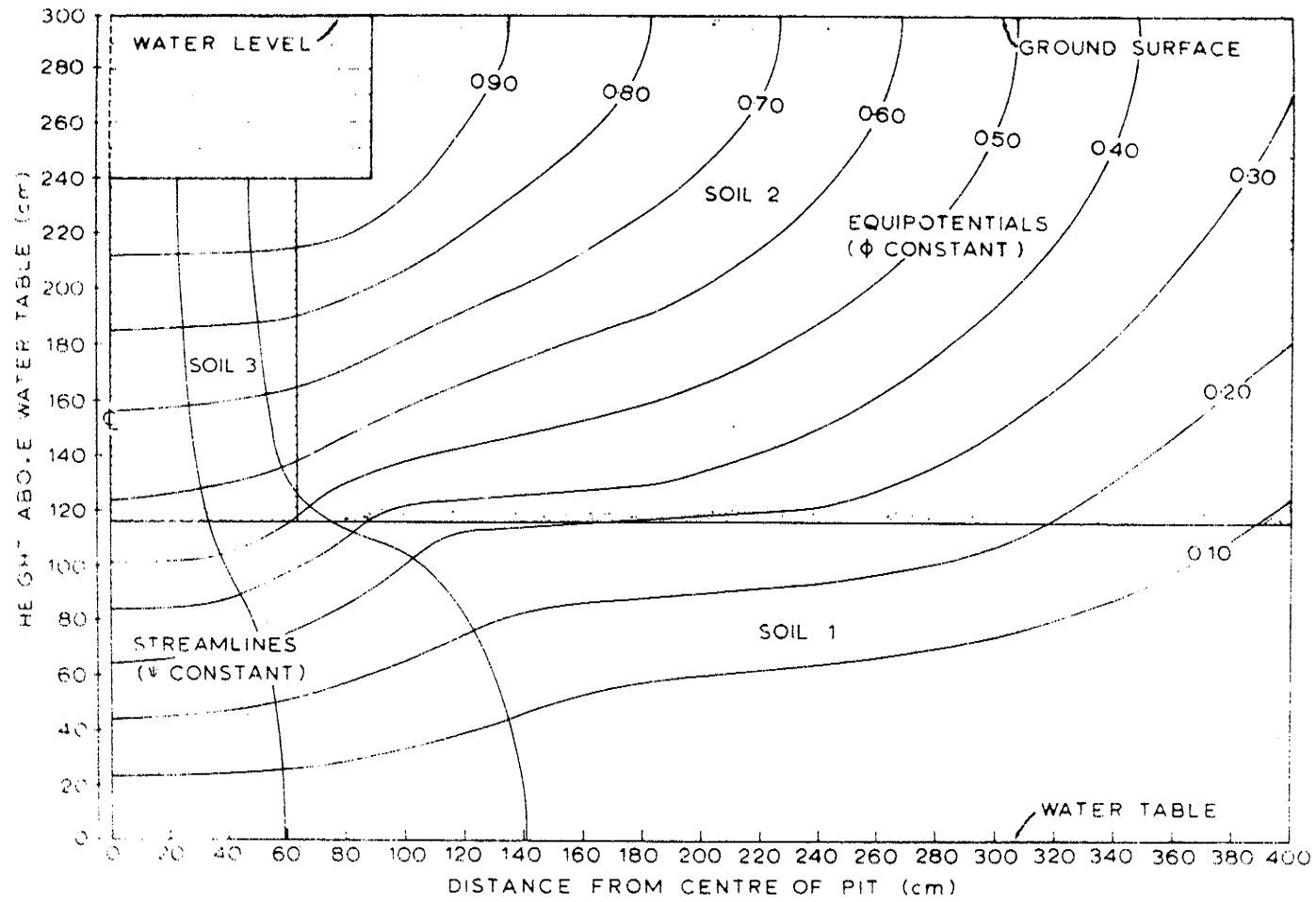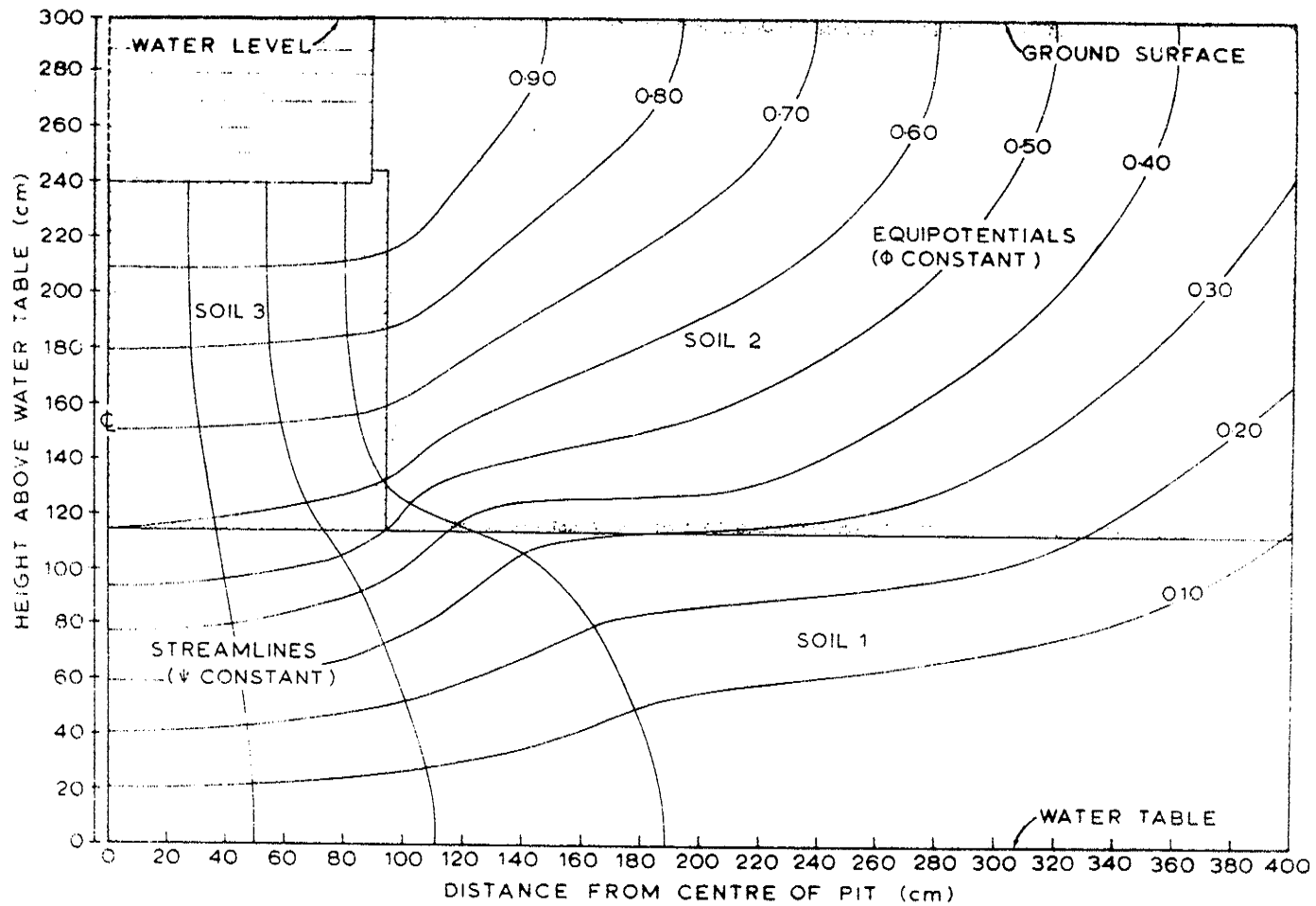
Figure 5.19:   Iyah Creek No. 1 Pit. Flow net for 60 cm depth of ponding into a
190 cm wide slot of high conductivity sand.

Figure 5.20: Iyah Creek No. 1 Pit. Water content profile corresponding to flow net given in Figure 5.19.

Figure 5.21: Shands No. 2 Pit. Flow net for a profile similar to Fig. 5.3, but with a thin layer of low conductivity material under the pit.

Figure 5.22: Shands No. 2 Pit. Water content profile corresponding to flow net given in Fig. 5.21.

Figure 5.23: Shands No. 2 Pit. Flow net for a profile similar to Fig. 5.3, but with a medium layer of low conductivity material under the pit.

Figure 5.24: Shands No. 2 Pit. Water content profile corresponding to flow net given in Fig. 5.23.

Figure 5.25: Shands No. 2 Pit. Flow net for a profile similar to Fig. 5.5, but with a thin layer of low conductivity material under the pit.

WATER LEVEL

GROUND SURFACE

0·380

0·292

0·200 0·100   0·060   0·055

MOISTURE CONTENT
BY VOLUME = θ

0·360

WATER TABLE

HEIGHT ABOVE WATER TABLE (cm)

135
130
120
110
100
90
80
70
60
50
40
30
20
10
0

0 10 20 30 40 50 60 70 80 90 100 110 120 130 140 150 160 170 180 190 200 210 220 230

DISTANCE FROM CENTRE OF PIT (cm)

94.

Figure 5.26: Shands No. 2 Pit.   Water content profile corresponding to flow net given in Fig. 5.25.
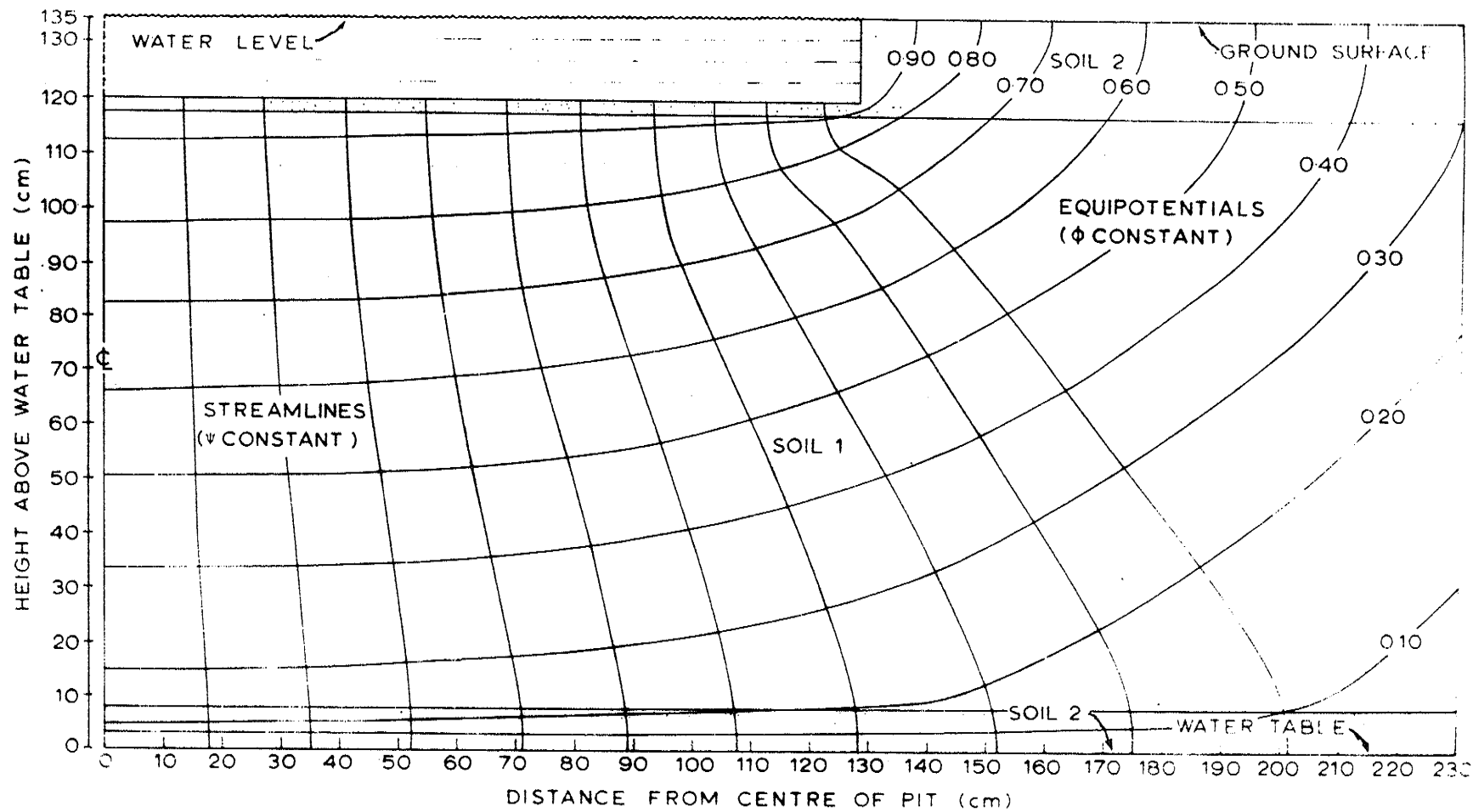
Figure 5.27: Shands No. 2 Pit. Flow net for a profile similar to Fig. 5.21, but with a thin layer of low conductivity material across the base.
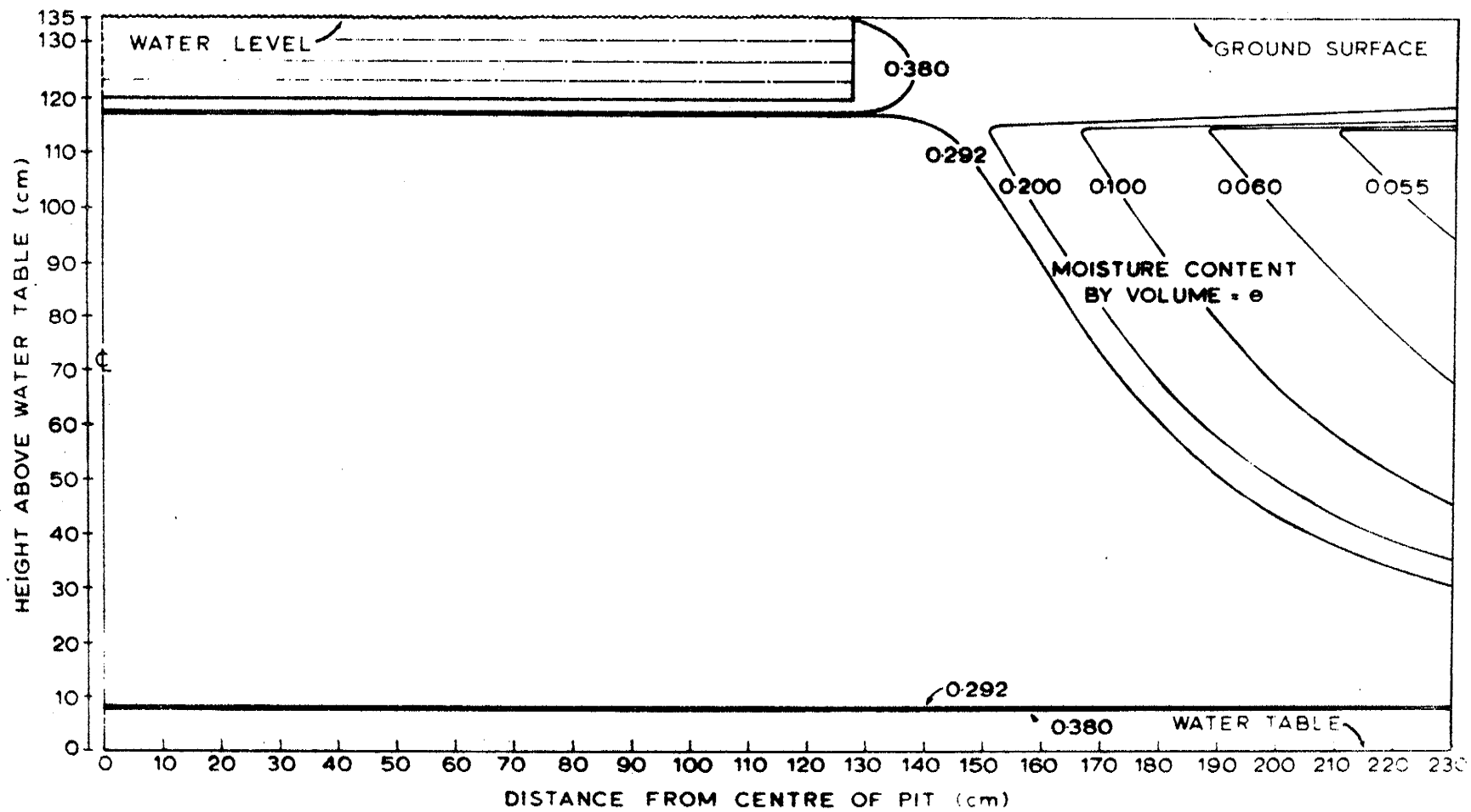
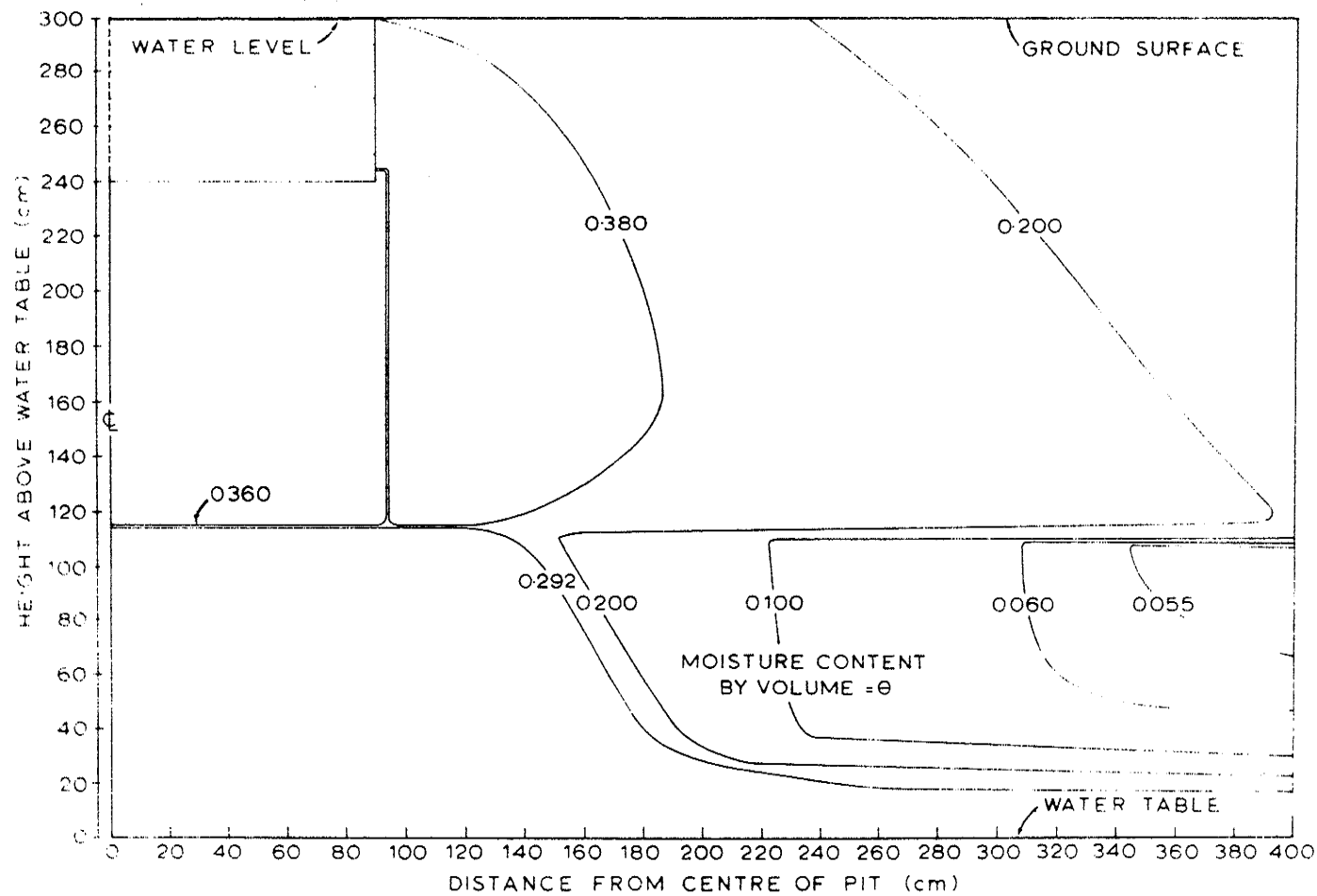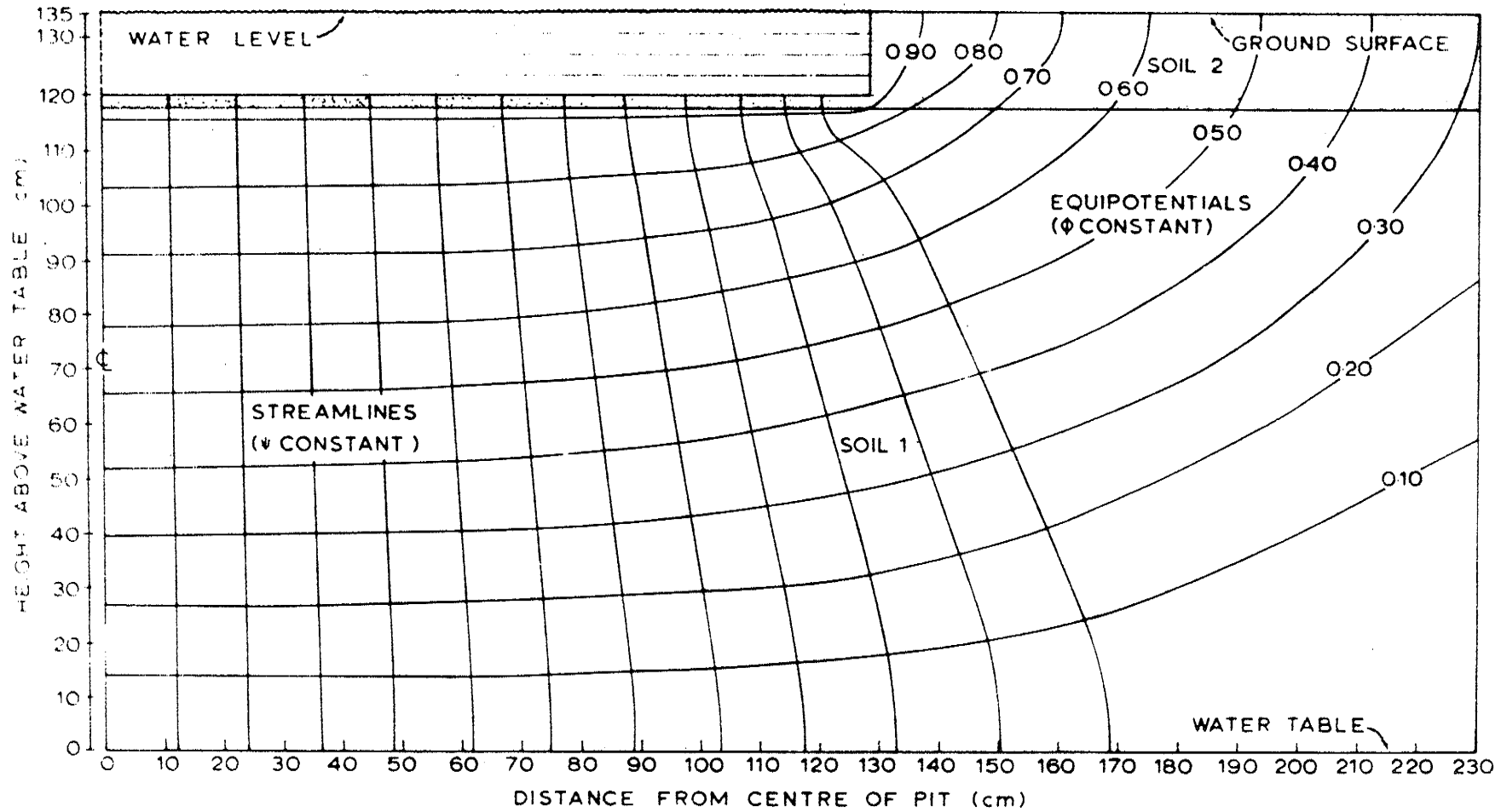Figure 5.28:   Shands No. 2 Pit. Water content profile corresponding to flow net given in Fig. 5.27.
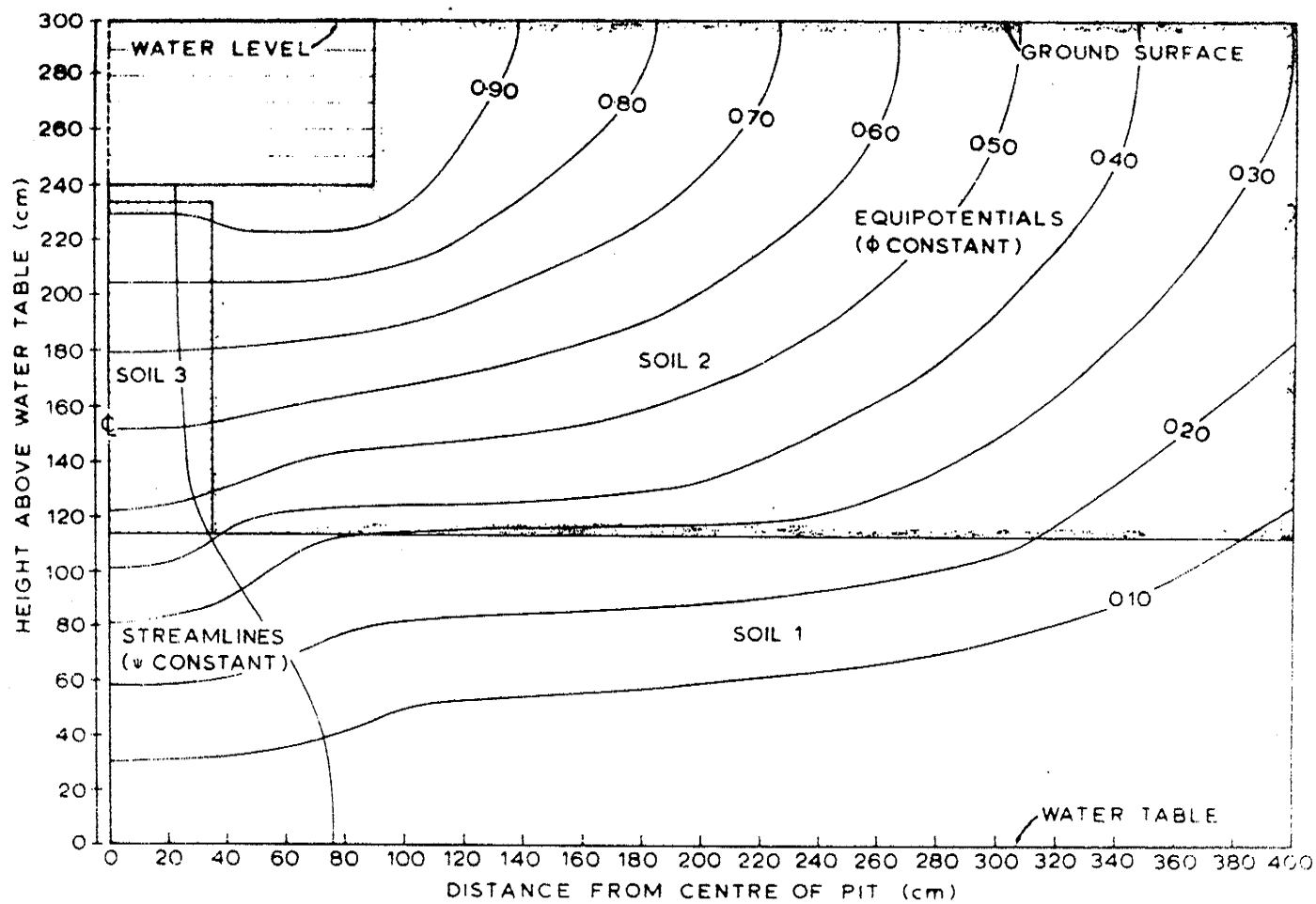
Figure 5.29: Iyah Creek No. 1 Pit. Flow net for a profile similar to Fig. 5.15, but with a thin layer of low conductivity material under the pit.
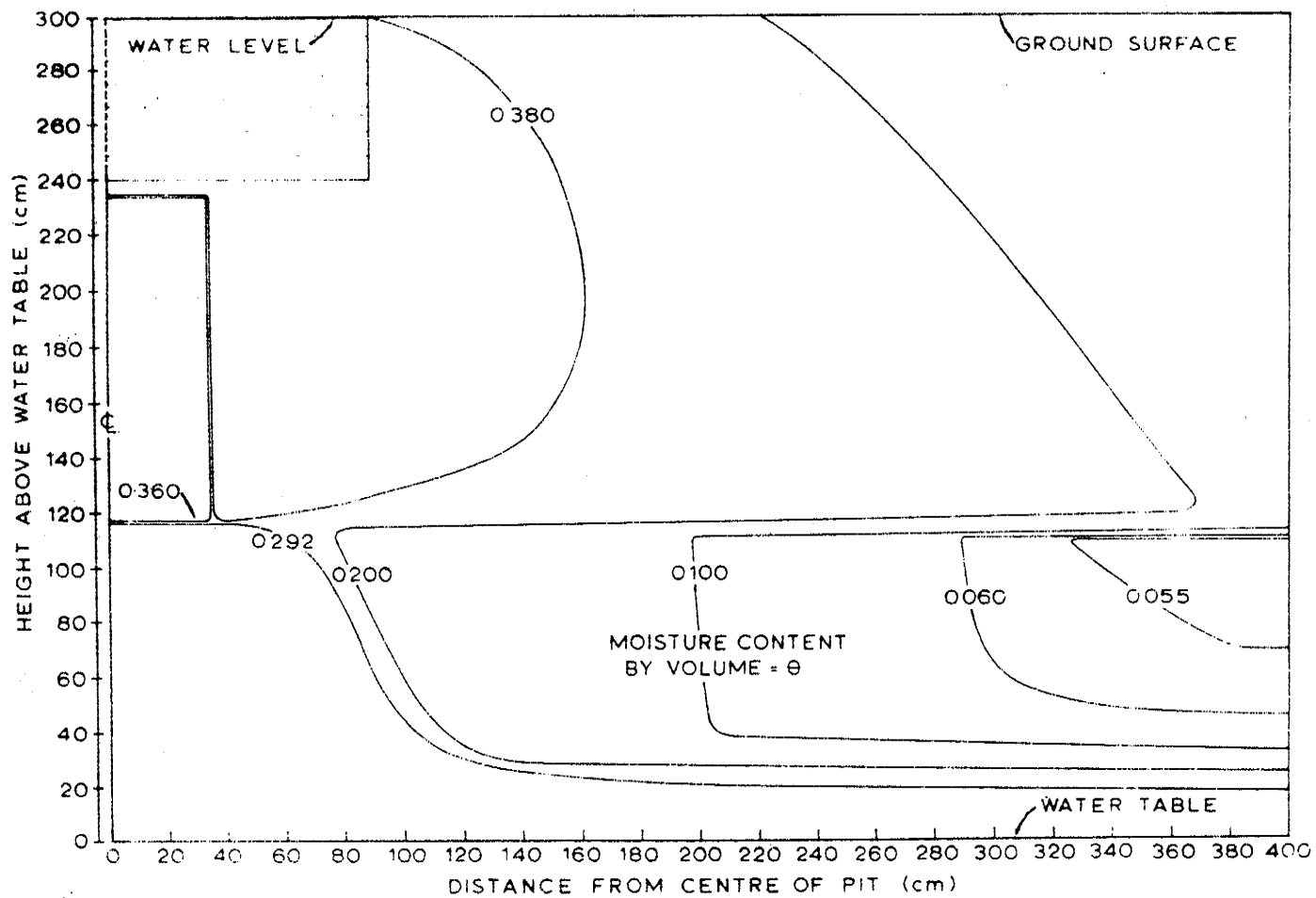
Figure 5.30: Iyah Creek No. 1 Pit. Water content profile corresponding to flow net given in Fig. 5.29.
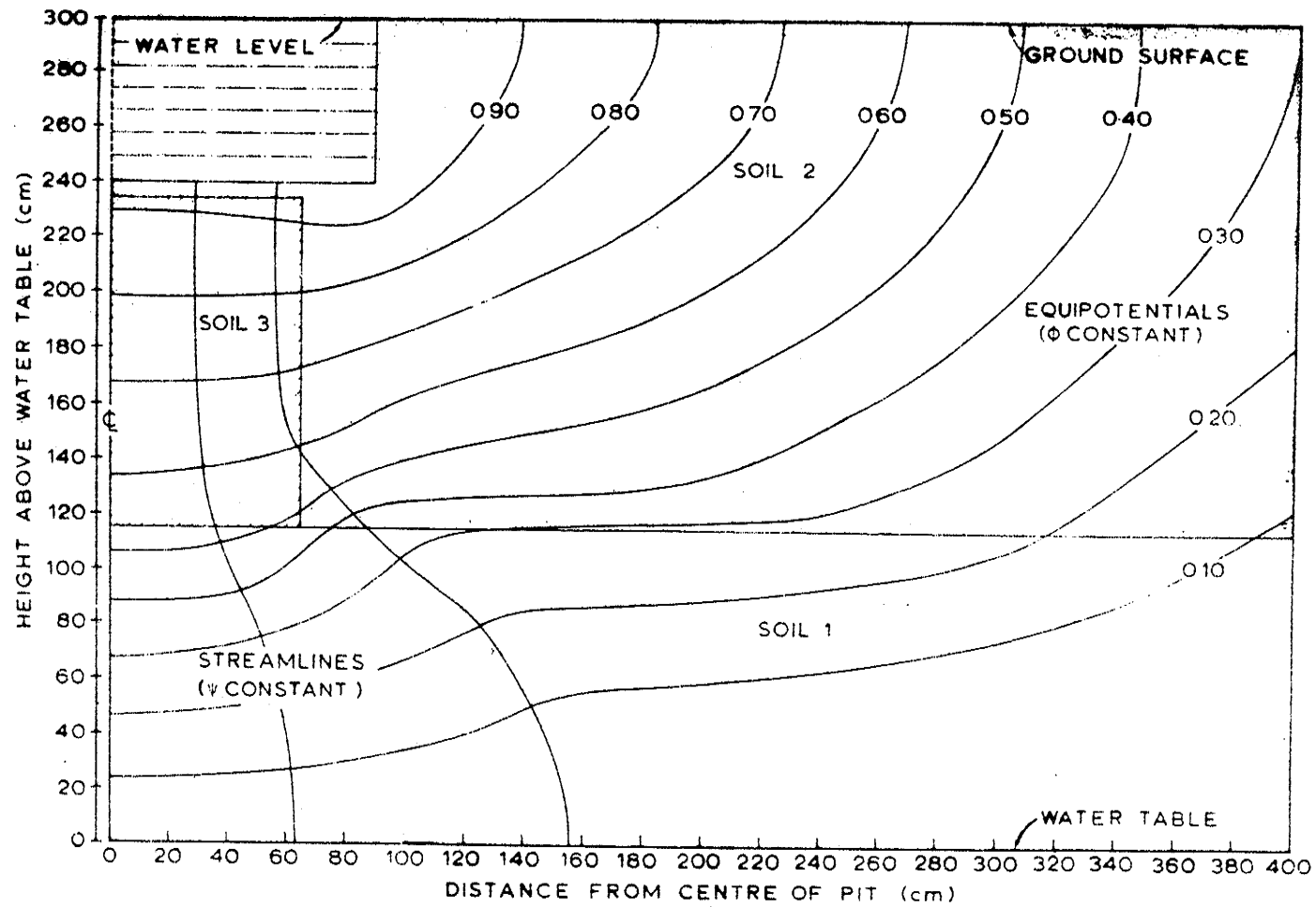
Figure 5.31: Iyah Creek No. 1 Pit. Flow net for a profile similar to Fig. 5.17, but with a thin layer of low conductivity material under the pit.
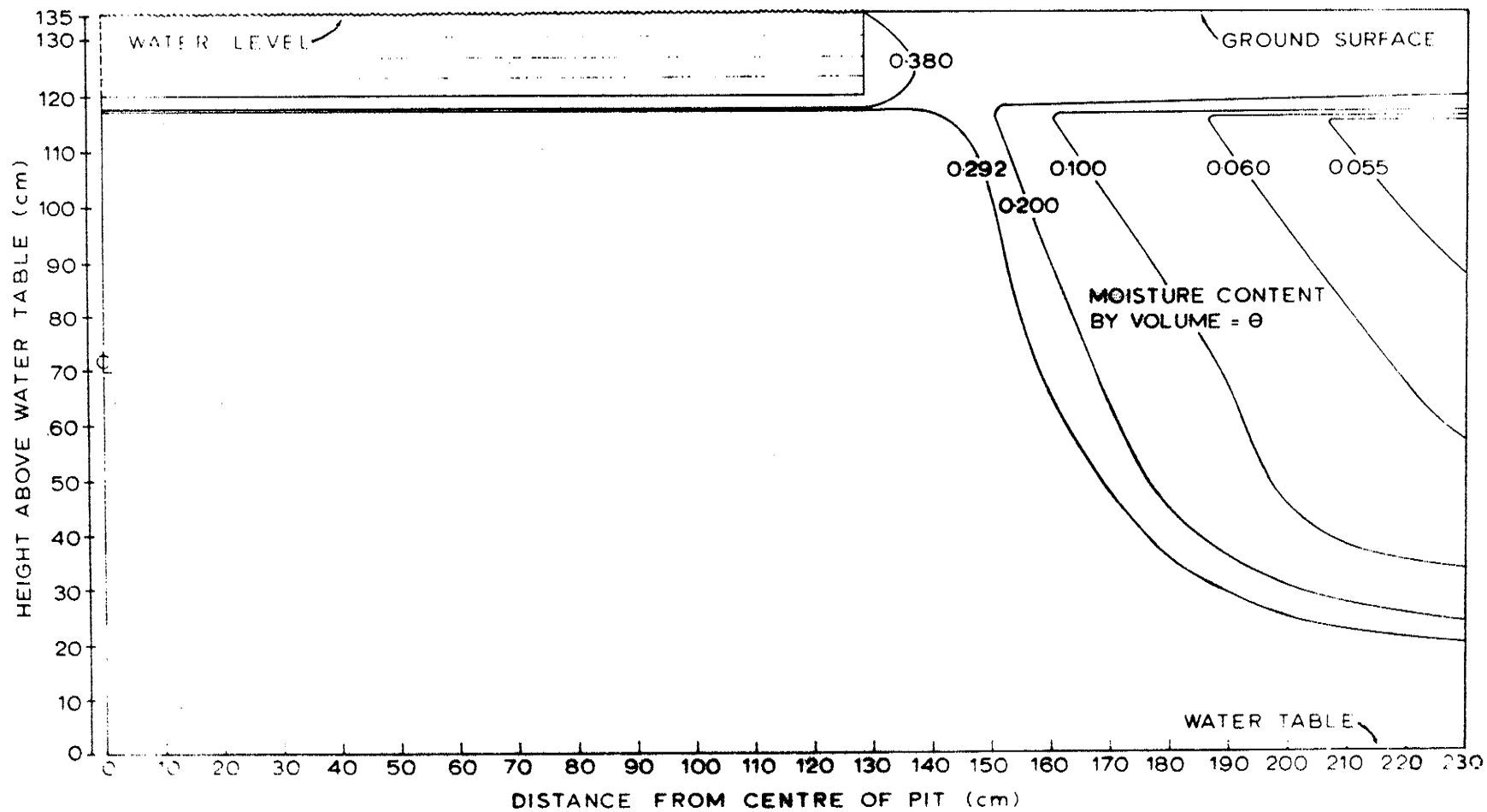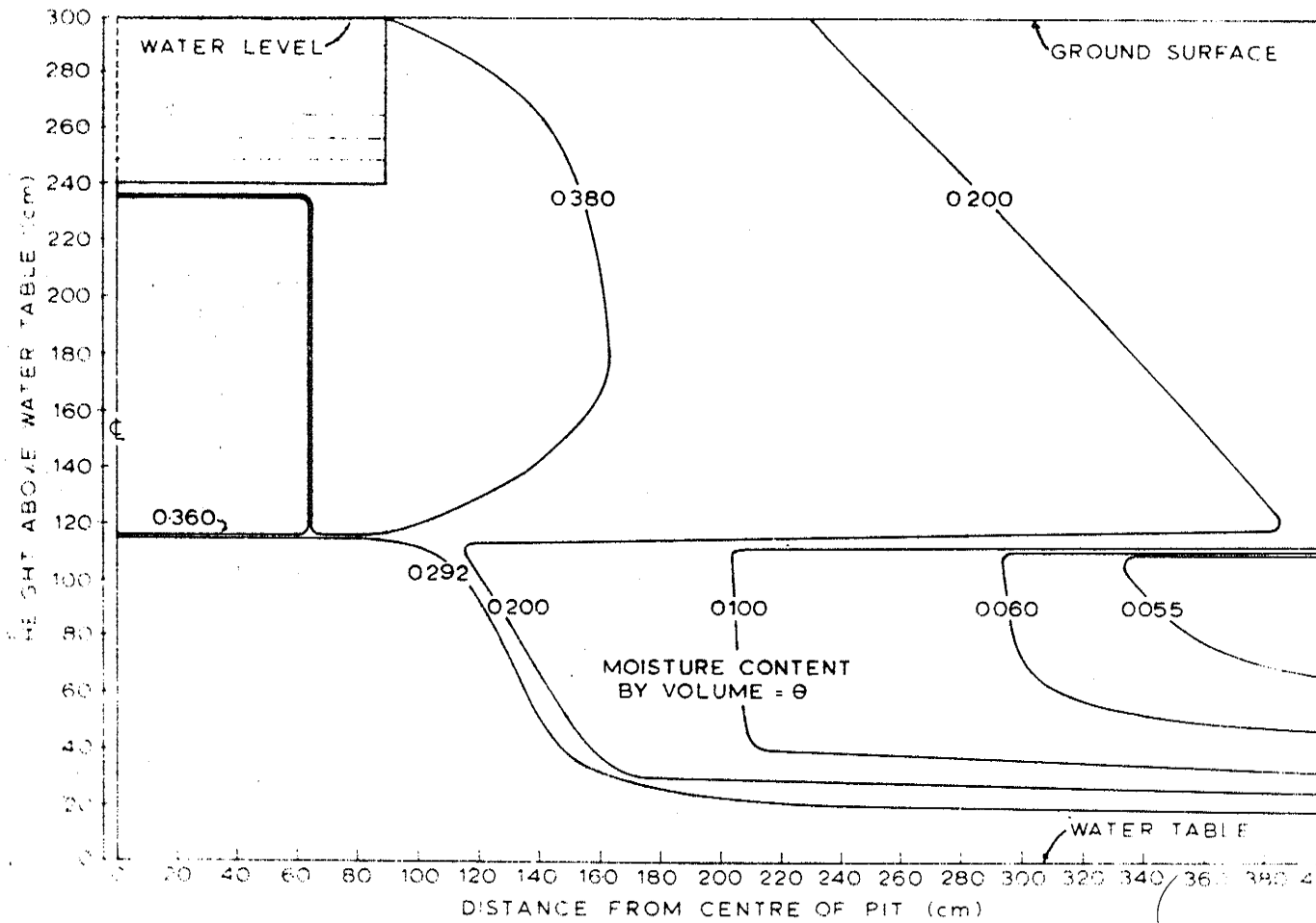
Figure 5.32:   Iyah Creek No. 1 Pit.   Water content profile corresponding to flow net given in Fig. 5.31.

Figure 5.33: Iyah Creek No. 1 Pit. Flow net for a profile similar to Fig. 5.19, but with a thin layer of low conductivity material under the pit.
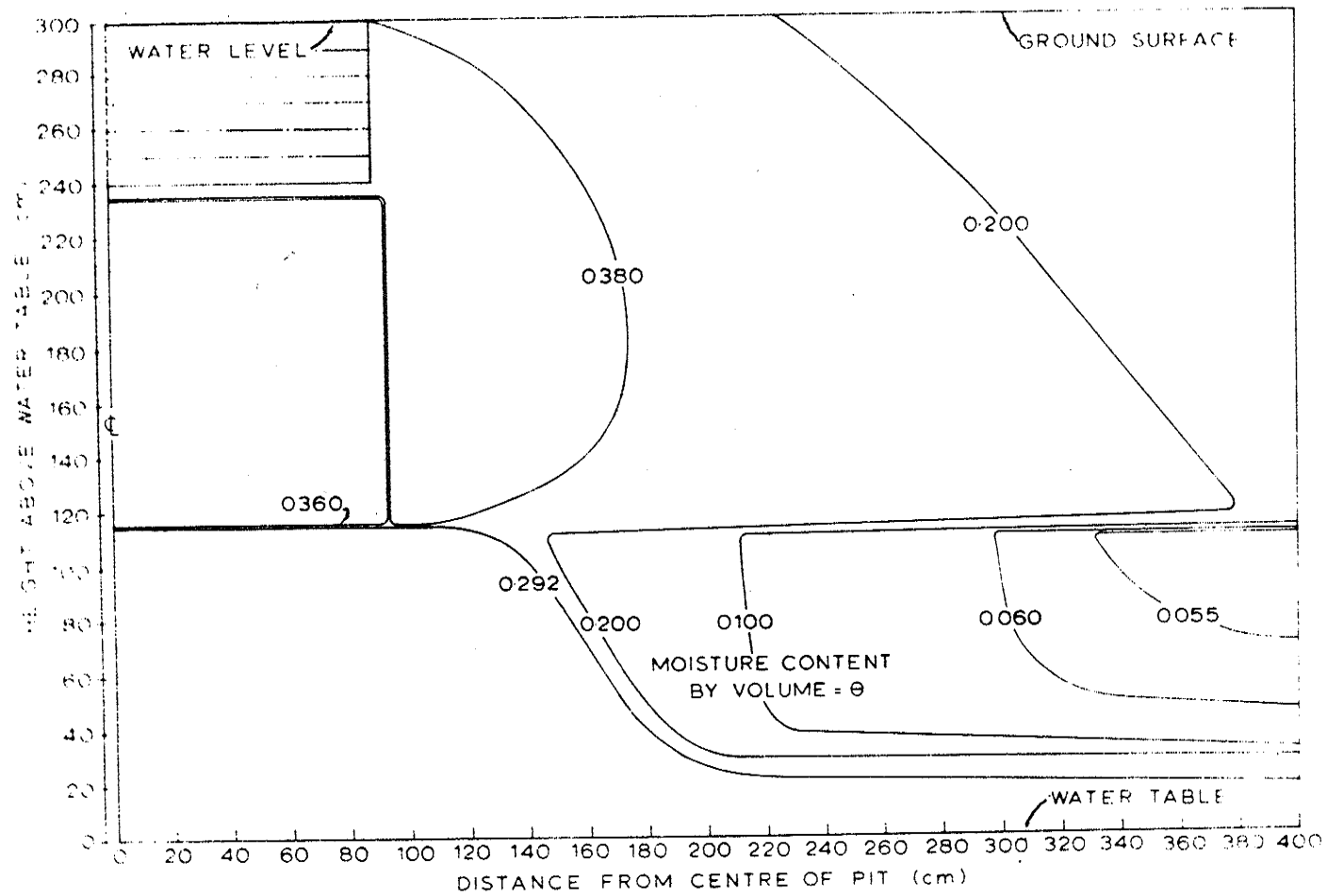
Figure 5.34: Iyah Creek No. 1 Pit. Water content profile corresponding to flow net given in Fig. 5.33.
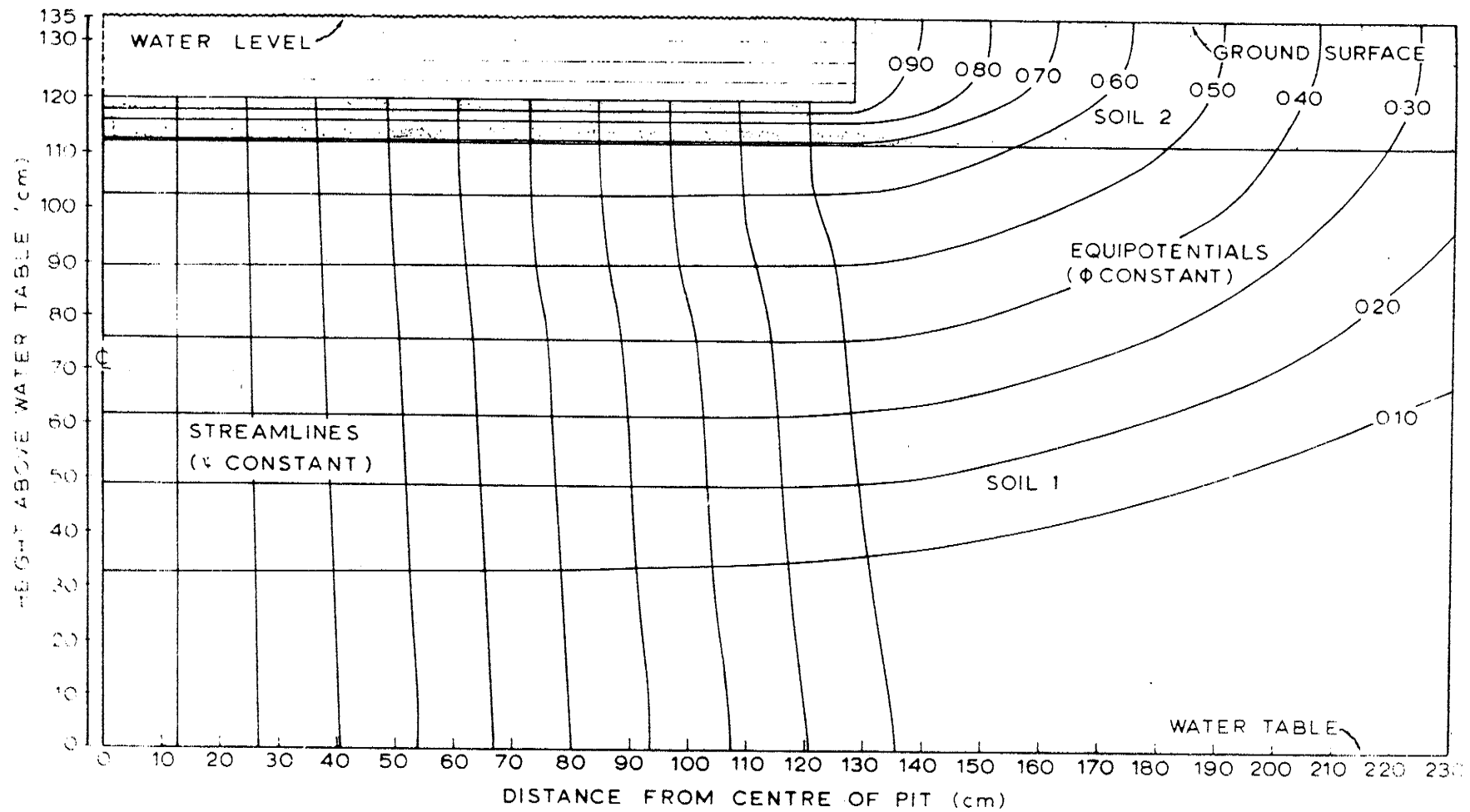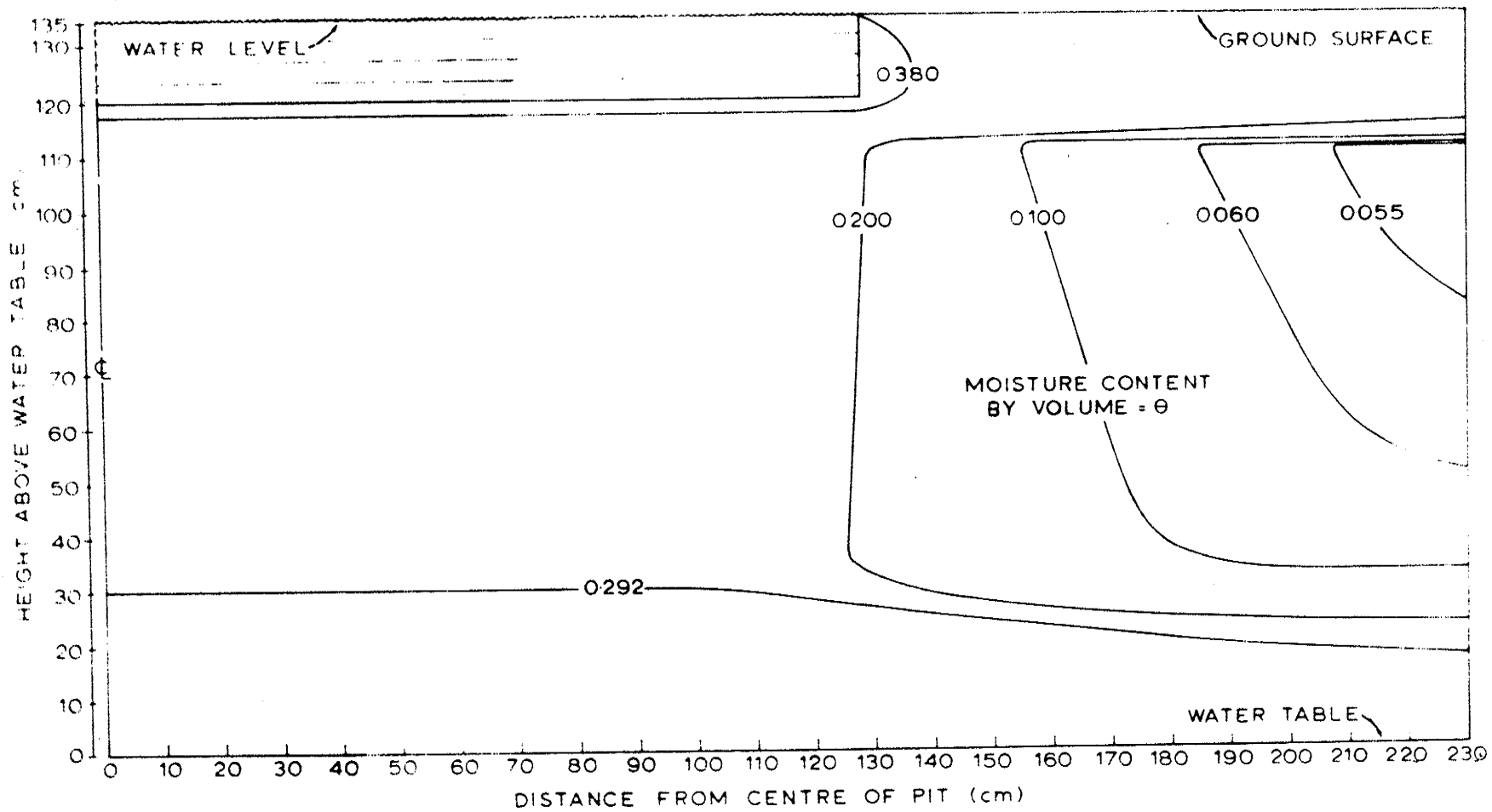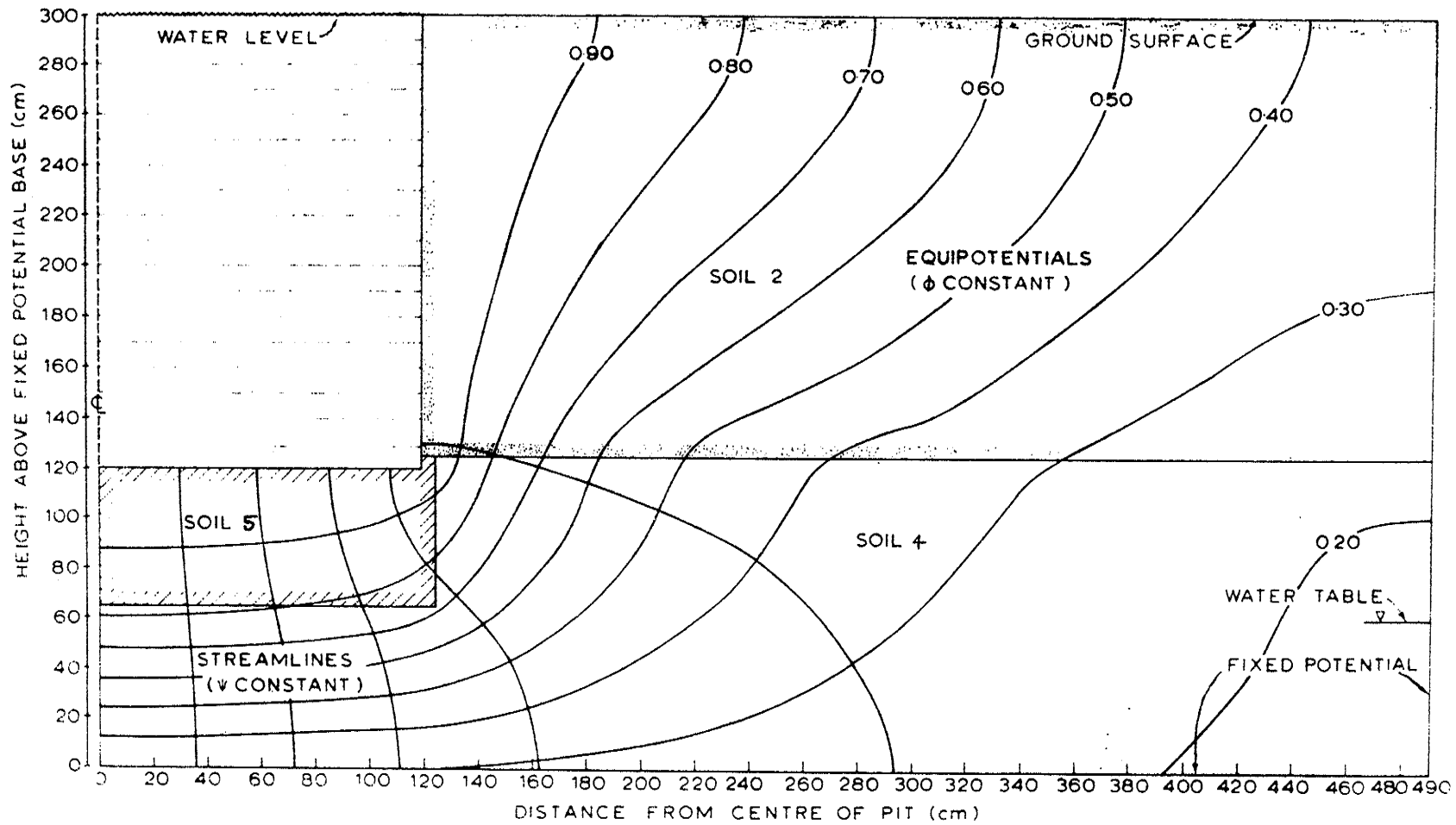
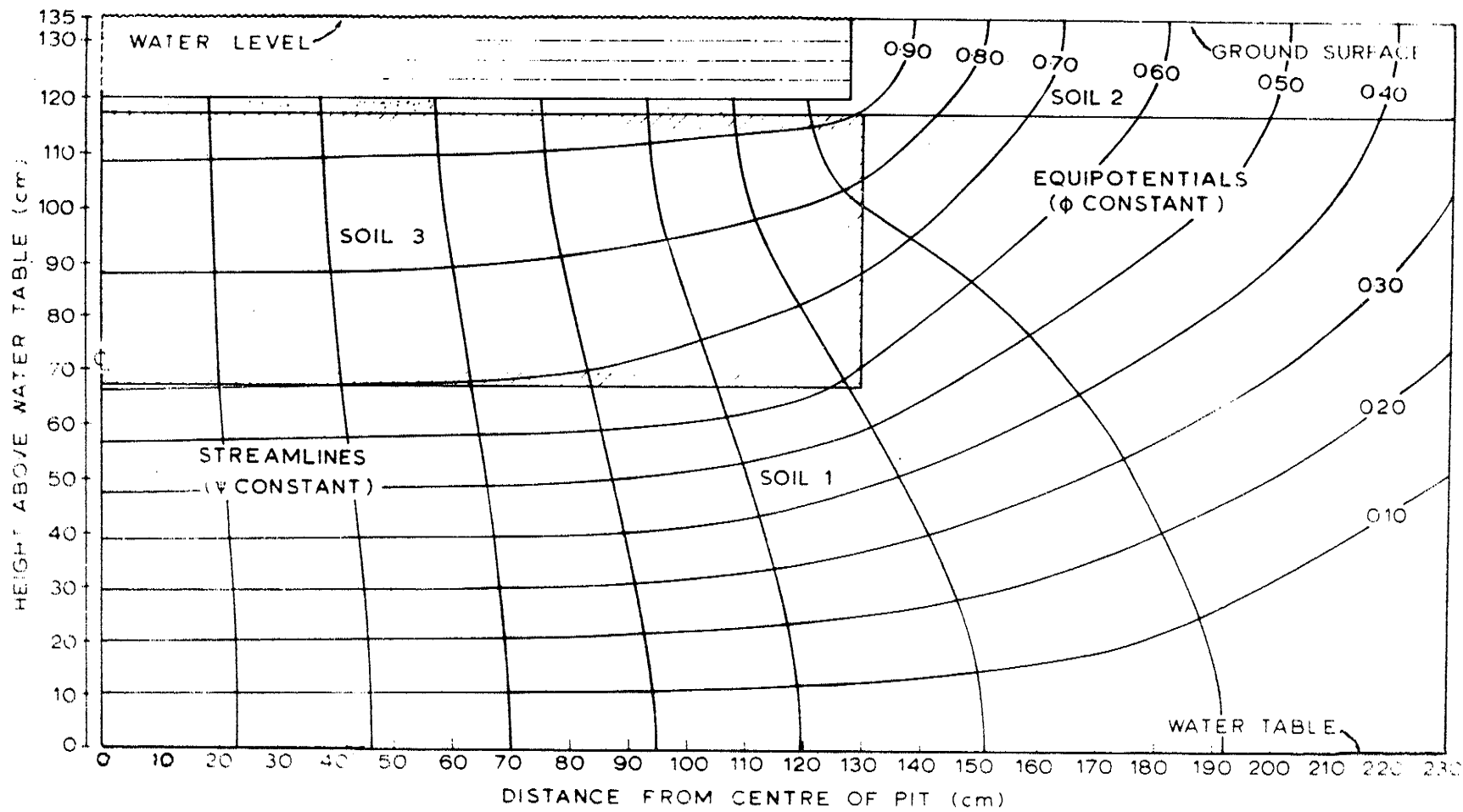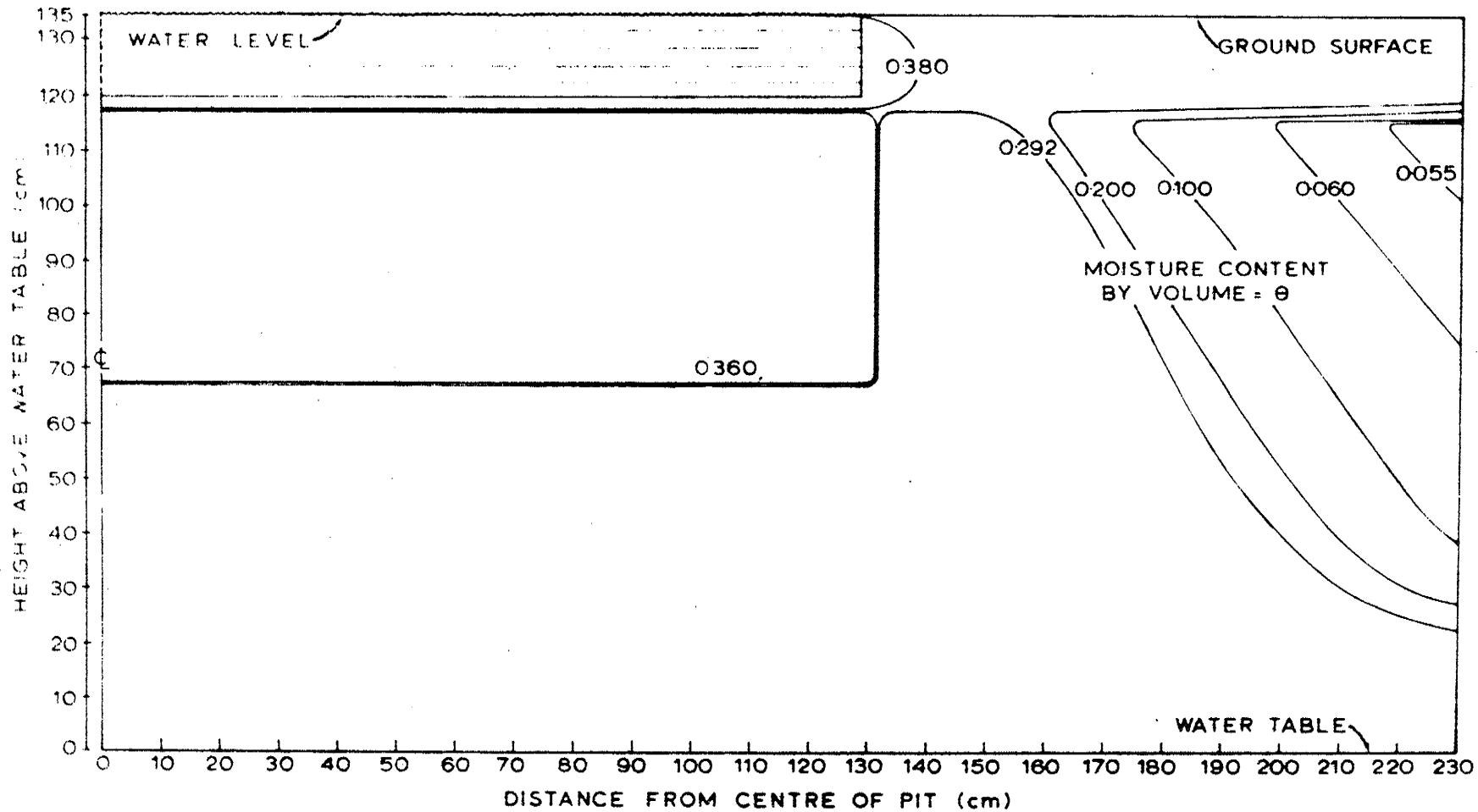Figure 5.35: Shands No. 2 Pit. Flow net for a profile similar to Fig. 5.13, but with a fixed potential base and side portion to demonstrate water table mounding.
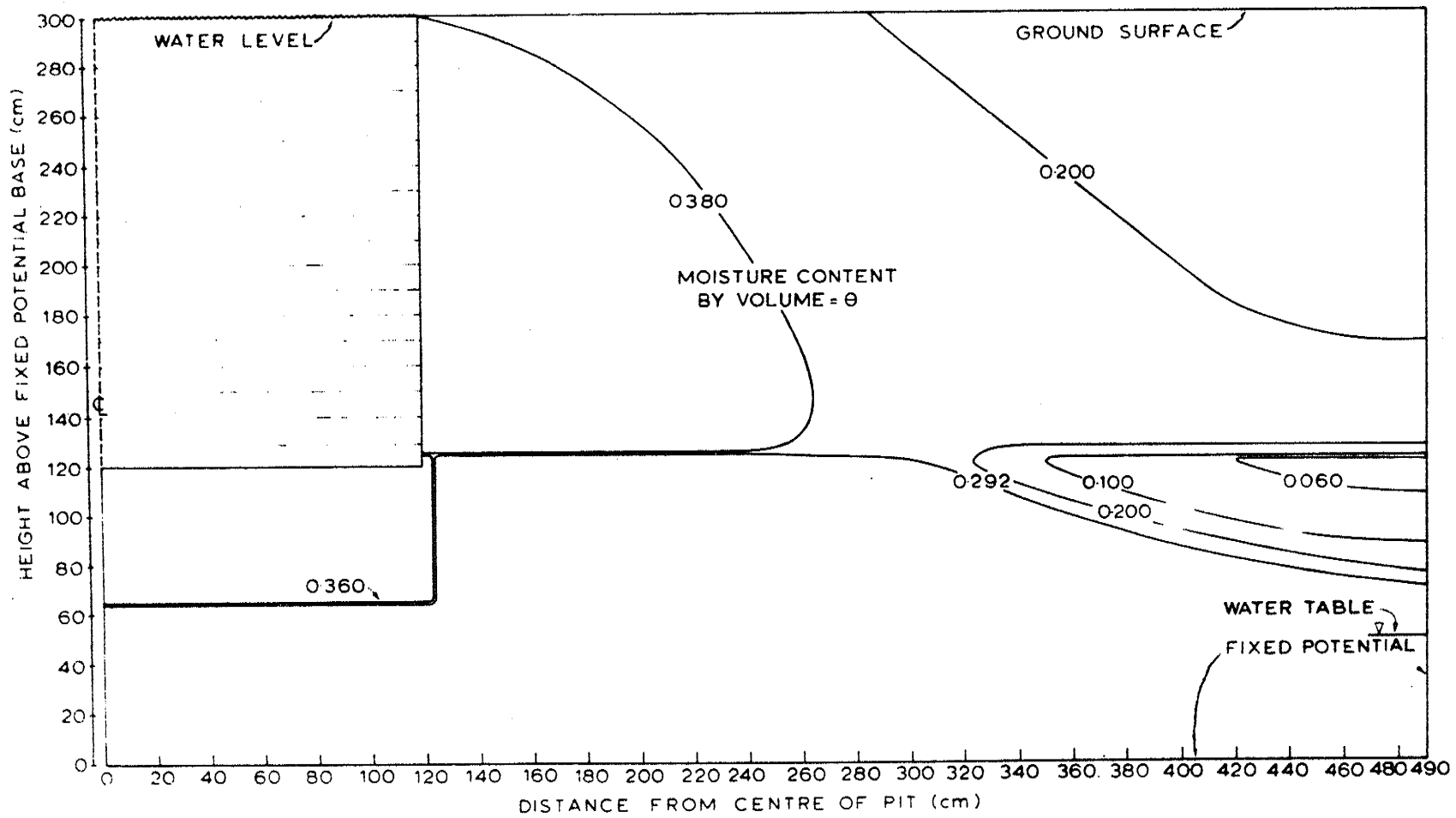
Figure 5.36: Shands No. 2 Pit. Water content profile corresponding to flow net given in Fig.5.35.

5.3.1 Simulation of Shands No. 2 Pit
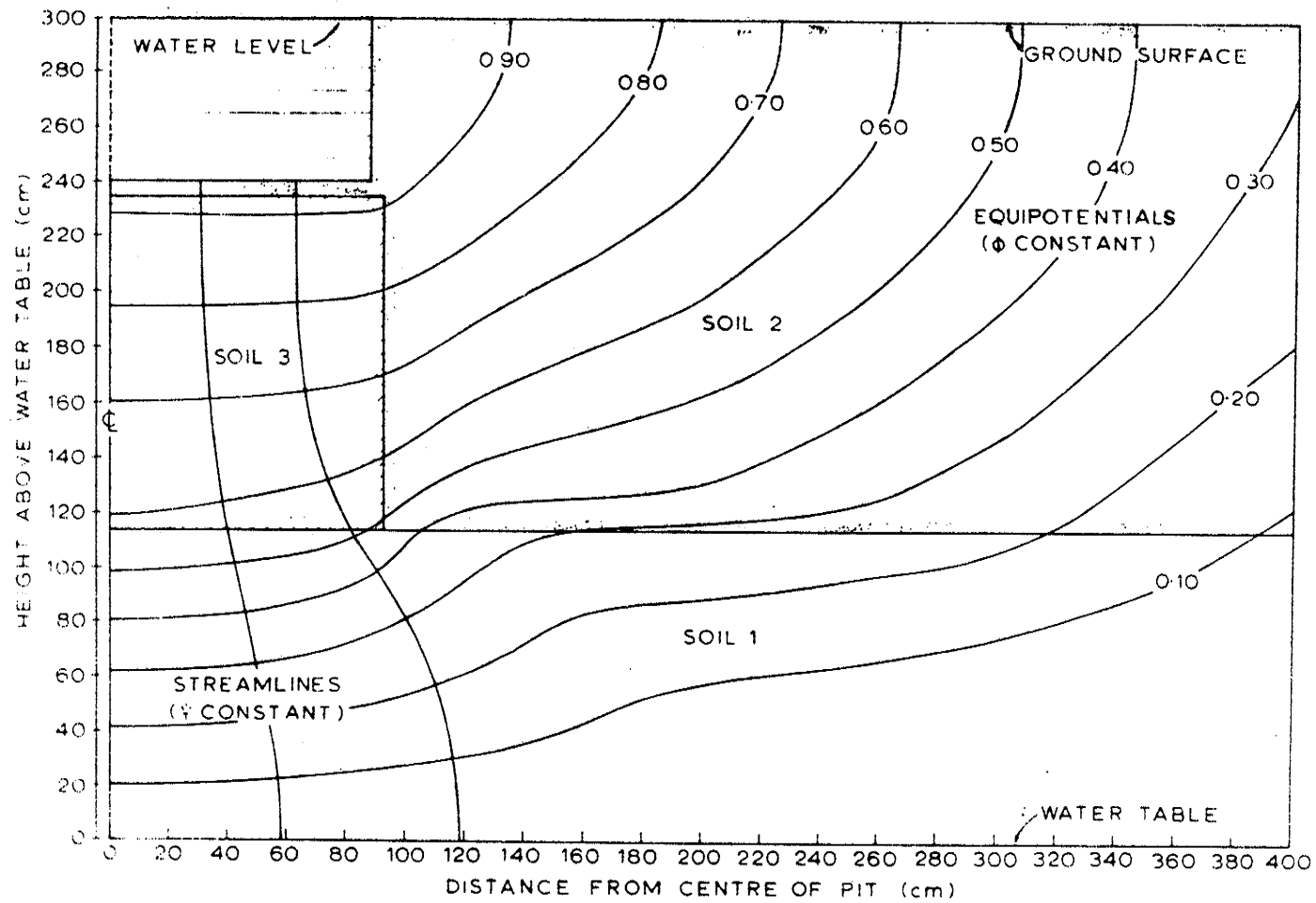
The results for Shands No. 2 Pit discussed in this section are shown in Figures 5.1 to 5.14, and the corresponding intake rates are listed in Table 5.2. The results for 15 cm of ponding into a 120 cm deep profile will be discussed first. Figures 5.1 and 5.2 give the flow net and water content distribution for the simplest case where the entire profile consists of #17 sand. It might be noted that the flow tubes are distributed along the base and up the side of the pit. The width of the saturated zone is only slightly greater at the base of the profile compared with the width of the zone near the bottom of the pit. This indicates that the flow is predominantly vertical; a similar observation was noted in the unsteady state study discussed in Chapter 4.

Figures 5.3 and 5.4 give the flow net and water content distributions for a profile similar to that of Figure 5.1, but with a bank of low conductivity material on the edge of the pit. This profile is very similar to Shands No. 2 Pit before the beach sand was introduced. The main difference caused by the change in bank material, lies in the distribution of the flow tubes at the edge of the pit. The water content profile is also quite different at this point. This flow case is very similar to that considered in the unsteady state case. When Figure 5.4 is compared with Figure 4.1 in Chapter 4, it can be seen that the saturation line for the steady state case corresponds very closely to the saturation line at 50 minutes in the unsteady state study. This shows that steady state flow has almost been attained after 50 minutes of ponded infiltration.

Comparing the intake rates given in Table 5.2 for the two cases (one with a #17 sand bank and the other with a Rubicon bank), it may be noted that the introduction of a low conductivity bank causes only a marginal reduction in intake rate. This is not surprising as the bank is a relatively small part of the area in contact with the recharge water.

Figures 5.5 and 5.6 describe a third case for Shands No. 2 Pit in which a layer of high conductivity material is placed under the recharge pit. This corresponds closely to the introduction of beach sand to Shands No. 2 Pit half way through this Research Project. The comparison of these figures with Figures 5.3 and 5.4 indicates that the introduced sand has a considerable effect on the flow pattern.

The saturated zone is forced away from the pit and the recharge rate (see Table 5.2) increases from 4260 to 6280 m^3 per day. These results clearly demonstrate how the actual introduction of beach sand at Shands No. 2 Pit caused an almost twofold increase in recharge rate. The increase is not twofold in the steady state examples because the properties of the in situ soils at Shands No. 2 Pit are not well enough defined to carry out an exact simulation. However, the potential effect of introducing a layer of high conductivity sand is clearly demonstrated in these examples.

A fourth case for Shands No. 2 Pit is shown in Figures 5.7 and 5.8. In this case a medium layer (approximately 8 cm) of low conductivity material has been placed across the base of the profile to simulate the effect of a clay band or semi-impervious layer. Clay bands are present under this pit but they have discontinuities in them which allows a relatively unimpeded flow of recharge water to the water table. This case was investigated to see what effect a continuous layer of low conductivity material would have on the recharge rate.

A comparison of Figures 5.7 and 5.8 with Figures 5.3 and 5.4 reveals that the impeding layer causes the flow net to move outwards from the pit centreline; the corresponding zone of saturation is also wider. However, the intake rate (see Table 5.2) is only reduced from 4260 to 3690 m^3 per day by the impeding layer. This is a reduction of 13.3%. It is apparent therefore that a continuous layer of low conductivity material, at a reasonable depth in the profile, may only have a marginal effect on the recharge rate.

Three other flow cases simulated for Shands No. 2 Pit are shown in Figures 5.9 to 5.14. In each case the depth of ponding is 180 cm and a low conductivity bank zone exists. The soil profile configuration is the same but different soil properties are used in the two zones below the pit to observe the effect of these on the recharge rate. The cases simulate the expected steady state flow conditions when the pit is full of water. It can be seen that the flow nets are similar in shape but the spacing of the equipotentials and streamlines differ in each case. The water content profiles are almost identical.

The intake rates for the first two cases (Figures 5.9 and 5.11) are very similar although the different soils used in the top zone in each case have quite different conductivity values. It seems therefore that a reasonably large increase in the conductivity of the introduced beach sand

has a negligible effect on the intake rate. In the third case with 180 cm depth of ponding (Figure 5.13) the soils used in the two zones below the pit are the same as those used in Figure 5.5 in which the depth of ponding was 15 cm. The change in intake rate (Table 5.2) due to the greater depth of ponding is considerable, increasing from 6280 to 13900 m^3 per day. It can also be seen by comparing Figures 5.6 and 5.14 that the width of the saturated zone is much greater when the pit is full of water. When this third case (Figure 5.13) is compared with the other two cases having the same soil configuration (Figures 5.9 and 5.11) we note that the higher conductivities used in the third case have approximately doubled the intake rate. It might also be noted from Table 5.1 that the conductivities of the two soil zones below the pit are almost doubled for the third case. The intake rate of 13900 m^3 per day obtained for this case is slightly higher than the maximum rate of about 11100 m^3 per day obtained in the operation of Shands No. 2 Pit. However, the intake rate found for the other two cases (Figures 5.9 and 5.11) with this soil profile shape, and using laboratory determinations of the saturated conductivities of the soils under the pit, gave an intake rate of only 6980 m^3 per day approximately. This is lower than the measured recharge rate of 11100 m^3 per day in the pit.

There are two major factors which could cause this difference. Firstly it has been assumed in all these cases that the water table is fixed at a depth of 120 cm below the base of the pit. In practice the water table would rise from this position as recharge proceeds. Secondly, the laboratory determination of the saturated conductivities of the field soils in their disturbed state may not relate very closely to the in situ field conductivities. More exacting field tests would have to be carried out to derive a closer correspondence between field intake rates and simulated intake rates. However, such an exercise would be of limited usefulness as the most important aspect of these simulation studies is that it enables comparisons of various configurations to be made. The absolute values of the intake rates are less important.

The cases described in this section give a clear picture of the behaviour of Shands No. 2 Pit under different flow conditions. Further information on the response of this pit to surface clogging conditions is given in Section 5.3.3, and the effect of water table mounding under Shands No. 2 Pit is discussed in Section 5.3.4.

5.3.2 Simulation of Iyah Creek No. 1 Pit

During the course of this Research Project the question arose as to the effect the widening of the slot of introduced sand in Iyah Creek No. 1 Pit would have on the intake rate. To this end three cases were investigated for this pit with slot widths of 70 cm, 130 cm and 190 cm. The results are shown in Figures 5.15 to 5.20. In each case the depth of ponding is 60 cm and the profile depth between the bottom of the pit and the water table is 240 cm. Three soils are used to simulate the soil profile in each case. The slot material is a high conductivity sand; the natural soil from the surface to the bottom of the slot is a low conductivity sandy loam; and the natural sand below the tongue is a medium conductivity sand. The properties of each soil are listed in Table 5.1.

Ideally the width of the slot would have been increased in even multiples of the initial width, but this was not possible because of the need to define the width by a fixed number of node points. Only half the profile was simulated using the same assumption as for Shands No. 2 Pit, namely that the profile is symmetrical about the pit centreline.

Referring to Figures 5.15, 5.17 and 5.19 it can be seen that the basic shape of the flow net is similar for each case. Virtually all the flow passes through the slot of introduced sand, and the flow is predominantly vertical. The shapes of the water content profiles given in Figures 5.16, 5.18 and 5.20 are also very similar. As the width of the slot is increased the saturated zone is offset further away from the pit centreline.

In Table 5.2 the intake rates for the three cases are given as 3070, 4750 and 6220 m^3 per day respectively. By taking a basic slot width of 65 cm and correcting the 70 cm width reading downwards, and the 190 cm width reading upwards to 195 cm, it is possible to get a measure of the increase in intake rate for doubling and trebling the slot width. The readings after correcting them to the new widths (65 cm, 130 cm and 195 cm) become 2850, 4750 and 6380 m^3 per day respectively. This indicates that doubling the slot width increases the intake rate by 67%, and trebling it increases the rate by 124%. Although doubling of the slot width causes an increase of 67% in intake rate, increasing the width by the same amount again only causes an additional

increase of 57% in the intake rate (i.e. 124%-67%).

The actual percentage increases to be expected in Iyah Creek No. 1 Pit would be similar to those given above, but slight differences may arise if the soil profile shape, ponding depth, or soil properties, are different from those assumed in the examples.

The effects of surface clogging on the three Iyah Creek profiles are discussed in the following section.

5.3.3 Studies of Surface Clogging

As has been discussed earlier in this report, the build up of sediment on the bottom of a recharge pit, together with biological activity, causes a reduction in intake rate with time. To simulate the effect of this clogging action on the flow nets and water content profiles, steady state studies were carried out using the same soil profiles described in the preceding two sections, but with a layer of low conductivity material just under the bottom of the pit.

The surface clogging cases investigated using the Shands No. 2 Pit profiles are given in Figures 5.21 to 5.28. Figures 5.21 and 5.22 give the surface clogging case equivalent to Figures 5.3 and 5.4. In this case the impeding layer has been defined in the computer model by assigning the properties of Rubicon sandy loam to the top row of nodes across the base of the pit. This is equivalent to an impeding layer of approximately 0.8 cm in thickness, hereafter termed a 'thin' impeding layer. The flow nets indicate that the equipotentials are more closely spaced near the bottom of the pit for the surface clogging case. As a consequence the equipotentials are spaced further apart in the rest of the profile. Comparing the water content profiles, the saturation zone is seen to be wider for the unimpeded flow case. There are also differences just under the pit due to the layer of finer soil being present. The intake rate for the surface clogging case is 3690 m^3 per day and for the unimpeded case is 4260 m^3 per day. Accordingly, the layer causes a reduction of 13.3% in the intake rate.

Figures 5.23 and 5.24 describe a similar profile to that discussed above but with a greater thickness of Rubicon material under the bottom of the pit. In this case the impeding layer has been formed by assigning the properties of Rubicon sandy loam to the two top rows of nodes across the base of the pit; these are spaced 5 cm apart in the vertical direction. This is equivalent to a layer approximately 8 cm in thickness hereafter termed a 'medium' impeding layer. Comparing

these figures with Figures 5.3, 5.4, 5.21 and 5.22 it may be noted that the increased depth of fine material (simulating a more severe case of surface clogging) causes a significant change in the flow net and water content profiles. The equipotentials are spaced close together near the bottom of the pit and are then uniformly spaced at a wider interval through most of the profile except near the base where the spacing is wider again. The water content profile in Figure 5.24 reveals that there is a uniformly unsaturated zone through-out most of the profile depth with zones of saturation just below the bottom of the pit, and above the water table. It is clear that the surface clogging effect has reduced the flow to such an extent that the profile has become largely unsaturated. The intake rate from Table 5.2 for this case is 1040 m^3 per day compared with the original unimpeded intake rate of 4260 m^3 per day. This is a reduction of 75.7%. The development of this unsaturated zone under severe clogging condit-ions was detected in field measurements taken at Shands No. 2 Pit. This aspect will be discussed in Part B.

The third surface clogging case investigated for Shands No. 2 Pit is given in Figures 5.25 and 5.26. The soil profile is the same as the case described by Figures 5.5 and 5.6. Comparing the figures it can be seen that the flow nets are very similar except in the zone just under the pit where the spacing of equipotentials is closer for the surface clogging case. The water content profiles are also similar except in the region near the bottom of the pit but the saturation zone is wider for the unimpeded flow case. The intake rates given in Table 5.2 for the two cases (i.e. Figures 5.5 and 5.25) indicate that the reduction in flux is from 6280 to 6110 m^3 per day. This is a reduction of only 2.8%. The reduction in flux is much less for this soil configuration compared with the 13.3% reduction experienced when there is only one soil present below the pit (Figures 5.3 and 5.21). It is apparent that the very high conductivity of the SOIL 3 zone compensates for the impeding layer of low conductivity material.

The last surface clogging case considered for Shands No. 2 Pit is shown in Figures 5.27 and 5.28. This profile is similar to that given in Figures 5.7 and 5.8. Comparing the flow nets for the two cases it may be noted that they are almost the same except near the impeding layer. The water content profiles show that the impeding

layer has narrowed the zone of saturation slightly. The only other difference in the water content profiles is in the region near the impeding layer. The low conductivity zone has reduced the intake rate from 3690 to 3120 m^3 per day; an effective reduction of 13.3%.

The three surface clogging examples for Iyah Creek No. 1 Pit are shown in Figures 5.29 to 5.34. The soil profiles are identical (except for the thin layer of low conductivity material under the pit) to examples given in Figures 5.15 to 5.20, and discussed in Section 5.3.2. Comparing the figures with the same widths of slot material, it can be seen that the introduction of the impeding layer has reduced the width of the saturated zone in each case, and distorted the equipotentials near the bottom of the pit. The distortion is most noticeable in Figure 5.29 for the 70 cm slot width, and as in all the other surface clogging examples, the equipotentials near the bottom of the pit are more closely spaced.

Table 5.2 shows that the impeding layer has caused a reduction in intake rate for each case. For the 70 cm slot the reduction in flux is 20.9%, for the 130 cm case the reduction is 13.2%, and for the 190 cm slot the impeding layer reduces the flux by 6.7%. The effect of the impeding layer is much more severe with the narrowest width of slot material. The reason for this can be seen by comparing the flow nets for the three surface clogging examples. In Figure 5.29 (70 cm slot width) the position of the equipotentials is largely controlled by the SOIL 2 material and the equipotentials in the slot material can only distort to a limited extent to compensate for the impeding layer. As the width of the slot increases the equipotentials distort more freely to compensate for the low conductivity zone.

5.3.4 <u>A Study of Water Table Mounding</u>

One case of water table mounding was investigated to see how the flow net and intake rate are affected by the formation of a water table mound. In all the steady state cases considered in the preceding sections, the water table was assumed to remain horizontal and at the same elevation under recharge conditions. This can only occur in practice when a gravel substratum underlies the profile or when the zone below the water table has a very high horizontal conductivity compared with the vertical conductivity of the material above the water table.

The water table mounding case is shown in Figures 5.35 and 5.36.
The soil properties and configuration are the same as the case
described by Figures 5.9 and 5.10. The right hand boundary of the
profile was set up as a fixed hydraulic head boundary in the lower
part, and in the upper part was set as a no-flow boundary. The base
boundary was set up as a fixed hydraulic head boundary by assuming
the pressure head at the base to be 90 cm under the pit tapering to
60 cm of water at the right hand boundary. By comparing this figure
with Figure 5.9 it can be seen that the flow has a greater tendency
to move horizontally because of the mound under the pit. An examin-
ation of the water content profiles for the two cases shows that the
zone of saturation is wider in the water table mounding case.

It is difficult to simulate a fixed hydraulic head or impermeable
base using a steady state program because there must necessarily be
flow through the right hand boundary of the profile. There is how-
ever insufficient information to tell how deep the flow zone should
be on the boundary and this has to be assessed before the profile can
be simulated. The development of a steady state flow system under
these types of base boundary condition would be dependent on boundary
conditions imposed at a large distance from the pit. In fact it is
unlikely that a true steady state profile could develop under a
recharge pit with a fixed potential base boundary condition unless
there was some recognizable boundary nearby, such as a river.

This water table mounding case is given purely as an example of
how the flow system would be affected by a water table mound. The
actual behaviour of Shands No. 2 Pit probably depends on a combination
of a water table and a fixed hydraulic head boundary. A true steady
state system would only exist for a short time if at all because of
variations in the intake rate due to surface clogging, pit water
level fluctuations, and other factors such as interaction with other
recharge pits and pumping from a well nearby. However it can be
seen from this water table mounding example, that if a mound develops
it will tend to inhibit the flow of recharge water, and it is
probably a combination of this factor, together with sedimentation
and biological activity, that causes the intake rate of this pit to
decrease with time. The intake rates for Figures 5.9 and 5.35 in
Table 5.2, indicate that the water table mound in this example has
reduced the intake rate from 7000 to 4470 m^3 per day - a reduction of
36.2%. If the depth of profile between the bottom of the pit and the

water table was greater, the effect of the water table mound would be much less severe.

5.4 SUMMARY OF RESULTS

The use of steady state solutions enabled a comprehensive study of the behaviour of Shands No. 2 Pit and Iyah Creek No. 1 Pit to be carried out. These solutions considerably expand the amount of information available from the unsteady state studies discussed in Chapter 4. The results summarized below are for assumed soil profile shapes, which closely resemble the measured configuration of the two pits when this research project was carried out.

Summary of results for Shands No. 2 Pit.

- the effect of an impermeable bank on the flow net and intake rate was minimal as most of the flow took place through the bottom of the pit.

- the introduction of a layer of high conductivity material under the pit increased the intake rate by 47.5%.

- increasing the depth of ponding in the pit from 15 cm to 180 cm improved the intake rate by 122%.

- the effect of a medium layer of low conductivity material deep in the profile was to reduce the recharge rate by 13.3%.

- the position of the saturated front in a steady state profile similar to the profile used in Section 4.3 (unsteady state flow), was almost the same as the saturation line at 50 minutes from the start of infiltration. This indicates that the unsteady state flow case had almost reached steady state flow conditions at that time.

- a water table mound base boundary condition was used in one case. It reduced the intake rate by 36.2% compared to the same profile with a water table base. If the profile depth between the base of the pit and the initial water table level had been greater, the percentage reduction would have been less.

- the introduction of a thin layer of low conductivity material along the bottom of the pit reduced the intake rate by 13.3% when the profile consisted of uniform sand. When the layer of beach sand was introduced, the same layer of low conductivity material only reduced the intake rate by 2.8%.

- a medium layer of the same low conductivity material across the bottom of the pit, and overlying a uniform sand profile, reduced the intake rate by 75.7%. An unsaturated zone developed under the pit due to the surface clogging effect of this layer.

Summary of results for Iyah Creek No. 1 Pit.

- this pit was simulated using three widths of introduced slot material. The smallest slot width (approximating the actual width of this slot in the pit) was doubled and then trebled in width. Doubling caused a 67% increase in intake rate and trebling an increase of 124%.

- each of the three widths of slot material was simulated with a thin layer of low conductivity material overlying the slot. The reduction in intake rate for the smallest slot was 20.9%, for the doubled width it was 13.2%, and for the trebled width it was 6.7%. It is apparent therefore that the narrower the width of the slot material, the more sensitive the pit is to surface clogging effects.

The results produced in this Chapter are only a limited sample of the many different cases that could be simulated using the steady state program. It is apparent that such a program could be used to great advantage in the design of new recharge pits and in the modification and management of existing pits. A careful assessment would need to be made of the importance of simulating various cases, as a considerable amount of computer time and analysis time is required for each case.

REFERENCES

AMERMAN, C.R. (1969). Finite difference solutions of unsteady two-dimensional, partially saturated porous media flow. Ph.D. thesis, 136 pp., Purdue University.

AIREY, P.L., CALF, G.E., HARTLEY, P.E., ROMAN, D. and SPRAGG, W.T. (1974). The use of environmental isotopes and artificial tracers to study recharge to groundwater in the Burdekin Delta, Queensland. IAEA Symposium on Isotope Techniques in Groundwater Hydrology, Vienna, Austria.

BRUTSAERT, W.E. (1971). A functional iteration technique for solving the Richards equation applied to two-dimensional infiltration problems. Water Resour. Res. 7(6), 1583-1596.

DOUGLAS, J., PEACEMAN, D.W. and RACHFORD, H.H. (1959). A method for calculating multi-dimensional immiscible displacement. A.I.M.E. Trans., 216, 297-308.

FREEZE, R.A. (1971). Three-dimensional, transient, saturated-unsaturated flow in a groundwater basin. Water Resour. Res., 7(2), 347-366.

NELSON, R.W. (1962). Steady darcian transport of fluids in heterogeneous partially saturated porous media, Part 1, Mathematical and numerical formulation. HW - 72335 PT1, 30 pp.

NWA, E.U., TAYLOR, G.S., CURRY, R.B. and TAINGANIDES, E.P. (1971). Two-dimensional analysis of natural rainfall infiltration into a sloping plane, 1. Theory. A.S.A.E. Annual Meeting, Washington State Univ.

O'SHEA, J.A. (1967). Replenishment of underground water supplies - Burdekin Delta, Queensland. Civil Engineering Transactions, Inst. of Engineers, Aust., CE9, 117-126.

PERRENS, S.J. and WATSON, K.K. (1976). Two dimensional infiltration and redistribution with non-uniform surface flux. Submitted for publication to Water Resources Research.

PEACEMAN, D.W. and RACHFORD, H.H. (1955). The numerical solution of parabolic and elliptic differential equations. J. Soc. Indust. Appl. Maths., 3, 28-41.

REISENAUER, A.E., NELSON, R.W. and KNUDSEN, C.N. (1963). Steady darcian transport of fluids in heterogeneous partially saturated porous media, Part 2, The computer program. HW-72335 PT2, 88 pp.

RICHTMEYER, R.P. and MORTON, K.W. (1967). Difference methods for initial value problems. Wiley, New York.

RUBIN, J. (1968). Theoretical analysis of two-dimensional transient flow of water in unsaturated and partially saturated soils. Soil Sci. Soc. Amer. Proc., 32, 607-615.

TOPP, G.C. (1969). Soil-water hysteresis measured in a sandy loam and
    compared with the hysteretic domain model. Soil Sci. Soc. Amer.
    Proc., 33, 645-651.

VERMA, R.B. and BRUTSAERT, W. (1970). Unconfined aquifer seepage by
    capillary flow theory. A.S.C.E. Proc., J. Hyd. Div., 69(HY6), 1331-1344.

VOLKER, R.E. and STARK, K.P. (1973). Development of a numerical model
    of a coastal aquifer subject to recharge. Hydrology Symposium,
    Perth, pp.111-118.

WATSON, K.K. (1971). Numerical analysis of finite depth problems in
    soil-water hydrology. Nordic Hydrol., 2, 1-22.

WATSON, K.K. and CURTIS, A.A. (1974). Numerical analysis of vertical water
    movement in a bounded profile. 5th Australasian Conference on
    Hydraulics and Fluid Mechanics, Christchurch, New Zealand.

WATSON, K.K. and WEBB, S.N. (1974). Studies in water movement from groundwater
    recharge trenches. 5th Australasian Conference on Hydraulics and
    Fluid Mechanics, Christchurch, New Zealand.

WHISLER, F.D. and KLUTE, A. (1967). Rainfall infiltration into a vertical
    soil column. Trans. Amer. Soc. Agr.Eng., 10, 391-395.

WHISLER, F.D. and WATSON, K.K. (1969). One-dimensional gravity drainage
    of uniform columns of porous materials. J. Hydrol., 6, 277-296.

44.

er

lwater

l

PART B
FIELD STUDIES

1. INTRODUCTION

Part A of this report entitled "Numerical Studies" summarized the one dimensional and two dimensional numerical approaches and contained the results of several numerical simulations of the behaviour of two recharge pits—Shands No. 2 Pit and Iyah Creek No. 1 Pit. In Part B the results of field studies carried out at Shands No. 2 Pit are presented.

The data and results of the field studies are presented in three chapters. Chapter 2 details the equipment used in obtaining the various field measurements and the design and installation of this equipment. Several photographic plates describing various phases of the installation process are included in the chapter. The results of a study investigating diurnal recharge variations are presented in Chapter 3 whilst Chapter 4 contains the results of several recharge experiments carried out at Shands No. 2 Pit. Soil water pressures, water content measurements, and temperature profiles are presented for a variety of conditions including filling, draining and intermittent recharge sequences. Results showing temperature variations in the soil profile over a one-day period are also presented.

Conclusions and summaries of results are presented at the end of the relevant chapters.

2. MEASURING EQUIPMENT AND
COLLECTION OF DATA

2.1 INTRODUCTION

Shands No. 2 Pit in the South Burdekin Water Board District in the Burdekin Delta was chosen as the best site to collect data for this study. A general view of the pit when full is given in Plate 1. The pit had only recently been completed when this study commenced and had not been used for recharge. It was planned therefore to collect data for analysis from the beginning of the recharge life of this pit, with the objective of observing any changes in the recharge pattern of the pit with progressive usage. However instrumentation problems, to be discussed later in this chapter, delayed the collection of useful data until the second recharge season for this pit, approximately eight months later.

Shands No. 2 Pit was formed by excavating through an overburden consisting of loam and clay loam (0 to 0.2 m), heavy clay (0.2 m to 0.8 m), and sandy clay loam (0.8 m to 2 m) to clean aquifer sand at approximately 2 metres below the natural surface. The pit was excavated parallel to Iyah Creek and was connected to it by a pipe with a butterfly valve on the inlet end. A flow meter was installed in this pipe to record the total amount of recharge water entering the pit. Part way through this investigation approximately 0.5 metres of sand were excavated from the bottom of the pit and replaced with Alva Beach sand. This sand had a higher hydraulic conductivity than the natural sand and it had the effect of considerably improving the overall intake rate of the pit.

Plate 2 shows a general view of Shands No. 2 Pit when empty taken from the western end. The instrument hut is located on the left hand side, and Iyah Creek is located to the right of the pit. In the foreground can be seen the inlet pipe from Iyah Creek and the concrete blocks and protective works to reduce scouring by the incoming water. At a later stage the inlet works were improved by installing an upright 0.5 metre diameter culvert pipe in the middle of the pit and connecting the inlet pipe through its side. The incoming water cascaded over the edge of the culvert pipe and its energy was dissipated by large rocks placed around the edge.

Shands No. 2 Pit appeared to be ideal for the purposes of this investigation and it was instrumented thoroughly to measure all the parameters which could have an influence on the movement of the recharge water from the pit to the aquifer. At the time of installation the depth to the
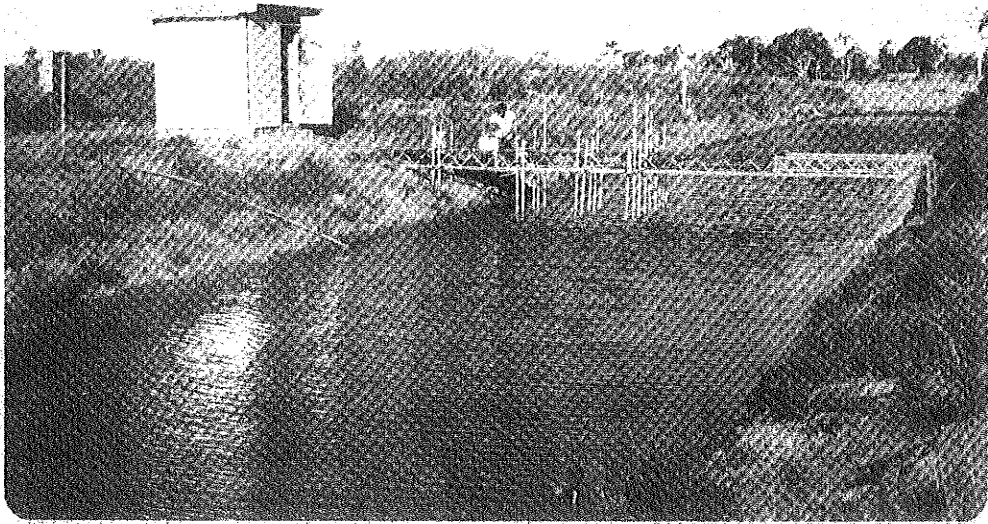
y.

d

y

ed

und

er
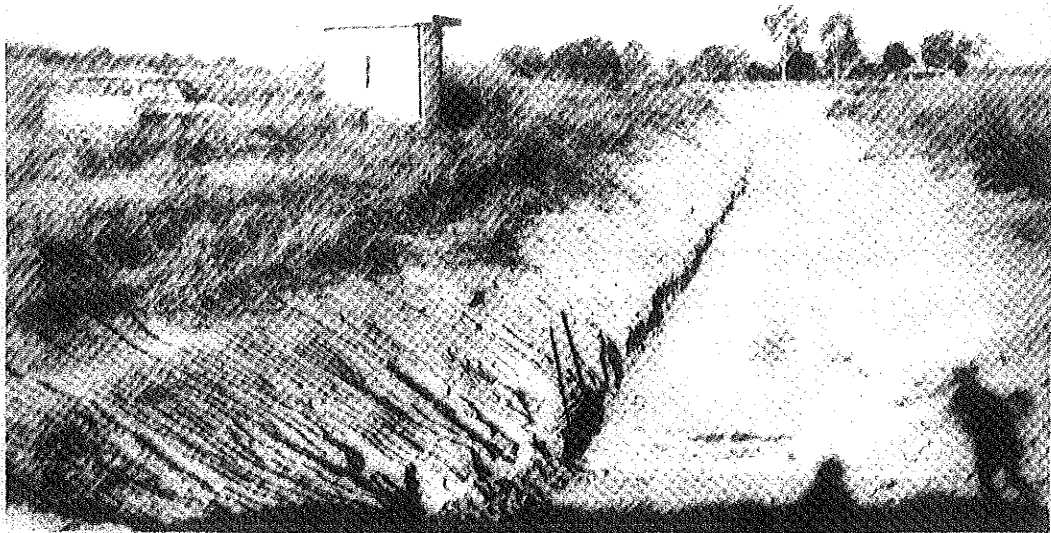
e

Plate 1:   General view of Shands No. 2 Pit when full

Plate 2:   General view of Shands No. 2 Pit when empty

water table from the bottom of the pit was approximately 5.2 metres. A total of nineteen tensiometer-transducer units were installed between the bottom of the pit and the water table with one below this level to measure water table fluctuations. The purpose of this installation was to measure the distribution of soil water pressure during the normal operation of the recharge pit. Unfortunately, after the installation was completed there was a significant rise in the regional water table during the exceptional 1973-74 rainy season. During the period when most of the useful results were collected on soil moisture distributions, the water table was only 1 to 2 metres below the base of the pit. Some of the transducers were re-positioned above the new water table, but the shorter flow path from the pit to the water table meant that it was more difficult to trace the development of a pressure mound under the pit.

Nine copper-constantan thermocouples were installed on one vertical profile of the pit to measure temperature gradients through the profile. Four access holes were drilled to below the water table and lined with plastic pipe. These were used both as piezometer holes and for neutron moisture meter measurements of water content profiles. Three piezometer holes were also installed at approximately half way along the pit and on a line at right angles to the pit centreline. These were used to detect water level changes, and the development of any water table mound under the pit. A pressure-bulb water level recorder was used to monitor the depth of water in the pit. Several other measurements were made by field staff and these are discussed in detail later in the chapter.

In the following sections each of the data collection facilities is discussed separately.

2.2 PRESSURE MEASURING EQUIPMENT

2.2.1 Tensiometer-Pressure Transducer Unit

The twenty pressure transducers used in this investigation were purchased from Statham Instruments Inc., Oxnard, California. They are known as thin film strain gauge pressure transducers, the model number being PA856-25. Their range is 0 to 173 kPa absolute (0-25 lb in^{-2}). Since these are absolute pressure transducers it was necessary to have one transducer in the instrument hut with its diaphragm exposed to the atmosphere so that atmospheric pressure changes could be monitored. The soil water pressures in the profile were then found by assuming that air present in the unsaturated zone below the pit was at atmospheric pressure.

A typical tensiometer-pressure transducer unit, including the necessary connectors and seals, is shown in Plate 3. All the metal parts were machined from stainless steel to minimise corrosion. The tensiometer housing was made from solid stainless steel with a cavity in the end to contain the water in contact with the membrane of the pressure transducer. A disc of 1 bar high flow ceramic was cemented with special epoxy resin to the end of the cavity and was used to provide continuity between the water in contact with the transducer and the soil water in the profile material.

The tensiometer-pressure transducer units were installed at depths up to 5.5 metres below the soil surface. Since the electrical connections on the transducer had to be kept free of moisture a water tight assembly was developed to carry the electric cable from the transducer to the ground surface. It was found that 25 mm internal diameter heavy gauge galvanised water pipe was suitable for this purpose. The connectors used to join lengths of pipe together were also machined from stainless steel and rubber rings were recessed in the end of each connector to prevent water entering the pipe. The galvanised pipe was fabricated in lengths of 1.53 metres and 3.05 metres. For a particular tensiometer installation a suitable combination of these lengths was made up so that the pipe extended a convenient distance above the ground surface. Each end of the lengths of galvanised pipe was threaded on the inside to match the stainless steel connectors. The length that protruded above the ground surface was threaded on the outside at the top end so that a standard galvanised end cap could be screwed on.

A brass insert and threaded screw were welded in the end cap so that the electric cable from the pressure transducer could be brought out of the pipe. Again the gap between the cable and brass screw was sealed by a rubber ring. A small bag of silica gel was hung inside the pipe to absorb any moisture in the enclosed air. The end cap, a length of pipe, a connector, and a tensiometer unit are shown in Plate 4. Also shown is the electrical lead used to supply the 10V DC excitation voltage to the transducer and to return the signal to the datalogger. Four leads are necessary but in fact the cable used was 5 core microphone cable with metal shielding and with a waterproof plastic skin on the outside. Even though some of the cables between the logger in the instrument hut and the pressure transducer were up to 25 metres long, no problems were encountered in lack of sensitivity of the transducer response, and no water leaked into the system.
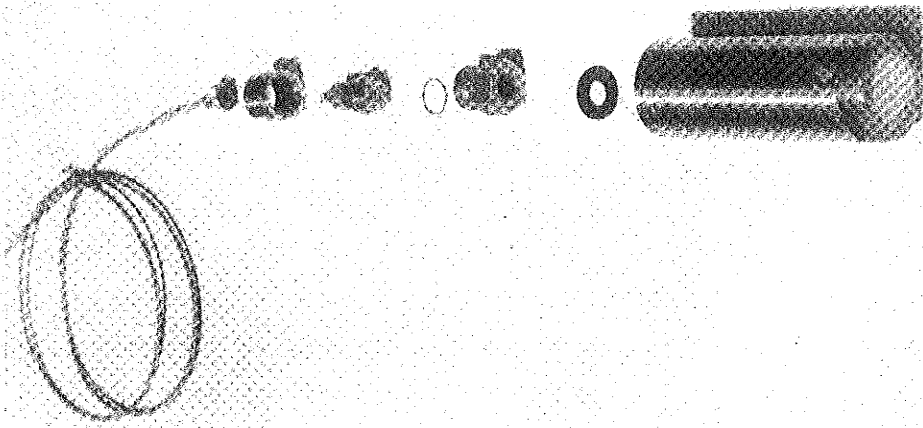
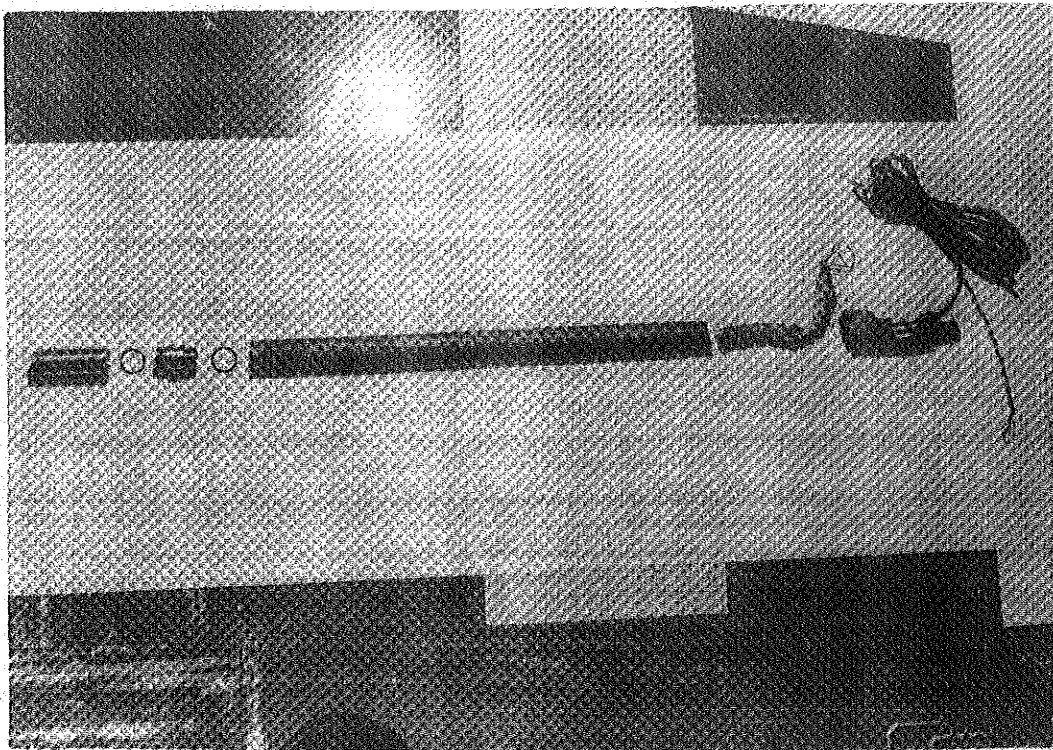Plate 3:   Tensiometer-pressure transducer unit and connectors

Plate 4:   Complete pressure-measuring probe assembly

2.2.2 Calibration and Performance of Transducers

Each of the 20 transducers was individually calibrated in the soil water laboratory at the University of New South Wales before transporting them to the field site. This calibration was used to determine a calibration factor which was measured in terms of the change in millivolt output per 100 cm change in water pressure. A testing rig was set up in which a zero head, a positive head of 50 cm of water, and a negative head of the same magnitude were imposed on each transducer in turn. Readings of the millivolt output from the transducer were recorded for each setting as well as the reading of a transducer always exposed to atmospheric pressure, and henceforth designated as the atmospheric pressure transducer. It was necessary to set aside a transducer for this purpose as all the transducers measured absolute pressure; therefore corrections had to be made to the pressure readings to allow for atmospheric pressure changes.

In the field a second calibration had to be carried out prior to installation of the tensiometer-transducer units in the soil profile. The purpose of this calibration was to obtain a reading from all tensiometer-transducer units when they were subjected to a common pressure, namely atmospheric pressure. The transducers were tightened in their tensiometer units and connected to their respective lengths of cable. All the 19 tensiometer-transducer units were stood in a tray of water, with the ceramic facing downwards and the depth of water in the tray was adjusted until the water was at the same level as the diaphragms of the transducers inside the units. Hence the pressure on the diaphragms was atmospheric and the same as that existing on the special atmospheric transducer.

The output from the 20 transducers was then monitored using a datalogger until the readings stabilised. At the same time the voltage supply to the transducers was monitored. The outputs from the 20 transducers were then corrected for any departure of the voltage supply from the nominal 10 volts specified. These corrected readings were then noted and used as the HZERO calibration values to be discussed later in this section.

Upon completion of the field calibration the tensiometer-transducer units were installed in the soil profile and their outputs together with the atmospheric pressure transducer and the voltage supply were monitored and recorded by a datalogger at pre-defined time intervals.

Later the recorded values were converted to soil water pressure readings using the following formulae -

$$h_{ATMOS} = [((VOLT(19) \times 10.0)/VOLT(20)) - HZERO(19)]$$
$$\times (100.0/CALFAC(19))$$

$$h_I = [((VOLT(I) \times 10.0)/VOLT(20)) - HZERO(I)]$$
$$\times (100.0/CALFAC(I)) - h_{ATMOS}$$

where h_{ATMOS} = difference between atmospheric pressure transducer reading at field calibration and atmospheric pressure at time of reading (cm of water),

VOLT(19) = voltage output for atmospheric pressure transducer at time of reading,

VOLT(20) = voltage reading of DC power supply to transducers at time of reading (at calibration was 10.0 volts but tended to vary slightly from this due to local supply fluctuations). Recorded in volts,

HZERO(19) = reading of atmospheric pressure transducer when field calibration carried out (millivolts),

CALFAC(19) = calibration factor derived in the laboratory for atmospheric pressure transducer (millivolts per 100 cm of water),

VOLT(I), HZERO(I), CALFAC(I) = readings for transducer I. Similar definitions to those for transducer 19,

h_I = soil water pressure measured by tensiometer-transducer unit I (cm of water).

The performance of the transducers themselves was more than adequate under fairly exacting field conditions. Problems that arose during the period they were installed (approximately 18 months) were mainly due to the development of faulty electrical connections either in the instrument hut or at the union between the electrical disconnect and the 5-core cable in the transducer pipe. Other problems in incorrect readings were found to be due to datalogger malfunctions. These are discussed in a later section. It is felt that the tensiometer-transducer system used in this investigation could be used up to 25 metres or more below the soil surface providing suitable installation techniques could be devised. When the transducers were returned to the University of New South Wales after the investigation was completed, it was found that the calibrations of the transducers had not varied and they performed as well as when they were first installed in the tensiometer assembly.

2.2.3 Installation of Pressure Transducers

A total of nineteen tensiometer-transducer units were installed in the soil profile at Shands No. 2 Pit. Ideally the tensiometers were to be installed on vertical profiles at the pit centreline and at several other points extending to the northern side of the pit, so that the two-dimensional development of the moisture profile and the water table mound could be examined. In practice it was not possible to space the tensiometers on a vertical line because of the need to have separate drill holes for each tensiometer. Drill holes were therefore spaced approximately 0.3 metres apart on lines parallel to the pit centreline.

One line of tensiometers was installed on the centreline of the pit (8 units), and extending out to the northern side of the pit at distances of 1.2 (4 units), 2.4 (4 units), 4.3 (2 units), and 6.1 metres (1 unit) were installed additional tensiometers, each installation being on a line parallel to the pit centreline.

As mentioned in the Introduction to this chapter the regional rise in water table elevation necessitated the repositioning of several tensiometers part way through this project, so that units below the new water table could be lifted into the unsaturated zone, and hence be used to record the pressure profile development during recharge. After this change the number of tensiometers on the lines from the pit centreline outwards were 9, 3, 4, 2 and 1. The relative elevations of the tensiometers are given with the results in a later chapter.

The installation of the tensiometer-transducer units in the soil profile proved to be a difficult task. Since it was desirable that the tensiometers be placed in undisturbed soil it was not possible to use the percussion drilling technique which is normally utilised for drilling holes in the Burdekin Delta. This method, because of vibration and drilling water, causes severe disturbance to the soil in the vicinity of the hole. It was decided that an auger drilling technique would have to be used to minimise disturbance. Unfortunately most commercially available augers are at least 75 mm diameter and this would also tend to provide a large disturbed soil zone around the 34 mm transducer pipes. The only available auger of suitable size was a 40 mm coal auger, and although this has a very poor lifting capacity because of the small grooves for carrying the cuttings, it was found to be suitable for drilling in sandy soils.

The auger was powered by a 4 H.P. Mate Post-Hole digger which can be operated by one man. Because of the weight of the Mate and auger (approx. 80 Kg for the Mate with 12 metres of auger attached) it was necessary to use a tripod and block and tackle arrangement to support the weight. The auger was fabricated in 1.5 metre lengths and screwed at each end so that additional pieces could be connected as the drill penetrated progressively deeper into the profile.

The sequence of drilling operations carried out at Shands No. 2 Pit is shown in Plates 5 to 8. In Plate 5 the Mate Post-Hole digger has been suspended from the tripod by the block and tackle and drilling operations are about to commence. Plate 6 shows the holes along the pit centreline completed and the equipment being set up for the new row of holes. In the drilling procedure the hole was initially drilled through the soil to approximately 0.3 metres above the final location of the tensiometer. A plastic liner made from 40 mm nominal bore plastic pipe was then inserted into the hole and the shavings and debris in the bottom of the hole removed by augering through the liner or by using a sampling tube. The final 0.3 metres of spoil between the end of the plastic liner and the final tensiometer location was also extracted using the sampling tube. The plastic pipe was fabricated in 1.5 metre lengths with a male spigot turned down on one end of the pipe for approximately 40 mm and a corresponding female socket turned on the inside of the other end. Lengths of pipe could then be glued together to line any desired depth of hole. The resulting joints were flush on both the inside and outside and did not interfere with the passage of the pipe into the ground or the free movement of the auger bit.

Drilling on the edge of the bank of the pit was found to be a difficult exercise. Two of the tripod legs had to have extensions fitted to enable the Mate and auger to be lifted through at least 2 metres of height. An assistant was required to hold the weight of the digger and auger and raise and lower them when necessary. Considerable difficulties were encountered in drilling through the hard clay bank material. Plate 7 shows the auger being used through the plastic liner with the liner being prevented from rotating by a clamp. Plate 8 shows the installation after completion of the tensiometer holes.

A layer of clay, approximately 30 mm in thickness and embedded in the sand was present in all drill holes but varied in depth from 1 to 2.5 metres and also varied in thickness and composition. It was one of the prime causes of drilling problems when augering through the plastic liner.
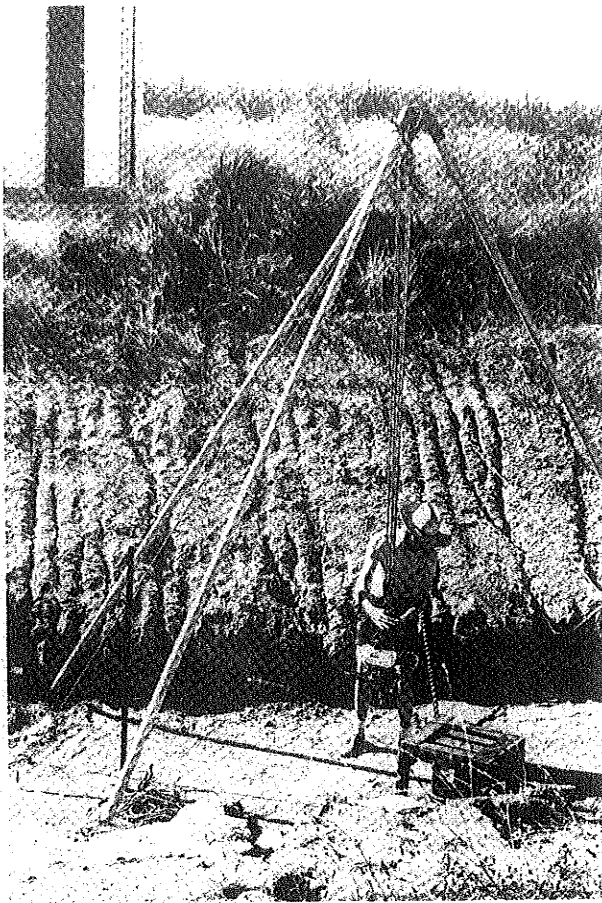
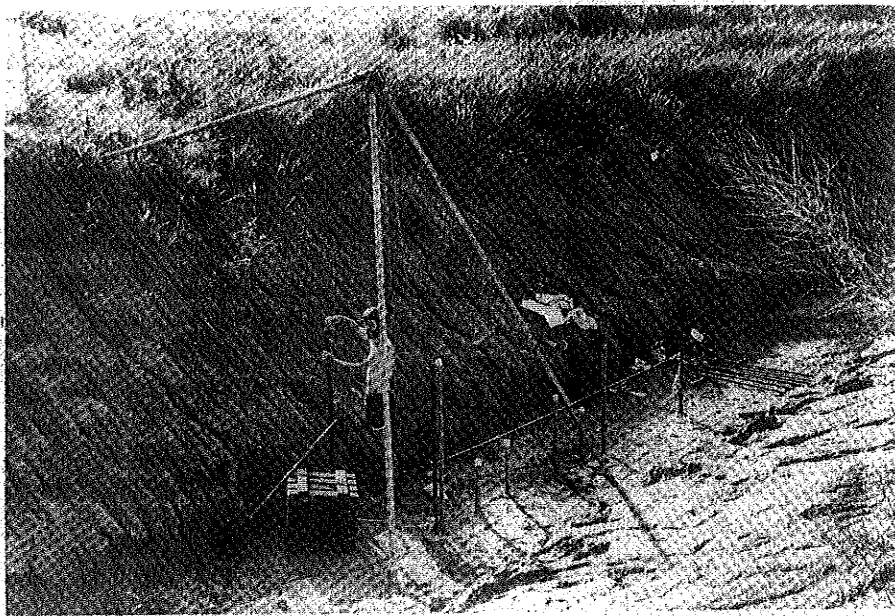Plate 5: Mate post-hole digger suspended from tripod

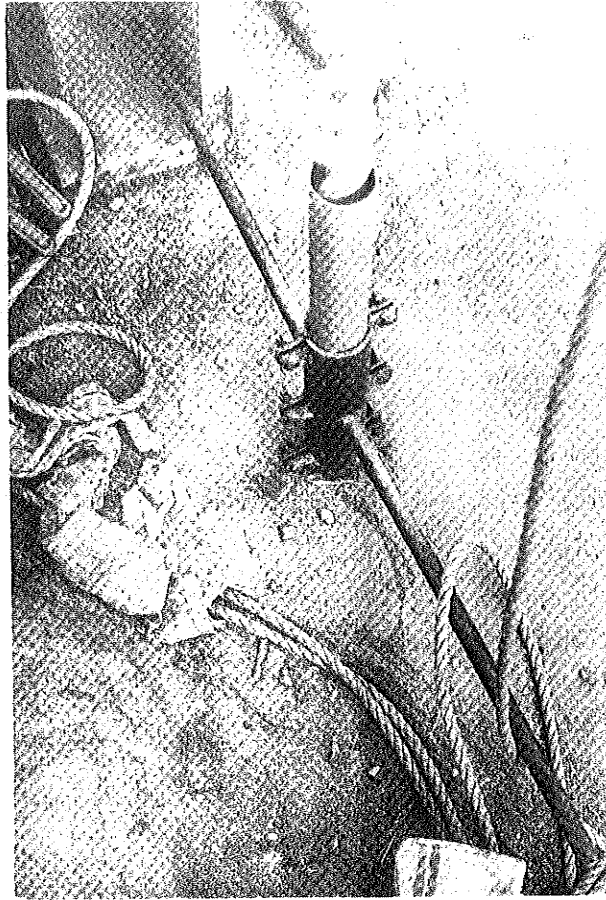Plate 6: Equipment being set up for second row of holes

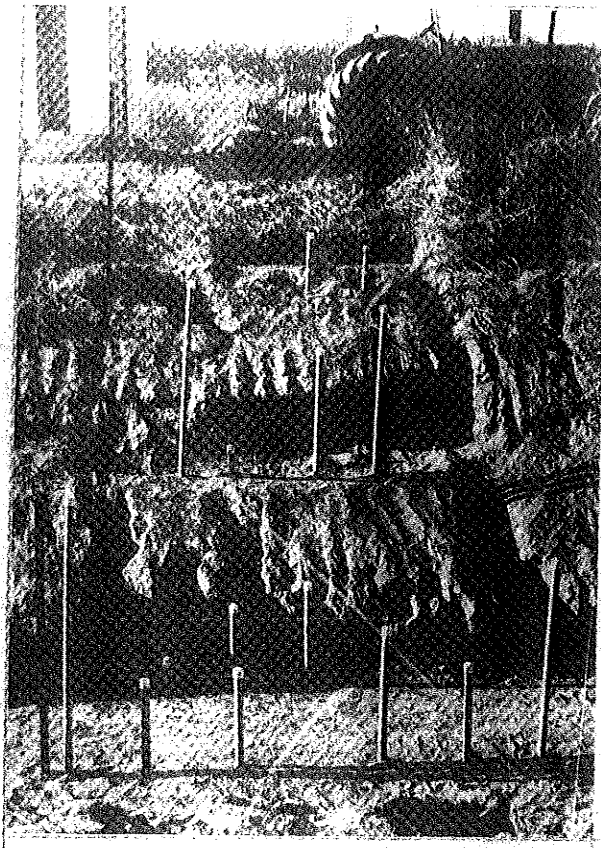Plate 7:   Auger being used through the plastic liner

Plate 8:   Installation after completion of tensiometer holes

The clay tended to jam between the auger and liner and collect stones which jammed and sometimes fractured the pipe. It is clear that the conditions and equipment were not ideal but still the installation was completed in a little over one month by two men.

The installation of the tensiometer-transducer units was then carried out. Where the length of pipe and tensiometer did not exceed 8 metres the pipes were assembled and installed in one piece. For deeper installations pipes had to be joined on as the pipe was lowered down the plastic liner. Once the tensiometer pipe had been lowered to the bottom of the plastic liner, the liner was removed taking care to pack the sand around the pipe as it was withdrawn. Plate 9 shows a view of the access bridge with all the pipes installed but with the cables still to be connected to the datalogger in the hut.

The purpose of the access bridge was to provide support for the tensiometer pipes and access to the neutron moisture meter holes, one of which was positioned at the pit centreline and one at each of the next three transducer installations towards the northern side of the pit. Each of the two supporting beams was formed by bolting four sections together. These were pre-fabricated in Sydney from light weight galvanised water pipe braced with steel webbing. Three wooden platforms, also pre-fabricated in Sydney, were laid on the beams to form the decking. The beams were braced at the top by the decking and at the bottom by steel tension rods.

2.3 TEMPERATURE MEASURING EQUIPMENT

A total of ten thermocouples were purchased; nine were installed in the soil profile and one was kept in the instrument hut to monitor the ambient temperature. The thermocouples were made from copper-constantan and were coated with a non-corrosive sheath. A cold junction was attached to the datalogger (see Section 2.4) and readings were recorded by the datalogger at the same time as the transducers were monitored. Each of the thermocouple cables was 23 metres long.

The thermocouples were installed on a vertical profile at 1.2 metres from the pit centreline and on the same line as the second set of tensiometers. They were placed at depths ranging from 0.3 to 3.98 metres below the bottom of the pit in intervals of 0.46 metres. The auger was used to drill a hole to approximately four metres and it was then lined with plastic pipe. All the thermocouples were bound together, lowered into hole, and the plastic liner withdrawn. At the same time the soil was

compacted around the thermocouple wires.

The purpose of installing the thermocouples was to investigate the development of temperature gradients within the soil profile during the on-off operation of the recharge pit. It was also expected that the thermocouple readings would be of relevance to the biological studies carried out in one of the related projects.

The thermocouples were calibrated from 0° to 100^oC in the laboratory and were found to be of very high accuracy. It was also found that the calibration curve was related almost exactly to the theoretical curve for copper-constantan. An accuracy of $\pm$ 0.5^oC could be expected in field use. A greater accuracy could be expected in a laboratory where the ambient temperature was controlled.

Results produced by the thermocouples and recorded by the datalogger are presented in a later chapter.

2.4 DATA ACQUISITION EQUIPMENT

Both the pressure transducers discussed in Section 2.2 and the thermocouples discussed in Section 2.3 were monitored by a data acquisition and recording system. This unit was installed in the instrument hut which was air-conditioned to provide a satisfactory operating environment for the equipment. A photograph of the datalogger and peripheral equipment installed in the hut is shown in Plate 10.

The data acquisition system was purchased from Schlumberger Instrumentation Australia Pty. Ltd. and consisted of elements of their Series Three Data System. It consisted of five free-standing components - a data transfer unit, a digital voltmeter, an analogue scanner, a paper tape punch, and a strip printer. The data transfer unit basic assembly contained a power supply module which supplied both DC and AC power to all the other units as required. Other components included an interface to the digital voltmeter, a controller, a scanner controller, a clock, two output drivers (one each for the punch and printer), and a display unit (only one output driver can be used in conjunction with this unit). A special days generator was added to the clock module so that days, hours, minutes and seconds could be recorded. The clock was used to initiate scans of all the channels at preset time intervals. Usually scans were initiated by the clock at 2 hour intervals but during filling and emptying of the pit shorter time intervals were chosen. Scans could be initiated at intervals of 1, 2, 10, 20 seconds; 1, 2, 5, 10, 20, 30 minutes, and at 1 or 2 hours. The scans were triggered automatically so that operator intervention was only required for changing paper
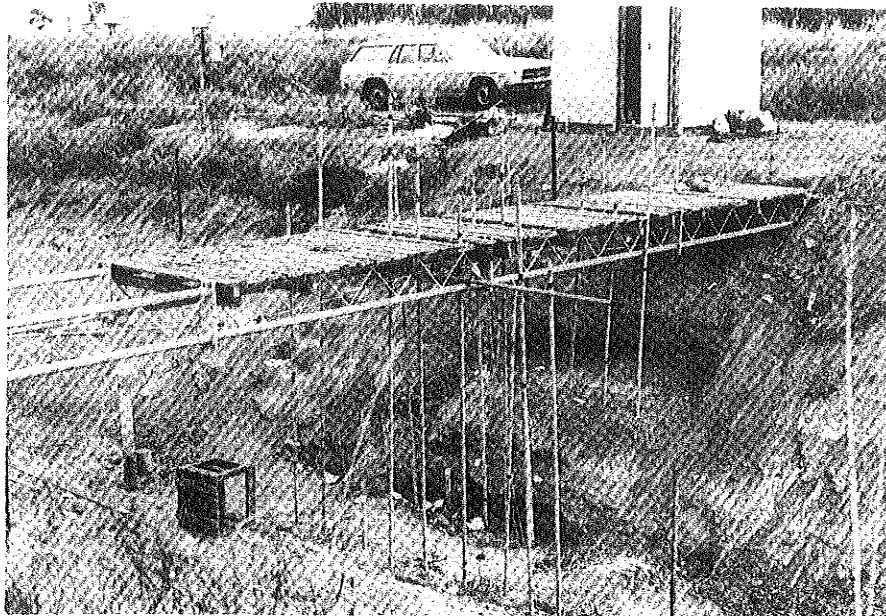
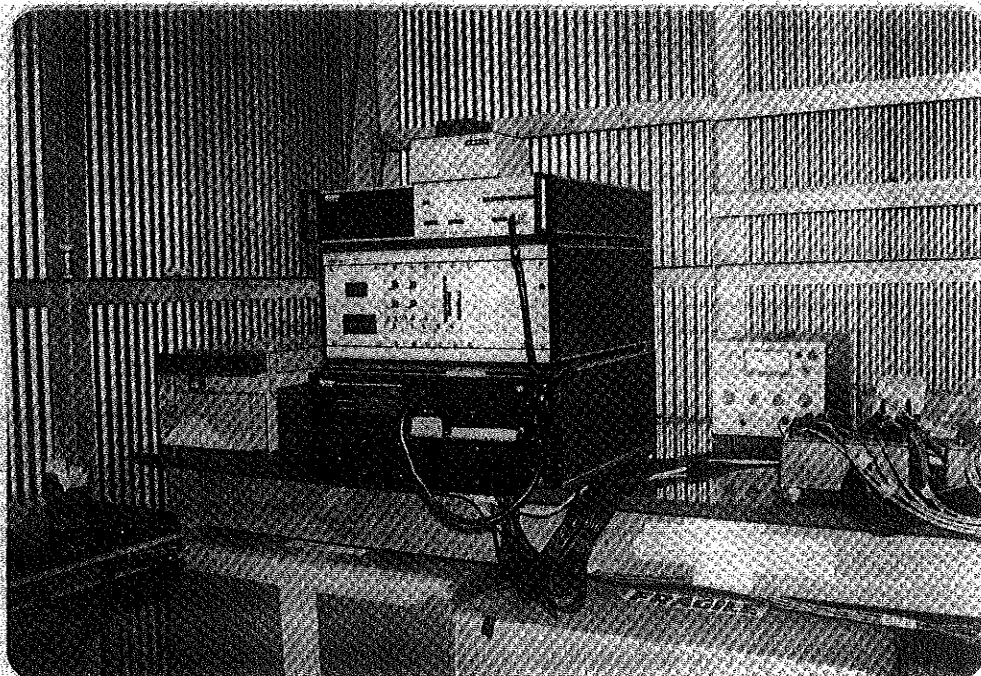Plate 9:   View of access bridge with tensiometer pipes installed

Plate 10:   Datalogger and peripheral equipment

on the output devices or changing the scan time intervals.

The digital voltmeter used in the system was a Schlumberger
Solarton Model A210/214. It had a resolution of 1 μV and produced
6 digit output. It could be set on auto range, in which the voltmeter
automatically selected the optimum range for reading a particular
signal, or it could be set on one of five voltage ranges. These were
100 mV, 1V, 10V, 100V and 1000V with an over-range of 20% on each
range (i.e. readings of up to 120 mV could be recorded on the 100mV
range). The scan rate was up to 100 channels per second, but this
speed was limited by the capacity of the output device being used,
unless a special buffer unit was included in the system.

The free standing unit known as the Series Three analogue scanner
3301 received the electrical inputs from the transducers and thermo-
couples. The unit has a capacity of 100 channels made up of ten input
selector modules each of which can provide 4-pole switching for ten
channels. If necessary several scanners can be linked together to give
a potential capacity of 1000 channels for the system. A cold junction unit
was attached to the analogue scanner to provide signal conditioning for
the ten thermocouple inputs.

The main output device was a FACIT 4070 paper tape punch. It had
a capacity of 75 characters per second which is equivalent to 5 to 6
channels per second - well within the capacity of the digital voltmeter.
The paper tape for the punch which came in 305 metre rolls was changed
when necessary and processed on the IBM 360/50 computer at the University
of New South Wales. A second output device was also attached to the
system, this being a FACIT 4552 Alphanumerical strip printer. This
device could output data at approximately one channel per second and
was only used for testing of the system or for taking twice-weekly
check readings. Mr. T.E. Musgrave of the South Burdekin Water Board
regularly took these readings on the printer and posted them to Sydney,
so that faults occurring in the system could be detected and remedied
before they seriously affected the quality of the records.

Considerable difficulties were experienced in the first six months
of operation of the datalogger. Some of these were due to hardware
faults in the system, but the biggest problem lay in the susceptibility
of the system to faults due to extremes of temperature and humidity. The
module most affected by these climatic factors was the interface in
the analogue scanner. After this unit was replaced and an air-conditioning

system installed in the hut, the datalogger performed remarkably well for the conditions.

Another problem with the system was its vulnerability to power fluctuations. The punch unit in fact was designed to cut out with a greater than 10% fluctuation in the mains supply. Power fluctuations of this order and complete power cuts were very common during the period of installation of this equipment. Most of the problems caused by fluctuations were overcome by placing an AC voltage regulator in the circuit but the problem of power cuts could not be overcome. Whenever a power cut occurred the clock in the datalogger was reset to zero and the punch was permanently switched off until an operator reset it.

2.5 WATER CONTENT MEASUREMENT

Water content profiles under Shands No. 2 Pit were determined by means of neutron moisture meter logging. The equipment for this was loaned by the Australian Atomic Energy Commission, although the radio-active source was supplied by the University of New South Wales. Mr. Len McGowan of the Irrigation and Water Supply Commission, Queensland was responsible for taking the readings.

The equipment consisted of two portable battery operated units - a ratemeter and a scaler. They were operated by standard torch batteries. The two units were linked together by cable and the ratemeter was connected by means of a 25 metre length of heavily insulated cable to the probe unit. A paraffin wax shield was used to store the probe unit when it was not being used.

The probe unit was made of stainless steel tubing with an outside diameter of approximately 25 mm. It was 400 mm long and was completely water-proofed. Contained within the probe were a fast neutron emitter and a slow neutron detector separated by a lead plug. The fast neutrons were generated by means of a 300 mCi Am-241/Be source. This source was sufficiently large to enable an accurate count to be taken in relatively dry sand over a count period of one minute. A 30 second count was adequate in wet sand. The only problem limiting the effectiveness of this system, was the lack of an automatic timer. The count had to be manually timed using a stopwatch which of course introduced an element of human error.

The water content measurements were monitored at four locations - at the pit centreline and at the next three tensiometer - pressure transducer installations towards the instrument hut. The access holes for the neutron moisture meter readings were drilled with the same power auger as the transducer pipes, and were lined with 40 mm nominal bore plastic pipe. All the holes were drilled to approximately 2 metres below the standing water level at the time of installation (i.e. to 7.2 metres below the base of the pit). These holes were also used as piezometer holes. Access to the pipes was provided by means of the prefabricated bridge discussed earlier.

It was found that the neutron moisture meter was very effective in determining the moisture content profiles under Shands No. 2 Pit. The biggest problem in using the data from these measurements was in devising a suitable calibration curve to convert the count rate to a moisture content reading. In general the relationship between count rate and volumetric water content is linear for a neutron moisture meter probe. With a homogeneous sand profile an adequate calibration curve can be obtained by taking standard counts in a dry sample of sand and a saturated sample, determining the volumetric water contents by oven-drying, and plotting the two points on a calibration sheet. A straight line joining these points should be sufficiently accurate for field investigations. However the soil profile under Shands No. 2 Pit was heterogeneous. The layer of sand immediately below the base was Alva Beach sand (a fine sand of uniform grain size) and below this the natural sand tended to have layering of fine and coarser sands, and a layer of clay at one point. The best approach with such a profile, without massive excavation, was to determine the saturated count rate when the profile was saturated just after a new recharge cycle had commenced, and estimate the probable volumetric water content at saturation. A calibration point for the upper layer of sand when it was dry was obtained by taking soil samples, and a corresponding neutron moisture meter count at the same elevation.

Although the above technique was not ideal it was possible to derive useful results from the moisture meter readings for comparison with pressure readings taken at the same times. The results are presented in a later chapter.

2.6 ADDITIONAL DATA COLLECTED BY FIELD STAFF

Additional data were collected by field staff of the Irrigation and

Water Supply Commission, Queensland as part of AWRC Project 71/29.
Details of the methods and purpose of these additional measurements
are set out below.

Water table levels in the vicinity of Shands No. 2 Pit and at
several other locations were monitored at regular intervals using
piezometer holes installed for this purpose. At Shands No. 2 Pit three
piezometer holes were installed approximately 30 metres towards the
eastern end of the pit from the instrument site. One hole was located
on the edge of the pit and the other two spaced out on a line away
from the pit centreline. The purpose of these holes was to monitor the
rise and fall of the water table mound during recharge cycles. Water
levels were also monitored in the four holes installed at the instrument
site for neutron moisture meter readings (see Section 2.5). These holes
did not have screens in the bottom section of the pipe so the readings
from them probably displayed a damped response. However they were useful
in checking the accuracy of the pressure transducers located below
the water table.

Water levels in the pit were recorded automatically using a
Cambridge pressure recorder. Charts were generally changed for each
recharge cycle or at more frequent intervals. During the period of the
investigation of diurnal recharge variations, to be discussed in a later
chapter, a Leupold and Stevens Type F water level recorder was installed
on the access bridge to monitor the water level more accurately. During
filling operations the water level on a staff gauge was recorded manually
at frequent intervals as levels could be read more accurately by this
means than from the recorder charts. Monitoring of the pit water level
was important as the depth of water in the pit affected the potential
intake rate of the pit. Also the comparison of inlet flow meter readings
and pit water levels was necessary to define the instantaneous intake
rate in the early stages of filling, or during fluctuations in the supply
of water from the recharge channel.

The intake rate of Shands No. 2 Pit was monitored regularly by
field staff using several different approaches. Firstly the inlet flow
meter was read regularly to give a measure of the average intake rate
since the previous time the meter was read. This was not a very reliable
reading as the blades on the meter were frequently fouled with weeds
passing through the inlet pipe from the recharge channel. A second
approach to determining the intake rate was to close the inlet valve

for a short period and measure the drop in water level in the pit. From a depth-area curve for the pit it was then possible to estimate the instantaneous intake rate. The intake rate was also estimated by taking flow meter readings over short time intervals but these readings were again dependent on the accuracy of the flow meter at that time. The measurement of the intake rate was important in the overall management of the pit. Whenever the rate dropped to an unacceptable level the pit was shut off and allowed to drain and dry. Cleaning operations were then carried out if necessary.

Other data collected by field staff included turbidity measurements using a turbidity stick. This gave an indication of the sediment level in the recharge water. Water temperature was also monitored at regular intervals, and data on rainfall and barometric pressure were provided from records kept at Home Hill and Claredale. The rainfall records were important because the occurrence of a rainstorm while the pit was empty usually caused a change in the tensiometer-pressure transducer readings to be detected. In the absence of rainfall records such changes could have been attributed to instrument malfunctions. The barometric records were used to check the performance of the transducer kept in the instrument hut for monitoring atmospheric pressure changes.

3. DIURNAL RECHARGE VARIATIONS IN
SHANDS NO. 2 PIT

3.1 INTRODUCTION

Diurnal variations in the recharge at Shands No. 2 Pit were first detected in an examination of the pressure transducer outputs recorded by the datalogging system. Initially it was assumed that the variations were caused by an instrument malfunction as similar patterns of diurnal changes in the readings had been recorded in the early stages of the installation when humidity and temperature had affected some electronic components (see Chapter 2). However careful checking of the data showed that the pressure variations detected were real, and that they were probably due to fluctuations in the recharge rate.

Once the pressure variations had been confirmed, a field exercise was carried out to provide additional confirmation, and to get an exact measure of the magnitude of the recharge fluctuations. To this end the flow meter at Shands No. 2 Pit was monitored over a period of 56 hours by three observers. The results of this exercise are presented in this chapter.

3.2 COLLECTION OF DATA

Several measurements were carried out to define the various parameters which could cause variations in the recharge rate. The pit water level was monitored as it affected the pressure head at the bottom of the pit and hence the potential recharge rate. Also variations in the pit water level affected the volume of storage in the pit. Changes in storage had to be applied as a correction to the flow meter readings so that the actual recharge into the aquifer in a given interval could be determined. The water level in the supply channel was also monitored as it determined the water level in the pit for a specified intake rate.

Both the pit and channel water levels were read off gauge boards and the pit water level was also monitored using a Leupold and Stevens Type F water level recorder. This instrument was installed to complement the gauge board readings. Normally the pit water level was monitored using a Cambridge pressure recorder but this did not have a high enough resolution to monitor the minor water level changes caused by the recharge variations.

The flow meter had to be read manually as it had no provision for automatically recording the flow. Only the accumulated flow up to a

particular time could be read from a digital counter recording to 0.01 of an acre-foot (12.3 m^3). Pressure and temperature readings were automatically recorded by the datalogger. All readings were taken at half-hourly intervals over the full 56 hour period of the test.

3.3 RESULTS AND DISCUSSION

The results derived from the test are summarized in Figure 3.1. As can be seen, the recharge rate is plotted as the recharge occurring during half hour periods between readings. The recharge rate for the interval was calculated as the volume of recharge divided by the time interval. The datalogger was inadvertently left off in the early part of the test so no pressure data are available in this period. No temperature data are plotted as these data did not reflect the variations in recharge over the test period. Due to the shutdown of one of the supply pumps there was a significant drop in the channel water level early in the test but the water level was essentially constant for the remainder of the test. The recharge water was clean (< 40 p.p.m.) during the test period so that the influence of sediment deposition could be neglected.

From a close examination of the relative heights of the pit and channel water levels it can be seen that the variation in the recharge rate is reflected in the relative head difference between the channel and pit. The scatter in the intake rate values over the first part of the test is due to the flow meter only being read to 0.01 of an acre-foot (12.3 m^3). During the latter part of the test the flow meter was read to 0.001 of an acre-foot (1.23 m^3) by interpolation.

It is clear from Figure 3.1 that there was a systematic diurnal variation in recharge at Shands No. 2 Pit during the period of the test. This variation is reflected in the response of the pressure transducer located 78 cm below the base of the pit. A similar response was noted with the other transducers located in the profile near the base of the pit. The minimum recharge rate occurred over the time 0900 to 1600 hours and the maximum over the period 2300 to 0400 hours. The minimum intake rate was approximately 17% less than the maximum rate.

Figure 3.2 shows the response of 3 transducers during a normal recharge cycle. Recharge commenced at 1506 on the 196th day of the year. From the figure it can be seen that the oscillations due to algal activity become significant at about 4 days after recharge commenced. Transducers 4 and 6 are in the upper part of the soil profile and transducer 7 is well below the water table. The initial dip in transducer 7 on the 199th
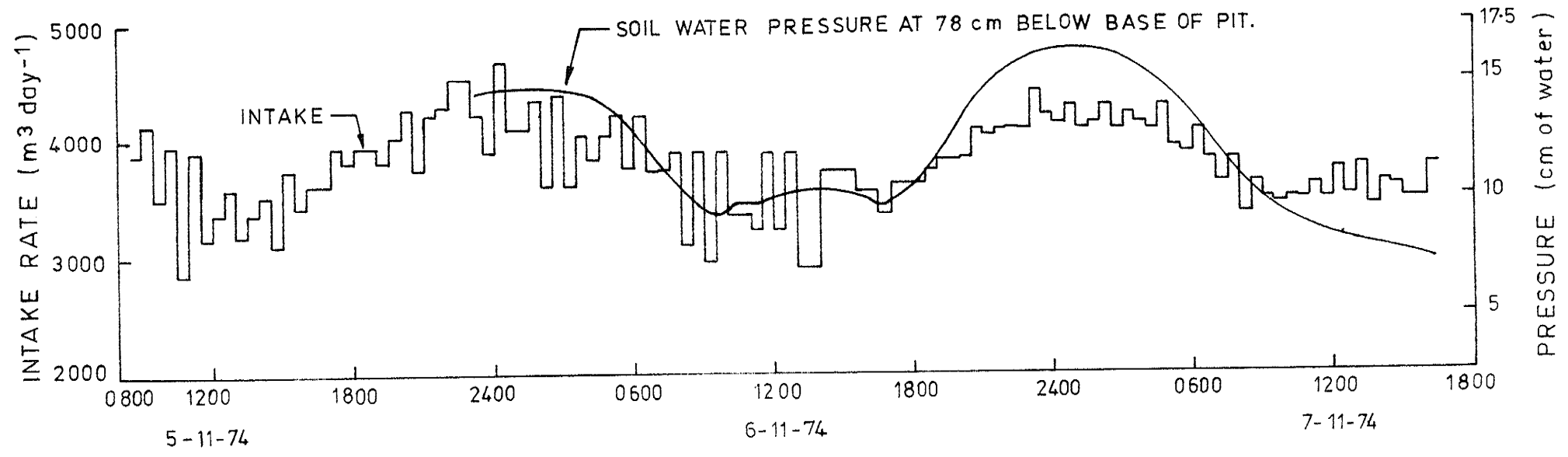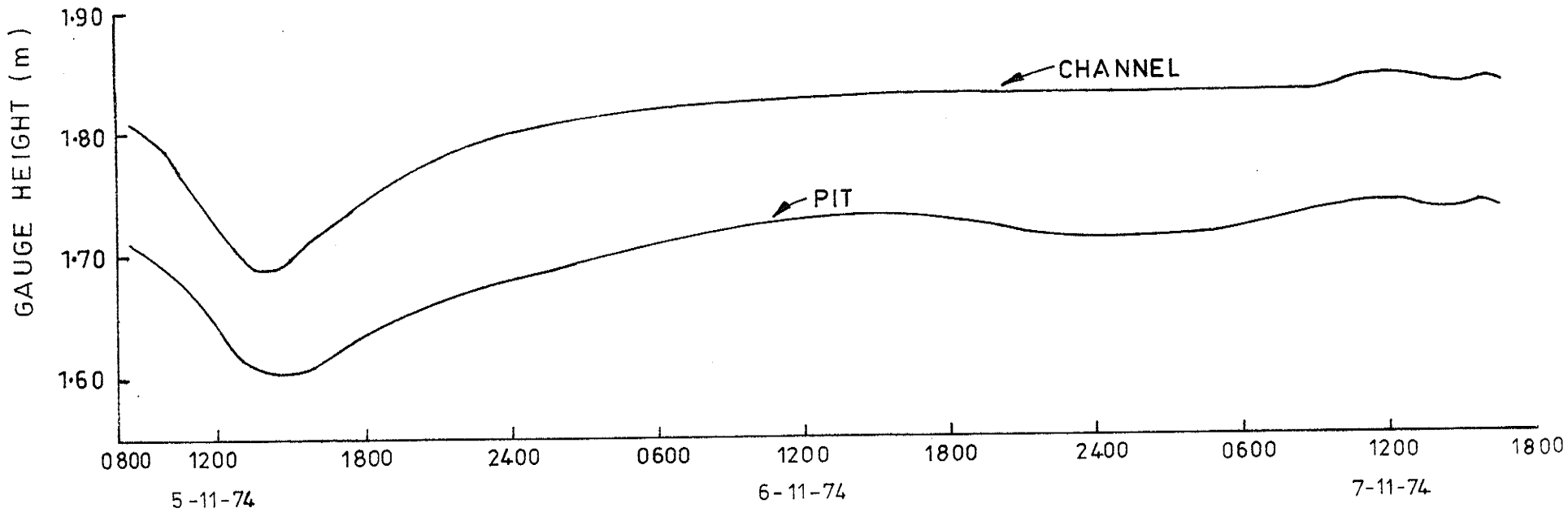
Figure 3.1: Diurnal variation in recharge recorded at Shands No. 2 Pit

Transducer No.	Location Z (cm)	Pressure (cm of water)
4	-28	as shown
6	-78	add 10
7	-577	add 470

RELATIVE TRANSDUCER PRESSURES (cm of water)

No. 6

No. 4

No. 7

135.

TIME (days)

Figure 3.2:   Pressure plots for three transducers during a recharge cycle

day was due to the operation of an irrigation pump approximately 200 m from the pit and reflected the drop in water table position. It might be noted also that there is a general rise in readings from the 211th day onwards. This was due to an increase in water level in the supply channel and pit.
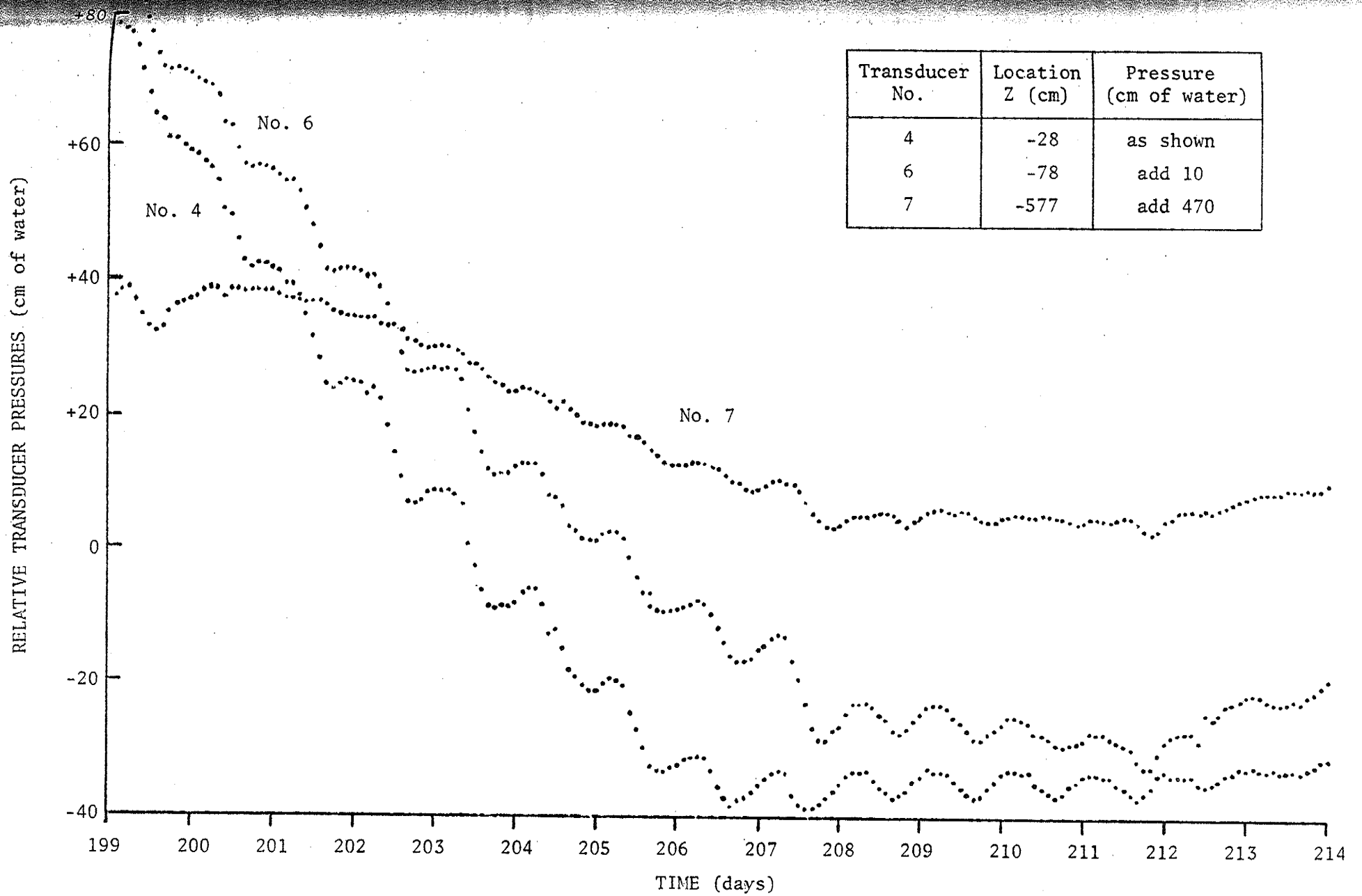
When a gradual decrease occurs in the surface flux of a recharging profile the pressure head at points within the profile will decrease (become more negative) as the flux decreases. In addition, prior to the commencement of desaturation in the profile, the absolute value of the pressure head difference between any two points will increase resulting in a decrease in the hydraulic gradient. In terms of these observations the hydraulic response of the profile as the flux decreases is illustrated by the readings given in Figure 3.2 for transducers 4 and 6. The general pressure head decrease with time is clearly shown together with the superimposed diurnal pressure head fluctuation. The fall in recharge is very significant between days 200 and 207; thereafter the decrease is slight until the rise from the 212th day onwards due to the increase in pit water level. The response of transducer 7 in tracing the rise and fall of the groundwater mound shows the same pattern of decreasing and increasing recharge.

Field recharge measurements were made on days 197, 198, 200, 203, 205, 207, 210 and 212. They confirm that the pit was operating at near its maximum intake rate up until the 200th day, thereafter the rate dropped significantly to about one third its maximum value on the 210th day, with a slight increase to the 212th day. This pattern is in complete agreement with the transducer responses discussed above.

From an examination of pressure transducer data given in Figure 3.2 and for other recharge cycles it was apparent that the diurnal variation in recharge starts a few days (approximately 3 to 5 days) after water is put on the pit, and reaches a maximum amplitude after water has been on the pit for a week or more.

It appears from the results that there are two parallel phenomena acting to affect the intake rate of the pit. The predominant factor is the clogging of the bottom of the pit and the surface layer of sand caused by algal material and sediment, the sediment deposition being assisted by the presence of algal material. A second factor which affects the pattern of the recharge rate is the generation of oxygen by the algae, and it is apparently this factor which causes the 17% variation in re-

charge between day and night. During the day photosynthesis takes place generating oxygen gas and this reduces the water saturation and potential hydraulic conductivity of the surface layer. At night algal activity is at a minimum and recharge is hence greater. According to Jackes (1975), the dominant algae in Shands No. 2 Pit during the 1974 recharge season when this investigation was carried out, were the filamentous forms, particularly the blue-green Aulosira, and to a lesser extent several species of Oscillatoria.

During the first few days of a recharge cycle there is little algal activity and the diurnal variation in recharge is either not present or insignificant. However, at later stages in the inundation period the effect of the oxygen given off during photosynthesis by the algae is a significant factor although of course it is less significant than the clogging action of the developing algal mat. At high intake rates in the early part of the inundation phase of the recharge cycle the percentage change in recharge due to algal activity would not be as high as 17% but would be some lesser amount depending on the level of algal activity. The field exercise was carried out when the pit was due for emptying and cleaning, and it can be expected that the diurnal variation was at a maximum on the basis of a percentage of the intake rate.

Diurnal variations in oxygen production due to photosynthesis have been measured and modelled in rivers (Odum, 1956; Odum, 1957; Edwards and Owens, 1962; O'Connell and Thomas, 1965; Thomas and O'Connell, 1966; Westlake, 1966; O'Connor and Di Toro , 1970; Kelly et al., 1974a; Kelly et al., 1974b; Hornberger and Kelly, 1975), in lakes (Verduin, 1957; Tilzer, 1973) and in the laboratory (McIntire et al., 1964). Some of the river measurements were carried out where higher order plants contributed to the diurnal periodicity of oxygen concentration, and in other cases algae of similar species to those found in Shands No. 2 Pit were predominant. In the laboratory study by McIntire et al. (1964) artificial illumination was varied and the corresponding productivity of the laboratory stream measured.

Referring again to Figure 3.1 it may be noted that the transducer reading follows the recharge variation almost exactly. Although the transducer pressure data points are not shown, none of the points in fact deviated from the curve by more than 2.5 mm. This is an indication of the high accuracy of the field tensiometer-pressure transducer equipment used, and the high performance of the measuring equipment. Further results from the pressure measurements are presented in the following chapter.

4. PRESSURE, WATER CONTENT AND TEMPERATURE
PROFILE DEVELOPMENT AT SHANDS NO. 2 PIT

4.1 INTRODUCTION

This chapter presents the results of field measurements of various parameters investigated at Shands No. 2 Pit in the Burdekin Delta. The details of how these various measurements were taken are given in Chapter 2. In Chapter 3 some limited pressure measurements are presented because of their relevance to the diurnal recharge variations described in that chapter. However the systematic development of pressure, water content and temperature profiles during recharge cycles at Shands No. 2 Pit are presented in this chapter.

The following two sections detail the locations of the various measuring points and the conversion of the field data to pressure, water content and temperature values. The results are then presented in four sections - during filling of the pit at the beginning of a recharge cycle; during drainage of the pit at the end of a cycle; during intermittent on-off infiltration into the aquifer, and finally a set of results comprising temperature profile variations over a one-day period. The first three sections of results contain corresponding pressure, water content and temperature profiles for each event with the fourth section consisting only of temperature profiles.

A summary of the results is presented in a final section.

4.2 LOCATION OF MEASURING POINTS

The locations of the tensiometer-pressure transducer units for measuring soil water pressure are given in Figure 4.1. It should be noted that the positions of transducers 4, 5, 6 and 11 were changed early in July, 1974, the old positions being marked by circles. This relocation was made necessary by the rise of water level between the time of installation (September, 1973) and July, 1974. It was also necessary to position a transducer in the Alva Beach sand placed in the pit in March, 1974. In Figure 4.1 the bottom of the pit prior to the introduction of the beach sand is shown as a dotted line. A solid line defines the ground surface after renewing of the sand. It should be noted that the bed level of the pit was subject to minor variations due to cleaning, scouring by recharge water and sediment deposition, during the period of this investigation. However the variations caused by these factors were relatively minor.
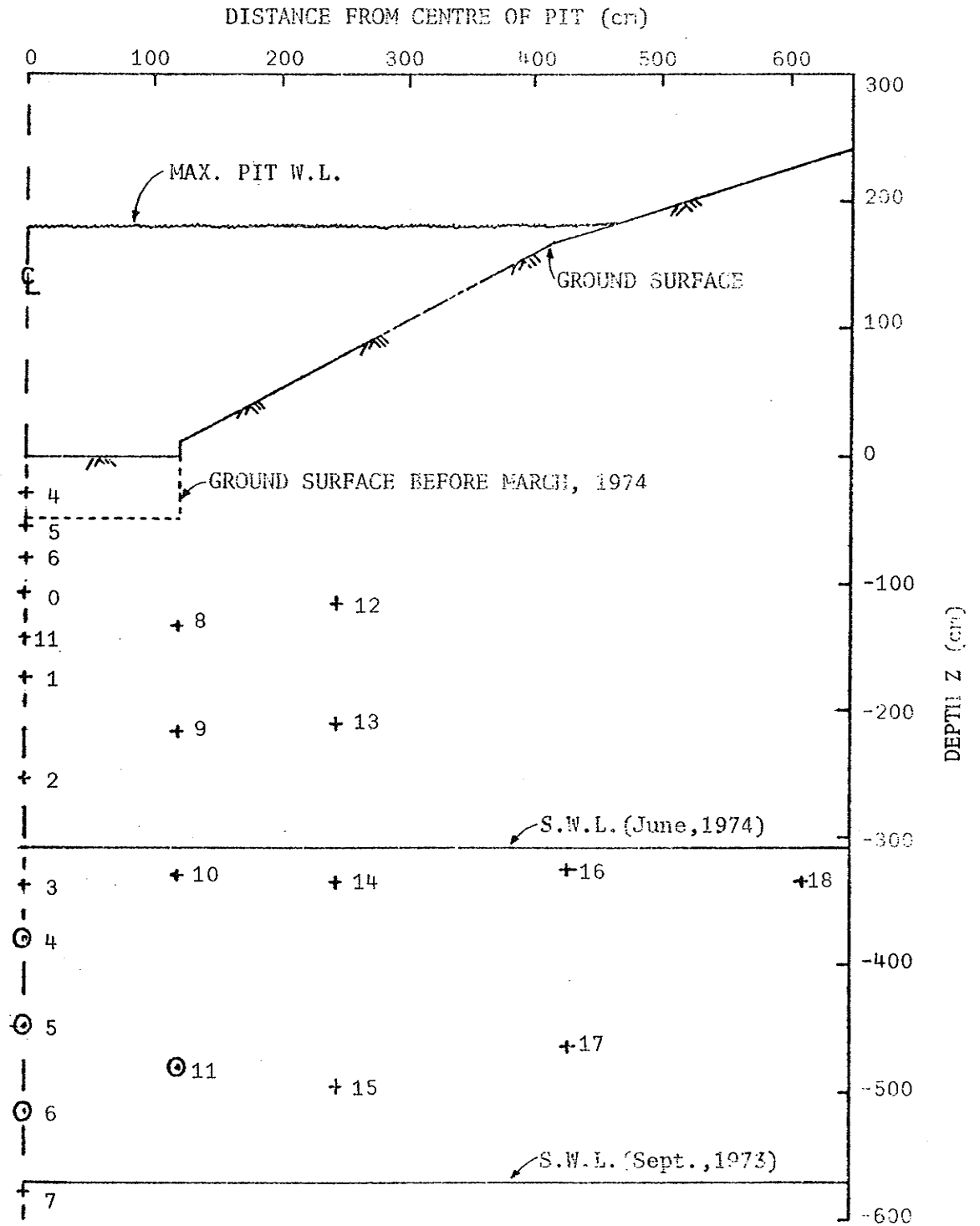
DISTANCE FROM CENTRE OF PIT (cm)

Figure 4.1: Cross-section through transducer installation at
Shands No. 2 Pit.

Referring to Figure 4.1, it should be noted that although the tensio-meter-pressure transducer units are shown on a vertical cross-section of the pit, they were in fact located on lines parallel to the pit centreline. They were spaced as close together as possible, this being about 0.3 m. Any closer spacing than this made it difficult to operate the drilling unit.

During the period when most of the detailed results were collected in July, 1974, the water table rose to a level between 1 m and 1.5 m from the base of the pit. The only transducers which were not below this new water level were numbers 4, 5, 6, 0, 11, 8, and 12. Four of these transducers were initially below the level and had to be raised as noted above. It was therefore not possible to draw two dimensional plots of pressure profile development because of the lack of tensiometer-transducer installations at suitable depths away from the pit centreline. Although the regional rise in water level in the Burdekin Delta during the exceptional 1973-74 rainy season was of undoubted benefit to the local landowners, it can be seen from Figure 4.1 that it effectively 'drowned out' the majority of the trans-ducer installation and restricted the results to one dimensional profiles.

Water content measurements described in Section 2.5 were made at four positions across the pit. The first was located on the pit centreline, the second on the same vertical profile as transducers 8, 9, etc., the third on the same line as transducers 12, 13, etc., and the fourth on the same line as transducers 16 and 17. Neutron moisture meter counts were taken from 0.15 m below the base of the pit in increments of 0.3 m to the standing water level in the access tubes. Care was taken to ensure that the measure-ments were taken at corresponding elevations for each set of readings.

As described in Section 2.3, thermocouples were installed on a vertical profile on the same line as transducers 8, 9, etc., and located from 0.3 m to 3.98 m below the base of the pit in increments of 0.46 m. The thermo-couples were not installed on the pit centreline because there was insuffi-cient room for another hole to be drilled at that location.

All the pressure results presented in this chapter relate to the pit centreline and the corresponding water content measurements were also taken at this location. Temperature profiles are given for the thermocouple installation approximately 1.2 m from the centreline but still located with-in the horizontal pit area. Because of the predominantly vertical movement of the recharge water it can be expected that the temperature measurements would correspond closely to the temperature values occurring at the pit centreline.

4.3 CONVERSION OF FIELD MEASUREMENTS TO PRESSURE, WATER CONTENT AND TEMPERATURE READINGS

The formula used to convert the millivolt outputs from the pressure transducers to pressure in cm of water is described in Section 2.2.2. This conversion process was carried out using the IBM 360/50 computer at the University of New South Wales. The transducer outputs in millivolts were recorded by the data acquisition equipment on punched paper tape. This tape was sent to Sydney and converted to pressure readings using two programs reproduced in Appendix A.

The first program (PTRAN1) was used to convert the punched coding to a character set and write this set onto a magnetic tape file which was then kept as a permanent record. PTRAN3, the second computer program, read in the file created by PTRAN1 and performed character manipulations, firstly to check that there were no data errors on the punched tape (frequent power cuts caused erroneous coding in some instances), and secondly, to store the transducer outputs in arrays ready for conversion.

The conversion from millivolts to pressure values was performed in subroutine INTPRT which is part of program PTRAN3. Once the conversion was performed the pressure values were outputted to the line printer and card punch. Suitable data for plotting were found by scanning the line printer output. The appropriate card output for the times to be plotted were then used as input to program PLOTTER, also reproduced in Appendix A. The plotting was carried out on the CYBER 72-26 computer currently in use at the University of New South Wales. Plotter outputs are presented in the sections of this chapter giving the results.

The thermocouple readings were also recorded in millivolts by the data acquisition system on the same punched paper tape with the pressure transducer readings. Each time the datalogger initiated a scan it read all the transducers and then the 10 thermocouples. The temperature readings in °C were derived from the punched paper tape in the same manner as the pressure readings using PTRAN1 and PTRAN3. The conversion equation from millivolts to °C is included in subroutine INTPRT. As noted in Section 2.3 the theoretical values for copper-constantan were used in the conversion, and these were found in laboratory calibrations to be the same as the actual thermocouple readings. The computer program PLOTTER was also used to plot the temperature results presented later in this chapter.

The neutron moisture meter readings in counts per minute were corrected to volumetric water content values manually using a calibration graph.

As described in Section 2.5 there were deficiencies in the data available to perform this conversion, but useful results were still obtained. It was assumed in the conversion that the saturated water content of the natural sand at Shands No. 2 Pit was 30%, and for the Alva Beach sand 35%. Because the neutron moisture meter could only take a reading at one point in the profile at a particular time, there was less information available for drawing the water content profiles in contrast with that available for the pressure and temperature profiles. Readings at certain times had to be interpolated to complete the water content plots.

4.4 RESULTS

The results of the field studies are presented in four separate subsections. A general summary of the results is then presented in the final section of this chapter.

4.4.1 Results Recorded During Filling

Three filling sequences at Shands No. 2 Pit are described in this section. The first two have corresponding pressure, water content and temperature data but the last sequence has no temperature data since the thermocouples were not installed at that time.

The first case is described in Figures 4.2 to 4.4. Figure 4.2 shows the progressive increase in soil water pressure as the moisture front moves down the profile. The initial water table level for this case was -200 cm. Recharge commenced at 1034 on the 187th day of the year and it can be seen that the profile became completely saturated approximately 30 minutes later (see Figure 4.3). The first four profiles given in the water content plot in Figure 4.3 correspond to the first four pressure plots. The fifth water content profile corresponds to the sixth pressure plot. As mentioned earlier there was generally less data available for plotting the water content profiles because of only one measuring device being available. However it is clear that the water content profiles correspond closely with the pressure profiles.

Figure 4.4 shows the temperature profiles at the same times as the pressure plots given in Figure 4.2. Curve 2 in the temperature profiles is identical to the temperature plot at the time the water entered the pit. It is clear that there is no significant trend in the temperature profiles until the water has been on the pit for about one hour (curve 6). Thereafter the temperature gradually decreases in the upper part of the profile until the temperature becomes almost uniform throughout the profile in
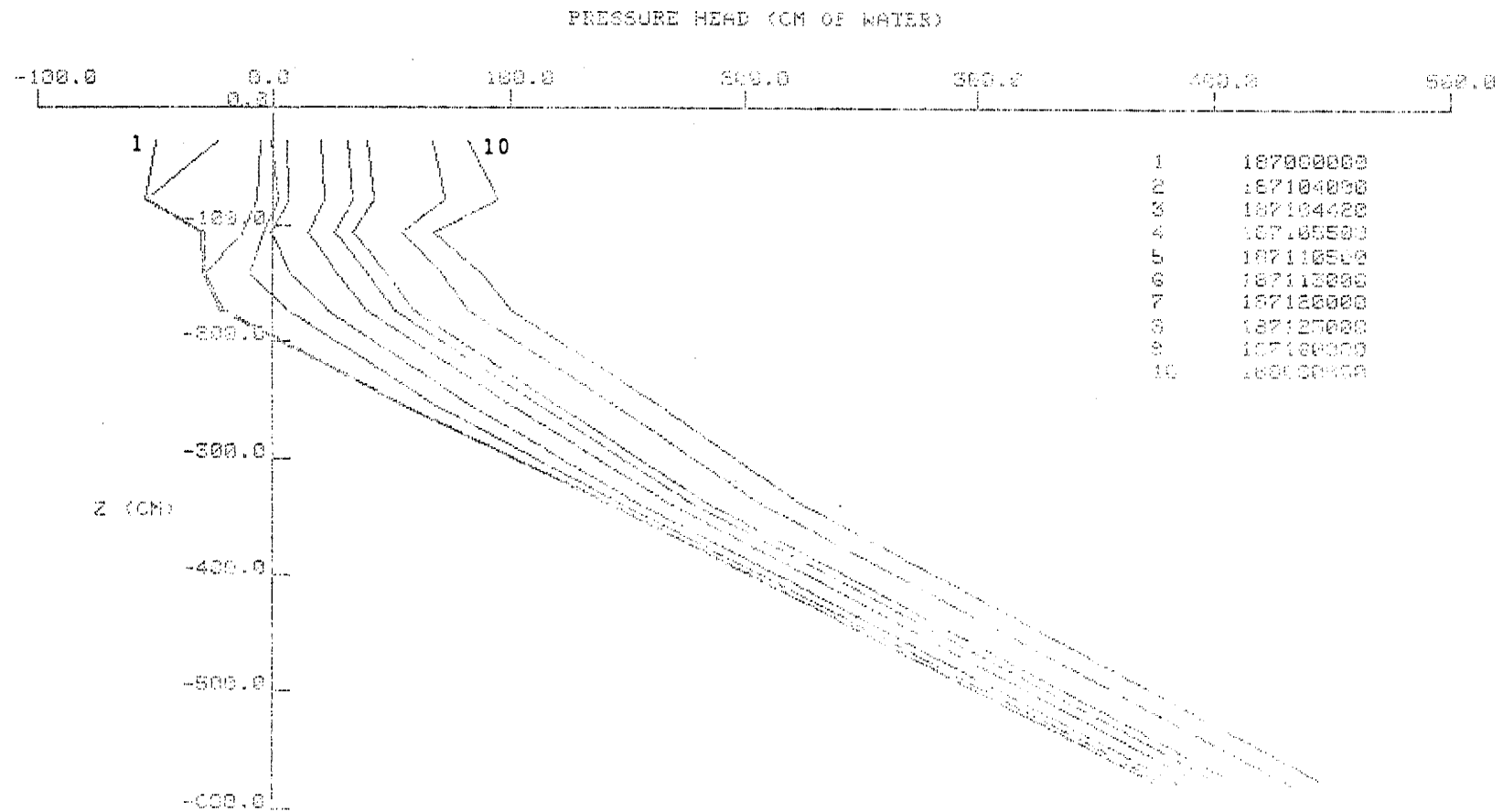
PRESSURE HEAD (CM OF WATER)

Figure 4.2:   Pressure profiles during filling (Case 1)

WATER CONTENT (cm^3cm^{-3})
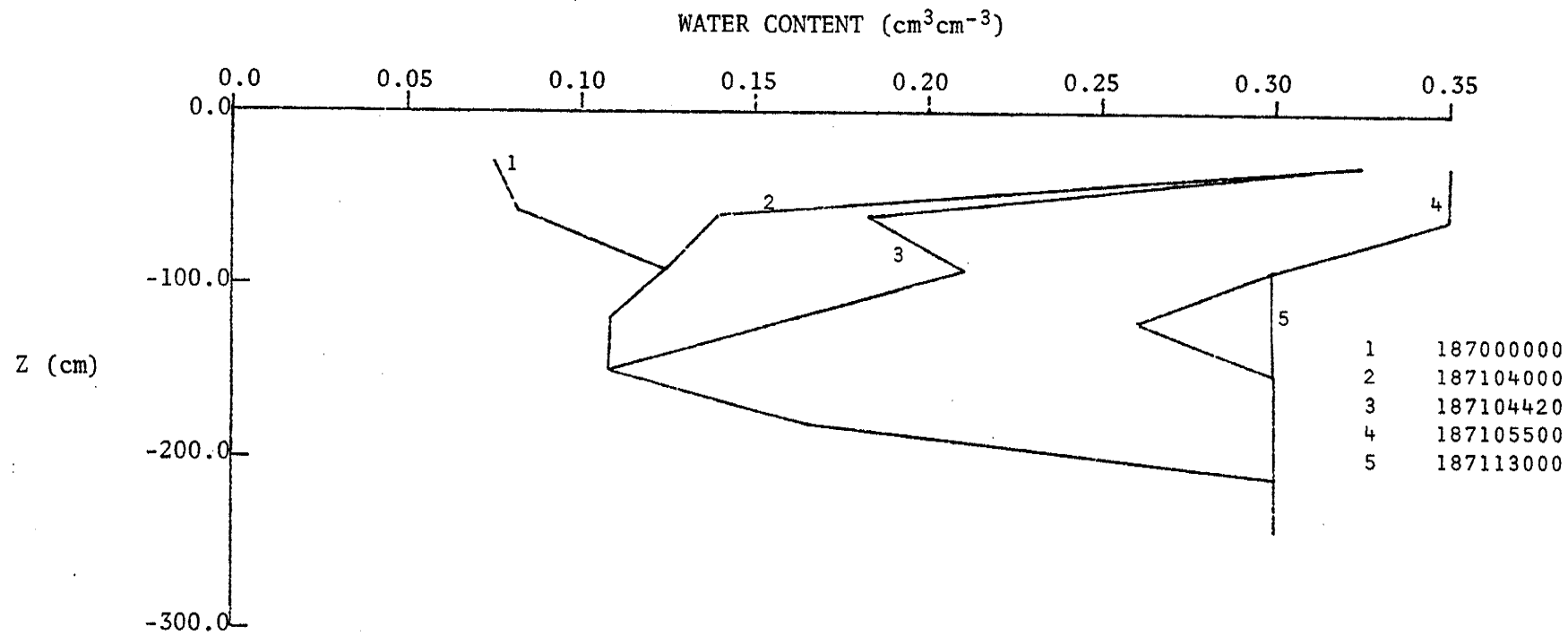
Figure 4.3: Water content profiles during filling (Case 1)

1	187000000
2	187104000
3	187104420
4	187105500
5	187113000

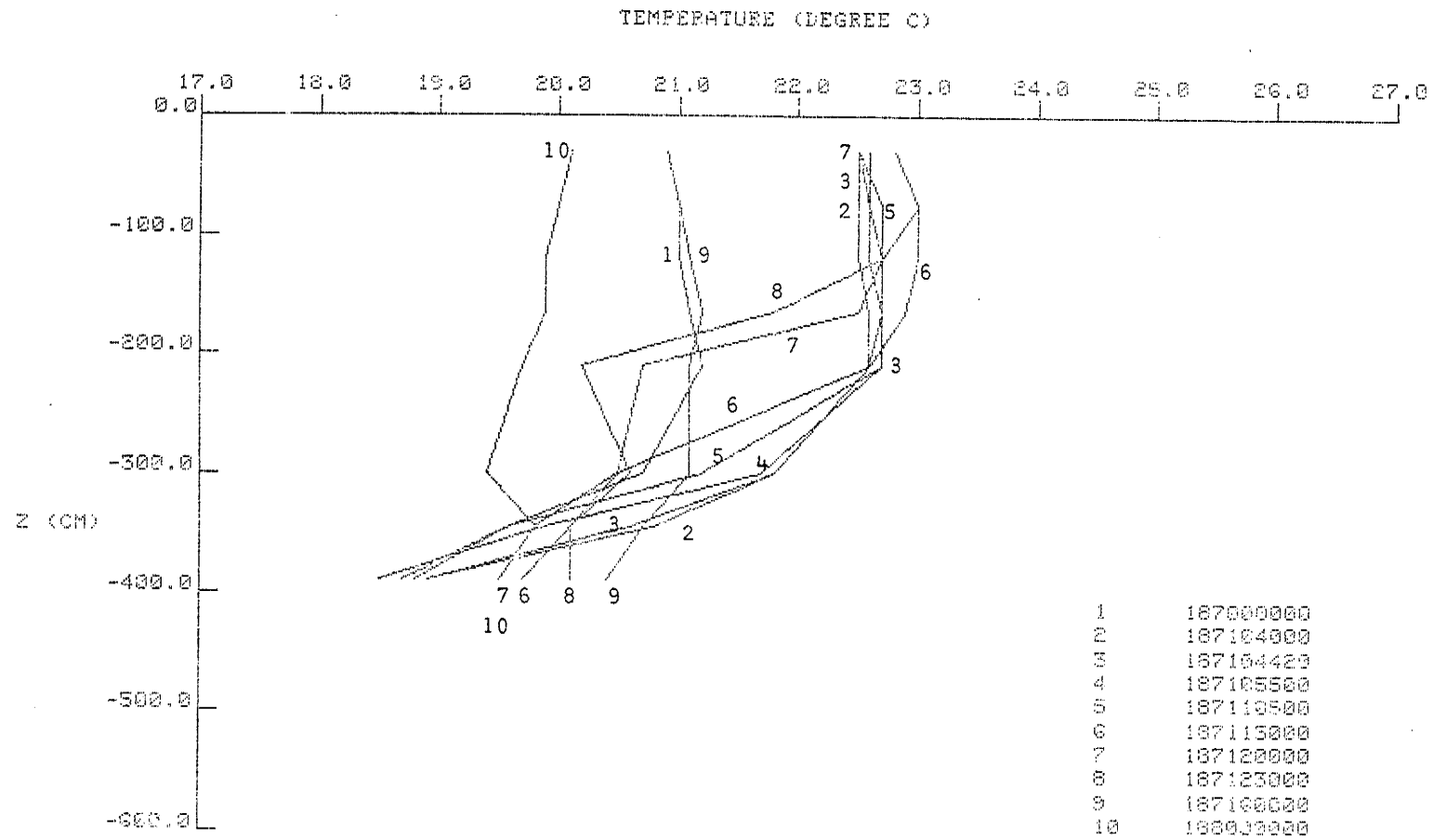Z (cm)

TEMPERATURE (DEGREE C)

Figure 4.4:   Temperature profiles during filling (Case 1)

curve 10. It should be noted that the temperature values at any point are only accurate to approximately ± 0.5°C so in fact curve 10 could represent a completely uniform temperature profile. The change from a non-uniform to a uniform temperature profile was characteristic of the behaviour of the temperature profile when filling the pit after it had been thoroughly drained. This behaviour is not demonstrated in the temperature profiles for case 2, as water had only recently been drained from the pit before the filling operation started.

The second set of filling data are presented in Figures 4.5 to 4.7. For this case the water entered the pit at 1447 on the 191th day of the year. The very clear detail of the pressure profile development in the upper part of the profile should be noted in Figure 4.5. From this figure the initial water-table level can be seen to be -180 cm. As a consequence, the water content distribution given in Figure 4.6 is less detailed because of the fewer measuring points. The temperature profiles for this case given in Figure 4.7 show that the temperature is practically uniform throughout the profile with a slight increase in temperature below the water table as the recharge water reaches that point.

The final filling case is given in Figures 4.8 and 4.9. For this case the tensiometer-transducer units were in their original positions (see Figure 4.1) before four of the transducers were relocated. As a consequence there is no pressure information for the top part of the profile. The initial water table was at -280 cm for this case which allowed a much greater scope for the water content profile to develop as shown in Figure 4.9. Recharge commenced at 1455 on the 144th day of the year.

This last filling case is of particular interest because the depth of water in the pit was maintained between 0.1 m and 0.2 m for the entire infiltration sequence. Because of this low head and a thin crust of sediment on the base of the pit, this example shows evidence of being a limiting flux case. Referring to the pressure profile in Figure 4.8 the soil water pressure at -110 cm remains at approximately -5 cm pressure head from 1508 to 1630 hours. In both the other filling cases the pressure became positive as the wetting front passed a point. The water content profile in Figure 4.9 shows that the profile does not become completely saturated until some time after 1545 although the wetting front reached the water table at approximately 1515.

4.4.2 Results Recorded While Draining

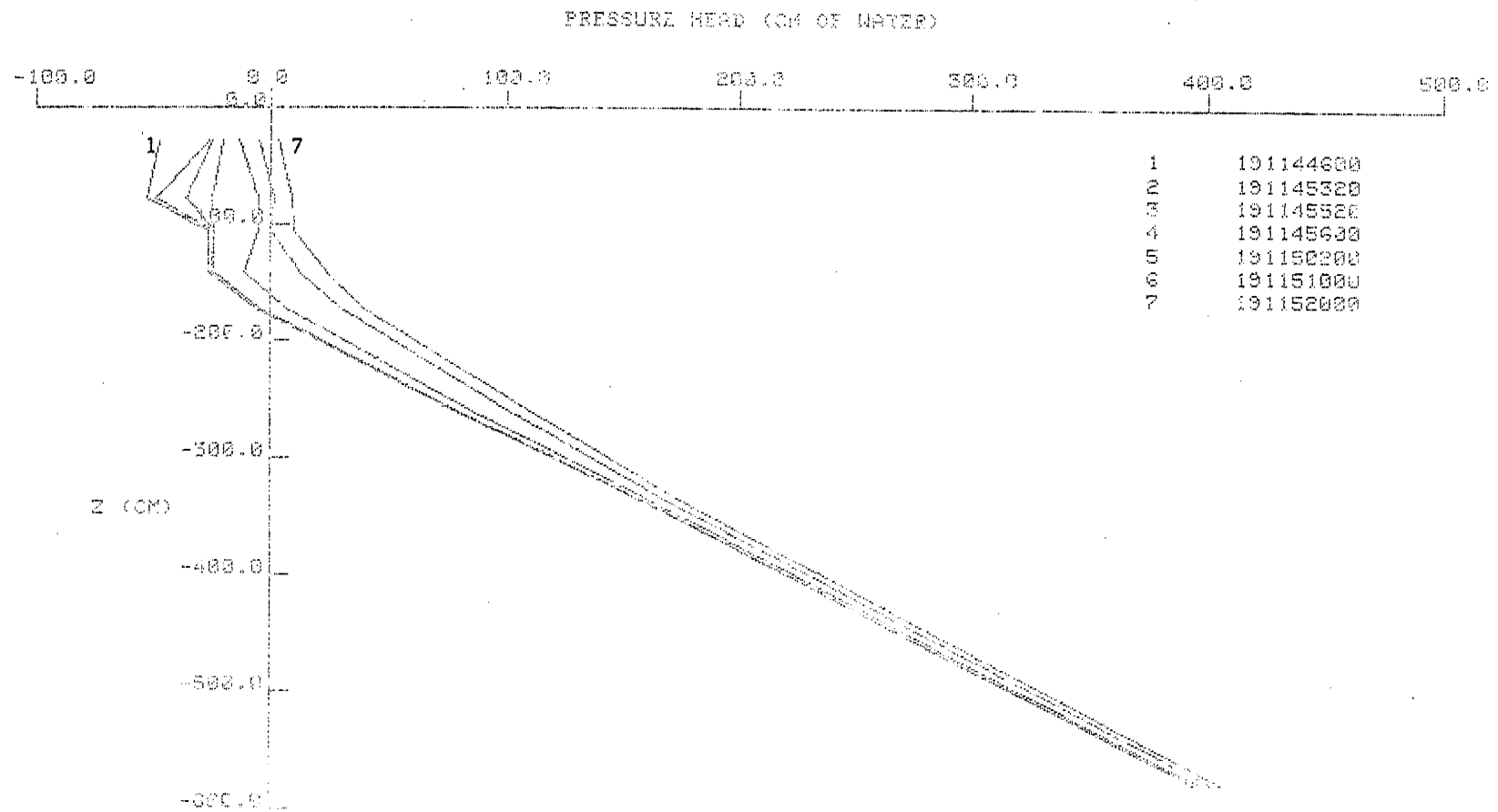Two cases are reproduced for draining of the soil profile at Shands

PRESSURE HEAD (CM OF WATER)

		1	191144600
		2	191145320
		3	191145520
		4	191145630
		5	191150200
		6	191151000
		7	191152000

Z (CM)

Figure 4.5: Pressure profiles during filling (Case 2)
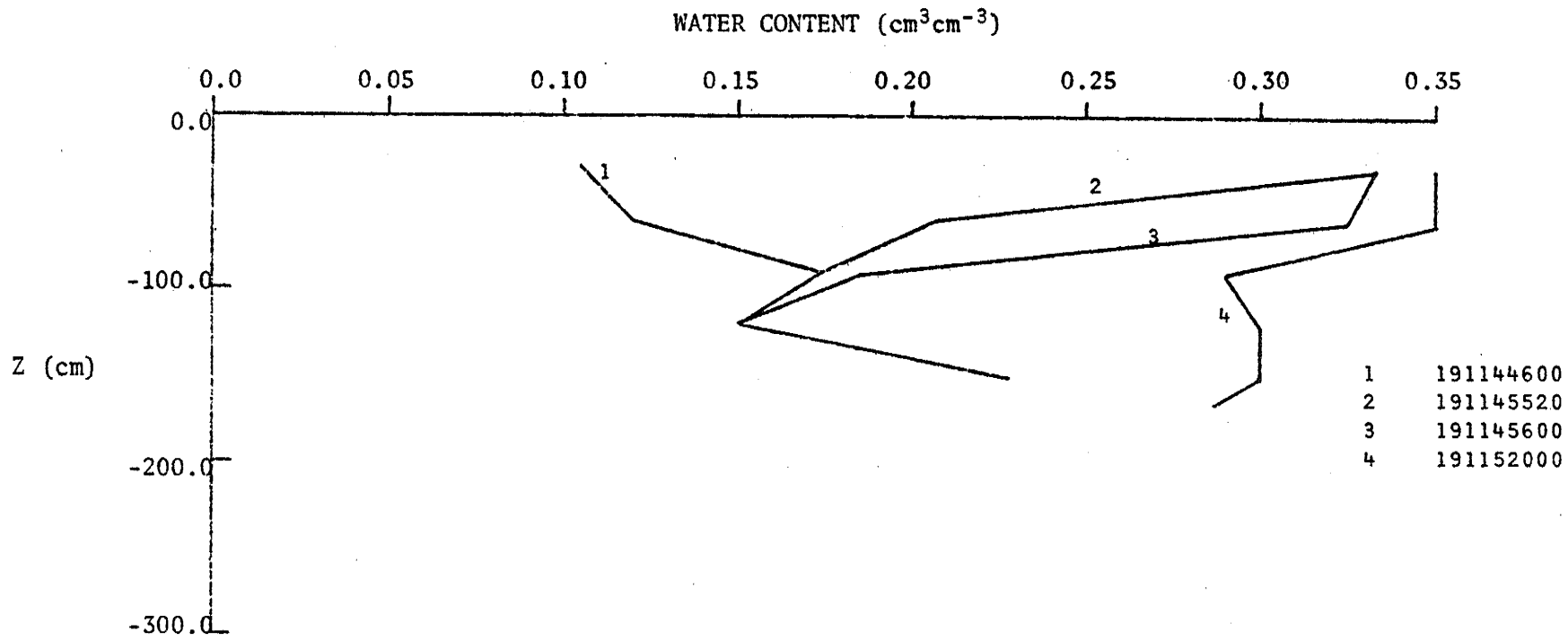
Figure 4.6:   Water content profiles during filling (Case 2)

TEMPERATURE (DEGREE C)

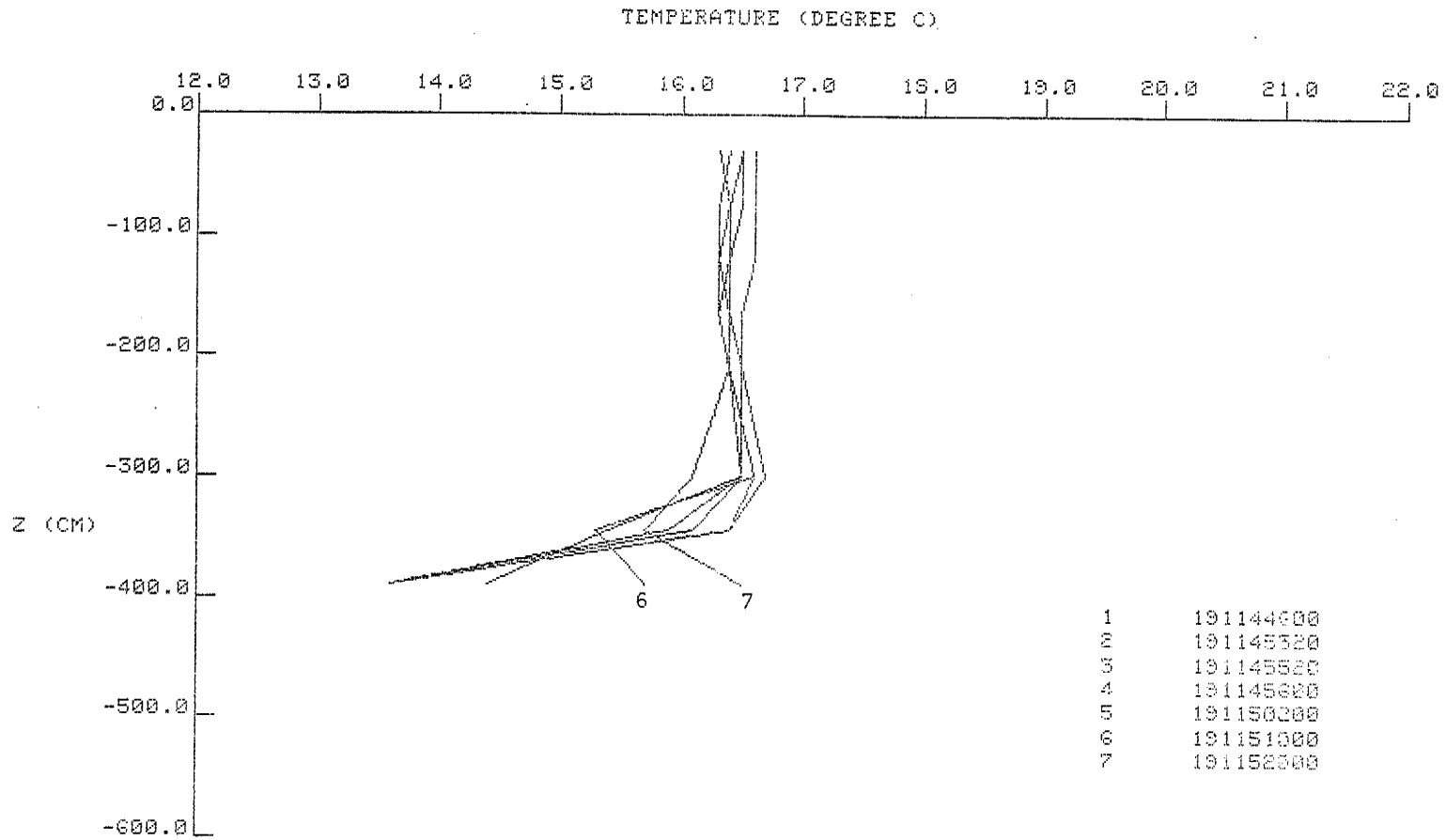|	1	191144600
	2	191145320
	3	191145520
	4	191145600
	5	191150200
	6	191151000
	7	191152300

Figure 4.7: Temperature profiles during filling (Case 2)

Figure 4.8: Pressure profiles during filling (Case 3)
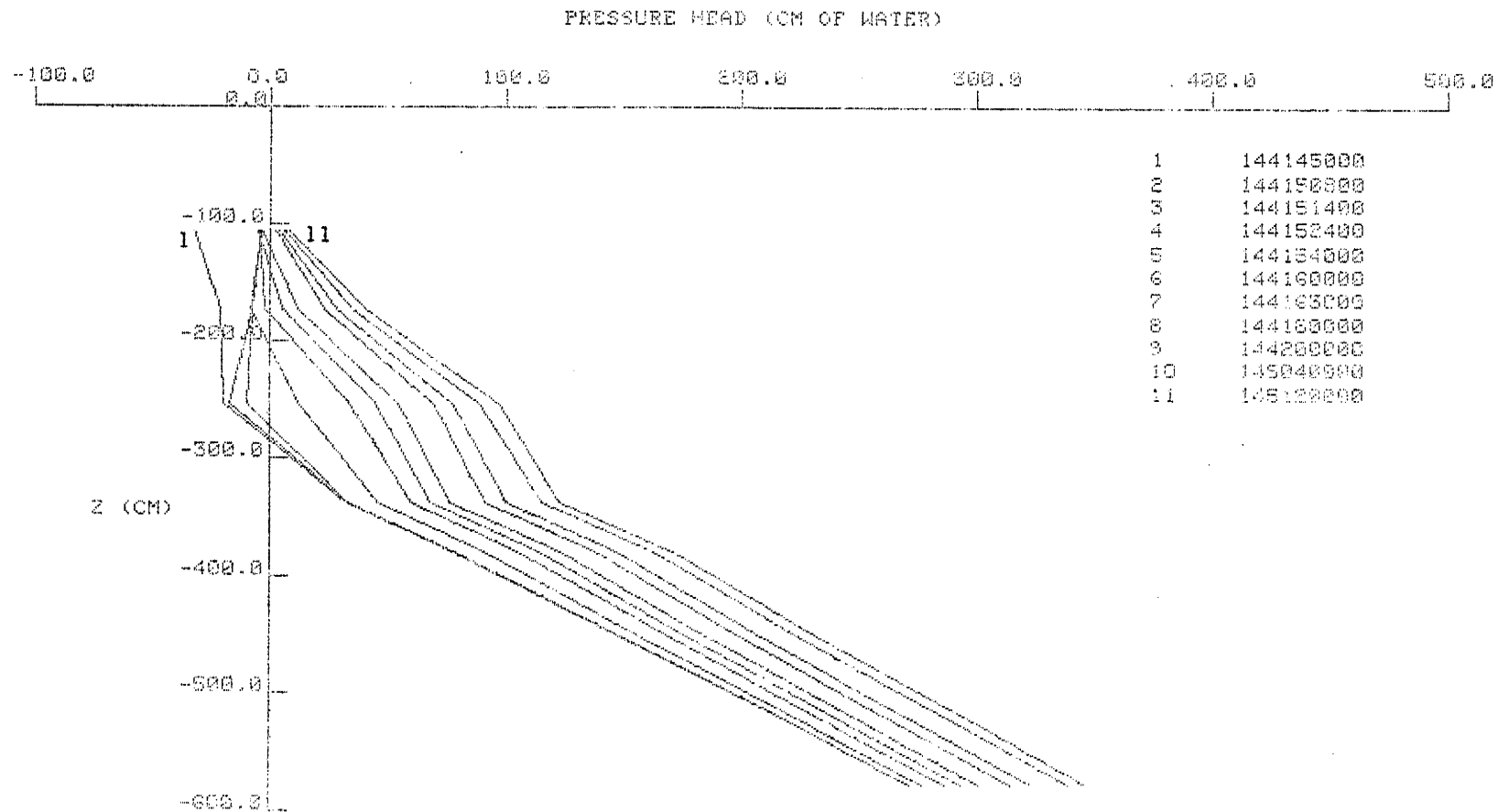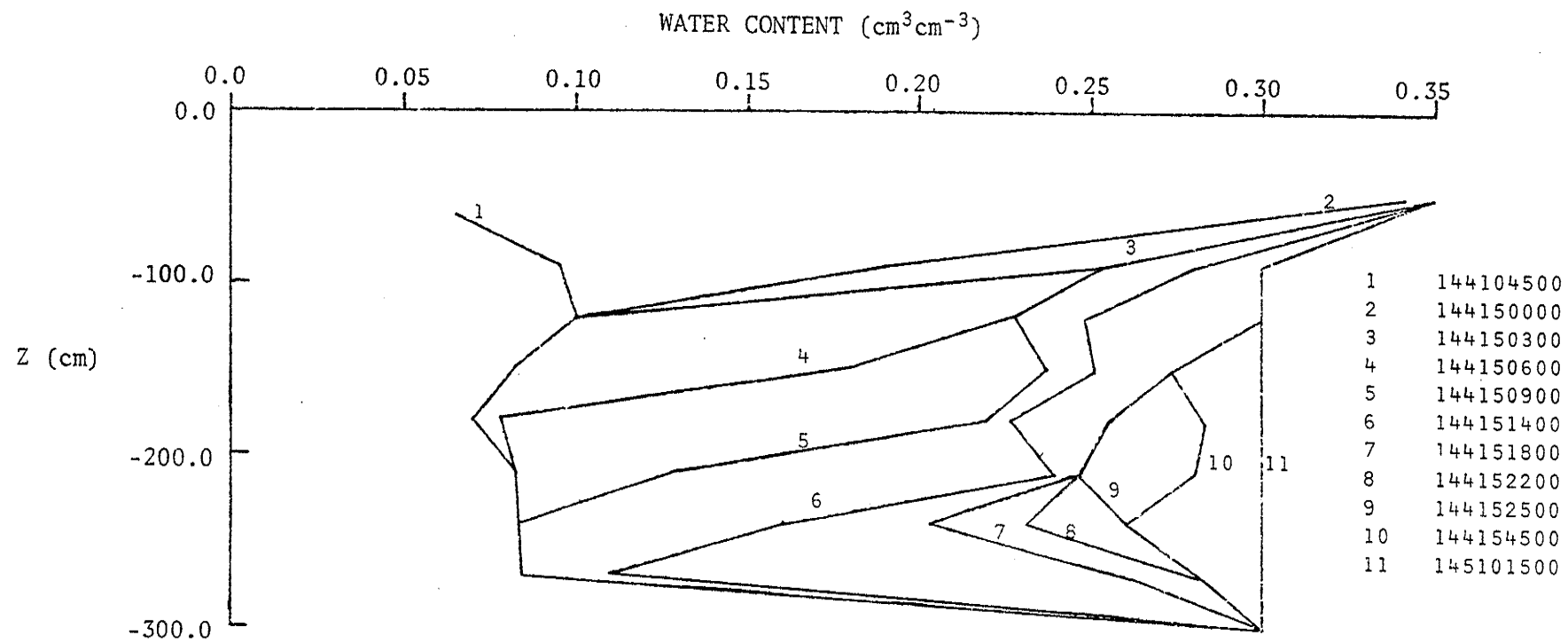
Figure 4.9: Water content profiles during filling (Case 3)

1	144104500
2	144150000
3	144150300
4	144150600
5	144150900
6	144151400
7	144151800
8	144152200
9	144152500
10	144154500
11	145101500

No. 2 Pit. The first case is described by Figures 4.10 to 4.12. For this case the ponded water disappeared through the sand surface at 1420 hours on the 188th day of the year. This time occurs between curves 3 and 4 and corresponds with negative soil water pressures developing in the upper part of the profile. The valve in the inlet pipe to the pit was shut at 1244, just before curve 2, so it can be seen that there is a significant pressure redistribution throughout the profile as the water level drops in the pit and before drainage commences.

Examining Figure 4.10 it can be seen that the upper part of the profile drains first and the rest of the profile drains more slowly. The drainage process is noticeably slower than the filling operation discussed in the preceding section. Figure 4.11 gives the water content distribution for several times. Again it should be noted that drainage is from the surface downwards corresponding to the pressure profile changes.

The temperature profiles given in Figure 4.12 show that there is no significant temperature gradient beneath the pit. There is a slight tendency for the temperature to cool down when the water has drained but this may be due to normal daily temperature fluctuations. A study of temperature profile changes over a one-day period is presented in a later section.

Figures 4.13 to 4.15 describe the second filling case. For this case the inlet valve to the pit was turned off at 0938 hours on the 190th day of the year and the ponded water was gone by 1219 hours which is between curves 5 and 6 in Figure 4.13. Negative pressures developed in the upper part of the profile before the ponded water disappeared but, as is shown in Figure 4.14, little, if any, water had drained from the profile by this time.

In Figure 4.13 it might be noted that curves 1 and 2 cross at approximately -100 cm. This is due to the fact that in the lower part of the profile the pressure is still increasing from the filling sequence started the previous day, whereas the upper part of the profile is reflecting the decreasing head of water in the pit as the water level drops. After curve 3 there is a systematic decrease in soil water pressure as drainage proceeds. The temperature profiles for this case are given in Figure 4.15. They show that there is an insignificant change in the temperature profile during the drainage sequence.

4.4.3 Results Collected During Intermittent Infiltration

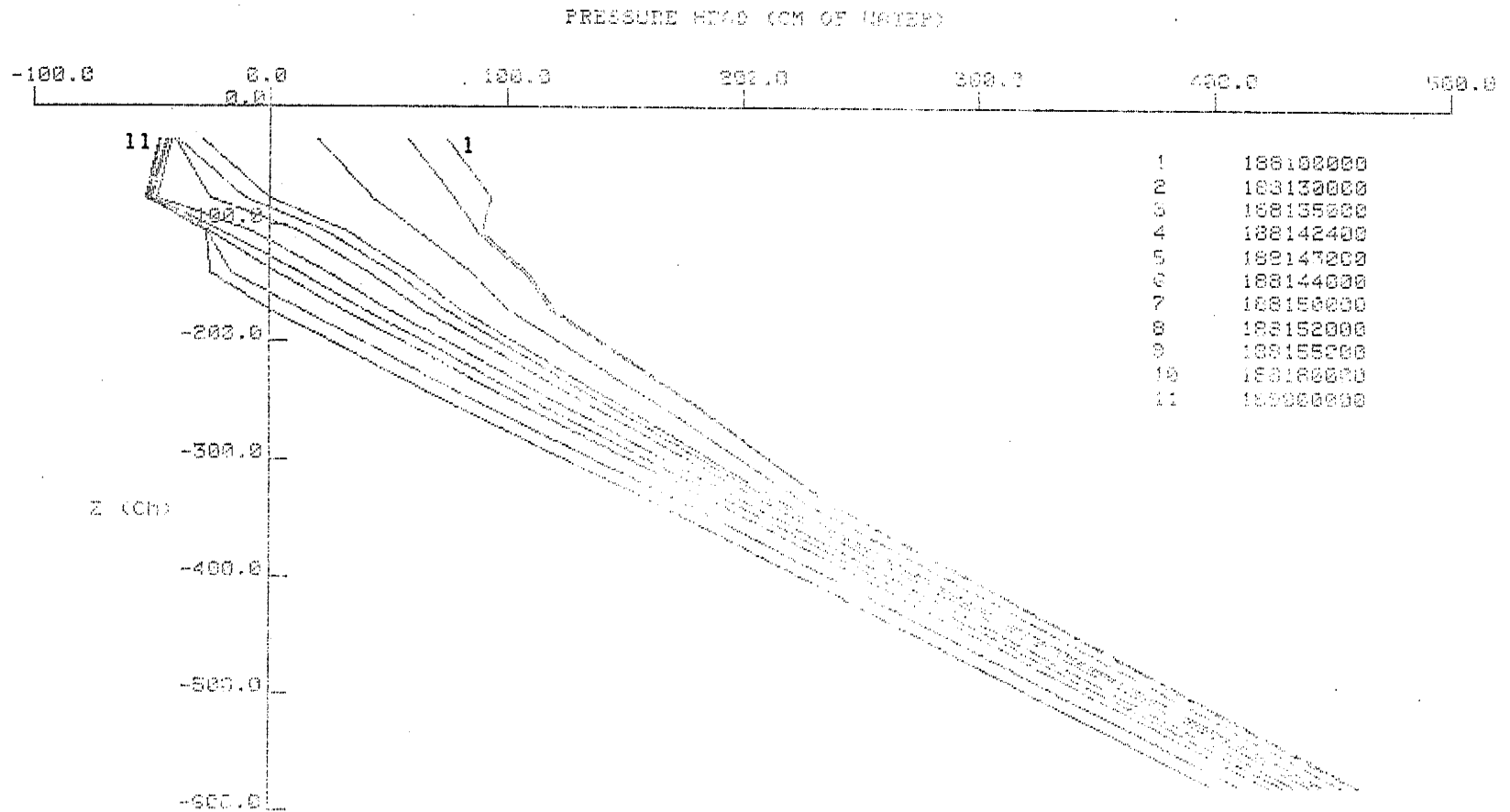One case is considered for intermittent recharge from Shands No. 2 Pit.

PRESSURE HEAD (CM OF WATER)

Figure 4.10: Pressure profiles during draining (Case 1)
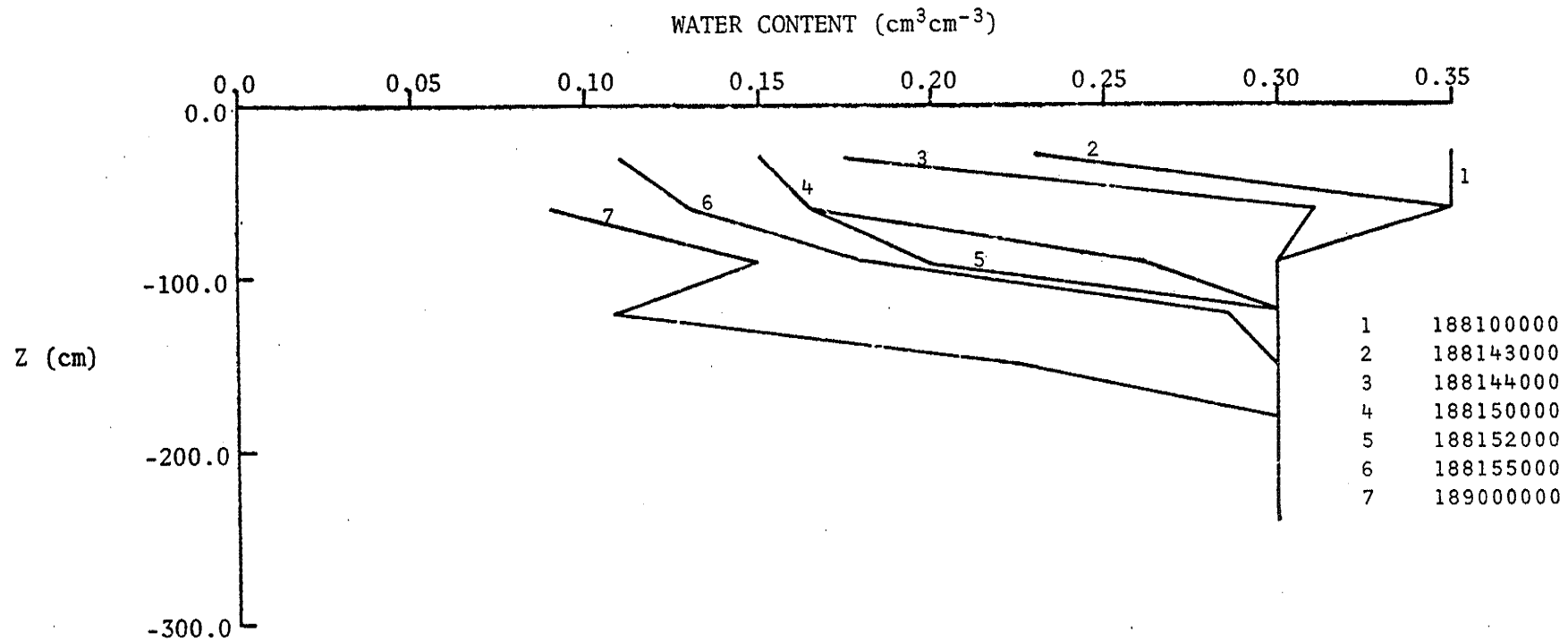
Figure 4.11: Water content profiles during draining (Case 1)

TEMPERATURE (DEGREE C)

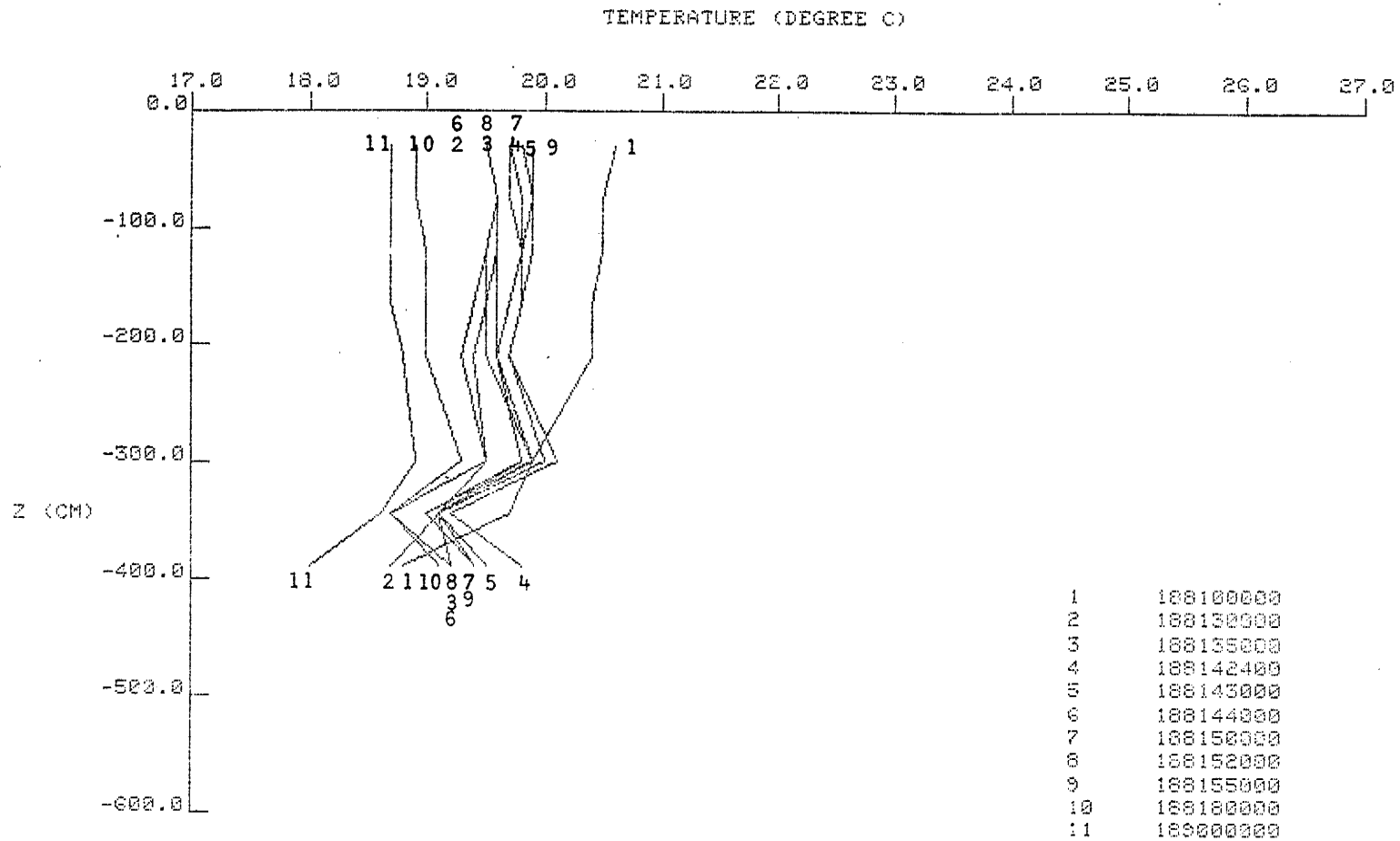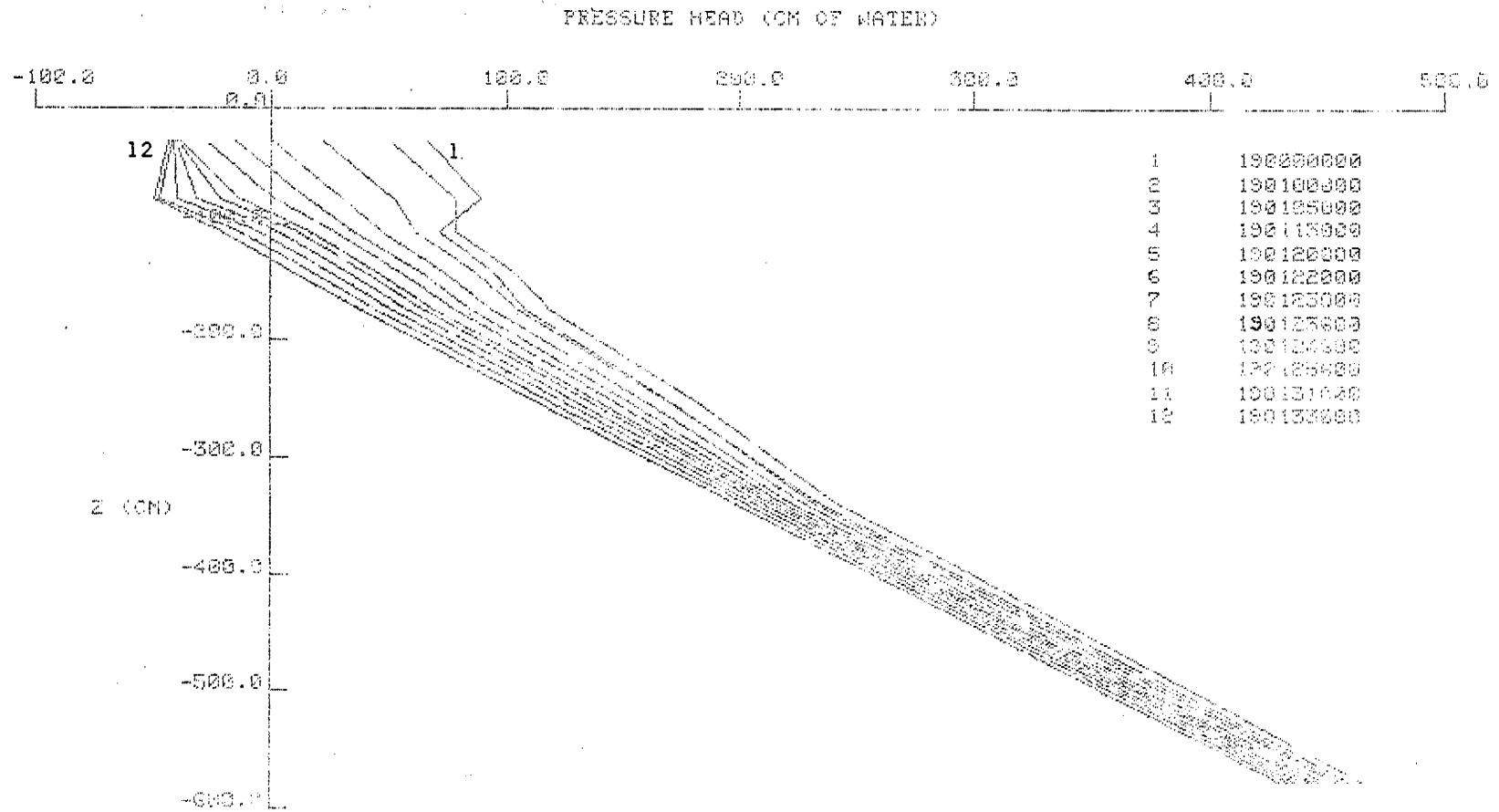Figure 4.12: Temperature profiles during draining (Case 1)

PRESSURE HEAD (CM OF WATER)

Figure 4.13: Pressure profiles during draining (Case 2)

WATER CONTENT (cm^3cm^{-3})

Figure 4.14:   Water content profiles during draining (Case 2)

TEMPERATURE (DEGREE C)

```
     12.0    13.0    14.0    15.0    16.0    17.0    18.0    19.0    20.0    21.0    22.0
     0.0

   -100.0

   -200.0

   -300.0

Z (CM)

   -400.0
                                                        1      190000000
                                                        2      190100000
                                                        3      190105000
                                                        4      190113000
                                                        5      190120000
   -500.0                                               6      190122000
                                                        7      190123000
                                                        8      190123600
                                                        9      190124600
                                                       10      190125600
   -600.0                                               11      190131000
                                                       12      190133000
```
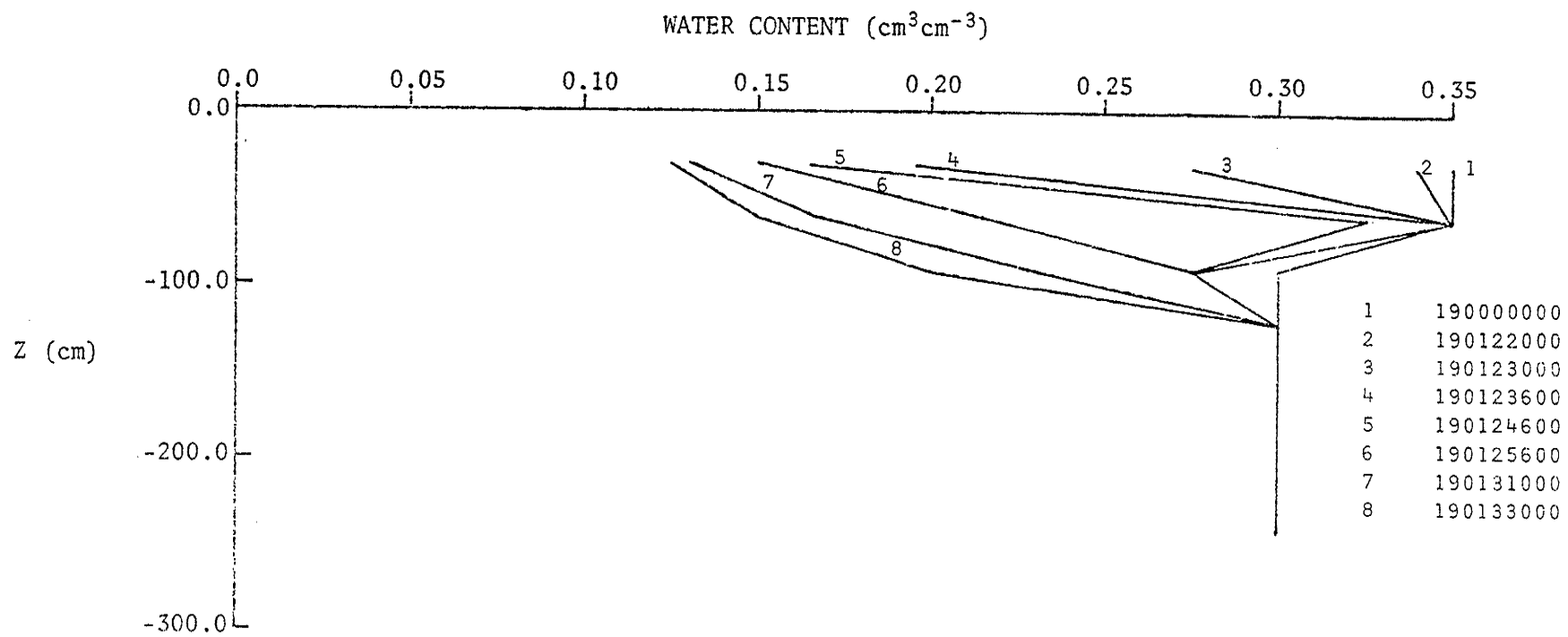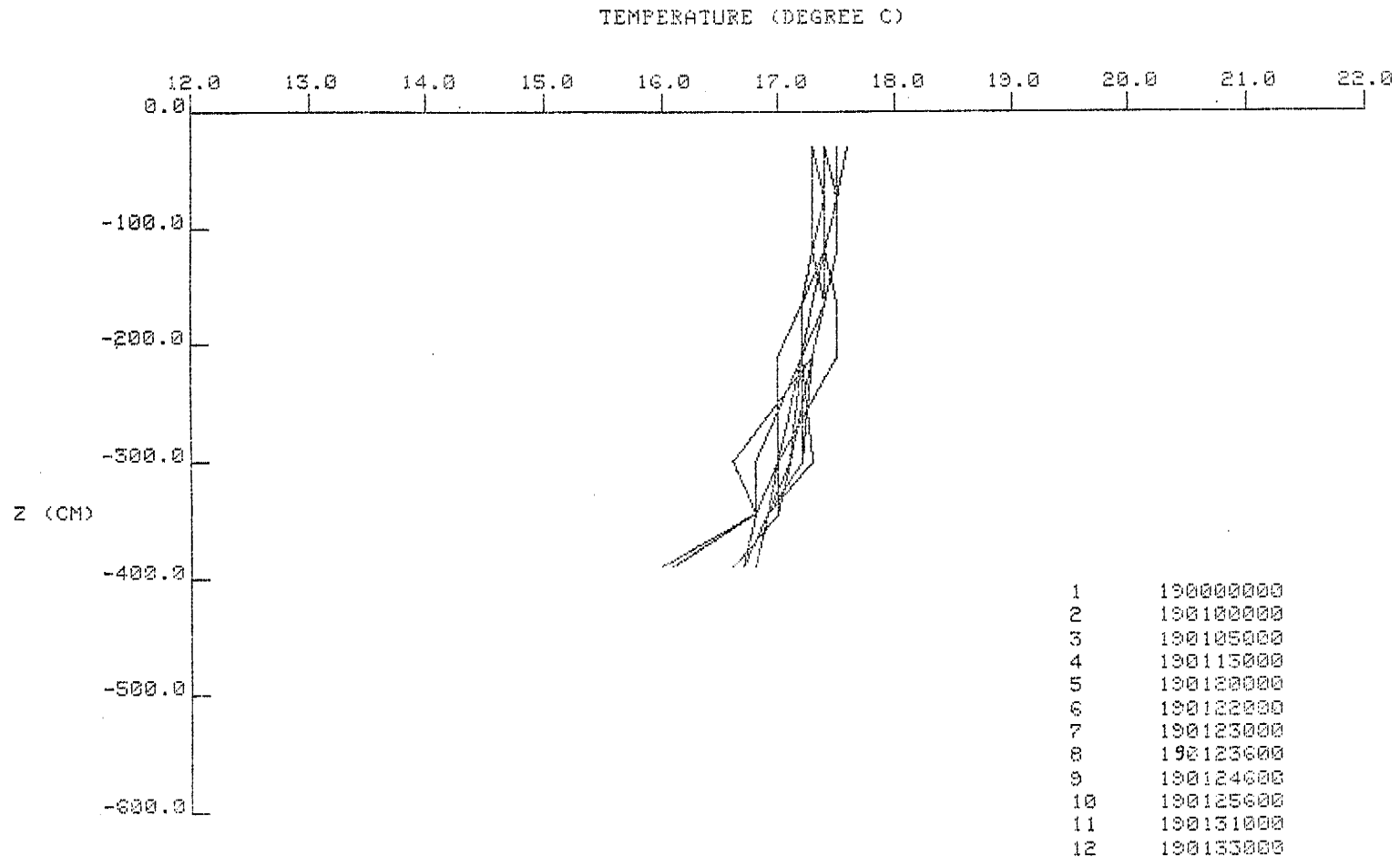
Figure 4.15: Temperature profiles during draining (Case 2)

Water was put on the pit for two short periods with a short time for drainage in between. The inlet valve was then opened and left on for a longer period. The response of the soil profile to this sequence of events is shown in Figures 4.16 to 4.18. Figure 4.16 shows the soil water pressure response to the on-off operation of the pit and this is reflected in the water content variations given in Figure 4.17. The temperature profiles in Figure 4.18 show little evidence of the pit operations.

The times of the on-off operations are given below, all the times being on the 196th day of the year.

Water on	1424
Pit drained	1430
Water on	1442
Pit drained	1449
Water on	1506

All the times are given to the nearest half minute. Referring to Figures 4.16 and 4.17 (note that the first 12 curves of each are at corresponding times), it can be seen that curves 1 to 3 describe the first filling sequence with the profile progressively wetting up. Curves 4 and 5 represent the first draining sequence. The upper part of the profile drains but the lower part continues to wet up slowly. Curves 6 and 7 describe the second filling sequence with the upper part of the profile wetting up and the lower part starting to wet up faster again. Curves 8 and 9 represent the second draining period. Again the upper part drains and the lower part of the profile wets up initially and then, as shown by curve 9, all the profile to about -130 cm commences to drain. Curves 10 to 13 represent the early part of the final filling sequence. In curve 10 the upper part of the profile wets up as the lower part continues to drain; this is then followed by the gradual wetting of the entire profile.

It might be noted that the water content profiles in Figure 4.17 are not completely in agreement with the pressure profiles at some times. This is due to a shortage of data for plotting the water content as discussed earlier. However the general pattern of behaviour is consistent for the two sets of data.

It is pleasing to note that the response of the tensiometer-pressure transducer units is in close agreement with the sequence of on-off operations of the recharge water. This provides evidence of the accuracy and fast response times of these units which were specially designed for this study.
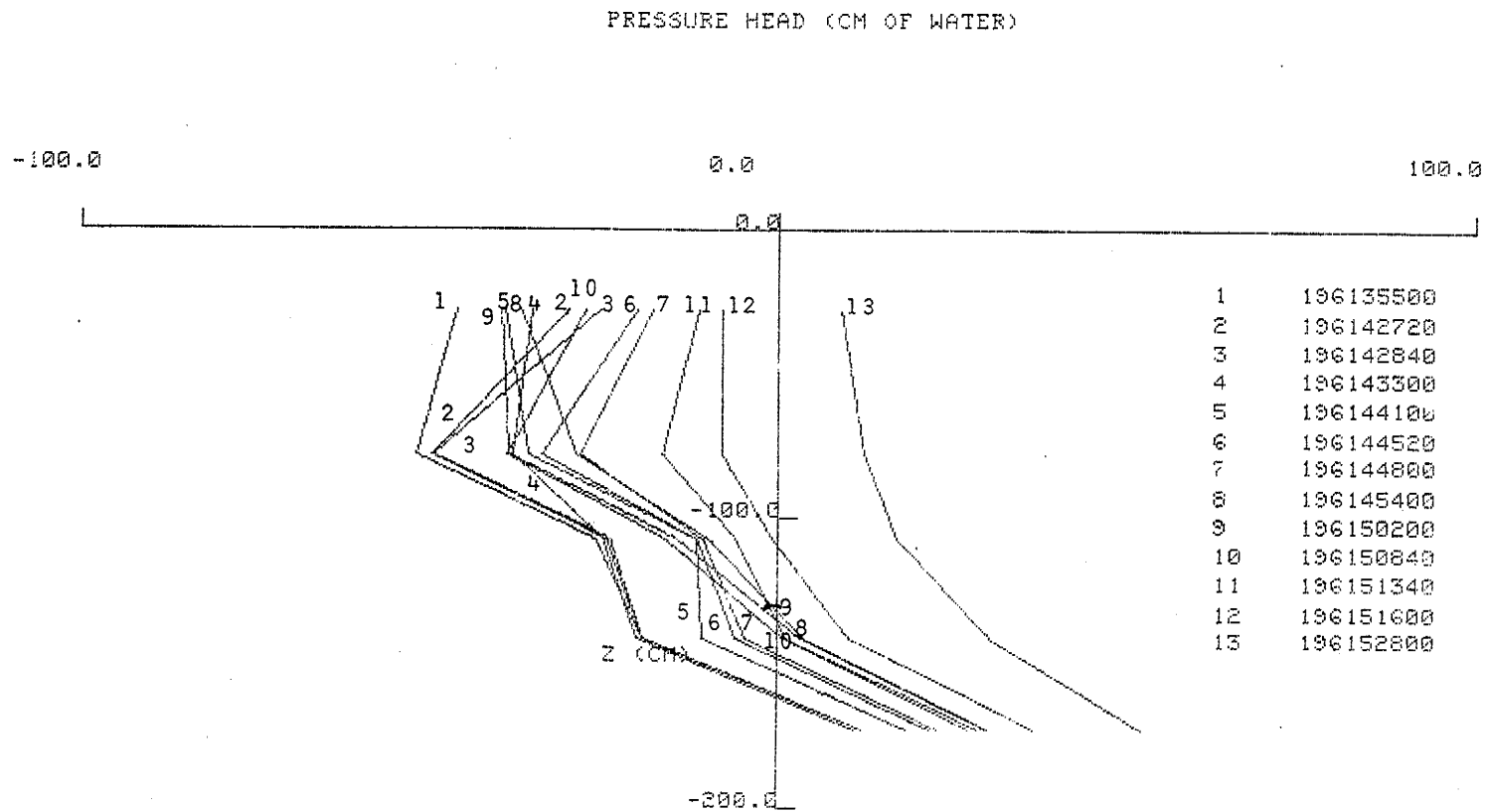
PRESSURE HEAD (CM OF WATER)

Figure 4.16: Pressure profiles during intermittent infiltration

WATER CONTENT (cm^3cm^{-3})

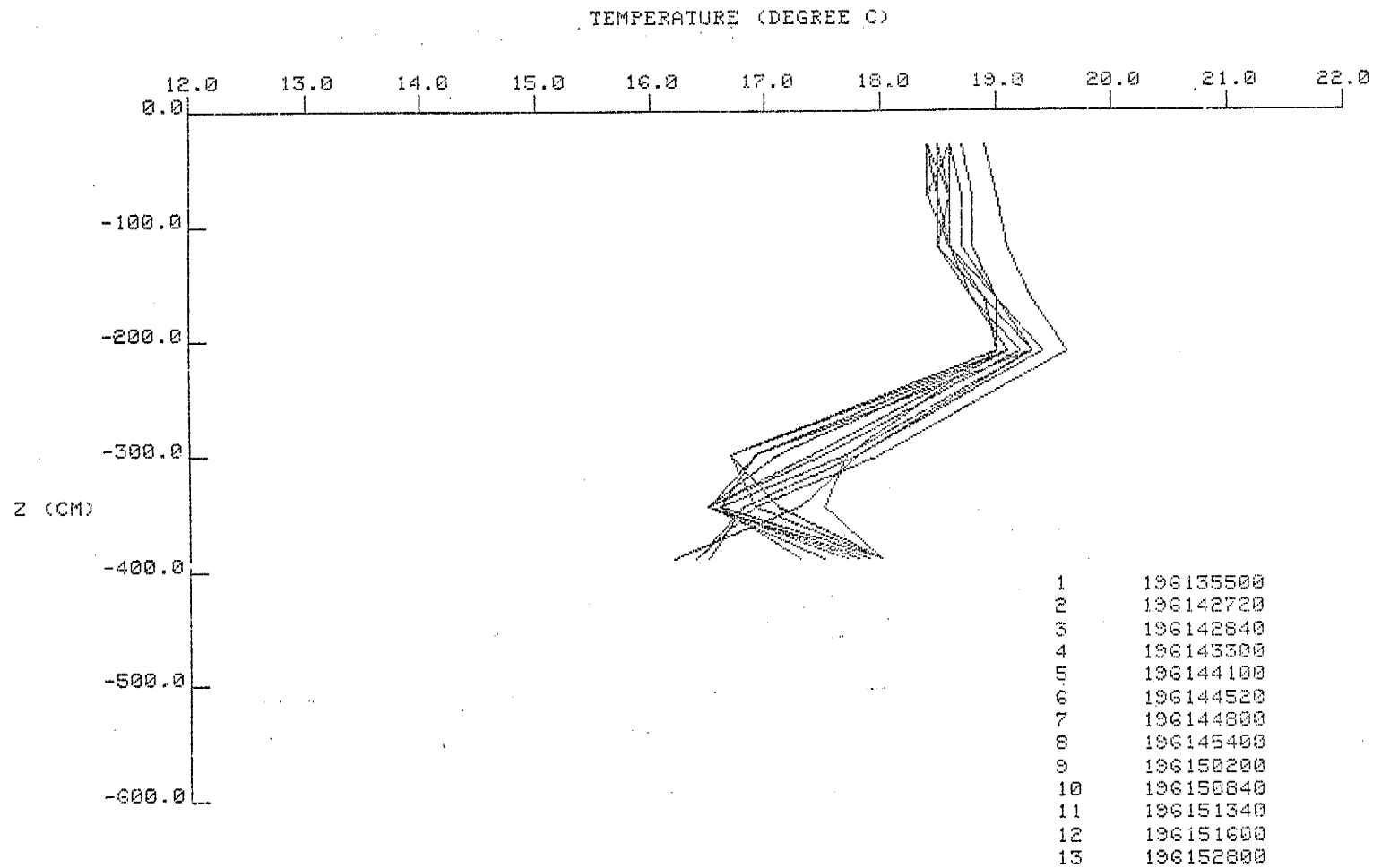| 1 | 196135500 |
2	196142720
3	196142840
4	196143300
5	196144100
6	196144520
7	196144800
8	196145400
9	196150200
10	196150840
11	196151340
12	196151600
13	197100700
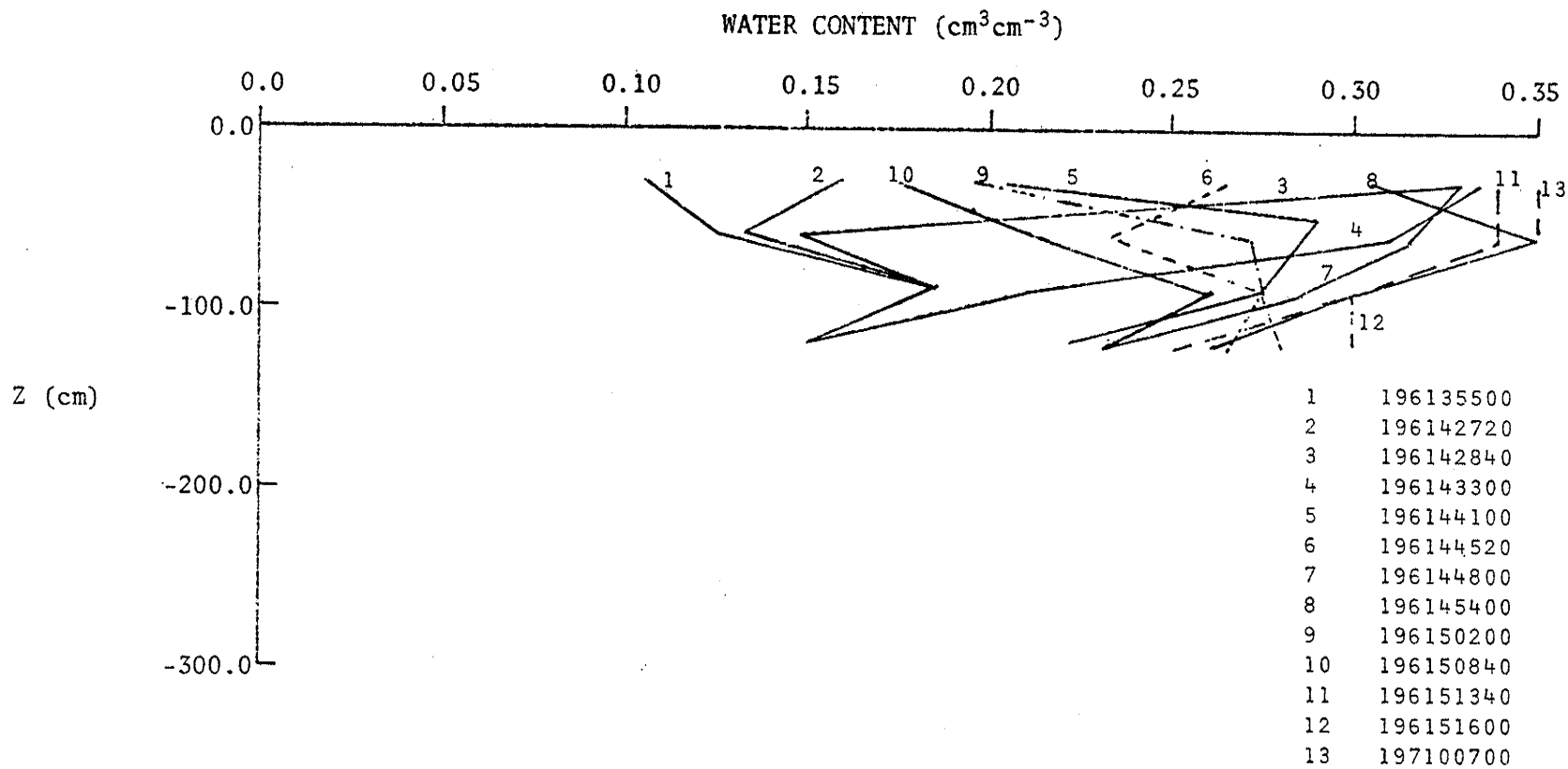
Figure 4.17: Water content profiles during intermittent infiltration

Figure 4.18:   Temperature profiles during intermittent infiltration

Another point of interest that was noted in this investigation was the large number of air bubbles that rose from the bottom of the pit during the second filling sequence. This would have been caused by air entrapment between the wetting zone from the first filling sequence, and the second wetting front. Although there are insufficient data to demonstrate the effect of this phenomena, it probably slowed the progress of the second wetting front significantly.

4.4.4 Temperature Trends Over a One-Day Period

During the diurnal recharge study discussed in Chapter 3 the datalogger was set to scan the transducers and thermocouples at half-hourly intervals. The temperatures derived from the thermocouple outputs for approximately one day of this period are presented in this section to examine more closely the temperature variations over a long time period. Temperature variations during the short filling and draining sequences are presented in the preceding results sections.

The temperature profiles are presented in Figures 4.19 to 4.25. It should be noted that the sharp zig-zags in the profiles are probably due to differences in the thermocouple calibrations rather than real differences in temperature. However, the relative temperature changes would be correct to within a fraction of a degree centigrade. The most noticeable feature of the curves is that there is a cyclic pattern of temperature change, with a much greater fluctuation in the upper part of the profile than in the lower. This difference would be due to the lower thermocouples being submerged below the standing water level. As a consequence there would be less movement of new recharge water in this zone and temperature variations in the new recharge water would tend to be damped out.

The fluctuations in temperature in the upper part of the profile tend to follow a diurnal pattern with the maximum temperatures occurring in the period 0800 to 1030 hours and the minima occurring at about 1930 hours. It would appear that the timing of the temperature fluctuations must be due to heating of the water in the river during the day and cooling at night. The lag in time between the probable maximum temperature in the river (late afternoon), and the maximum experienced in the pit, would be due to the travel time of the recharge water from the Burdekin River.

It is apparent from examining the figures that there are very significant temperature gradients in the soil profile at some times. For example in Figure 4.25 some of the temperature gradients are of the order
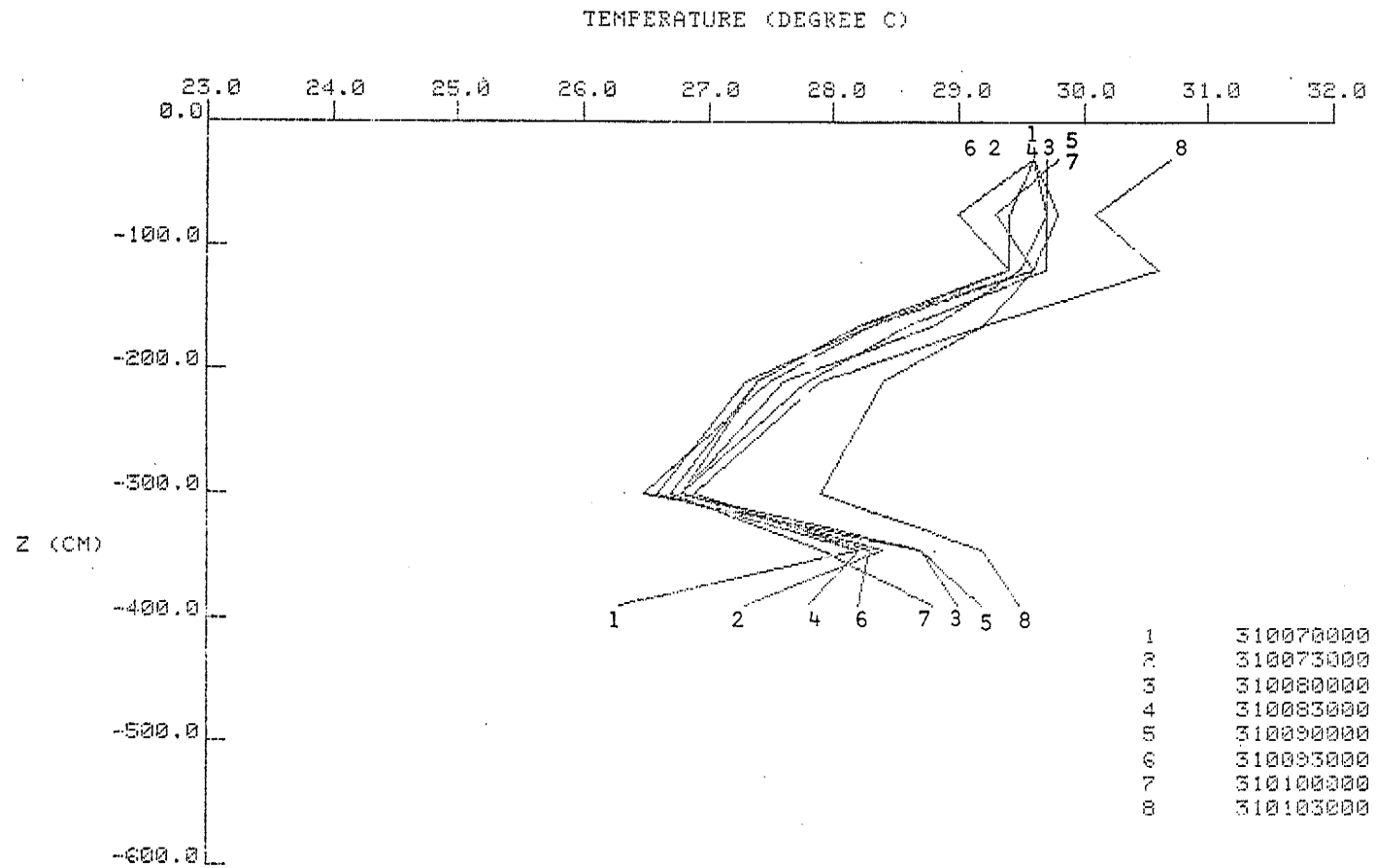
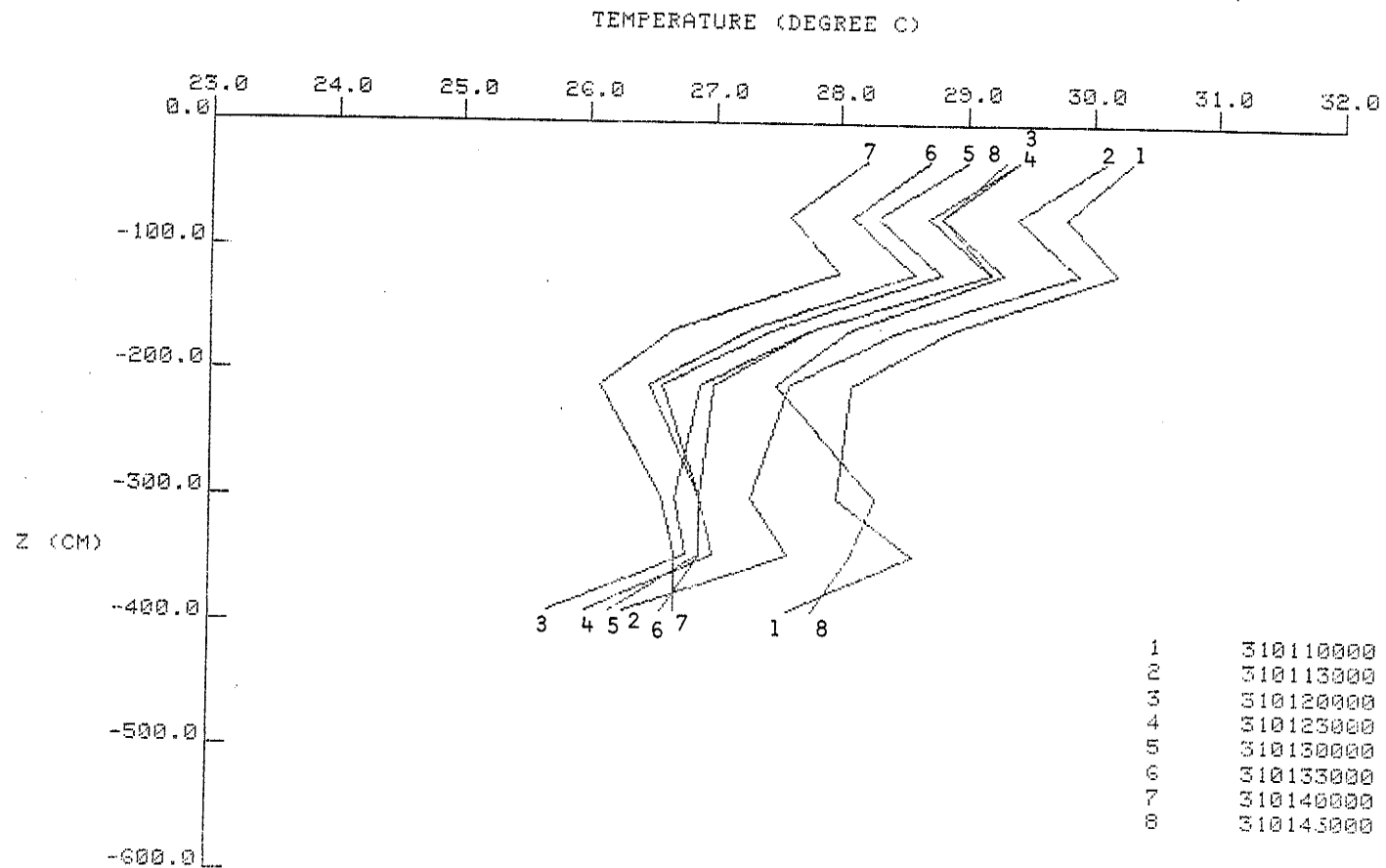Figure 4.19: Temperature profiles below Shands No. 2 Pit

TEMPERATURE (DEGREE C)

Figure 4.20:   Temperature profiles below Shands No. 2 Pit

TEMPERATURE (DEGREE C)

Figure 4.21:   Temperature profiles below Shands No. 2 Pit

Figure 4.22: Temperature profiles below Shands No. 2 Pit
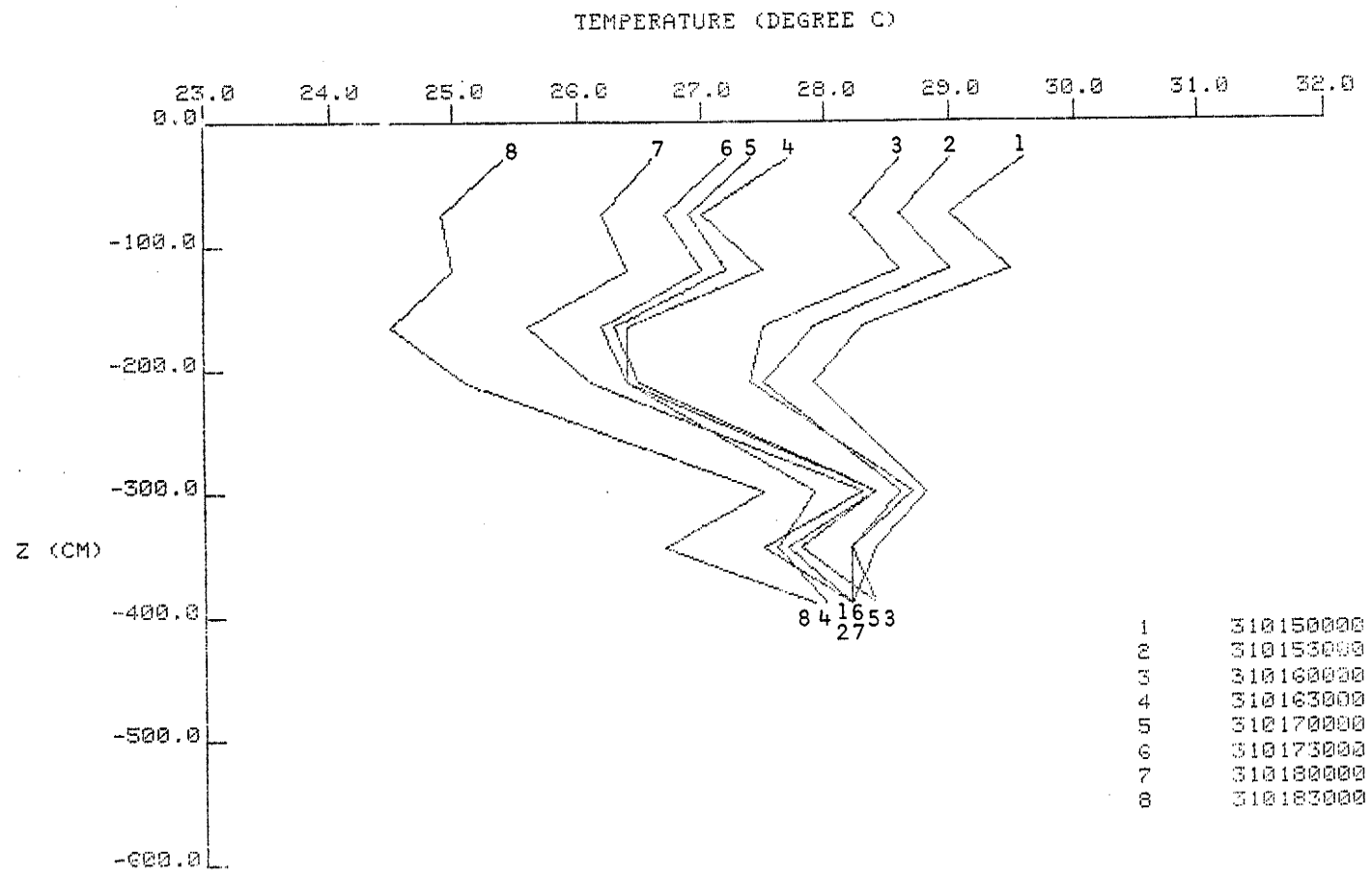
TEMPERATURE (DEGREE C)

Figure 4.23: Temperature profiles below Shands No. 2 Pit

Figure 4.24: Temperature profiles below Shands No. 2 Pit

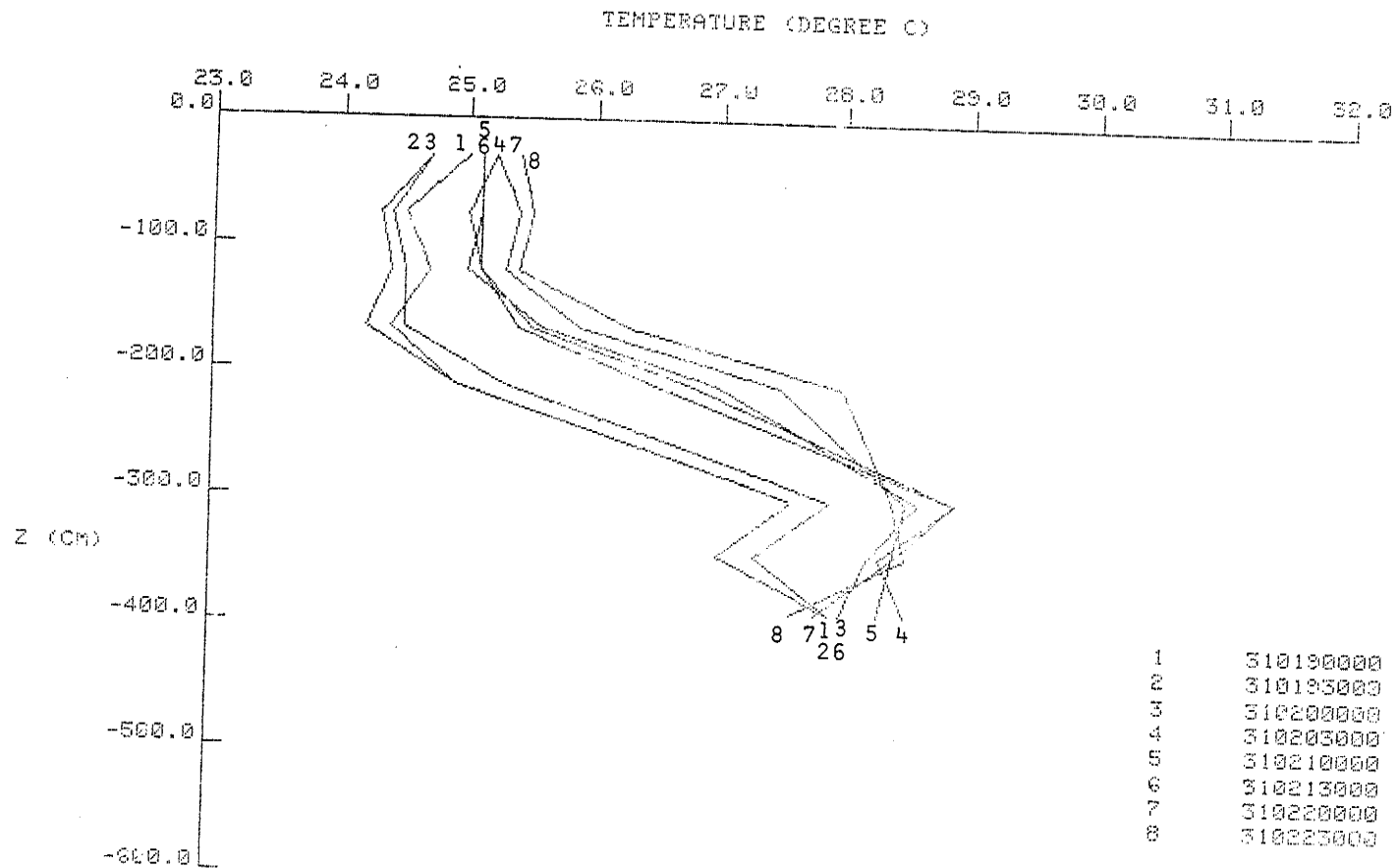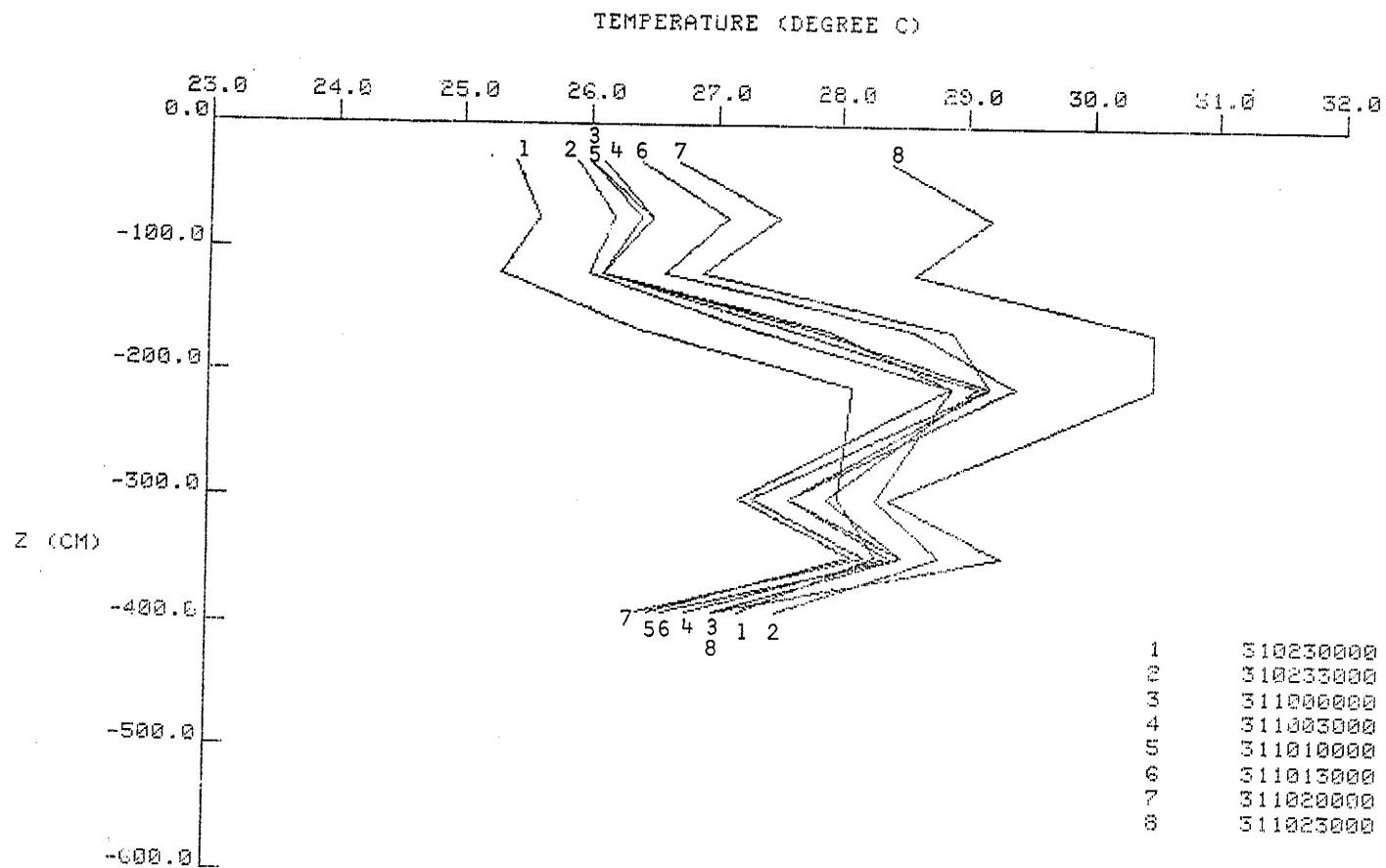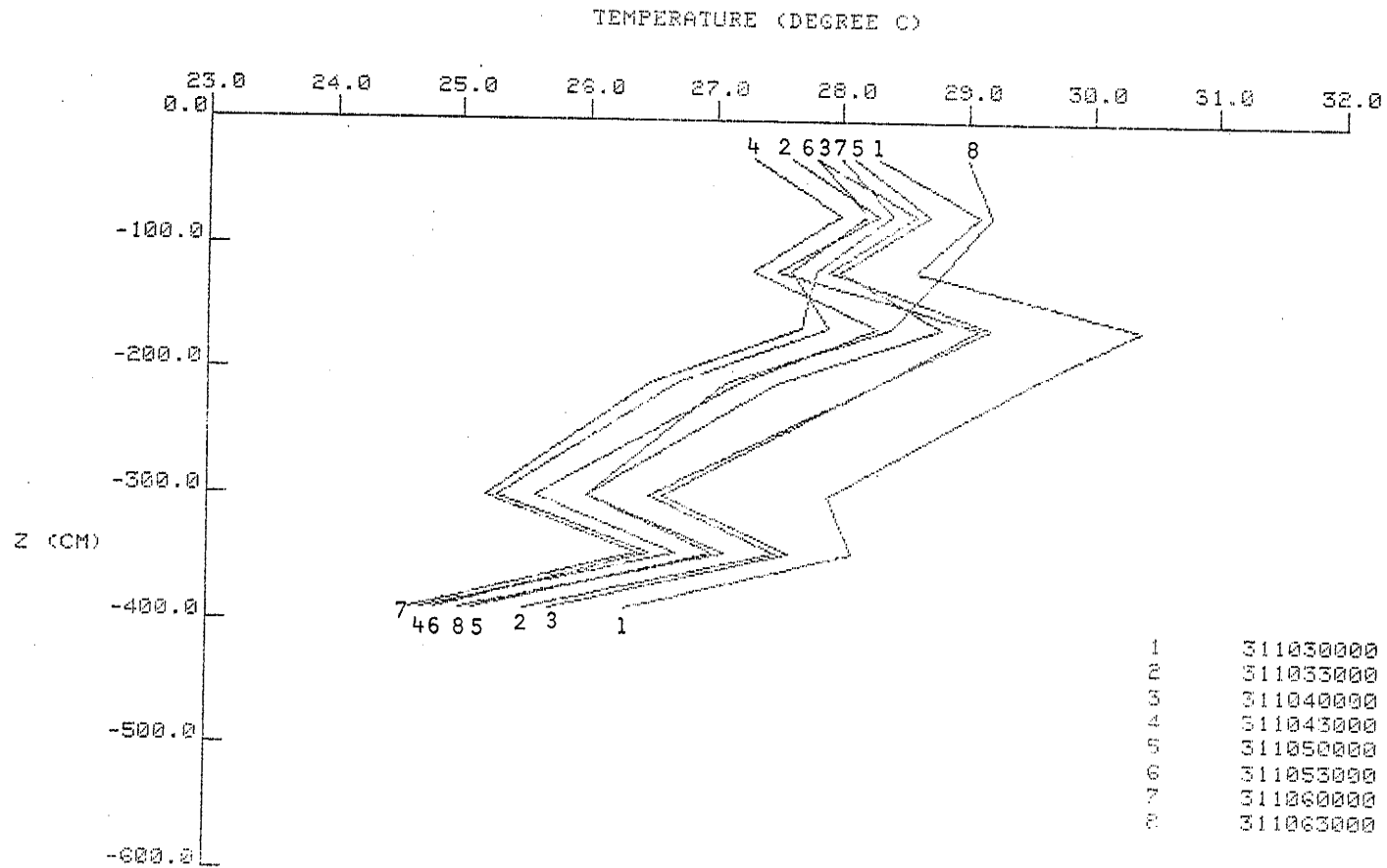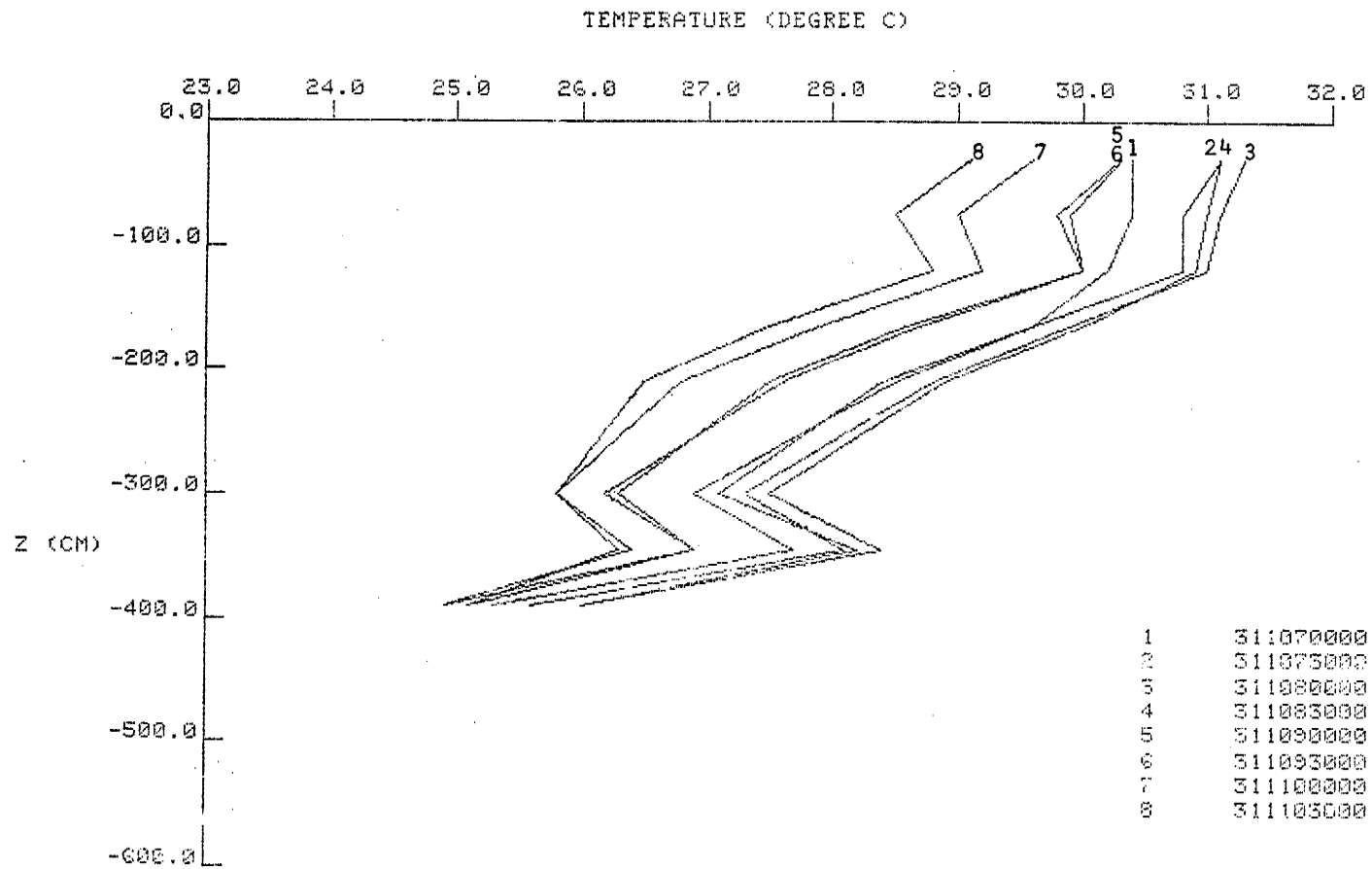Figure 4.25:   Temperature profiles below Shands No. 2 Pit

of 5°C in 4 m. Since recharge was proceeding with the pit full during the entire period covered by this figure it is clear that the new recharge water did not penetrate very far into the water table mound under the pit, and probably tended to flow predominantly in the horizontal plane after penetrating perhaps 2 m into the soil profile (it can be seen from the figure that temperatures diverge from uniformity after 1.5 to 2 m below the base of the pit).

Thermal gradients of the magnitude shown here would be sufficient to cause the soil water to flow under their influence, but any flow that did occur would be insignificant relative to the flow due to recharge. When there was no water on the pit there was evidence from the transducer readings of minor cyclic changes in pressure head which were probably due to the movement of soil water under thermal gradients.

The great variations in temperature in the upper part of the profile and the temperature gradients within the profile would presumably have a significant effect on the pattern of biological activity at the surface and within the soil profile. The temperature data collected in this investigation would therefore appear to be highly relevant to any biological studies conducted at Shands No. 2 Pit.

4.5 SUMMARY OF RESULTS

The pressure, water content and temperature profiles presented in this chapter provide a clear picture of the response of the soil profile under Shands No. 2 Pit to recharge cycles. Under intermittent infiltration into the pit it is possible to trace the movement of the successive wetting fronts as they proceed down the profile. One filling case is presented in which the depth of water in the pit was maintained at a very low level. This resulted in a limiting flux case in which the profile wet up, but did not become saturated until the wetting front had reached the water table. The crust of algal material and sediment on the base of the pit provided the low conductivity layer for this case.

The temperatures are shown to be substantially uniform throughout the profile during draining sequences, and when filling the pit soon after it had been drained. When filling the pit after it had been drained for some time, it is shown that there is initially a very steep temperature gradient which tended to a uniform profile as recharge proceeded.

An investigation of temperature profiles over a one-day period shows that significant diurnal fluctuations in temperature occur in the upper

1.5 to 2 m of the profile. This is probably due to the fact that the recharge water moves in a predominantly horizontal direction after penetrating to this depth. Below the 2 m level the water in the soil probably has a long resident time. Significant temperature gradients of the order of 5°C in 4 m developed in the profile even during continuous recharge operations because of the small penetration of the new recharge water.

REFERENCES

Edwards, R. L. and Owens, M. (1962). The Effects of Plants on River Conditions. J. of Ecol., 50, 207-220.

Hornberger, G. M. and Kelly, M. G. (1975). Atmospheric Reaeration in a River using Productivity Analysis. ASCE, J. Sanit. Engg Div., 101, 729-739.

Jackes, Betsy R. (1975). Final Report on A.W.R.C. Project 71/39—Burdekin Artificial Groundwater Recharge Study: Biological Problems in Artificial Recharge of Groundwater. School of Biological Sciences, James Cook University of North Queensland, 67pp.

Kelly, M. G., Church, M. R. and Hornberger, G. M. (1974a). A Solution of the Inorganic Carbon Mass Balance Equation and Its Relation to Algal Growth Rates. Water Resour. Res., 10(3), 493-497.

Kelly, M. G., Hornberger, G. M. and Cosby, B. J. (1974b). Continuous Automated Measurement of Rates of Photosynthesis and Respiration in an Undisturbed River Community. Limnology and Ocean., 19(2), 305-312.

McIntire, C. D., Garrison, R. L., Phinney, H. K. and Warren, C. E. (1964). Primary Production in Laboratory Streams. Limnology and Ocean., 9, 92-102.

O'Connell, R. L. and Thomas, N. A. (1965). Effect of Benthic Algae on Stream Dissolved Oxygen. ASCE, J. of Sanit. Engg Div., 91(SA3), 1-16.

O'Connor, D. J. and Di Toro, D. M. (1970). Photosynthesis and Oxygen Balance in Streams. ASCE, J. Sanit. Engg Div., 96(SA2), 547-571.

Odum, H. T. (1956). Primary Production in Flowing Waters. Limnology and Ocean., 1, 102-117.

Odum, H. T. (1957). Primary Production Measurements in Eleven Florida Springs and a Marine Turtle-grass Community. Limnology and Ocean., 2, 85-97.

Thomas, N. A. and O'Connell, R. L. (1966). A Method for Measuring Primary Production by Stream Benthos. Limnology and Ocean., 11, 386-392.

Tilzer, M. M. (1973). Diurnal Periodicity in the Phytoplankton Assemblage of a High Mountain Lake. Limnology and Ocean., 18(1), 15-30.

Verduin, J. (1957). Daytime Variations in Phytoplankton Photosynthesis. Limnology and Ocean., 2, 333-336.

Westlake, D. F. (1966). A Method for Quantitative Studies of Photosynthesis by Higher Plants in Streams. Air and Water Poll. Int. Jour., 10, 883-896.

A.W.R.C. Technical Papers

No. 1   Field study of evaporation: Installation, operation and maintenance of equipment. Snowy Mountains Engineering Corporation, March 1971.

No. 2   Field study of evaporation: Notes on the extraction and computation of data. Snowy Mountains Engineering Corporating, March 1971.

No. 3   A design procedure for the conjunctive use of surface and groundwater storages by P.R. Johnson, E.M. Laurenson and D.T. Howell. Australian Government Publishing Service, Canberra 1972.

No. 4   Water quality assessment practice in Australia by B.J. Lyons and C.D. Parker, Australian Government Publishing Service, Canberra 1973.

No. 5   Hydrologic investigation and design in urban areas — A review by A.P. Aitken, Australian Government Publishing Service, Canberra 1973.

No. 6   Hydrologic data for small rural catchments in Australia 1973 by J.A.H. Brown, Snowy Mountains Engineering Corporation, Cooma 1973.

No. 7   A compilation of Australian water quality criteria by Barry T. Hart, Australian Government Publishing Service, Canberra 1974.

No. 8   Examination of waters: Evaluation of methods for selected characteristics by J.A. McGlynn, Australian Government Publishing Service, Canberra 1974.

No. 9   Survey of corrosion of prestressing steel in concrete water-retaining structures by E. Phillips, Australian Government Publishing Service, Canberra 1975.

No. 10   Hydrologic investigation and design of urban stormwater drainage systems by A.P. Aitken, Australian Government Publishing Service, Canberra 1975.

No. 11   Field study of evaporation — Catalogue of data for phase 1 by R.D. Hoy and S.K. Stephens, Australian Government Publishing Service, Canberra 1975.

No. 12   Corrosion of groundwater pumping equipment in Australia by G.J. Kelly and R.G. Kemp. This title not published.

No. 13   A review of the potential applications of remote sensing techniques to hydrogeological studies in Australia by C.D. Ellyett and D.A. Pratt, Australian Government Publishing Service, Canberra 1975.

No. 14   Guidelines for the selection of turbine pump materials for use in groundwaters by G.J. Kelly and R.G. Kemp, Australian Government Publishing Service, Canberra 1975.

No. 15   An assessment of eutrophication in Australian inland waters by Gavin Wood, Australian Government Publishing Service, Canberra 1975.

No. 16   Suitability of containers for storage of water samples by D.C. Bowditch, C.R. Edmond, P.J. Dunstan and J.A. McGlynn, Australian Government Publishing Service, Canberra 1976.

No. 17   Drilling mud invasion of unconsolidated aquifer materials by C.R. Dudgeon and R.J. Cox, Australian Government Publishing Service, Canberra 1976.

No. 18   Effects of near-well permeability variation on well performance by C.R. Dudgeon and P.S. Huyakorn, Australian Government Publishing Service, Canberra 1976.

No. 19   Influence of metering, pricing policies and incentives on water use efficiency by D.R. Gallagher and R.W. Robinson, Australian Government Publishing Service, Canberra 1977.

No. 20   Efficiency in industrial, municipal and domestic water use by D.P. Heeps, Australian Government Publishing Service, Canberra 1976.

No. 21   Field study of evaporation — analysis of data from Eucumbene, Cataract, Manton and Mundaring by R.D. Hoy and S.K. Stephens, Australian Government Publishing Service, Canberra 1976.

No. 22   Hydrologic design data for water wells in unconsolidated sediments by C.R. Dudgeon and R.J. Cox, Australian Government Publishing Service, Canberra 1976.

No. 23   Effects of siltation on rates of recharge by S.E. James and J.L. Henry, Australian Government Publishing Service, Canberra 1977.

No. 24   Analysis of the movement of water from recharge channels and pits by S.N. Webb and K.K. Watson, Australian Government Publishing Service, Canberra 1977.

Copies of these publications are distributed within Australia and overseas to major libraries and those libraries of organisations which have been identified by the AWRC Secretariat as key water information centres.

Copies still in print may be purchased from AGPS Bookshops in all Australian capital cities or through the mail from Mail Order Sales, Australian Government Publishing Service, P.O. Box 84, Canberra, A.C.T. 2600 Australia.